

1  
2  
3  
4 **Chapter 3**

---

5  
6 **Polar Stratospheric Ozone**

7  
8 **Lead Authors:**

9  
10 Paul A. Newman  
11 John A. Pyle

12  
13 **Co-Authors:**

14 John Austin  
15 Geir Braathen  
16 Pablo Canziani  
17 Ken Carslaw  
18 Piers Forster  
19 Sophie Godin  
20 Bjorn Knudsen  
21 Karin Kreher  
22 Hideaki Nakane  
23 Steven Pawson  
24 V. Ramaswamy  
25 Markus Rex  
26 Ross Salawitch  
27 Drew Shindell  
28 Azadeh Tabazadeh  
29 Darin Toohey

30  
31 **Contributors:**

32 Doug Allen  
33 Linnea Avallone  
34 Stephen Beagley  
35 Greg Bodeker  
36 Christoph Brühl  
37 Anne Douglass  
38 Steve Eckermann  
39 Martin Dameris  
40 Florence Goutail  
41  
42

1  
2  
3  
4  
5  
6  
7  
8  
9  
10  
11  
12  
13  
14  
15  
16  
17  
18

Patrick Hamill  
Ulrike Langematz  
Elisa Manzini  
Tatsuya Nagashima  
Klaus Pfeilsticker  
Giovanni Pitari  
Eugene Rozanov  
Michelle Santee  
Christina Schnadt  
Theodore Shepherd  
Masanori Shitamichi  
Darryn Waugh

**Editorial Contributors:**

Rose Kendall  
Kathy Thompson

1			
2	<b>Executive Summary</b> .....		<b>5</b>
3	<b>0 Introduction</b> .....		<b>9</b>
4	<b>1 Observations and Trends of Ozone and Temperature in the Polar Stratosphere</b> .....		<b>11</b>
5	1.1 Measurements in the Antarctic/Arctic .....		11
6	1.2 Polar Ozone and Temperature Trends .....		13
7	1.2.1 Polar Ozone Trends .....		13
8	1.2.2 Polar Temperature Trends .....		16
9	<b>2 Basic Polar Stratospheric Processes</b> .....		<b>18</b>
10	2.1 Transport and Dynamics.....		18
11	2.1.1 The Polar Vortex: Mean Structure .....		18
12	2.1.2 Polar Vortex: Causes of Interannual Variability and Its Implications.....		19
13	2.1.3 Polar Transport and Mixing .....		25
14	2.2 Polar Stratospheric Clouds .....		29
15	2.2.1 Observations of PSC Physical Properties and Their Interpretation.....		30
16	2.2.2 Particle Composition .....		35
17	2.2.3 Denitrification.....		36
18	2.2.4 Dehydration.....		39
19	2.3 Polar Ozone Chemistry.....		39
20	2.3.1 Chlorine.....		40
21	2.3.2 Bromine.....		47
22	2.4 The Polar Summer Lower Stratosphere.....		51
23	2.4.1 Summertime NO <sub>x</sub> Chemistry.....		52
24	2.4.2 Summertime HO <sub>x</sub> Chemistry.....		53
25	2.4.3 Summertime Cl <sub>y</sub> Chemistry.....		54
26	<b>3 Quantification of Polar Ozone Loss: Observations and Models</b> .....		<b>56</b>
27	3.1 Approaches to Quantify Chemically Induced Ozone Loss in the Arctic .....		56
28	3.1.1 Approaches that Use Explicit Transport Calculations .....		57
29	3.1.2 Approaches that Use the Relation of Ozone to an Inert Tracer .....		60
30	3.2 Arctic Ozone Loss during the Last Decade .....		63
31	3.2.1 Ozone Loss Rates near the Maximum of the Ozone Concentration.....		63
32	3.2.2 Vertical Profiles of Ozone Loss .....		64
33	3.2.3 Effect of Ozone Loss on the Total Ozone Column .....		65
34	3.2.4 Chemical Ozone Loss in the Arctic Winter 1999/2000 .....		66
35	3.3 Consistency between the Different Observational Techniques .....		67
36	3.4 The Effect of Denitrification on Ozone Loss in the Arctic.....		68
37	3.5 Model Studies of Arctic Ozone Loss.....		70
38	3.5.1 Chemical Transport Models .....		71
39	3.5.2 Specific Model Studies.....		73
40	3.6 Quantifying Antarctic Ozone Loss .....		74
41	3.7 Model Studies of Antarctic Ozone Loss .....		75
42	3.8 Conclusion .....		76

1	<b>4</b>	<b>Causes of Polar Stratospheric Temperature Trends</b> .....	<b>76</b>
2	4.1	Introduction .....	76
3	4.2	Modeling Techniques .....	78
4	4.2.1	Fixed Dynamical Heating (FDH) Models .....	78
5	4.2.2	General Circulation Models (GCMs).....	78
6	4.3	Causes of Stratospheric Temperature Trends .....	79
7	4.3.1	Ozone .....	80
8	4.3.2	Well-Mixed Greenhouse Gases (WMGHG) .....	82
9	4.3.3	Combined Changes in WMGHGs and Stratospheric Ozone .....	82
10	4.3.4	Stratospheric Water Vapor .....	83
11	4.3.5	Solar Changes .....	84
12	4.3.6	Volcanoes.....	85
13	4.4	Timing of the Springtime Cooling Trend .....	85
14	4.5	Summary and Conclusions.....	86
15	<b>5</b>	<b>Chemistry-Climate Modeling of the Polar Stratosphere</b> .....	<b>89</b>
16	5.1	Introduction.....	89
17	5.2	The Uncertainties in Chemistry-Climate Models.....	92
18	5.2.1	Temperature Biases .....	92
19	5.2.2	The Simulation of Polar Stratospheric Clouds .....	94
20	5.2.3	The Position of the Upper Boundary of the GCM .....	96
21	5.2.4	Predictions of Planetary Waves .....	97
22	5.2.5	Uncertainties in the Rate of Water Vapor Increase.....	98
23	5.3	Model Assessments .....	100
24	5.3.1	The 1960 - 2000 Time Frame: Ozone Depletion.....	100
25	5.3.2	The 2000 - 2020 Time Frame: Start of Ozone Recovery.....	102
26	5.3.3	The 2020 - 2060 Time Frame: Complete Ozone Recovery .....	103
27	5.3.4	Attribution of Model Ozone Changes.....	104
28	5.4	Summary .....	104
29		<b>References</b> .....	<b>107</b>
30		<b>Chapter 3 Acronyms and Abbreviations</b> .....	<b>136</b>
31		<b>Chapter 3 Chemical Formulae and Nomenclature</b> .....	<b>140</b>

1  
2  
3  
4  
5  
6  
7  
8  
9  
10  
11  
12  
13  
14  
15  
16  
17  
18  
19  
20  
21  
22  
23  
24  
25  
26  
27  
28  
29  
30  
31  
32  
33  
34  
35  
36  
37  
38  
39  
40  
41  
42  
43  
44  
45

## EXECUTIVE SUMMARY

**Springtime Antarctic ozone depletion remains very large and is essentially unchanged since the early 1990s.** The minimum column abundance in 2001 was ~100 DU (Dobson unit), similar to the minimum values in the last decade. The processes are well understood.

**Certain estimates of the strength of the ozone hole, e.g., the area enclosed by the 220 DU contour, show interannual variability, so that it is not yet possible to say that the ozone hole has reached its maximum.** Much of the variability appears to be associated with processes at the vortex collar and is consistent with the almost constant halogen loading and meteorological variability.

**The degree of chemical loss of ozone for all Arctic winters during the last decade is now reasonably well documented.** The accuracy of state-of-the-art approaches to quantify chemical ozone loss from ozone observations is better than 20%.

**The Arctic winter/spring ozone column continues to be variable, reflecting the variable meteorology of the Northern Hemisphere stratosphere.** Lower column ozone was present during the cold winter of 1999/2000 than in the warmer, more disturbed winters 1998/1999 and 2000/2001. The variability arises from natural variability and a number of forcing factors. It is not possible to isolate the importance of these factors just from observations; model studies are needed to do this. The Arctic oscillation can be used as an index to describe variability, but not causality.

**There was very large local ozone depletion in the Arctic vortex in 1999/2000 reaching 70% by early April in a narrow region around 20 km.** Integrated column losses were greater than 80 DU. The winter of 1999/2000 was characterized by persistent low temperatures and a strong vortex. In contrast, in the warmer more disturbed polar vortex of 1998/1999 the estimated loss is very small. These observations are consistent with our expectation that Arctic ozone losses are expected to be variable and largest in cold stratospheric winters.

**Satellite and radiosonde observations show that the springtime polar lower stratospheres continue to cool.** Since 1979 there has been a trend of the order of -2K/decade at 70 degrees latitude. However, due to large springtime variability, particularly in the Arctic, the magnitude of this cooling remains uncertain. There has also been a statistically significant annually-averaged lower stratospheric cooling at both poles.

**Modeling studies now demonstrate that the springtime cooling in the Arctic lower stratosphere over the 1980-2000 period is, in part, due to stratospheric ozone depletion, but the degree of attribution is hindered by the large dynamical variability in this region.** In Antarctica modeling studies re-affirm that ozone loss is the major cause of the springtime cooling. They also indicate that well-mixed greenhouse gas (WMGHG) and stratospheric water vapor increases are likely contributors to the annually-averaged cooling. However, due to climate variability in the models, longer integrations are needed for attribution.

1 **Synoptic and mesoscale motions (baroclinic and gravity waves) can lead directly to, and**  
2 **enhance, PSC formation in both hemispheres.** For the first time, operational meteorological  
3 analyses have been demonstrated to contain credible information about the gravity wave field in  
4 high latitudes.

5  
6 **CIOOCl, the key intermediate in chlorine-catalyzed ozone loss in the perturbed polar**  
7 **regions, has been measured for the first time in the Arctic winter polar vortex.** These  
8 observations confirm the role of this species in ozone depletion, and the observed abundances  
9 agree well with inferred values that have appeared in previous assessments.

10  
11 **New studies indicate that the photochemical balance between ClO and CIOOCl is well**  
12 **understood during the winter,** using a termolecular rate constant for  $\text{ClO} + \text{ClO} + \text{M} \rightarrow \text{CIOOCl}$   
13  $+ \text{M}$  that is up to 25% larger than is currently recommended and absorption cross sections for  
14 CIOOCl as currently recommended.

15  
16 **Measurements of the inorganic chlorine species and the organic source compounds**  
17 **demonstrate that the budget of inorganic chlorine in the polar regions is balanced to within**  
18 **the uncertainties of the measurements,** insofar as our understanding of the photochemical  
19 balance between ClO and CIOOCl is fundamentally correct.

20  
21 **Modeling studies of the latitudinal, seasonal, and diurnal variations in BrO column**  
22 **abundances agree well with observations from eleven ground sites, indicating that the**  
23 **processes that govern ozone loss due to bromine in the polar regions are well understood.**  
24 There are some minor discrepancies between observations of BrO and the expected  
25 photochemical behavior, suggesting that there may be a small abundance of an unknown species  
26 or a small error in a rate constant. However, this result is largely inconsequential for assessing  
27 the role of bromine in polar ozone loss.

28  
29 **Observations of BrO in the winter Arctic vortex by *in situ* and remote detection techniques**  
30 **are in broad agreement and consistent with a total bromine budget of ~20 +/- 4 parts per**  
31 **trillion.** This result now allows for more accurate assessment of the contribution of bromine to  
32 polar ozone loss. At present, the fractional contribution of bromine to total ozone loss ranges  
33 from between 30 and 60%, depending on temperature and abundances of ClO. Considering the  
34 observed leveling off of abundances of sources of chlorine (reported in Chapter 1), the role of  
35 bromine in polar ozone loss will continue to increase relative to that of chlorine until the current  
36 upward trends of the bromine source gases reverse.

37  
38 **New laboratory and field studies have led to refinements in the recommendations for the**  
39 **rate constants of several key reactions that couple the photochemistry of HO<sub>x</sub> and NO<sub>x</sub>**  
40 **(species that are largely controlled by natural processes) and to the discovery of a new**  
41 **process (near-IR photolysis of HNO<sub>4</sub>).** Together with new observations of HO<sub>x</sub>, NO<sub>x</sub>, and  
42 ozone in late spring and summer, these studies have demonstrated that our understanding of the  
43 photochemistry of HO<sub>x</sub> and NO<sub>x</sub> in the lower stratosphere is fundamentally sound.

44

5/7/02

1 **Removal of nitrogen compounds (denitrification) has been observed to occur in the Arctic**  
2 **lower stratosphere in several cold winters.** Denitrification of up to 70% of the total reactive  
3 nitrogen was observed at some levels of the lower stratosphere in winter 1999/2000. Our  
4 understanding of what causes denitrification has improved considerably. It is now clear that  
5 sedimentation of large nitric acid hydrate particles can account for observed Arctic  
6 denitrification, although the mechanism of formation of the sedimenting particles remains  
7 uncertain. Sedimentation of ice containing dissolved nitric acid, which has been the preferred  
8 mechanism in stratospheric models, is not the dominant mechanism in the Arctic.

9  
10 **Observations and modeling results show that Arctic denitrification can increase lower**  
11 **stratospheric ozone loss by as much as 30% at a given level.** Model calculations suggest that  
12 the magnitude and vertical extent of denitrification could increase considerably in a future colder  
13 Arctic stratosphere, leading to increased ozone loss over a broader altitude range. The  
14 denitrification mechanism is not well represented in current global models, which currently  
15 limits the ability of the models to reproduce the large ozone losses observed in cold Arctic  
16 winters and to reliably predict future ozone losses in the Arctic.

17  
18 **The chemical composition of liquid and solid polar stratospheric cloud particles has been**  
19 **measured directly for the first time.** Measured compositions are in agreement with model  
20 calculations for liquid particles and nitric acid trihydrate, which have been used in stratospheric  
21 models for many years. These measurements give confidence in the microphysical models that  
22 are central to simulations of polar ozone loss.

23  
24 **Significant chemical loss of ozone (~0.5 ppmv) in the lower stratosphere during January**  
25 **has been observed in several cold Arctic winters.** The observations indicate that the loss  
26 occurred exclusively during periods when the air masses are exposed to sunlight. These January  
27 ozone losses cannot be fully explained with our current understanding of the photochemistry.  
28 For cold Arctic winters the ozone loss during January contributes about 25% to the overall loss  
29 of ozone over the winter.

30  
31 **Coupled chemistry-climate simulations generally agree with past trends in total ozone,**  
32 **particularly over the Antarctic.** Discrepancies with observations can, in some cases, be large  
33 and stem in particular from modal temperature biases and transport errors. These errors can be  
34 reduced with the use of higher spatial resolution and improved representations of sub-grid scale  
35 processes.

36  
37 **It is now possible to estimate the timing of the start of ozone recovery from several coupled**  
38 **models.** For the Arctic, this could occur within the timeframe 2004-2019 and for the Antarctic  
39 2001-2008. These dates are based on just three models and subject to large error. However,  
40 each model is consistent in showing a later start to recovery in the Arctic, which occurs several  
41 years after the peak in halogen amount in each model. This indicates that increases in well-  
42 mixed greenhouse gases have delayed the start of ozone recovery in the models. Interannual  
43 variability is also very large in the Arctic, so that unambiguous detection of ozone recovery may  
44 not occur there before 2030.

45

5/7/02

1 **Few 3-D models have been run beyond 2050.** These suggest that full Antarctic ozone recovery  
2 (to 1980 levels) may be expected by 2045-2055. In the Arctic, the model ozone changes are  
3 much smaller than in the Arctic and, once ozone recovery begins, the model results suggest that  
4 full ozone recovery may occur earlier, possibly as early as 2030. Hence, it is plausible that, by  
5 the time of unambiguous detection of the start of ozone recovery, Arctic ozone may have already  
6 fully recovered. However, some of the models do not include particle sedimentation that could  
7 delay the full recovery of Arctic ozone beyond 2030.

8



1 **0 INTRODUCTION**

2  
3 This chapter provides an update on our understanding of changes in polar ozone, and the  
4 polar vortex, in the recent past and considers possible future developments. It builds on earlier  
5 assessments, concentrating mainly, but not exclusively, on work reported since the last  
6 assessment report (World Meteorological Organization (WMO), 1999).

7 The last assessment reported that the Antarctic ozone hole continued unabated, with  
8 essentially near-complete destruction of ozone in the low stratosphere, and that the factors  
9 controlling the depletion - meteorological pre-conditioning, halogen activation, ozone depletion  
10 in sunlight - were well understood. In the Arctic, substantial ozone losses were reported in  
11 several winters during the 1990s, depending on the meteorological conditions. The report  
12 highlighted the vulnerability of the Arctic to large ozone losses in a cold winter while chlorine  
13 abundances remain high during the next decade or so. Less chemical loss was to be expected in  
14 the Arctic in winters with a warm, disturbed vortex. Difficulties with the precise quantification  
15 of Arctic ozone loss were indicated. The last assessment highlighted specific uncertainty issues  
16 surrounding the understanding of the different types of polar stratospheric clouds, and the  
17 process of denitrification, which can limit our ability to model present and future polar ozone  
18 loss.

19 The coupling between atmospheric chemistry and climate has been recognized increasingly  
20 in recent assessments. In WMO (1999) a late winter/springtime cooling in the polar lower  
21 stratospheric temperatures of ~3-4 K/decade was noted (although with the large dynamical  
22 variability in that region the statistical significance of the trend was not high) and the role of  
23 ozone, water vapor and the well-mixed greenhouse gases was explored. 3-D coupled chemistry-  
24 climate models were used for the first time to look at the possible recovery of the ozone layer;  
25 these models all indicated a delay in recovery beyond the time of the peak in stratospheric  
26 halogen abundance.

27 Since the last assessment there has been considerable progress in basic research that we  
28 report below. Satellite data sets on ozone and temperature have been further extended. In  
29 addition, scientific impetus has been provided by several major field campaigns to study the  
30 Arctic stratosphere. Results from the National Aeronautics and Space Administration's  
31 Photochemistry of Ozone Loss in the Arctic Region in Summer (NASA's POLARIS), aimed at

1 understanding the summer polar stratosphere, the European Union's (EU's) THESEO, a polar  
2 and middle latitude campaign, and the joint NASA/EU Stratospheric Aerosol and Gas  
3 Experiment (SAGE) III Ozone Loss and Validation Experiment-THESEO (SOLVE-THESEO  
4 2000) are reported here. These campaigns produced new data to address some of the  
5 uncertainties remaining after the last assessment.

6 Section 3.1 updates polar ozone measurements in both Antarctica and the Arctic,  
7 concentrating on the winter and spring seasons when the largest ozone depletion is observed. As  
8 well as considering the total ozone columns, updated information on various possible indicators  
9 of ozone recovery, suggested in the last assessment, are presented briefly. The updated polar  
10 temperature trends are also presented here.

11 Section 3.2 reviews our understanding of the relevant physical and chemical processes  
12 controlling the polar vortex and its composition. The Arctic field campaigns have provided new  
13 data on a disturbed winter with considerable exchange between polar and middle latitudes  
14 (1998/1999) and the cold polar winter of 1999/2000, which led to large local ozone depletion.  
15 Many new complementary constituent measurements provide an important constraint on  
16 chemical loss processes. Important new measurements of particles were also made in the winter  
17 polar stratosphere, leading to advances in our understanding of particle composition and  
18 denitrification. Improved understanding of the dynamics in and around the polar vortex has also  
19 been developed.

20 Section 3.3 looks in detail at our quantitative understanding of polar ozone loss. In earlier  
21 assessments it was recorded that models often fail to quantify correctly the observed ozone loss.  
22 A variety of methods to derive ozone loss from measurements are reviewed in this section.  
23 Estimated losses in recent Arctic and Antarctic winters are considered and compared with each  
24 other and with model estimates.

25 In WMO 1999, it was recognized that the future development of the ozone layer does not  
26 depend just on changes in stratospheric halogen loading but also, very importantly, on a number  
27 of other factors connecting chemistry and climate. These factors are discussed in Section 3.4.  
28 Temperature changes are particularly important since polar heterogeneous chemistry is strongly  
29 temperature dependent and, furthermore, temperature changes are related to the strength of the  
30 polar vortex, descent within the vortex, and mixing with lower latitudes. The attribution of the  
31 trends in polar stratospheric temperatures, presented in Section 3.1, is discussed and the role of

1 changes in well-mixed greenhouse gases, in ozone, water vapor and aerosol particles are  
2 reviewed. Future stratospheric temperature changes are discussed.

3 Finally, in Section 3.5, possible future states of the polar stratosphere are explored in  
4 sensitivity calculations using coupled chemistry/climate models. Results from these models  
5 were reported for the first time in an assessment in WMO 1999, and the models are still being  
6 developed. An extensive review of the present uncertainties in chemistry/climate models is  
7 presented here followed by some examples of sensitivity calculations to consider the polar  
8 stratosphere during the next 50 years.

## 9 1 **OBSERVATIONS AND TRENDS OF OZONE AND TEMPERATURE IN THE** 10 **POLAR STRATOSPHERE**

### 11 1.1 **Measurements in the Antarctic/Arctic**

12  
13 In this section, we update information on instruments that measure ozone and other species  
14 that are pertinent to polar ozone issues. We briefly review the status of a variety of ozone and  
15 related measurements for the Antarctic and Arctic. Total ozone observations and ozonesondes  
16 have been extensively discussed in previous reports, and are further reviewed in Chapter 4 of this  
17 assessment.

18 **Earth Probe (EP) Total Ozone Mapping Spectrometer (TOMS):** Data from the TOMS  
19 instrument have been extensively used to track Arctic and Antarctic ozone changes. The TOMS  
20 data are discussed in Chapter 4's Section 4.2.2.2. The EP/TOMS operational processing  
21 configuration has recently been changed in order to apply a correction to a cross-track bias error  
22 that has grown since 2000. While 2001 data are included herein, they are of slightly greater  
23 uncertainty (see discussion in the Earth Probes TOMS description in Section 4.2.2.2).

24 **Microwave Limb Sounder (MLS):** The MLS observations started in September 1991  
25 with the launch of the Upper Atmosphere Research Satellite (UARS). It gives column and  
26 profile data on ozone, ClO, and HNO<sub>3</sub>. Recently, the satellite and instrument have experienced  
27 problems and the instrument is only turned on when there are situations of particular interest. In  
28 particular, MLS was taken out of stand-by mode on 31 January 2000 and was operated during  
29 the 2-13 February and 27-29 March periods in conjunction with the SOLVE-THESEO 2000  
30 campaign (Santee *et al.*, 2000).

1       **Halogen Occultation Experiment (HALOE):** The HALOE observations also started in  
2 September 1991 with the launch of UARS. HALOE is a solar occultation instrument that makes  
3 measurements in the IR at both sunset and sunrise. HALOE measurements are used to retrieve  
4 profiles of O<sub>3</sub>, HF, HCl, CH<sub>4</sub>, H<sub>2</sub>O, NO, NO<sub>2</sub>, and aerosol extinction. The HALOE occultation  
5 latitudes are variable over the course of the northern winter, but do not reach the high northern  
6 latitudes. During the winter of 1999-2000, the maximum latitude sampled by HALOE was  
7 approximately 63°N in mid-March. HALOE typically has difficulty sampling the polar vortex  
8 during mid-winter, but does sample the vortex edge region in the fall ([Pierce et al., 2001](#)).

9       **GOME:** The Global Ozone Monitoring Experiment (GOME) instrument was launched in  
10 1995 aboard the second European Remote Sensing (ERS-2) satellite. It measures column ozone,  
11 NO<sub>2</sub>, BrO and OCIO, and O<sub>3</sub> profiles. Details on the GOME instrument can be found in  
12 Burrows *et al.* (1999). The GOME data have been subject to validation exercises (Hansen *et al.*,  
13 1999; Hoogen *et al.*, 1999; Corlett and Monks., 2001; Ionov *et al.*, 2001; Piders *et al.*, 1999;  
14 Rathman *et al.*, 1997).

15       **The Polar Ozone and Aerosol Measurement (POAM)** is a solar occultation instrument  
16 that provides ozone, water vapor, NO<sub>2</sub>, and aerosol extinction profiles in the polar regions.  
17 POAM II was launched in 1993 aboard the French Satellite Pour l'Observation de la Terre  
18 (SPOT)-3 satellite. These measurements were interrupted by the failure of the SPOT-3 satellite  
19 in November 1996. POAM III was subsequently launched on the French SPOT-4 satellite in  
20 March 1998 and is currently operational.

21       Intercomparisons between POAM III and other instruments have been published by Lucke  
22 *et al.* (1999); [Lumpe et al. \(2002\)](#); [Randall et al. \(2002\)](#). Results from POAM III include studies  
23 on dehydration ([Nedoluha et al., 2000](#)); ozone loss ([Randall et al., 2002](#); [Hoppel et al., 2002](#));  
24 and PSCs ([Bevilacqua et al., 2002](#)).

25       **The Improved Limb Atmospheric Spectrometer (ILAS)** is a satellite instrument that  
26 uses solar occultation technique ([Sasano et al., 1999](#); [Nakajima et al., 2002](#)). ILAS was  
27 launched onboard the ADvanced Earth Observing Satellite (ADEOS) on 17 August 1996. ILAS  
28 made measurements over high latitude regions from 57°N to 71°N and from 64°S to 88°S from  
29 late October 1996 until late June 1997.

30       ILAS consists of an infrared spectrometer that covers the wavelength region from about 6  
31 to 12 micron. ILAS made measurements of vertical profiles of O<sub>3</sub>, HNO<sub>3</sub>, NO<sub>2</sub>, N<sub>2</sub>O, methane

1 (CH<sub>4</sub>), and H<sub>2</sub>O from the infrared spectrometer as well as vertical profiles of aerosol extinction  
2 coefficient at 780 nm from the visible spectrometer. Ozone data are validated by correlative and  
3 coincident measurements from several instrumental techniques (Sugita *et al.*, 2002). Nitric acid,  
4 NO<sub>2</sub>, and H<sub>2</sub>O data have also been validated (Koike *et al.*, 2000; Kanzawa *et al.*, 2002; Irie *et*  
5 *al.*, 2002).

## 6 **1.2 Polar Ozone and Temperature Trends**

### 7 **1.2.1 POLAR OZONE TRENDS**

8  
9 Ozone is primarily produced in the mid-latitudes and tropics by photo dissociation of  
10 oxygen by hard UV-radiation (below 242 nm), and is transported towards the poles by the  
11 Brewer-Dobson circulation. An annual cycle in ozone results, shown by the climatological  
12 values in Figure 1.2-1. Because of the stronger Brewer-Dobson circulation in the Northern  
13 Hemisphere (NH), the Arctic is both warmer and has larger column ozone amounts than the  
14 Antarctic. In the Northern Hemisphere there is usually a maximum in the column in late  
15 winter/early spring. At South Pole, there is less annual variation (larger annual variations are  
16 expected at the vortex edge). In recent years, the annual cycle has been modified by polar ozone  
17 depletion, most obviously in the Southern Hemisphere.

18 Figure 1.2.1 also shows recent year-round ozone measurements from the Arctic Ny  
19 Ålesund station (78.9°N, 11.9°E) and the South Pole station, updating polar observations since  
20 the last assessment. The Antarctic observations in the last few years continue to show the  
21 extremely low spring ozone values that have characterized the ozone hole during the 1990s. The  
22 low Antarctic values begin with the chemical ozone losses during August and September and end  
23 upon the break-up of the vortex in November or December. During the summer, ozone is  
24 destroyed photochemically, especially at the poles during continuous sunlight conditions (Brühl  
25 *et al.*, 1998), and the climatological seasonal minimum is reached in autumn.

26 In the Arctic, the March-April ozone maximum is occasionally reduced below the  
27 climatology in some years (*e.g.*, in 1997, the magenta triangles) because of severe chemical  
28 ozone loss and reductions in ozone transport (Andersen and Knudsen, 2002). In these low ozone  
29 years, the column ozone rapidly increases with the break-up of the vortex (*e.g.*, early April  
30 1997). Of the most recent winters, 1999/2000 also has somewhat lower ozone columns than the

1 climatology, to be discussed later. Extremely low Ny Ålesund column ozone values at the  
2 beginning of 1996 (Figure 1.2-1 gold triangles) can partially be explained by the early onset of  
3 the ozone depletion that year (see Section 3.2). The lowest 1996 values occur in an 'ozone  
4 minihole' event ([Weber \*et al.\*, 2002](#)) (see Section 2.1.2). A complicating factor in the upper  
5 panel in Figure 1.2-1 is that occasionally Ny Ålesund is outside the vortex, as is evident from the  
6 large variations on a broad range of spatial and temporal scales.

7 Extremely high Ny Ålesund column ozone values in December 1998 (Figure 1.2-1 black  
8 diamonds) and February 2001 (red circles) were caused by sudden warmings. The warmings in  
9 these years also result in high temperatures, thereby preventing the formation of polar  
10 stratospheric clouds.

11 The largest ozone depletion occurs in the polar vortices during springtime. Figure 1.2-2  
12 shows the springtime ozone values in the Arctic and Antarctic (63° to 90°) since 1970 (updated  
13 from Newman *et al.*, 1997). The Arctic column ozone averages were extremely low during the  
14 mid-1990s, but have been relatively high in 4 of the last 5 winters. As noted in the previous  
15 paragraph and as is apparent in Figure 1.2-1, these higher ozone values are associated with  
16 stratospheric sudden warmings. The downward secular ozone trend apparent through 1997 and  
17 its reversal over the last few years can be associated with a long-term variation of stratospheric  
18 warmings.

19 Figure 1.2-2 also shows that the Antarctic ozone hole continues to display the low values  
20 over the last 4 years that were apparent during the early and mid-1990s. The notably higher  
21 value in October 2000 resulted from greater dynamical activity, as is also apparent in Figure 1.2-  
22 1.

23 The polar column ozone averages of Figure 1.2-2 in the 63° to 90° region generally  
24 coincide with the polar vortices. However, in the NH the vortex is usually smaller and the 63° to  
25 90° region may contain air outside the vortex. The absolute minimum in the NH occurred in  
26 1997, when the vortex was cold, very large and pole-centered. However, the column chemical  
27 ozone loss in the vortex was probably much larger in 1995, 1996, and 2000 (see Section 3.2).  
28 However, [Andersen and Knudsen \(2002\)](#) have argued that about 75% of the 63° to 90°N  
29 depletion from 1992-2000 relative to the 1979-1982 average is due to ozone depletion inside the  
30 vortex, so the plot does give quite a good indication of the Arctic vortex depletion.

1 The two previous figures have shown recent ozone observations. We now turn attention to  
2 the trends derived from these observations. Large total column ozone trends have been seen in  
3 both the Arctic and Antarctic polar vortices during the spring (Figure 1.2-3). To obtain these  
4 trends with better correlation with the polar vortices, a potential vorticity coordinate (equivalent  
5 latitude) remapping technique was applied to a trend analysis of homogenized satellite data from  
6 TOMS and GOME (Bodeker *et al.*, 2001). In this coordinate the center of the vortices are at  
7 about 90° and the edges at 60° to 75° (as shown). After applying a regression model including  
8 trends and variability (seasonal cycle, QBO, solar cycle, volcanic effects, ENSO) to the data  
9 from 1978 to 1998, statistically significant linear trends were obtained.

10 The largest Arctic negative trend ( $1.93 \pm 0.40$  %yr<sup>-1</sup>) is observed in March, while the  
11 largest Antarctic negative trend ( $2.95 \pm 0.40$  %yr<sup>-1</sup>) is observed in October. In the Arctic vortex  
12 the 1978-2000 trend has almost doubled compared to the 1978-1991 period ( $1.05 \pm 0.96$  % yr<sup>-1</sup>)  
13 due to severe vortex depletions in the 1990s (Section 3.2). In the Antarctic vortex trends have  
14 weakened due to saturation of the ozone losses, but the total depletion over the whole period has  
15 in fact increased. Figure 1.2-3 shows the trends when 1999 and 2000 data are added, which  
16 results in slightly smaller negative trends than previously in the Antarctic spring column ozone.  
17 In the Arctic adding the exceptionally warm winter of 1998/1999, when no significant ozone  
18 depletion in the vortex occurred, leads to a substantial reduction of the downward trends. Figure  
19 1.2-3 shows steep gradients in the trends across the edge of the vortex. It also reveals  
20 statistically significant negative ozone trends in May, June, and July just inside the Antarctic  
21 vortex, which were not found in previous trend analyses, but confirms earlier findings (Roscoe *et*  
22 *al.*, 1997; Lee *et al.*, 2001) (see Section 3.7.2).

23 As the ozone loss mainly occurs in the 12- to 20-km layer, the partial column ozone from  
24 12 to 20 km provides a good representation of the long term decrease of the stratospheric ozone  
25 in Antarctica and could be used as an indicator of ozone recovery (see WMO, 1999). Figure 1.2-  
26 4 gives monthly averaged partial column ozone in September, October, and November based on  
27 the ozone sonde observation at Syowa (1968-2001). The partial column ozone has decreased  
28 considerably from the early 1970s (~80% in September, ~85% in October, ~80% in November).  
29 The October partial column has not shown appreciable change since 1992. On the other hand,  
30 the September and November partial columns continue to show small reductions during the  
31 1990s. The averaged partial column ozone over the three months (September to November) has

1 also shown decreases during the 1990s, with relatively smaller interannual variability. Because  
2 Syowa is located near the vortex edge region, these September and November ozone reductions  
3 during the 1990s may be related to cooling near the vortex collar.

4       Spatially averaged characteristics of the Antarctic ozone hole from 1979 to 2000 based on  
5 the total column ozone observed by satellites (TOMS series and TOVS for 1995) are shown in  
6 Figure 1.2-5. These parameters include the maximum area, the minimum total column ozone,  
7 the ozone mass deficiency, and the date of the ozone hole's disappearance. The maximum area  
8 of the ozone hole increased rapidly during the 1980s and gradually during the 1990s, with year-  
9 to-year variations, and reached the maximum in 2000. The minimum total ozone, which usually  
10 appears in late September or in early October, has been approximately 100 DU since 1993  
11 (Figure 1.2-5) after the considerable decrease during the 1980s and the early 1990s. The ozone  
12 mass deficiency in the ozone hole ( $O_3$  MD) is defined as the ozone mass deficiency from 300  
13 DU in the sunlit area poleward of  $60^\circ S$  averaged for 105 days (1 September – 15 December).  $O_3$   
14 MD varied in concert with the Antarctic ozone hole area and was at the highest level ever in  
15 2000. The date of the disappearance of the Antarctic ozone hole (disappearance of the total  
16 ozone values below 220 DU), has generally been occurring later in the season. As a whole,  
17 observations show that the Antarctic ozone hole has been slightly larger in the last few years in  
18 comparison to the mid 1990s. These observational results could be explained by ozone  
19 decreases near the vortex edge (*e.g.*, Bodeker *et al.*, 2001, 2002; Lee *et al.*, 2001). Although the  
20 size of the Antarctic polar vortex has not increased, it has been stronger as shown in Figure 1.2-  
21 6. There has been a tendency towards a cooling of the vortex due to ozone depletion (the  
22 temperature trends are discussed immediately below) and the polar vortex has been more  
23 persistent with some interannual variability. These conditions could result in more extensive  
24 PSCs in the sunlit vortex edge, and larger chemical depletion of ozone. This would expand the  
25 area of the hole, and delay its disappearance.

## 26 **1.2.2 POLAR TEMPERATURE TRENDS**

27  
28       There is substantial observational data on the polar stratosphere available from ~1979,  
29 including radiosonde and satellite measurements, and analyses of various types (Ramaswamy *et*  
30 *al.*, 2001). Figure 1.2-7 illustrates the time series of temperatures at  $70^\circ N$  (March) and  $70^\circ S$   
31 (November) from National Center for Environmental Protection (NCEP) reanalyses and CPC



1 analyses (for descriptions, see WMO, 1999, Chapter 5). There are large interannual variations  
2 manifest in both hemispheres which generally complicates the determination of statistically  
3 significant trends.

4 The Microwave Sounding Unit channel-4 (MSU-4) data and the Stratospheric Sounding  
5 Unit (SSU) derived temperature trends (1979-1998) for 70°N and 70°S are shown in Table 4.1  
6 (see also Figure 1.2-8). These are an update to the 1979-1994 trends presented in Ramaswamy *et*  
7 *al.* (2001). The 70° latitude is chosen for the comparisons as this is the highest latitude for which  
8 SSU trend data is available. Both MSU-4 and SSU-15X signals originate from a range in  
9 altitude in the stratosphere and do not conform to one particular height. The SSU peak signal  
10 corresponds to a pressure of roughly 50 hPa and shows a statistically significant (at the 2 $\sigma$  level)  
11 cooling of nearly 3K/decade at 70°N in MAM and 70°S in SON, and approximately 1.2K/decade  
12 for the annual average temperature change at both poles. The instrument also shows cooling  
13 significant at the 1 $\sigma$  level for most other seasons. The MSU-4 data (peak signal from  
14 approximately 100 hPa) also shows a significant cooling during the spring in both hemispheres (-  
15 1.8 K/decade at 70°N and -1.1 K/decade at 70°S) and at both poles. These MSU-4 trends are  
16 roughly half the magnitude of the SSU trend. The observed satellite trends for this period are  
17 one of cooling in all seasons at both 70°N and 70°S.

18 It should be noted that the magnitude and statistical significance of the trends in both  
19 regions are dependent on the end year considered. This is more crucial for the Arctic, especially  
20 during winter/spring when the time series reveals large interannual variations in temperatures  
21 (see Figure In 1.2-8; also Labitzke and Van Loon, 1995). The trend sensitivity can be  
22 appreciated by comparing the latest (1979-1998) MSU trend at 70°N (March, as shown in Figure  
23 1.2-8) with the corresponding MSU trends shown in WMO (1995) (Figure 8.11 for the period  
24 1979-1991).

25 Comparing the satellite 1979-2000 annual-mean trends with those obtained for the 1979-  
26 1994 period (WMO, 1999), there is now a statistically significant cooling at the 95% confidence  
27 level in the mid-to-high southern latitudes (Ramaswamy *et al.*, 2002a). The northern  
28 midlatitudes continue to exhibit a statistically significant cooling trend (see WMO, 1999) while  
29 the higher latitudes (Arctic region) now have a cooling trend significant at the 90% confidence  
30 level. As in the satellite data, the 1979-2000 sonde trends yield a annually averaged cooling  
31 trend in the northern polar region. The sonde trend is somewhat smaller than the satellite trend

1 (see Table 4.1), although this may be partially due to the time period for the trend analysis being  
2 longer in the sonde data (note that 3 of the last 4 years have been relatively warmer, see Figure  
3 1.2-7). The CPC analysis at 50 hPa also shows a cooling at both poles, consistent with the  
4 satellite data and sonde data.

## 5 **2 BASIC POLAR STRATOSPHERIC PROCESSES**

### 6 **2.1 Transport and Dynamics**

7  
8 This section discusses the structure and dynamics of the polar stratosphere, including trace  
9 gas transport. Section 2.1.1 gives a brief overview of the mean vortex structure, providing a  
10 context for the later assessment. Section 2.1.2 assesses recent studies of the dynamics and  
11 structure, including variability and trends. An important point is the apparent delay in polar-  
12 vortex breakdown in springtime of both hemispheres; extending the cold winter season is a  
13 critical factor in increasing the likelihood of chemical ozone loss, but even in the absence of  
14 chemical processes, the continued isolation of the polar region into the springtime leads to a  
15 ‘dynamical’ ozone deficit. Section 2.1.3 examines transport processes, including the mean  
16 meridional circulation and issues of transport inside, outside, and across the boundary of the  
17 polar vortex; these play a crucial role in fixing the distributions of ozone and other trace gases,  
18 which impacts both the physical processes (such as radiative heating) and chemical ozone loss.

#### 19 **2.1.1 THE POLAR VORTEX: MEAN STRUCTURE**

20  
21 The winter stratospheric circulation is dominated by the polar night jet, which is at the edge  
22 of the polar vortex. Understanding the polar vortex dynamics is central to our ability to  
23 understand recent ozone change and to predict future ozone.

24 The polar vortex structure is well understood: absence of solar heating in winter leads to  
25 strong radiative cooling, which is offset by the adiabatic warming caused by the descending  
26 branch of the Brewer-Dobson circulation. This circulation is caused by the damping of planetary  
27 and gravity waves in the middle atmosphere (*e.g.*, Fels, 1985). An illustration of the polar vortex  
28 (Figure 2.1-1) shows the polar night jet (peaking near 60°N at about 45 km) and the strong  
29 descent (shown by the meridional stream function) which is proportional to the radiative cooling.  
30 Descent in the polar region leads to (diabatic) downward transport, carrying ozone and other

1 trace gases from the mesosphere to the lower stratosphere during winter (*e.g.*, Rosenfield and  
2 Schoeberl 2001).

3 The asymmetry of the polar vortices in the two hemispheres is a consequence of the  
4 different topographic features: the weaker wave activity propagating from the Southern  
5 Hemisphere troposphere provides less forcing and therefore a weaker Brewer-Dobson circulation  
6 than in the Northern Hemisphere (*e.g.*, Randel and Newman, 1998). The Antarctic vortex is  
7 more symmetric, stronger and colder than the Arctic, as illustrated by the 50-hPa geopotential  
8 height distributions in middle winter (Figure 2.1-2). Even in the absence of chemical ozone  
9 destruction, these dynamical differences lead to substantially more ozone in the Arctic than in  
10 the Antarctic vortex, especially in springtime.

11 The main impacts of these dynamical differences on Arctic (compared to Antarctic) ozone  
12 are from the stronger diabatic descent, which transports trace species downwards more rapidly,  
13 and the decreased likelihood of PSC formation. Since PSCs form at temperatures near 195 K at  
14 50 hPa (see Section 2.2), they can form every winter in the Antarctic vortex core, but only on  
15 colder-than average days in the Arctic (*e.g.*, Pawson *et al.*, 1995; Pawson and Naujokat, 1999).

16 While these basic mechanisms that determine the vortex structure and tracer transport in  
17 polar regions are now well understood, there are important aspects for which the complexity is  
18 only partially described. Recent results pertaining to these uncertainties are assessed in the next  
19 section.

### 20 **2.1.2 POLAR VORTEX: CAUSES OF INTERANNUAL VARIABILITY AND ITS IMPLICATIONS**

21  
22 Differences between the hemispheres, caused by the stronger wave driving in the Northern  
23 Hemisphere, are also evident in the year-to-year variations. Figure 1.2-8 shows what appear to  
24 be robust temperature trends in the springtime, but interpretation of such trends is complex,  
25 because of the large interannual variability of high-latitude temperature (Figure 1.2-7), which  
26 varies with time of year and is different in the two hemispheres (Figure 2.1-3: *e.g.*, Scaife *et al.*,  
27 2000b). Southern hemispheric variability peaks in late winter and spring (*e.g.*, Kuroda and  
28 Kodera, 1998), while northern hemispheric variability is large throughout the season (*e.g.*,  
29 Labitzke, 1982). The variability of the stratosphere (defined in terms of departures from the  
30 long-term mean) is characterized by a 'see-saw' of temperature and mass between the polar  
31 region and mid-latitudes (*e.g.*, Labitzke, 1982): anomalously weak wave forcing leads to a strong

1 polar vortex and a weak Brewer-Dobson circulation (*e.g.*, Figure 2.1-1), with a cold polar region  
2 and warmer mid-latitudes (the converse is true for strong wave forcing). Newman *et al.* (2001)  
3 demonstrated the quantitative linkage between the upward-propagating wave activity through the  
4 tropopause region and the strength of the polar vortex.

5 The occurrence of a strong, cold polar vortex leads to anomalously low ozone in the polar  
6 region, since the transport of ozone-rich air is weak and because the potential for PSC  
7 processing, a precursor to chemical ozone loss, is enhanced. This means that in years with weak  
8 tropospheric wave forcing a stronger polar vortex will result in less ozone in the polar region.  
9 Chipperfield (1999) reported results from a 6-year simulation using the SLIMCAT chemistry and  
10 transport model (CTM), driven by UKMO analyses of the meteorology. The horizontal winds  
11 and temperatures are taken from the UKMO analyses, and the vertical motion is diagnosed using  
12 a radiation scheme. The model simulates the interannual variations in chlorine activation during  
13 northern winters, and reproduces the repeatable pattern of activation observed during southern  
14 winters. Chipperfield and Jones (1999) utilized the same model to evaluate the relative  
15 contributions of photochemical and dynamical processes to interannual variability in northern  
16 high latitude ozone, and show that dynamical variations dominate interannual variability.  
17 [Hadjinicolaou \*et al.\* \(2002\)](#) find similar results using a long run of the same model, driven by  
18 ECMWF analyses.

19 In the Northern Hemisphere, the anomalies in polar vortex strength are a part of what is  
20 now known as the Arctic Oscillation (AO) (Thompson and Wallace, 1998). The AO and its  
21 Southern-Hemispheric counterpart are also referred to as the annular modes. The annular  
22 structure of the AO in the stratosphere can be traced to the surface, with a strong link to the  
23 North Atlantic Oscillation (NAO) in the Northern Hemisphere (Thompson and Wallace, 1998).  
24 While there is some debate about the role of the stratosphere in forcing anomalies in the  
25 tropospheric component of the AO (*e.g.*, Perlwitz and Graf, 2001; Ambaum *et al.*, 2001), that is  
26 beyond the scope of this assessment of stratospheric ozone. This discussion focuses on the  
27 stratospheric component of the AO.

28 A high (low) AO index corresponds to a strong (weak) vortex and low (high) polar ozone  
29 column values (Thompson and Wallace, 2000; Hartmann *et al.*, 2000). Thompson *et al.* (2000)  
30 estimated that approximately 40% of recent apparent polar ozone loss in March could be  
31 explained by the tendency of the AO to remain positive in the springtime, which describes a

1 strong, cold and isolated polar vortex. However, on the basis of the observations, it cannot be  
2 determined whether the signal in ozone is caused by the AO anomaly, or whether the AO  
3 anomaly is a consequence of ozone depletion, or whether both are coherently forced by some  
4 other factor.

5 There is strong evidence that the AO signal originates near the subtropical stratopause and  
6 propagates poleward and downward through the mechanism of wave forcing (*e.g.*, Baldwin and  
7 Dunkerton 1999; Kuroda and Kodera 1999; Kodera *et al.* 2000; and Christiansen, 2001). Kodera  
8 and Kuroda (2000) show how the interannual variability of wave forcing can cause such  
9 anomalies to take different phases in different years.

10 Isolating causes of variability and the factors that drive trends is not straightforward. Apart  
11 from the link between the AO strength and the upward propagation of planetary waves, other  
12 mechanisms have been related to the polar vortex. Model simulations reveal that a substantial  
13 year-to-year variability in the stratospheric vortex (and hence the AO) can exist in the absence of  
14 variations in boundary conditions or other forcing mechanisms (*e.g.*, Yoden *et al.*, 1999;  
15 Hamilton, 1999). This variability, forced by internal dynamics of the atmosphere, means that  
16 many factors often invoked as causes of interannual variability in the real atmosphere may or  
17 may not be significant. Despite this, there is some evidence of coupling between the polar vortex  
18 and other atmospheric variations: the main relationships that have been studied are the quasi-  
19 biennial oscillation (QBO) of tropical winds, the 11-year variability of solar radiation, the phase  
20 of the El Niño-Southern Oscillation (ENSO), and major volcanic eruptions. While polar vortex  
21 composites grouped according to these mechanisms show apparent signals, several factors  
22 complicate their interpretation and robustness. The most severe complications are that the  
23 observational record covers only about four decades and that some of the forcing factors vary in  
24 unison. For instance, following Labitzke and van Loon (1997) and grouping northern mid-  
25 winter polar vortex structure according to the solar cycle (high or low) and the phase of the QBO  
26 (East or West) leads to twelve winters in the low/West category, with a strong polar vortex;  
27 however, five of these twelve winters coincide with ENSO cold events or volcanic eruptions,  
28 which have the same anomalies (see Figure 2.1-4). Determining robust relationships from  
29 observations on the basis of these overlapping factors and the internal variability is thus  
30 impossible.

1 Models have been used to address these questions. The SKYHI General Circulation model  
2 (GCM) with an artificially forced QBO reproduces observed QBO-related interannual variability  
3 in the Arctic vortex (stronger when the tropical winds are westerly, weaker when easterly) and  
4 variations in wintertime stationary wave patterns (Hamilton, 1998). Shindell *et al.* (1999b)  
5 found that the QBO significantly modulated the strength and propagation of planetary wave  
6 energy in the troposphere in the Goddard Institute for Space Studies (GISS) model, leading to  
7 warmer (3- to 5-K) zonal-mean temperatures at high southern latitudes for late winter and early  
8 spring during the QBO easterly phase. Niwano and Takahashi (1998) studied the influence of  
9 the QBO on the Northern Hemisphere winter circulation; their model reproduced the relationship  
10 between the polar vortex strength and the QBO phase and a related North Atlantic Oscillation  
11 (NAO) pattern in the troposphere. These and earlier studies have worked on the premise that the  
12 lower stratospheric winds impact planetary wave propagation, while more recent work (Gray *et*  
13 *al.*, 2001) has shown that the polar vortex anomalies are more strongly related to winds near the  
14 tropical stratopause (which are indirectly affected by the QBO).

15 There are two important factors in isolating the impacts of solar forcing on the circulation  
16 and climate. First, stratospheric ozone changes modulate the response of the temperature to the  
17 changes in solar irradiance (Haigh, 1994). However, studies of solar impacts on ozone, mostly  
18 using two-dimensional models, have been plagued by an inability to reproduce the solar-ozone  
19 relationship detected in observations (*e.g.*, Brasseur, 1993; Hood and Zhou 1999). Second,  
20 inclusion of the correct spectral dependence of solar irradiance variations in the atmospheric  
21 heating rate calculations is essential to capture the correct vertical structure of heating rates  
22 (Haigh, 1999; Shindell *et al.*, 1999a; Larkin *et al.*, 2000). However, even incorporating these  
23 feedbacks, climate model studies generally remain inconclusive about the role of solar-induced  
24 perturbations in the variability of the Arctic polar vortex.

25 Volcanic aerosol loading impacts polar ozone by perturbing stratospheric chemistry and  
26 transport. Chemical perturbations from heterogeneous reactions on aerosols are discussed in  
27 Section 2.2. Here, circulation perturbations arising from anomalous radiative forcing is  
28 discussed. Increased volcanic aerosol loading of the tropical lower stratosphere leads to a  
29 warmer tropical lower stratosphere some months after a volcanic eruption (*e.g.*, Robock, 2000),  
30 which is discussed in more detail in Chapter 4. The polar response to this tropical warming has a  
31 northern polar vortex remaining anomalously cool in the winter following the eruption (*e.g.*,

1 Kodera, 1994), as shown in Figure 2.1-4. Figure 2.1-4 shows that the three volcanic eruptions  
2 affected winters with ENSO warm events and that they ‘reverse’ the ENSO anomalies, leading to  
3 anomalously strong, cold polar vortices (van Loon and Labitzke, 1987; Labitzke and van Loon,  
4 1989), thereby increasing the likelihood of negative polar ozone anomalies. Based on only three  
5 events (and because of the factors discussed above), these results must be interpreted with  
6 caution. This relationship has also been isolated in models (Kirchner *et al.*, 1999; Ramachandran  
7 *et al.* 2000).

8  
9 ***The importance of synoptic and mesoscale waves for PSC formation [2.1.1.3]***

10  
11 While temperatures low enough for PSC formation occur on the large scales (*e.g.*, Pawson  
12 and Naujokat 1997, 1999), the likelihood of their occurrence is enhanced by the temperature  
13 perturbations induced by medium-scale waves (*e.g.*, Grewe and Dameris, 1997; Sato *et al.*, 2000;  
14 Teitelbaum *et al.*, 2001), as well as by topographic and inertial gravity waves (*e.g.*, Dörnbrack *et*  
15 *al.*, 2001, 2002). The temperature perturbations induced by these waves can cause sufficient  
16 additional cooling for PSCs to form in locations where the large-scale flow would not support  
17 them. This is particularly important on the vortex edge, where the processed air can be  
18 irreversibly transported into the middle latitudes (in the presence of breaking waves) and where  
19 the air masses are more likely to be illuminated, enhancing the potential for ozone depletion.

20 Ozone mini-holes occur due to synoptic-scale, reversible advection (*e.g.*, McKenna *et al.*,  
21 1989; Newman *et al.*, 1988), related to upper tropospheric anticyclonic structures. The high  
22 tropopause, coupled with ascending motion, leads to extremely low total ozone values with  
23 lifetimes of up to several days. Steinbrecht *et al.* (1998) show that correlations in tropopause  
24 height correlate with ozone concentration changes in the region up to 23 km, illustrating the  
25 depth of the disturbances. However, the low ozone values themselves are short-lived features  
26 that are unrelated to chemical loss. The dynamical forcing which causes ozone mini-holes also  
27 causes adiabatic cooling, which can lead to synoptic-scale temperature perturbations of sufficient  
28 magnitude to allow PSC formation (*e.g.*, McKenna *et al.*, 1989; Grewe and Dameris, 1997). The  
29 importance of baroclinic disturbances in producing PSC formation near the polar vortex edge has  
30 been discussed by Hood *et al.* (2001) and Teitelbaum *et al.* (2001). Orsolini and Limpasuvan  
31 (2001) showed how these disturbances are linked to the storm tracks, which vary in unison with

1 the AO. There is thus a flow-dependent nature to the likelihood of synoptic-scale PSC formation  
2 and to the likelihood that they contribute to ozone loss on the vortex edge region.

3 Just as baroclinic waves help PSC formation on the synoptic scales, mesoscale disturbances  
4 from gravity waves are also important. Volkert and Intes (1992) demonstrated PSC formation in  
5 wave crests over Scandinavia in their model of topographically forced gravity waves. The  
6 importance of gravity-wave PSCs was also demonstrated by Deshler *et al.* (1994) and Meilinger  
7 *et al.* (1995). High-resolution radiosonde data have recently provided much needed information  
8 on stratospheric gravity wave morphologies in and around the Antarctic (Pfenniger *et al.*, 1999;  
9 Zink and Vincent, 2001) and Arctic (Whiteway and Duck, 1999; Yoshiki and Sato, 2000).  
10 While the microphysical effects of a background spectrum of gravity waves are smaller than first  
11 thought (Bacmeister *et al.*, 1999), it is now accepted that mesoscale temperature decreases due to  
12 large-amplitude gravity waves, particularly mountain waves, can lead to temperatures low  
13 enough for PSC formation (Carslaw *et al.*, 1998b, 1999; Schulz *et al.*, 2001), and lead to  
14 structure inside larger-scale PSCs (Toon *et al.*, 2000). The detailed microphysics associated with  
15 PSCs is discussed in Section 2.2.1 of this chapter.

16 Important advances have been made in our ability to model lower stratospheric gravity  
17 waves and, especially, to resolve such waves in global meteorological analyses. Dörnbrack *et al.*  
18 (2001) demonstrated that the high-resolution ECMWF operational meteorological analyses  
19 capture gravity wave structures over Scandinavia. This represents an important advance for  
20 applying the analyses to our understanding of the gravity-wave morphology and its importance  
21 for PSC formation. An additional advance of some importance was made by Dörnbrack *et al.*  
22 (2002), who detected inertia-gravity waves over Scandinavia in the ECMWF analyses and *in situ*  
23 data, noting their role for PSC formation. The isolation of gravity waves in such operational  
24 analyses points to their potential utility in mountain wave forecasting and analysis, meaning that  
25 the off-line models that have been used for such studies could eventually become unnecessary.

26 Another important role played by gravity waves (from all sources) is that they transport  
27 momentum into the middle atmosphere; as these waves break, they deposit momentum to the  
28 mean flow, constituting an important driving mechanism for the Brewer-Dobson circulation.  
29 The importance of these waves for driving the flow and reducing biases in global models is  
30 discussed in more detail in Section 5.2.1 below.



1 **2.1.3 POLAR TRANSPORT AND MIXING**

2  
3 This section discusses in detail the physical processes that lead to the redistribution of trace  
4 gases in the polar regions. Trace gas distributions are determined by the balance between the  
5 slow mean meridional circulation and the more rapid, quasi-isentropic mixing (*e.g.*, Holton  
6 1986); the following discussion examines these components of transport in and around the polar  
7 vortex and the exchange across the vortex edge.

8 [Manney \*et al.\* \(2002\)](#) examines impacts of using different meteorological analyses, which  
9 impact the amount of exchange between middle latitudes and the vortex. Despite the  
10 uncertainties, the consensus is that the vortex remains quite isolated in wintertime. Vertical  
11 transport (discussed in Section 2.1.3.1) leads to descent in and around the vortices, while mixing  
12 (Section 2.1.3.2) redistributes ozone and trace gases on isentropic levels; there is some exchange  
13 across the vortex edge, associated with large-scale mixing events.

14  
15 ***Descent in the polar vortex [2.1.3.1]***

16  
17 Descent inside the polar vortex builds up (or maintains) lower stratospheric ozone over the  
18 winter, making it an important process to understand. The descending branch of the Brewer-  
19 Dobson circulation is driven by wave forcing of the flow (see Section 2.1.1). Descent rates can  
20 be determined in several manners: (i) ‘directly’ from the vertical velocities produced in routine  
21 meteorological analysis systems, such as the UKMO (Swinbank and O’Neill, 1994) and the  
22 DAO (Rood *et al.*, 1997), (ii) based on the cross-isentropic transport determined by diabatic  
23 heating rates, and (iii) using measurements of long-lived trace gases with well-understood  
24 vertical gradients. The various estimates are in reasonably good agreement, showing stronger  
25 descent in the upper stratosphere than in the lower stratosphere and unmixed descent from the  
26 upper to the lower stratosphere. The strongest descent occurs in the Antarctic vortex, but is more  
27 variable in the Arctic, where it can occur on the vortex edge when the temperature is higher there  
28 (*e.g.*, Manney *et al.*, 1999).

29 Schoeberl *et al.* (1995) used HALOE CH<sub>4</sub> data to estimate the descent rate as 1.8  
30 km/month inside the Antarctic vortex in February-October 1992. Descent rates over Antarctica  
31 were deduced from ISAMS CO data for April to July 1992 by Allen *et al.* (2000) and from  
32 POAM-III H<sub>2</sub>O data by Nedoluha *et al.* (2000). Abrams *et al.* (1996) demonstrated strong

1 descent in the upper stratosphere (3.2 km/month at 40 km) with weak descent in the lower  
2 stratosphere (0.8 km/month at 20 km) based upon the Atmospheric Trace Molecule Spectroscopy  
3 (ATMOS) data from November 1994. Kawamoto and Shiotani (2000) also used HALOE data  
4 and United Kingdom Meteorological Office (UKMO) meteorological analyses to investigate the  
5 interannual variability of the descent rate, using the for the February-October (winter) averages  
6 in 1992-1997 HALOE CH<sub>4</sub> data. They find that the descent varies between 1.2-1.8 km/month  
7 using the 0.6 ppmv CH<sub>4</sub> contour inside the polar vortex and is consistent with the wave driving  
8 determined from the UKMO analyses To summarize, the various estimates of Antarctic descent  
9 rates give reasonably consistent results, given that they are presented for different levels, seasons  
10 and years.

11  
12 ***The vortex core [2.1.3.2]***

13  
14 The degree of mixing within the vortex core has come under scrutiny because of  
15 assumptions about representing the bulk behavior of the vortex with irregular temporal and  
16 spatial sampling. If the core is well mixed, then measurements anywhere within the vortex will  
17 suffice to characterize its behavior. If the core is not well mixed, then more frequent sampling at  
18 separated locations is necessary to do this. Schoeberl *et al.* (1990) assumed that the vortex was  
19 relatively well mixed in assessing ozone loss using ER-2 data from the Airborne Arctic  
20 Stratospheric Expedition (AASE)-I mission during the Arctic winter of 1988-1989. Richard *et*  
21 *al.* (2001) used ER-2 data from the SOLVE-THESEO 2000 campaign to show that tracer-tracer  
22 relationships inside the vortex during the Arctic winter of 1999-2000 are distinct and compact,  
23 suggesting a rapid mixing in the Arctic. While current evidence suggests that the Arctic vortex  
24 is relatively well mixed in the absence of intrusions of air from the vortex edge, Lee *et al.* (2001)  
25 present evidence that the Antarctic vortex is separated into two regions: a strongly mixed vortex  
26 core and a weakly mixed ring of air extending to the vortex boundary. This may arise from the  
27 fundamentally different meteorology of the two hemispheres.

28  
29 ***Transport across the vortex edge and mixing [2.1.3.3]***

30  
31 The balance of mass and trace gases in and around the polar vortex is determined by the  
32 downward transport and exchange across the vortex edge. Any vertical gradient in the vortex-  
33 averaged mass flux will be compensated for by flow across the vortex edge. The discussion

1 below will separate the transport across the vortex edge in winter from transport occurring as the  
2 polar vortex breaks down.

3 Planetary wave breaking can be responsible for vortex shrinking as well as sharpening of  
4 the vortex edge (*e.g.*, Thuburn and Lagneau, 1999). A number of studies have shown  
5 considerable variability in the width of the Antarctic vortex edge when it is perturbed  
6 (Teitelbaum *et al.*, 1999; Perez *et al.*, 2000), which result in non-linear irreversible transport and  
7 mixing of vortex air into mid-latitudes (Teitelbaum *et al.*, 1999). Lidar observations at Dumont  
8 d'Urville (66.4°S, 140°W) allow sampling at and around the moving vortex edge (Godin *et al.*  
9 2001); observations of Pinatubo aerosols, made during October and November 1992, show the  
10 sharpness of the vortex edge and low mixing between the inner vortex and the outside air above  
11 400 K.

12 The first obstacle to determining the cross-vortex flow is to unambiguously define the  
13 vortex edge. Chen (1994) defined it as the potential vorticity (PV) contour which has the  
14 smallest lengthening rate; he found a vertical dependence to the transport across the edge, with  
15 more transport out of the vortex at potential temperatures lower than 400 K than at higher levels.  
16 Tuck *et al.* (1995) reached similar conclusions using ER-2 data, showing also that the vortex  
17 edge region can be quite wide. This viewpoint of the polar vortex as a reasonably well-isolated  
18 entity is now generally accepted, but the amount of 'leakage' from the vortex (as a function of  
19 altitude) is not yet well understood. Different proposed definitions of the vortex edge include the  
20 wind maximum and the strongest gradients in PV (*e.g.*, Bowman, 1996; Nash *et al.*, 1996). The  
21 uncertainty in defining the vortex edge remains, so there is no unambiguous estimate of the  
22 vertical structure of cross-vortex transport. Mechanisms for the transport are at least  
23 qualitatively understood and are discussed here.

24 Recent results continue to sustain our understanding of the vortex edge impermeability  
25 (Chen, 1994) and of the polar vortex as a quasi-isolated containment vessel. Norton and  
26 Chipperfield (1995) and Jones and MacKenzie (1995) had argued that ozone-depleted air from  
27 the polar vortices makes only a small contribution to middle latitude ozone loss. High-resolution,  
28 single-level models with weak dissipation (*e.g.*, Jukes and McIntyre 1987; Mo *et al.*, 1998;  
29 Thuburn and Lagneau, 1999; Sobel and Plumb, 1999), have further confirmed that the export of  
30 air from the polar vortex is constrained. Vincent and Tranchant (1999) also found little mixing  
31 across the vortex edge at 520 K in the Antarctic. Li *et al.* (2002) used a CTM driven by analyzed

1 winds to show that less air is indeed exported from the Antarctic polar vortex to middle latitudes  
2 than descends into the troposphere.

3 Laminae and filaments could be an important mechanism in the mixing of air across the  
4 quasi-impermeable vortex edge. Such structures are common in winter and spring. As pointed  
5 out in WMO (1999) the filaments/laminae, *i.e.*, material sheets that tilt outward with increasing  
6 height (Schoeberl and Newman, 1995; Newman and Schoeberl, 1995) with initial horizontal  
7 scales of a few thousand kilometers, can lead to irreversible mixing on the timescale of 20-25  
8 days over which they decay. Laminae have been detected in a variety of data types, including in-  
9 situ aircraft observations (Newman *et al.*, 1996); sondes and lidar (Bird *et al.*, 1997; Orsolini *et*  
10 *al.*, 1997; Teitelbaum *et al.*, 2000); and satellites (Appenzeller and Holton, 1997; Manney *et al.*,  
11 1998, 2000). They have been successfully modeled (*e.g.*, Orsolini *et al.*, 1997). Waugh and  
12 Dritschel (1999) analyzed the relationship between Rossby wave breaking and vortex structure.  
13 These studies show that filamentation can lead to vortex air being peeled off and eventually  
14 mixed irreversibly into the surf zone, although some air may re-join the polar vortex.  
15 Furthermore Manney *et al.* (1998, 2001) have also shown that lamination processes within the  
16 polar vortex did not result from exchange across the vortex edge but rather from transport  
17 variations within the vortex.

18 Hence there is thus a need to assess the behavior of laminae and magnitude of their  
19 contribution to the total exchange between the vortex and midlatitudes. Appenzeller and Holton  
20 (1997) attempted to diagnose the production of tracer laminae using satellite data and  
21 meteorological analyses, as a first step in determining their contribution to transport.  
22 Nevertheless there arose some limitations regarding the use of such a diagnostic (Kettleborough  
23 and Holton, 1999), because (a) it does not include small vertical scales that are relevant in  
24 defining tracer lamination and (b) there can be a reversible contributions. In other words the  
25 proposed diagnostic could overestimate the transport and mixing.

26 A principal challenge to modeling the polar ozone in the Northern Hemisphere and the  
27 effects of polar processes on middle latitudes is to ensure that the models produce the appropriate  
28 balance among the many processes that contribute directly or indirectly to the polar lower  
29 stratospheric ozone tendency. Both transport and photochemical processes contribute. The year-  
30 to-year variability in meteorological fields is significant, and the northern vortex may be cold  
31 and strong, as the winters 1996-1997 and 1999-2000, or warmer and more disturbed, as the

1 winter 1997-1998 (Sinnhuber *et al.*, 2000; Guirlet *et al.*, 2000). Simulations have focused on  
2 replicating observations for ozone and other trace gases, and quantifying model sensitivity to  
3 various processes (Chipperfield and Pyle, 1998). Such studies point out the importance of  
4 developing a better understanding of the physical processes leading to denitrification, so that  
5 model parameterizations respond appropriately to changes in temperature, water vapor, or nitric  
6 acid that may result from climate change.

7 Millard *et al.* (2001) utilized advanced diagnostics developed by (Lee *et al.*, 2001) to  
8 quantify the importance of polar processes to ozone change at middle latitudes. Both the  
9 chemical processes that contribute to polar ozone loss and the transport process that impact  
10 mixing between high latitudes and middle latitudes vary depending on the meteorology of a  
11 particular year. CTMs have been utilized to address questions concerning specific winters. For  
12 example, Lefèvre *et al.* (1998) utilized a CTM forced by winds from ECMWF to show that both  
13 transport and photochemical processes contribute to the record low ozone observed by TOMS  
14 during northern spring 1997 (Figure 1.2-2). Like the studies of Guirlet *et al.* (2000), results are  
15 broadly consistent with observations. However, as shown by Douglass *et al.* (2001), the model  
16 results separating photochemical and transport contributions are sensitive to the vertical velocity  
17 and to the ozone vertical gradient.

18 The breakdown of the polar vortex, whether by a major midwinter warming or in the final  
19 warming, allows vortex air to be mixed relatively easily with that from middle latitudes.  
20 Atkinson and Plumb (1997) showed that as the Antarctic vortex breaks down, a substantial  
21 amount of ozone-depleted air is transported to middle latitudes. Once there, it can effectively  
22 mix with the ambient air masses. Effective diffusivity has been used as a diagnostic for mixing  
23 by Allen and Nakamura (2001), who show increases in mixing lengths as the polar vortices break  
24 up.

## 25 **2.2 Polar Stratospheric Clouds**

26

27 PSCs play two important roles in polar ozone chemistry. First, the particles support  
28 chemical reactions leading to active chlorine formation, which can catalytically destroy ozone.  
29 Second, nitric acid removal from the gas phase can increase ozone loss by perturbing the reactive  
30 chlorine and nitrogen chemical cycles in late winter and early spring.

1 PSCs are divided into two main categories. Type I PSC particles contain nitric acid, either  
2 in the form of liquid ternary solutions with water and sulfuric acid or as solid hydrates of nitric  
3 acid. Type II PSCs are made of ice particles. Knowledge of PSC particle sizes, number  
4 concentrations, composition, phase and evolution is central to efforts to develop prognostic  
5 models of how PSCs affect the chemistry of the polar stratosphere. *In situ* observations of PSCs  
6 from balloons or aircraft are often used to obtain detailed information on cloud particle size  
7 distribution and composition. Remote sensing platforms, such as lidar and satellites, provide  
8 complementary information on phase and large-scale time evolution of PSCs, respectively. We  
9 now briefly review recent advances in our understanding of PSC properties and their effect on  
10 denitrification and dehydration.

## 11 **2.2.1 OBSERVATIONS OF PSC PHYSICAL PROPERTIES AND THEIR INTERPRETATION**

### 12 13 *In situ*

14  
15 The last assessment (WMO, 1999) described considerable improvements in our  
16 understanding of liquid PSCs, but highlighted the outstanding uncertainties in the properties of  
17 solid particles. Solid nitric acid-containing PSC particles are important because, in contrast to  
18 the sub-micron liquid aerosol, they may be present with sufficiently low number concentrations  
19 ( $< 10^{-2} \text{ cm}^{-3}$ ) to allow a few particles to grow to large sizes, leading to sedimentation and  
20 denitrification. Our understanding of the range of solid particle number concentrations and sizes  
21 that can form in the polar stratosphere has improved since the last assessment as a result of new  
22 *in situ* observations.

23 Observations in the Arctic stratosphere at altitudes from 16 to 20 km in January to March  
24 2000 detected a population of large nitric acid particles with very low number concentrations  
25 (Fahey *et al.*, 2001; Northway *et al.*, 2002a), see Figure 2.2-1. Large particles, with similar sizes  
26 and number concentrations as those observed by Fahey *et al.* (2001), were detected by the  
27 Multiangle Aerosol Spectrometer Probe (MASP) (Carlaw *et al.*, 2002). These measurements  
28 (Fahey *et al.*, 2001; Northway *et al.*, 2002a) are very important because they provide conclusive  
29 evidence that such large particles are composed principally of nitric acid (probably present as  
30 nitric acid hydrates).

31 Observations of large nitric acid particles raises several questions. The most obvious  
32 question is how these particles compare with previous observations in the Arctic and Antarctic.

1 Balloon-borne instruments such as the Optical Particle Counter (OPC) (*e.g.*, Deshler *et al.*, 1991,  
2 1994; Deshler and Oltmans, 1998; see also WMO, 1999 and references therein), which has flown  
3 in many previous Arctic winters, is capable of detecting particles up to 20  $\mu\text{m}$  in diameter with  
4 number concentrations greater than about  $6 \times 10^{-3} \text{ cm}^{-3}$ . However, this is higher than average  
5 particle concentrations ( $\sim 10^{-4} \text{ cm}^{-3}$ ) measured by Fahey *et al.* (2001). Further, the forward  
6 scattering spectrometer probe (FSSP) instrument, which measured PSC size distributions during  
7 the 1989-1990 Arctic winter (Dye *et al.*, 1992), could not have detected PSCs with number  
8 concentrations below about  $10^{-3} \text{ cm}^{-3}$ . Thus, if large nitric acid particles were present in  
9 previous Arctic winters, at number concentrations near and below  $10^{-4} \text{ cm}^{-3}$ , then the available  
10 *in situ* instruments at the time would not have been able to detect them (Table 2.2.1). However,  
11 it is interesting to note that in earlier Antarctic measurements the OPC instrument, which  
12 operated at a different inlet flow rate, detected large PSC particles with number concentrations as  
13 low as  $10^{-4} \text{ cm}^{-3}$  (Table 2.2.1). Thus populations of very few ( $\sim 10^{-4} \text{ cm}^{-3}$ ) large PSC particles  
14 have been observed previously, but it is only through recent measurements (Fahey *et al.*, 2001)  
15 that we have learned such large particles are indeed enriched in nitric acid.

16  
17

18 **Table 2.2.1. Observations of solid PSC particle size and number density**

19  
20  
21  
22  
23  
24  
25  
26  
27  
28  
29  
30  
31

Number density ( $\text{cm}^{-3}$ )	Average Diameter ( $\mu\text{m}$ )	Atmospheric References	Location
10 <sup>-1</sup> -1	1-2	Voigt <i>et al.</i> , 2000a, b	Arctic
10 <sup>-3</sup> -10 <sup>-2</sup>	1-4	Dye <i>et al.</i> , 1992*	Arctic
10 <sup>-4</sup> -10 <sup>-2</sup>	4-10	Hofmann and Deshler, 1991*	Antarctic
10 <sup>-5</sup> -10 <sup>-3</sup>	10-20	Fahey <i>et al.</i> , 2001# Northway <i>et al.</i> , 2002a#	Arctic

32 \*Note that these measurements are mode diameters of a log normal distribution.

33 #These observations on the average show PSC number densities of about  $2 \times 10^{-4} \text{ cm}^{-3}$   
34 with a mode diameter centered near 14  $\mu\text{m}$ , assuming a nitric acid trihydrate (NAT) composition.  
35  
36

1 The second question is whether these large particles present at very low number  
2 concentrations can denitrify the stratosphere. Simple calculations presented by Fahey *et al.*  
3 (2001) demonstrate that large nitric acid particles can grow to their optimal observed sizes in  
4 about 5 to 8 days, implying that they must have nucleated several kilometers above the aircraft  
5 flight altitude. Instantaneous downward flux calculations of nitric acid contained in such large  
6 particles indicate that they were capable of causing significant denitrification (Fahey *et al.*, 2001,  
7 [Northway \*et al.\*, 2002b](#)). 3-D model simulations of particle growth further show that the  
8 observed PSC sizes are consistent with growing NAT and/or nitric acid dihydrate (NAD)  
9 particles ([Carslaw \*et al.\*, 2002](#)). However, it is important to note that PSCs with size  
10 distributions different to those measured in winter 1999/2000 have been observed in previous  
11 winters in both hemispheres (see Table 2.2.1). Model simulations by [Jensen \*et al.\* \(2002\)](#) show  
12 that previously observed PSC particle size distributions (Dye *et al.*, 1992; Hofmann and Deshler,  
13 1991), with number concentrations in the range of  $10^{-2}$  to  $10^{-3}$   $\text{cm}^{-3}$ , are also capable of  
14 efficiently denitrifying the polar stratosphere.

15 A third question is how these large nitric particles form in the polar stratosphere. Both  
16 homogeneous (Tabazadeh *et al.*, 2001) and heterogeneous (Tolbert and Toon, 2001; [Drdla \*et al.\*,  
17 2002](#)) freezing mechanisms have been suggested to account for the formation of large nitric acid  
18 particles. For such nucleation mechanisms to operate, the cooling caused by synoptic-scale  
19 uplift of air masses (Teitelbaum *et al.*, 2001; Spang *et al.*, 2001; Hendricks *et al.*, 2001; [Saitoh \*et al.\*,  
20 2002](#)) can provide favorable conditions for solid PSCs to form. Laboratory observations  
21 show that concentrated aqueous nitric acid aerosols can homogeneously crystallize into hydrates  
22 of nitric acid (Disselkamp *et al.*, 1996; Bertram *et al.*, 1998 a, b; Prenni *et al.*, 1998; Salcedo *et al.*,  
23 2001). The stratospheric particle system has also been studied using thin films, where gas  
24 phase  $\text{HNO}_3$  and  $\text{H}_2\text{O}$  are absorbed by cold aqueous sulfuric acid solutions (Iraci *et al.*, 1994,  
25 1995, 1998). The results of these thin film experiments show that  $\text{HNO}_3$  uptake in sulfuric acid  
26 can cause freezing of nitric acid hydrates in solution. Tabazadeh *et al.* (2001) have recently  
27 extrapolated the laboratory homogeneous freezing rates of Salcedo *et al.* (2001) and obtained  
28 nucleation rates sufficient to produce large nitric acid particles in a microphysical model. Note  
29 that the nucleation rates extrapolated from Salcedo *et al.* (2001) are much higher than upper  
30 limits derived from earlier bulk freezing experiments with 1-milliliter samples, which used  
31 stratospheric temperatures and liquid phase compositions (Koop *et al.*, 1995; 1997). Modeling



1 studies (Drdla *et al.*, 2002) further show that heterogeneous freezing can also produce large  
2 particles if only a very small fraction ( $< 0.1\%$ ) of stratospheric aerosol particles contained an  
3 effective freezing nucleus, although it is not clear what the freezing nucleus should be (Biermann  
4 *et al.*, 1996). In addition to direct homogeneous and heterogeneous freezing mechanisms, the  
5 large particles may also form by a gradual sedimentation from the base of ‘mother clouds’  
6 containing much higher number concentrations of small solid particles (Füglister *et al.*, 2001;  
7 Dhaniyala *et al.*, 2001), such as those generated by lee wave clouds (Carslaw *et al.*, 1998a).

8 The freezing mechanisms described above are all capable of producing low number  
9 concentrations of sedimenting nitric acid particles. However, model simulations do strongly  
10 suggest that the large nitric particles, observed during the winter of 1999-2000 winter, were  
11 unlikely to have nucleated in synoptic-scale ice clouds, which were not sufficiently prevalent in  
12 the days preceding the observations (Carslaw *et al.*, 2002, Drdla *et al.*, 2002). Further analysis of  
13 satellite data in the Antarctic also seems to suggest that large nitric acid particles formed in the  
14 winter of 1992 independent of synoptic-scale ice clouds (Tabazadeh *et al.*, 2000).

15 A final question is whether these large particles observed *in situ* can also be detected by  
16 lidar. Aircraft lidar observations in January to March 2000 detected regions of enhanced aerosol  
17 backscatter in regions where large nitric acid particles were detected (Flentje *et al.*, 2000).  
18 However, Flentje *et al.* (2000) inferred an approximate size for the particles based on the  
19 sedimentation speed of the particle layer, rather than directly from the lidar signal. Their derived  
20 particle sizes are in reasonable agreement with *in situ* observations (Fahey *et al.*, 2001).

21 Overall, the assessment of both the Arctic and Antarctic studies, on observed and inferred  
22 PSC particle sizes, indicates that large nitric acid particles cannot initially nucleate on synoptic-  
23 scale ice clouds. However, the formation mechanism of large nitric acid particles still remains  
24 uncertain. Thus more laboratory and field studies are needed the better to test which of the  
25 above mechanisms is most likely to dominate the rate of large nitric acid particle production in  
26 the polar stratosphere.

27  
28 **Remote**

29  
30 Lidar observations are useful for constraining PSC particle sizes. Depolarization  
31 measurements by lidar can also provide strong evidence for the presence of solid PSC particles.  
32 As indicated above, only large solid PSC particles can cause denitrification, and lidar

1 observations provide valuable information on the horizontal and vertical extents of solid PSC  
2 particle distributions in the stratosphere.

3 Lidar studies provide new estimates of the occurrence of solid PSC particles, which is an  
4 important parameter for constraining microphysical models. Toon *et al.* (2000) have re-analyzed  
5 lidar observations from all DC 8 flights during the 1989-1990 Arctic winter and find that large  
6 solid PSC particles are more common in the Arctic stratosphere than the smaller liquid PSC  
7 particles (type 1b). From 3 years of lidar observations from Ny Ålesund (79°N), Biele *et al.*  
8 (2001) have shown that at least 50% of PSCs contained solid particles, with some of these clouds  
9 being of type 1b, normally attributed to pure liquid clouds. Several studies have also derived  
10 new estimates of solid particle number concentrations. Gobbi *et al.* (1998) have analyzed many  
11 Antarctic lidar vertical profiles and estimate that solid PSC particles comprised less than 1% of  
12 the available condensation nuclei (therefore, typically less than 0.1 particles cm<sup>-3</sup>). Toon *et al.*  
13 (2000) derived similar values for the 1989-90 winter Arctic stratosphere. Biele *et al.* (2001) and  
14 Tsias *et al.* (1999) estimate that many depolarizing clouds must typically contain fewer than  
15 about 0.005 - 0.01 cm<sup>-3</sup> solid particles and that such particles can rarely grow to their  
16 equilibrium sizes. In summary all the lidar studies discussed here suggest that large solid  
17 particles that can cause denitrification are widely distributed in both hemispheres.

18 Some clouds observed by lidar are consistent with high number densities of small solid  
19 nitric acid particles (typically >1 cm<sup>-3</sup> and < 2 μm diameter) (Tsias *et al.*, 1999; Toon *et al.*,  
20 2000; Hu *et al.*, 2002). These clouds are frequently associated with the outflow from mountain  
21 waves (*e.g.*, Hu *et al.*, 2002). Efficient NAT nucleation on numerous small ice particles formed  
22 in wave clouds could be an important mechanism for generating such a dense population of  
23 small solid PSC particles (Carslaw *et al.*, 1998a, 1999; Wirth *et al.*, 1999; Larsen *et al.*, 2002).  
24 Some studies suggest that small solid PSC particles generated by wave clouds may also play a  
25 central role in producing large nitric acid particles that lead to denitrification (see Section 2.2.1).

26 Satellite instruments are also capable of observing PSC particles. SAM II (McCormick *et*  
27 *al.*, 1981); CLAES (Mergenthaler *et al.*, 1997); POAM (Steele *et al.* 1999; Fromm *et al.*, 1999;  
28 Fromm *et al.*, 1997; Bevilacqua *et al.*, 2002) and ILAS (Kondo *et al.*, 2000, Irie *et al.*, 2001)  
29 instruments have taken many aerosol extinction vertical profiles of PSCs in the Arctic and  
30 Antarctic stratosphere over the last two decades. Several recent studies have paired up aerosol  
31 extinction measurements with water and nitric acid gas phase measurements onboard the same

1 (Tabazadeh *et al.*, 2000; Stone *et al.*, 2001; Nedoluha *et al.*, 2000; Dessler *et al.*, 1999) or  
2 different satellites (Santee *et al.*, 2002) to determine the scale and magnitude of denitrification  
3 and dehydration in both polar regions (see Sections 2.2.3 and 2.2.4).

## 4 **2.2.2 PARTICLE COMPOSITION**

### 5 6 *Inferred particle compositions*

7  
8 PSCs that exist at temperatures greater than the ice frost point have long been accepted to  
9 be composed of nitric acid and water, either in the form of a nitric acid hydrate or as supercooled  
10 solution droplets of nitric acid, sulfuric acid, and water (supercooled ternary solutions, STS).  
11 Numerous attempts have been made to infer the composition of nitric acid-containing PSCs by  
12 comparing particle volumes (either measured directly or derived from satellite extinction) and/or  
13 gas phase nitric acid concentrations with equilibrium model calculations assuming various  
14 particle compositions (WMO, 1999; Hopfner *et al.*, 1998; Steele *et al.*, 1999; Santee *et al.*, 2002;  
15 Saitoh *et al.*, 2002; Strawa *et al.*, 2002). These studies have provided strong support for the  
16 existence of STS droplets, but confirmation of the presence of different nitric acid hydrates has  
17 been more difficult to establish (WMO, 1999). This difficulty may be due to the fact that nitric  
18 acid hydrate particles, which can be considerably larger than STS droplets, are often not in  
19 thermodynamic equilibrium (*e.g.*, Tsias *et al.*, 1999; Biele *et al.*, 2001).

### 20 21 *Direct determinations of particle composition*

22  
23 New *in situ* observations using an aerosol mass spectrometer have measured PSC particle  
24 composition (Schreiner *et al.*, 1999, 2002; Voigt *et al.*, 2000a, b; Larsen *et al.*, 2000, 2002). The  
25 observed nitric acid to water mole ratio using an aerosol mass spectrometer in a mountain-  
26 induced gravity wave cloud over Scandinavia (Voigt *et al.*, 2000b) shows close agreement with  
27 an STS droplet composition predicted by a model. The same aerosol mass spectrometer flown in  
28 January 2000 detected NAT particles, identified by a H<sub>2</sub>O to HNO<sub>3</sub> mole ratio of 3:1 and  
29 confirmed to be solid particles from collocated backscatter measurements (Voigt *et al.*, 2000a;  
30 Larsen *et al.*, 2000); see Figure 2.2-2. These direct observations of particle composition in PSCs  
31 are important because they confirm that the thermodynamic models used to predict liquid aerosol  
32 compositions (*e.g.*, Carslaw *et al.*, 1997a) are reliable, and that NAT, long predicted to exist in  
33 the stratosphere (Hanson and Mauersberger, 1988), actually does exist there.

### 1 2.2.3 DENITRIFICATION

#### 2 3 *Observations of denitrification*

4  
5 *In situ* Arctic observations from the ER-2 aircraft in January to March 2000 detected the  
6 most severe and extensive denitrification observed in the Arctic stratosphere (Popp *et al.*, 2001),  
7 see Figure 2.2-3. Average removal of as much as 60% of NO<sub>y</sub> was observed throughout the core  
8 of the vortex near 20 km (Figure Popp). Waibel *et al.* (1999) have also analyzed balloon-borne  
9 observations of denitrification in 1995. These observations reveal an approximate 50%  
10 reduction in total reactive nitrogen (NO<sub>y</sub>) at 20 km. Using tracer measurements to eliminate  
11 deficits due to mixing (see Section 3), Waibel *et al.* (1999) concluded that at least 82% of the  
12 observed NO<sub>y</sub> loss at 20 km was due to denitrification. Sugita *et al.* (1998) and Hintsa *et al.*  
13 (1998) have also observed similar levels of Arctic denitrification near 20 km in 1995 and 1996  
14 winters, respectively. Together, these observations show that some Arctic air parcels were  
15 severely denitrified (> 50%) near 20 km in several cold winters.

16 Figure 2.2-4 shows the time evolution of HNO<sub>3</sub> in both hemispheres for a number of  
17 winters on three potential temperature surfaces, based on MLS observations. Large permanent  
18 depletions (> 80%) in HNO<sub>3</sub> vapor amounts occur only in the Southern Hemisphere (Santee *et al.*,  
19 1999), but much smaller irreversible depletions (~ 20%) have also been observed in cold  
20 Arctic air parcels (Dessler *et al.*, 1999; Santee *et al.*, 2000, 2002). However, large permanent  
21 depletions in HNO<sub>3</sub> concentrations (> 40%) have been observed in cold Arctic winters by  
22 satellite instruments with finer vertical resolution than MLS (~6 km vertical resolution), such as  
23 the ILAS instrument, which has a 1-2 km vertical resolution (Kondo *et al.*, 2000; Irie *et al.*,  
24 2002). Thus, extensive denitrification does occur in both hemispheres based on both *in situ* and  
25 remote sensing observations. However, severe denitrification in the Arctic must be narrow in  
26 depth because if the denitrified layers were deeper than 6 km, then MLS would have been able to  
27 detect this irreversible loss in gas phase nitric acid (Tabazadeh *et al.*, 2001). Individual nitric  
28 acid vertical profiles from the ILAS instrument (Kondo *et al.*, 2000; Irie *et al.*, 2002) during the  
29 winter of 1996-1997 further show that the vertical range of denitrification in the Arctic is  
30 typically ~2- to 3-km deep (from about 18 to 21 km) with immediate nitrification occurring  
31 below this altitude range.

1 Tabazadeh *et al.* (2000) have shown that denitrification over a broad altitude range (> 10  
2 km in depth) occurs rapidly in the Antarctic when the duration of an average PSC event is about  
3 2 weeks (defined to be the time spent by an isentropic air parcel below 195 K at 450 K potential  
4 temperature). Tabazadeh *et al.* (2000) suggest that deep extensive denitrification currently  
5 occurs only in the Antarctic because average Arctic PSC events last nearly half as long as those  
6 in the Antarctic, during the mid to late June time period, when denitrification occurs rapidly in  
7 the south pole (see the MLS plot). The short persistence of PSC events in the NH limits the  
8 extent of severe denitrification to only a few kilometers, as observed in many past cold Arctic  
9 winters (Popp *et al.*, 2001; Sugita *et al.*, 1998; Hints, *et al.*, 1998; Kondo *et al.*, 2000; Irie *et al.*,  
10 2001, 2002). In Section 3.3 the effect of denitrification depth on ozone loss is assessed for both  
11 hemispheres.

12

### 13 ***Model simulations of denitrification***

14

15 Improvements in our understanding of PSC particle sizes and number concentrations  
16 (Section 2.2.1) now allow for more sophisticated treatments of denitrification in models. Current  
17 3-D chemical transport models include a highly simplified representation of denitrification that is  
18 now recognized to be incorrect. These models assume that nitric acid is carried downwards on  
19 sedimenting ice particles wherever temperatures are lower than the ice frost point (Chipperfield  
20 *et al.*, 1993; Considine *et al.*, 2000). Removal of nitric acid on sedimenting ice particles is  
21 clearly not operating in the Arctic because models, using this assumption, have been unable to  
22 produce any denitrification by this mechanism (Chipperfield and Pyle; 1998; Davies *et al.*,  
23 2002).

24 Drdla *et al.* (2002) have used a coupled microphysical-chemistry trajectory model to show  
25 that synoptic-scale ice clouds could not have caused the massive denitrification observed during  
26 the 1999-2000 winter. They concluded that the large nitric acid particles that caused  
27 denitrification were not nucleated on ice particles.

28 Jensen *et al.* (2002) have used a 1-D version of the CARMA microphysics cloud model to  
29 show that solid nitric acid solid number densities in the range of  $10^{-2}$  to  $10^{-3}$   $\text{cm}^{-3}$  are the most  
30 efficient in causing rapid denitrification. The CARMA cloud model has also been used to show  
31 (see Figure 4 in Tabazadeh *et al.*, 2001) that the vertical range over which denitrification occurs  
32 is normally quite deep in the Antarctic (> 10 km) but limited in the Arctic, in general agreement

1 with many observations of denitrification in both hemisphere (*i.e.*, Santee *et al.*, 1999; Popp *et*  
2 *al.*, 2001; Sugita *et al.*, 1998; Hintsa, *et al.*, 1998; Kondo *et al.*, 2000; Irie *et al.*, 2001, 2002).  
3 The Arctic denitrified layers are shallow in depth mainly because the stratosphere, even in cold  
4 winters, is too warm below about 17 km for nitric acid hydrate particles to exist.

5 Waibel *et al.* (1999) simulated denitrification by assuming that ice acted as the nucleus for  
6 NAT formation. Most of the denitrification calculated in the model was caused primarily by  
7 sedimentation of NAT particles, with a fixed number concentration of  $5 \times 10^{-3} \text{ cm}^{-3}$ , released  
8 upon ice evaporation. In these 3-D model simulations, in which a simplified treatment of  
9 horizontal transport was used, NAT particles were assumed to be in equilibrium with gas phase  
10 nitric acid.

11 Davies *et al.* (2002) have included a parameterization in a 3-D CTM of NAT particle  
12 sedimentation assuming sizes and number concentrations representative of those observed by  
13 Fahey *et al.* (2001). NAT particles were assumed to be in equilibrium with gas phase nitric acid  
14 in these simulations. The calculated denitrification magnitude was similar to that observed in  
15 winter 1999/2000. In contrast, the modeled denitrification was significantly less than observed  
16 when NAT was allowed to only nucleate on ice particles. This result is consistent with previous  
17 simulations (Carslaw *et al.*, 2002; Drdla *et al.*, 2002) showing that the observed large nitric acid  
18 particles could not have nucleated on synoptic-scale ice clouds during the winter of 1999-2000.

19 Mann *et al.* (2002) have developed a 3-D model of denitrification that takes into account  
20 the time-dependence of both growth and sedimentation of large NAT particles. In these  
21 simulations NAT particle growth times are on the order of several days and therefore the  
22 magnitude of denitrification strongly depends on individual particle growth cycles. In fact, the  
23 extent of modeled denitrification is strongly amplified when areas of low temperature are stable  
24 and concentric with the vortex, allowing for individual particles to persist for a longer time and  
25 to grow to larger sizes. Thus the area of cold temperatures by itself is perhaps not the best  
26 indicator for predicting the severity of denitrification in the Arctic.

27 In summary, new model calculations show that the long-accepted mechanism of nitric acid  
28 removal on sedimenting ice particles cannot account for observed levels of denitrification.  
29 Denitrification is most likely caused by sedimentation of large nitric acid particles. Various  
30 models are able to reproduce, in broad terms, the observed levels of denitrification by assuming  
31 sedimentation of large nitric acid particles. In addition, recent model calculations show that

1 Arctic denitrified layers are normally shallow in depth because the stratosphere is too warm  
2 below about 17 km to allow for large particles to carry much nitric acid beyond this altitude.  
3 The sensitivity of ozone loss to denitrification is discussed in Section 3.3.

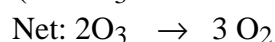
#### 4 **2.2.4 DEHYDRATION**

5  
6 Figure 2.2-5 shows the time evolution of water vapor in the Southern Hemisphere during  
7 1998 (Nedoluha *et al.*, 2000). Severe dehydration is observed over a 10 km altitude range.  
8 Similar results are also obtained from analysis of MLS water vapor data during the Antarctic  
9 winter of 1992 (Stone *et al.*, 2001). In the Arctic removal of ~ 1 ppm of water vapor over a 1-2  
10 km altitude range has been observed by the ILAS instrument (Pan *et al.*, 2002). The lack of  
11 extensive and deep dehydration in the Arctic is also supported by *in situ* observations (Vömel *et*  
12 *al.*, 1997; Hintsä *et al.*, 1998; Herman *et al.*, 2002). Overall, the Arctic climate, even in cold  
13 years, it too to allow for formation of widespread persistent ice clouds that lead to dehydration.  
14 The sensitivity of ozone loss to dehydration is discussed in Section 3.

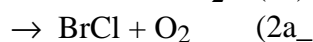
### 15 **2.3 Polar Ozone Chemistry**

16  
17 The chemical loss of polar ozone during winter and spring occurs primarily by two gas  
18 phase catalytic cycles that involve halogen oxide radicals:

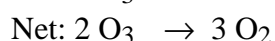
19  
20 Cycle 1



21  
22 Cycle 2



)



24  
25

1 Abundances of ClO in the polar vortex are greatly elevated by reactions of inactive  
2 chlorine reservoir species on various types of polar stratospheric clouds (PSCs) that form when  
3 temperatures drop below about 195 K (see Section 3.2.2). Abundances of BrO determine the  
4 removal rate by cycle (2), which contributes about 50% to the total chemical loss rate of polar  
5 ozone (Chipperfield and Pyle, 1998). In contrast to ClO, the abundance of BrO is not strongly  
6 affected by reactions involving PSCs because less than half of the available inorganic bromine  
7 budget is sequestered in reservoirs such as BrNO<sub>3</sub> and HBr prior to processing.

8 Since the last assessment, new studies have addressed the rates of ozone destruction by  
9 cycles (1) and (2) in an effort to reconcile apparent discrepancies between measured and  
10 modeled chemical loss rates of Arctic ozone (see Section 3.3). The chlorine and bromine cycles  
11 are discussed separately below. Model calculations reveal that, at present and for the foreseeable  
12 future, winter polar ozone loss will be dominated by reactions involving ClO and BrO (*e.g.*,  
13 Chipperfield and Pyle, 1998; Shindell *et al.*, 1998b).

### 14 **2.3.1 CHLORINE**

15  
16 A number of modeling studies have had difficulty accounting for observed chemical loss  
17 rates of Arctic ozone, particularly during mid-winter when insolation is weakest (see Section  
18 3.3). As a consequence, attention has focused on reducing uncertainties in key rate parameters,  
19 in particular those for formation and photolysis of the chlorine oxide dimer (ClOOCl), reactions  
20  $k_{1a}$  and  $J_{1b}$ . These reactions determine the rate of ozone loss by cycle 1, such that uncertainties  
21 in these kinetic parameters couple directly into the uncertainties in modeled ozone loss rates.  
22 Results of these studies are summarized in Section 3.2.3.1.1.

23 The loss of polar ozone via cycles 1 and 2 is determined by the temporal evolution of ClO.  
24 Numerous studies have examined the seasonal variations of inorganic chlorine partitioning,  
25 including production of high abundances of reactive chlorine (ClO<sub>x</sub>, defined as  
26 [ClO]+2[ClOOCl]) by PSCs ('activation'), maintenance of high abundances of ClO<sub>x</sub> throughout  
27 the winter, and deactivation of ClO<sub>x</sub> back to HCl and ClNO<sub>3</sub> ('recovery'). These results are  
28 summarized in Section 3.2.3.1.2.

29 Simultaneous measurements of the major inorganic and organic chlorine species have  
30 provided, for the first time, the ability to examine the overall chlorine budget for the Arctic  
31 stratosphere during a period of rapid ozone loss. These investigations can assess the possible



1 role of species not considered in standard models, such as higher oxides of chlorine. The results  
2 of these studies are summarized in Section 2.3.1.3.

3  
4 ***Chlorine Photochemistry [2.3.1.1]***  
5

6 Our understanding of the key kinetic parameters governing ozone loss by cycle 1 ( $k_{1a}$  and  
7  $J_{1b}$ ) has improved through new laboratory studies and atmospheric observations. Bloss *et al.*  
8 (2001) found  $k_{1a}$  to be up to 25% larger than the value recommended in the Jet Propulsion  
9 Laboratory (JPL) 00-3 compendium (Sander *et al.*, 2000) at temperatures below 210 K. The  
10 impact of this increase on calculated ozone loss rates depends on the manner in which the models  
11 treat ClO. In the case of models constrained by observed abundances of ClO, the rate of ozone  
12 loss due to cycle 1 is roughly proportional to the increase in  $k_{1a}$ . For models that allow ClO and  
13 ClOOCl to re-partition within the constraint of constant active chlorine, the total loss rate is  
14 largely independent of this change in  $k_{1a}$  because ClO abundances respond in the opposite sense  
15 to the change in the rate constant (Figure 2.3-1). Thus, the maximum effect of an increase in  $k_{1a}$   
16 based on the results of Bloss *et al.* (2001) is to increase total ozone loss rates by no more than  
17 25% under cold polar conditions. Such an increase is insufficient to fully resolve the factor-of-  
18 two discrepancies between modeled and measured Arctic ozone loss rates found in several recent  
19 studies (*e.g.*, Woyke *et al.*, 1999; Becker *et al.*, 2000).

20 The recommended absorption cross section for ClOOCl has not changed since the last  
21 assessment. However, there have been several important laboratory and theoretical studies  
22 (Moore *et al.*, 1999; Kaledin and Morokuma, 2000; and Toniolo *et al.*, 2000) of the product  
23 yields from photolysis of ClOOCl at wavelengths longer than 300 nm, the spectral region that  
24 contributes most to the overall photolysis rate of ClOOCl. These new results reduce a significant  
25 uncertainty in our knowledge of ozone loss rates. Only production of ClOO+Cl (leading to  
26  $2\text{Cl}+\text{O}_2$  upon the rapid thermal decomposition of ClOO at polar temperatures) results in catalytic  
27 loss of ozone; production of ClO+ClO from ClOOCl photolysis leads to a null cycle that has no  
28 effect on ozone. Prior to this assessment, fundamental assumptions regarding the products of  
29 ClOOCl photolysis had not been examined in the laboratory at key wavelengths.

30 Moore *et al.* (1999) recently reported that Cl and molecular oxygen ( $\text{O}_2$ ) are the primary  
31 products of photolysis of ClOOCl at 248 nm and at 308 nm. Further, they found that ClOO

1 products rapidly decompose due to excess vibrational energy. Thus, chlorine atoms and O<sub>2</sub> are  
2 the primary products of photolysis of ClOOCl under stratospheric conditions, a conclusion  
3 further supported by electronic structure calculations (Kaledin and Morokuma, 2000; Toniolo *et*  
4 *al.*, 2000).

5 Several new sets of atmospheric observations provide strong quantitative tests of our  
6 understanding of  $k_{1a}$  and  $J_{1b}$ . Recent balloon-borne *in situ* observations of the rate of decay of  
7 ClO immediately after sunset in the Arctic vortex are explained well by the larger value for  $k_{1a}$   
8 at temperatures near 190 K (Vömel *et al.*, 2001) (Figure 2.3-2). Similar conclusions were  
9 reached in studies of *in situ* observations of ClO and ClOOCl from the ER-2 aircraft that  
10 examined the ratio  $k_{1a}/J_{1b}$  in the Arctic vortex during the same winter (Stimpfle *et al.*, 2002) and  
11 of earlier ground-based ClO observations from McMurdo Station, Antarctica (Shindell and de  
12 Zafra, 1995).

13 The chemical loss rate of ozone, particularly during early winter, is also quite sensitive to  
14 the dependence of  $J_{1b}$  on solar zenith angle (SZA). The first atmospheric observations of  
15 ClOOCl, together with simultaneous observations of ClO provide important constraints on this  
16 parameter (Stimpfle *et al.*, 2002). In particular, the balance between ClO and ClOOCl in  
17 daylight, which is controlled by the ratio  $J_{1b}/k_{1a}$ , closely tracks a photochemical model that  
18 employs the Bloss *et al.* (2001) value for  $k_{1a}$  and the SZA dependence for  $J_{1b}$  based on the JPL  
19 00-3 recommended absorption cross sections for ClOOCl (Figure 2.3-3). The analysis of  $J_{1b}$  of  
20 Avallone and Toohey (2001) used JPL 00-3 recommendations for  $k_{1a}$ ; a reanalysis using the  
21 Bloss *et al.* (2001) value would lead to larger absolute values for  $J_{1b}$  that would be more  
22 consistent with those found by Stimpfle *et al.* (2002). The significantly smaller value for  $J_{1b}$   
23 based on absorption cross sections of Huder and DeMore (1995) can be ruled out by the  
24 combined results of these studies as well as Shindell and de Zafra (1995), Raffalski *et al.* (1998),  
25 Vömel *et al.* (2001), and Solomon *et al.* (2002). Furthermore, there is no evidence that supports  
26 the notion that ClOOCl may photolyze at an appreciable rate in optically thin spectral regions  
27 (*i.e.*, > 420 nm). Such a process could enhance ozone loss rates at high SZAs and account for  
28 some of the discrepancy between measured and modeled ozone loss rates in mid-winter (Rex *et*  
29 *al.*, 2002b and Section 3).

1 Finally, we note that Solomon *et al.* (2000) suggested that the ratio  $J_{1b}/k_{1a}$  is nearly 50%  
2 too low based on an analysis of ground-based measurements of ClO column over Antarctica in  
3 1996. However, a subsequent analysis of data obtained during 5 winters (1996 to 2000)  
4 (Solomon *et al.*, 2002) found good agreement between measurements of column ClO and model  
5 calculations employing the value of this ratio from current recommendations (Sander *et al.*,  
6 2000).

7  
8 ***Chlorine Seasonal Evolution [2.3.1.2]***  
9

10 Another element critical in accounting for ozone loss is the temporal evolution of the  
11 ozone-destroying halogen radicals. Mixing ratios of ClO remain elevated (~1 to 2 parts per  
12 billion by volume (ppbv)) from May/June until September (Figure 2.2-2) for all years over  
13 Antarctica for which observations are available (WMO, 1995; WMO, 1999; Santee *et al.*, 2000;  
14 Wagner *et al.*, 2001, 2002; Solomon *et al.*, 2002), where temperatures between 14 and 24 km  
15 remain very low (below PSC thresholds) for several months (Figure 2.1-3b). In addition, the  
16 southern polar vortex remains intact well into the spring season. Under these conditions, the  
17 total amount of ozone destroyed over Antarctica is nearly complete for an 8 to 10 km thick  
18 altitude layer (*e.g.*, Figure 2-1.2.4 (*this figure might be deleted*)), a condition that is relatively  
19 insensitive to the chemical loss rate at contemporary abundances of inorganic chlorine (WMO,  
20 1999).

21 Three-dimensional chemical transport models are able to simulate the seasonal evolution of  
22 ClO in the Antarctic polar vortex remarkably well (Ricaud *et al.*, 1998; Solomon *et al.*, 2000;  
23 2002). Figure 2.3-4 compares ground based column measurements of ClO above Scott Base,  
24 Antarctica (77.8°S) to calculations from the SLIMCAT model. Comparisons for the ClO mixing  
25 ratio at 480 K are also shown. During mid- to late-winter, the rise of ClO is determined  
26 primarily by increasing solar illumination at mid-day. The good agreement between theory and  
27 observations of column ClO during this time period suggests that the altitude range over which  
28 chlorine is activated is reproduced well by the model. During early spring, the short-term  
29 fluctuations in ClO are related to movement of the vortex over Scott Base, and the longer-term  
30 decline in ClO is the result of recovery into the reservoirs HCl (the primary sink for ClO<sub>x</sub> in the  
31 denitrified Antarctic vortex) and ClNO<sub>3</sub> (Solomon *et al.*, 2002). As a result of widespread  
32 suppression of gas-phase HNO<sub>3</sub> in SLIMCAT, high abundances of ClO are sustained throughout

1 the early spring season (September) until ozone is nearly completely removed. In October, HCl  
2 is observed to reappear much faster than  $\text{ClNO}_3$  in the core of the vortex due to the shift in  
3 partitioning of  $\text{Cl}/\text{ClO}$  and  $\text{NO}/\text{NO}_2$  to favor Cl and NO driven by exceedingly low ozone, while  
4 ClO recovers mainly to  $\text{ClNO}_3$  in the edge region of the Antarctic vortex (*e.g.*, Douglass *et al.*,  
5 1995; Ricaud *et al.*, 1998). Because most models simulate these features reasonably well, they  
6 are able to account for Antarctic ozone loss in a quantitative manner.

7 The situation for the Arctic winter is quite different, as chemical ozone loss depends more  
8 critically upon the details of chlorine activation, deactivation, and the timing of the break-up of  
9 the northern polar vortex. During cold Arctic winters, high levels of ClO are observed  
10 throughout the polar vortex (Raffalski *et al.*, 1998; Stachnik *et al.*, 1999, Klein *et al.*, 2000;  
11 Santee *et al.*, 2000; [Stimpfle et al., 2002](#)). Considerably more year-to-year variability is seen in  
12 Arctic measurements of ClO compared to Antarctic data, and peak values of Arctic ClO for cold  
13 winters are somewhat lower than observed in the Antarctic (Figure 2.2-2). Recent GOME  
14 measurements of OClO (Figure 2.3-5), which indicate much greater year-to-year variability in  
15 active chlorine for the Arctic as well as considerably higher levels of active chlorine for the  
16 Antarctic (Wagner *et al.*, 2001, [2002](#)), provide a picture consistent with the MLS observations of  
17 ClO. The GOME observations of Antarctic OClO are also consistent with earlier ground based  
18 observations of OClO (Miller *et al.*, 1999).

19 The MLS and GOME measurements show that elevated levels of  $\text{ClO}_x$  in the Arctic, even  
20 for cold years, decline rapidly in early spring, in contrast to the Antarctic, where high  $\text{ClO}_x$   
21 persists well into spring (Figures 2.2-2 and 2.3-5). Consequently, the total quantity of ozone  
22 destroyed in the Arctic vortex depends strongly on the rate of chlorine deactivation, which in  
23 turn is related to the extent of denitrification (*e.g.*, Rex *et al.*, 1997; Waibel *et al.*, 1999;  
24 Tabazadeh *et al.*, 2000) and the efficiency of chlorine reactivation (*e.g.*, Solomon, 1999; [Hanisco](#)  
25 [et al., 2002](#); [Drdla and Schoeberl, 2002](#)). Abundances of  $\text{ClO}_x$  over the Arctic decrease rapidly  
26 when temperatures increase above  $\sim 200$  K, due to photochemical release of  $\text{NO}_x$  from nitric acid  
27 that remains in excess of reactive chlorine throughout the winter. During this recovery period,  
28 observations have shown that  $\text{ClNO}_3$  is the primary inorganic chlorine species, representing  
29  $>80\%$  of the available chlorine (Chapter 3, WMO 1995). It has long been assumed that chlorine  
30 can be readily reactivated on PSCs during this recovery period (provided temperature drops

1 below ~195 to 200 K), leading to significant additional ozone loss. However, a recent study  
2 based on analyses of *in situ* observations of OH and HO<sub>2</sub> (Hanisco *et al.*, 2002) indicates that  
3 key heterogeneous reactions that reactivate chlorine proceed more slowly than currently  
4 recommended rates. The consequences of this finding have yet to be explored in photochemical  
5 model studies of Arctic ozone loss.

6 New simultaneous remote measurements of the major organic and inorganic chlorine  
7 species within the Arctic polar vortex during late autumn 1999, before widespread activation,  
8 indicated that abundances of HCl exceeded ClNO<sub>3</sub> for air masses that were soon to become  
9 activated (Salawitch *et al.*, 2002c). This result differs from that of Webster *et al.* (1993) during  
10 the same season in 1991, where HCl abundances were found to be significantly less than half of  
11 the available inorganic chlorine (*e.g.*, Figure 3-1 of WMO 1995). Variations in sulfate aerosol  
12 loading, which was highly enhanced in 1991 following the eruption of Mt. Pinatubo, may  
13 account for the differences in the initial HCl vs. ClNO<sub>3</sub> partitioning (*e.g.*, Webster *et al.*, 2000).  
14 Most importantly, three dimensional chemistry and transport models (Ricaud *et al.*, 1998; Massie  
15 *et al.*, 2000; van den Broek *et al.*, 2000) as well as trajectory simulations (Woyke *et al.*, 1999;  
16 Danilin *et al.*, 2000) are able to simulate well the high levels of ClO observed in the Arctic,  
17 indicating that chlorine activation schemes used in photochemical models are relatively accurate  
18 in describing large-scale features of chlorine activation. Recent model simulations also suggest  
19 that the rate and extent of halogen activation in the polar vortex are not as sensitive to PSC  
20 composition as previously thought (Carslaw *et al.*, 1997b; Becker *et al.*, 1998; Woyke *et al.*,  
21 1999; Danilin *et al.*, 2000). This lack of sensitivity arises because most heterogeneous halogen  
22 activation rates are much faster at low temperatures than deactivation rates of ClO<sub>x</sub> for air  
23 parcels outside of PSCs (*e.g.*, Solomon, 1999).

24 While models simulate the seasonal evolution of ClO in the Arctic reasonably well for cold  
25 winters, they have some difficulty for warm winters, where minimum temperatures are close to  
26 the threshold for formation of PSCs (*e.g.*, Klein *et al.*, 2000). For the winter of 1998/1999,  
27 ground-based observations of ClO from Ny Ålesund, Spitzbergen (78.9°N) revealed little or no  
28 enhancements above background levels, whereas the SLIMCAT model predicted ClO mixing  
29 ratios as high as 1.0 ppbv. This discrepancy has been attributed to a small cold bias (~1K) in the  
30 UKMO temperatures input to the SLIMCAT model (Klein *et al.*, 2000, Knudsen *et al.*, 2002),  
31 although it is also possible that the PSC nucleation scheme in SLIMCAT is unrealistic at

1 temperatures near NAT thresholds. In either case, such a problem highlights the extraordinary  
2 sensitivity of Arctic ClO to temperatures and microphysics schemes for winters where the  
3 minimum temperatures are very close to the threshold for formation of PSCs.

4  
5 ***Chlorine Budget [2.3.1.3]***  
6

7 Ideally, an assessment of the chlorine budget should be based on simultaneous  
8 measurements of the primary inorganic (*e.g.*, HCl, ClNO<sub>3</sub>, ClO, ClOOCl) and organic chlorine  
9 species (*e.g.*, chlorofluorocarbons and other chlorine containing halocarbons). Until recently,  
10 such a budget for the mid-winter periods of the polar stratosphere had to rely on calculated  
11 abundances of ClOOCl because there were no observations of this important reservoir of reactive  
12 chlorine. Nonetheless, a significant number of studies (all of which lack observations of  
13 ClOOCl) have indicated good agreement between the inorganic and organic chlorine budget for  
14 the lower polar stratosphere (*e.g.*, von Clarmann *et al.*, 1995; Engel *et al.*, 1997; Mickley *et al.*,  
15 1997; Ricaud *et al.*, 1998; Michelsen *et al.*, 1999; Pierson *et al.*, 1999; Stachnik *et al.*, 1999;  
16 [Salawitch \*et al.\*, 2002c](#)). Analyses of observations of ClO, constrained by the rate parameters for  
17  $k_{1a}$  and  $J_{1b}$  at values similar to those discussed in the previous section, have inferred that  
18 ClOOCl and ClO contain comparable amounts of chlorine during the period of maximum  
19 activation (Stachnik *et al.*, 1999; Avallone and Toohey, 2001). Although the rate of cycle (1)  
20 (and hence its contribution to ozone loss) can be inferred from measurements of ClO, photolysis  
21 of ClOOCl represents the true rate-determining step in this catalytic cycle. Thus, it is important  
22 to demonstrate the presence of ClOOCl at abundances necessary to explain observed ozone  
23 losses.

24 The most comprehensive set of measurements to date to assess the chlorine budget was  
25 obtained from the NASA ER-2 aircraft during the Arctic winter of 1999-2000. Measurements of  
26 ClO, ClOOCl, ClNO<sub>3</sub>, HCl, and numerous chlorofluorocarbons (CFCs) were all obtained  
27 simultaneously on a number of flights during times of rapid chemical loss of ozone. Based on  
28 these observations, the sum of concentrations of these major inorganic chlorine species (termed  
29  $Cl_{y,inorg}$ ) falls about 10 to 25% short of the inorganic chlorine content estimated from measured  
30 organic source compounds (termed  $Cl_{y,org}$ ) ([Stimpfle \*et al.\*, 2002](#)). However,  $Cl_{y,inorg}$  and  $Cl_{y,org}$   
31 agree within measurement error, so it is unclear whether this discrepancy is significant.

1 Further insight can be gained from examination of the chlorine budget from other  
2 instruments inside the Arctic vortex. These comparisons rely on calculated concentrations of  
3 ClOOCl, termed ClOOCl\*, assuming a steady state relation with measured ClO. Observations of  
4  $[HCl]+[ClNO_3]+[ClO]+2[ClOOCl^*]$  versus  $N_2O$  obtained by a balloon Fourier transform  
5 infrared (FTIR) instrument near the edge of the Arctic vortex on 15 March 2000 agree well with  
6 estimates for  $Cl_y^{org}$  (Salawitch *et al.*, 2002c). Additionally, balloon-borne microwave and whole  
7 air sampler measurements of  $[HCl]+[ClO]+2[ClOOCl^*]$  versus  $N_2O$  for air in the core of the  
8 Arctic vortex on 27 January 1995 (Stachnik *et al.*, 1999), made under conditions of highly  
9 elevated ClO, also agree well with estimates of  $Cl_y^{org}$ . These observations support the good  
10 understanding of the chlorine budget noted by the other studies cited in the first paragraph of this  
11 section, given the caveat that abundances of ClOOCl are based on calculations for all of these  
12 studies. Also, these findings are consistent with reasonably good agreement (differences of  
13 about  $\pm 15\%$ ) between the disappearance of organic chlorine and the appearance of inorganic  
14 chlorine observed for the summer polar stratosphere (Section 2.4.3), a region of the atmosphere  
15 for which the contribution to  $Cl_y^{inorg}$  is dominated by HCl and  $ClNO_3$ .

16 **NOTE: This material may be revised once a paper for the ER-2 measurement of ClOOCl**  
17 **exists. We will not refer to any paper that not has been submitted prior to the Les Diablerets**  
18 **meeting.**

### 19 **2.3.2 BROMINE**

20  
21 Cycle 2 (BrO + ClO) makes important contributions to polar ozone loss. As shown below  
22 in Section 2.3.2.1 there is now reasonably good agreement between measurements of BrO  
23 obtained by various techniques. This is a significant advance in our understanding because  
24 important differences had been noted in the previous assessment (WMO, 1999). This  
25 convergence of measurements allows for fairly accurate assessment of the contribution of  
26 bromine to chemical loss of polar ozone.

27 Profiles of inorganic bromine based on measurements of BrO have recently been  
28 compared to estimates based on the observed fall off (with increasing height) of the organic  
29 source species. These comparisons, discussed in Section 2.3.2.2, show a slight offset that may  
30 result from either direct influx of  $\sim 3$  parts per trillion by volume (pptv) of inorganic bromine

1 across the tropical tropopause or some organic species not accounted for. Finally, long-term  
2 measurements of BrO discussed also in Section 2.3.2.2 have been used to determine trends in  
3 total bromine loading that can be compared to trends based on the organic bromine content of the  
4 lower atmosphere. (This sentence will have to be modified if the bromine trends material below  
5 is removed or greatly altered).

6  
7 ***Bromine Monoxide (BrO) Abundances [2.3.2.1]***  
8

9 Harder *et al.* (1998) compared *in situ* BrO measurements from the ER-2 aircraft and a  
10 balloon flight with profiles of BrO obtained by the Differential Optical Absorption Spectroscopy  
11 (DOAS) technique (Figure 2.3-6). There is a systematic difference in these two sets of  
12 observations, where DOAS is somewhat larger than *in situ*, although this is within the combined  
13 uncertainties of the measurements. Consequently, the estimates of the inorganic bromine budget  
14 based on these sets of measurements have ranged from ~16 pptv (*in situ*) to ~20 pptv, (DOAS)  
15 (Avallone *et al.*, 1995; Pfeilsticker *et al.*, 2000). It is important to note that, because these sets of  
16 observations were obtained 5 years apart, more than half of this difference can be explained by  
17 trends in the bromine source gases, as discussed below.

18 Sinnhuber *et al.* (2002) compared ground-based zenith sky measurements obtained at  
19 eleven sites to simulations from the SLIMCAT model in an effort to examine the detailed  
20 processes that govern the partitioning of BrO. Comparisons for three sites are shown in Figure  
21 2.3-7. The simulated abundances of BrO generally agree to within ~10% of the observations  
22 over a wide range of seasons, latitudes, and solar zenith angles. The results are consistent with a  
23 total stratospheric bromine loading (sum of organic and inorganic) of 20±4 pptv, in agreement  
24 with the values deduced from previous remote measurements of BrO.

25 The SLIMCAT model tends to overestimate BrO column abundances at high latitudes,  
26 typically when ClO abundances are elevated (Figure 2.3-7). Conversely, Friess *et al.* (1999) find  
27 a discrepancy in the opposite sense between BrO slant column measurements made at Kiruna,  
28 Sweden (67.9°N) in winter and SLIMCAT model calculations that use JPL 97-4 kinetics  
29 (DeMore *et al.*, 1997) and a bromine loading of 20 pptv (the model underestimates midday  
30 measured BrO columns by 20 to 40%). Sinnhuber *et al.* (2002) note that the discrepancy  
31 highlighted in their study can be reduced by increasing the rate constant for reaction (2a\_) to the  
32 upper limit of the uncertainty of the Sander *et al.* (2000) recommendation. Friess *et al.* (1999),



1 however, report that the discrepancy they found is evidence for several pptv of BrO in the free  
2 troposphere. The Friess *et al.* (1999) interpretation is consistent with interpretations based on  
3 other remote observations of BrO (*e.g.*, Harder *et al.*, 1998; Fitzenberger *et al.*, 2000).

4 The discrepancies outlined above have a relatively minor impact on ozone loss rates  
5 calculated directly from cycle (2) or on observed abundances of ClO and BrO in the polar  
6 vortices. However, they do raise questions about the completeness of our understanding of  
7 coupled bromine/chlorine chemistry. Similar questions have been raised based on aircraft  
8 observations of BrO at 20 km (*in situ*) and 12 km (remote) within the perturbed polar vortex.  
9 Specifically, Avallone and Toohey (2001) report that mixing ratios of BrO did not drop to near-  
10 zero as expected with increasing SZA after sunset, when reservoir species like bromine nitrate  
11 (BrNO<sub>3</sub>), bromide chloride (BrCl), and hypobromous acid (HOBr) are expected to sequester  
12 nearly all available reactive bromine. Similarly, Wahner and Schiller (1992) previously reported  
13 non-zero BrO column abundances above 12 km in darkness that were difficult to explain.  
14 Avallone and Toohey (2001) suggest that thermal decomposition of a weakly bound molecule,  
15 such as BrOOCl, may be able to maintain a few pptv of BrO following sunset, but note that such  
16 a process would have little impact on ozone loss rates because of the rapid decline of ClO at  
17 sunset. The existence of adducts of bromine and chlorine oxides has been postulated in  
18 theoretical studies (Gleghorn, 1997; Bridgeman and Rothery, 1999; Gomez and Pacios, 1999;  
19 Papayannis *et al.*, 2001) and has been observed in an argon matrix (Johnsson *et al.*, 1995).

20 The previous assessment noted the spectroscopic detection of OBrO in the mid-latitude  
21 stratosphere, with implied mixing ratios as high as 20 pptv (Renard *et al.*, 1997). As such, OBrO  
22 would be the dominant nighttime reservoir for inorganic bromine in the mid-latitude  
23 stratosphere. The same group has since reported the presence of smaller amounts of OBrO in the  
24 nighttime, polar stratosphere (Renard *et al.*, 1998). However, abundances of even a few  
25 hundredths of a ppt of OBrO in the nighttime stratosphere are contrary to our present  
26 understanding of bromine photochemistry (Chipperfield *et al.*, 1998). Erle *et al.* (2000) recently  
27 reported measurements of upper limits for OBrO that are appreciably smaller than values  
28 observed by Renard *et al.* (1997, 1998), indicating that one of the sets of observations are in error  
29 or that abundances of OBrO are highly variable. The explanations for non-zero BrO mixing  
30 ratios in darkness and possible detection of OBrO remain a mystery.

31

1 ***Bromine Trends and Budget [2.3.2.2]***

2  
3 **Will need work based on lack of accepted papers by 7/02.**

4  
5 During the Arctic winter of 1998/1999, vertical profiles of all known major organic  
6 bromine species were measured between 9 and 28 km (Pfeilsticker *et al.*, 2000) (Figure 2.3-8).  
7 The expected profile for inorganic bromine that was inferred from the source gases agrees well  
8 (*i.e.*, differences are within the measurement uncertainties) with a second profile that was  
9 estimated from spectroscopic observations of BrO and a photochemical model estimate of the  
10 BrO/Br<sub>y</sub> ratio (see Figure 2.3-8) (Pfeilsticker *et al.*, 2000). This result indicates that the budget  
11 of bromine and its photochemistry in the lower stratosphere are reasonably well understood. For  
12 early 1999, the mixing ratio of total bromine estimated at 25 km in air of 5.6-year mean age was  
13 18.4 (+1.8, -1.5) pptv based on organic precursor measurements, and 21.5 ± 3.0 pptv from BrO  
14 measurements. This slight offset allows for the possibility of a bromine influx of 3.1 (-2.9, +3.5)  
15 pptv from the troposphere to the stratosphere (Pfeilsticker *et al.*, 2000).

16 **Remove some of the text below, unless we can refer to the EU Assessment? Also, the**  
17 **Toohey *et al.*, 2002 paper must be submitted in order to stay in the text below.**

18 Attempts to quantify temporal trends in inorganic bromine in the stratosphere traditionally  
19 have been hampered by the lack of long-term observations and the relatively small quantities  
20 (~10 pptv or less) of the bromine species. Two groups have recently examined different data  
21 sets that may shed some light on this issue, which is important in the context of polar ozone loss  
22 because the source of bromine to the stratosphere is expected to have increased by nearly 30%  
23 over the past decade (Wamsley *et al.*, 1998).

24 Pfeilsticker *et al.* (see Figure 2.12, EUR19867, 2001) have taken the approach of  
25 examining the fall-off of total bromine with altitude, deduced from measurements of BrO. They  
26 rely on separate measurements of carbon dioxide (CO<sub>2</sub>) or sulfur hexafluoride (SF<sub>6</sub>) and model  
27 simulations to determine the age of air versus altitude. Their results are consistent with a rate of  
28 increase of total bromine of about 0.7 pptv/year over the period 1995-2000. Using BrO  
29 observations at 20-22 km from the Arctic polar vortex when simultaneous measurements indicate  
30 high (> 1 ppbv) mixing ratios of ClO, Toohey *et al.* (2002) report that BrO increased about 30 to  
31 40% over the period 1989-2000, consistent with the trends in organic source gases reported by  
32 Wamsley *et al.* (1998). Assuming a budget of ~20 pptv for total bromine, these results imply a

1 rise rate of about 0.5 to 0.7 ppt/year, in good agreement with the results presented by Pfeilsticker  
2 *et al.* (see Section 2.3.2, EUR19867, 2001).

3 These results suggest that the contribution of bromine to ozone loss in the polar regions has  
4 increased faster than that of chlorine due to abundances of bromine that continue to increase at a  
5 time when those of chlorine are leveling off (see Chapter 1). Model studies indicate that  
6 catalytic cycles involving BrO account for as much as 60% (depending on abundances of ClO  
7 and temperatures) of the total chemical loss of ozone in the Arctic for cold winters (Chipperfield  
8 and Pyle, 1998). The contribution of BrO reactions to the total loss of Antarctic ozone is  
9 somewhat less than for the Arctic due to lower temperatures and widespread denitrification in the  
10 SH vortex. However, since ozone loss by the BrO cycle also depends on ClO, future major  
11 declines in Cl<sub>y</sub> are expected to lead to reductions in chemical loss of polar ozone essentially  
12 independent of changes to Br<sub>y</sub> (Chipperfield and Pyle, 1998).

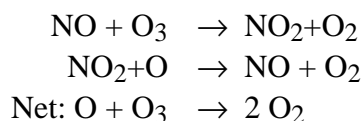
## 13 **2.4 The Polar Summer Lower Stratosphere**

14  
15 In both hemispheres, the annual cycle of total ozone has a strong decrease from the spring  
16 maximum to a minimum by mid-fall (*e.g.*, Dobson, 1966; Dütsch, 1974; Bowman and Krueger,  
17 1985). Column abundance of ozone declines by ~35% at high northern latitudes during summer  
18 (Toon *et al.*, 1999; Lloyd *et al.*, 1999). The rate of chemical ozone destruction in late  
19 spring/early summer is as large as in the polar stratosphere. This large decline, and the fact that  
20 the summer circulation is weak and quite zonally symmetric, makes the summer period a good  
21 test of understanding. Models typically have been unable to capture the full magnitude of the  
22 decline. To address this issue the POLARIS experiment was flown from Fairbanks, AK, with  
23 three deployments during the early spring, summer, and early fall of 1997. This mission  
24 examined the seasonal ozone decrease using a complete payload of instruments aboard the  
25 NASA ER-2 high altitude aircraft (Newman *et al.*, 1999).

26 The summer lower stratosphere is mixed vigorously by waves which penetrate in the  
27 presence of the weak summer westerlies (Wagner and Bowman, 2000). Orsolini (2001),  
28 however, has shown that remnants of polar vortex air can retain their identity until well into the  
29 summer in the lower stratosphere. Rosenlof (1999) has studied the annual cycle of ozone  
30 transport in high northern latitudes. She found that the seasonal cycle in transport was an  
31 important contributor to the seasonal march of ozone at high latitudes during middle to late

1 summer, with the eddy contribution to ozone reduction more than offsetting the ozone increase  
2 by advection at this time. In early summer transport is weak and *in situ* photochemical  
3 destruction dominates the ozone tendency. In contrast, Pierce *et al.* (1999) using a Lagrangian  
4 model with HALOE data found that the transport term was important

5 *In situ* measurements of NO<sub>x</sub>, HO<sub>x</sub>, and ClO<sub>x</sub> radical species (Fahey *et al.*, 2000) and long-  
6 lived tracers of stratospheric transport (Toon *et al.*, 1999) confirm the summertime loss of ozone  
7 is due primarily to the gas-phase catalytic cycle:



8  
9  
10 Fahey *et al.* (2000) calculated the ozone chemical tendency based on measurements of  
11 radicals from the major families and found that chemical processes dominate overall tendency in  
12 the mid-summer. Although this ozone loss process is generally understood (Brühl *et al.*, 1998),  
13 ozone abundances calculated using two- or three-dimensional models tend to exceed  
14 observations for high-latitude summer (*e.g.*, Chipperfield, 1999). This discrepancy has been  
15 attributed to inadequacies in model transport (*e.g.*, Fahey and Ravishankara, 1999).

16 New measurements of NO<sub>x</sub>, HO<sub>x</sub>, and ClO<sub>x</sub> species in the summer polar stratosphere have  
17 provided quantitative tests of our understanding of processes that regulate the abundance of  
18 radicals in each family. Measurements in the summer polar stratosphere are particularly useful  
19 because heterogeneous reactions, normally the dominant loss process for NO<sub>x</sub>, proceed at slower  
20 rates than gas phase loss reactions due to uninterrupted periods of solar illumination that restrict  
21 the build-up of N<sub>2</sub>O<sub>5</sub> (*e.g.*, Gao *et al.*, 1999; Osterman *et al.*, 1999). In the sections which  
22 follow, we briefly assess recent advances in our understanding of stratospheric photochemistry  
23 based on these observations.

#### 24 **2.4.1 SUMMERTIME NO<sub>x</sub> CHEMISTRY**

25  
26 Observations of NO, NO<sub>2</sub>, HNO<sub>3</sub>, and NO<sub>y</sub> obtained in the summer polar stratosphere  
27 revealed higher levels of NO<sub>x</sub> (relative to total NO<sub>y</sub>) and NO<sub>2</sub> (relative to HNO<sub>3</sub>) than could be  
28 accounted for by constrained photochemical box models using the JPL 97-4 set of recommended  
29 kinetic parameters (Gao *et al.*, 1999; Jucks *et al.*, 1999; Osterman *et al.*, 1999; Cohen *et al.*,

1 2000; Perkins *et al.*, 2001) (Figure 2.4-1). During polar summer, production and loss of NO<sub>x</sub> are  
2 regulated primarily by the OH + NO<sub>2</sub> and OH + HNO<sub>3</sub> reactions for a broad range of altitudes  
3 (*e.g.*, Osterman *et al.*, 1999). New laboratory data for OH + NO<sub>2</sub> (Dransfield *et al.*, 1999; Brown  
4 *et al.*, 1999a) and OH + HNO<sub>3</sub> (Brown *et al.*, 1999b) led to a re-evaluation of the rate constant  
5 for both of these reactions in the JPL 00-3 compendium. Use of the JPL 00-3 kinetic parameters  
6 significantly improves the agreement between measured and modeled ratios of NO<sub>x</sub>/NO<sub>y</sub> and  
7 NO<sub>2</sub>/HNO<sub>3</sub> (Gao *et al.*, 1999; Jucks *et al.*, 1999; Osterman *et al.*, 1999; Cohen *et al.*, 2000;  
8 Perkins *et al.*, 2001; [Salawitch \*et al.\*, 2002b](#)) (Figure 2.4-1).

9 Simultaneous measurements of NO, NO<sub>2</sub>, O<sub>3</sub>, ClO, and HO<sub>2</sub> during polar summer provide  
10 a stringent test of our understanding of the rapid photochemistry linking NO to NO<sub>2</sub> (Del Negro  
11 *et al.*, 1999). Photolysis rates for NO<sub>2</sub> (J<sub>NO<sub>2</sub></sub>) inferred from the chemical measurements are in  
12 excellent agreement with values calculated with radiative models and those measured with a  
13 spectroradiometer (Del Negro *et al.*, 1999). Recently, this comparison has been extended to  
14 larger SZAs of 80 to 93° (Gao *et al.*, 2001a). Values of J<sub>NO<sub>2</sub></sub> derived from the *in situ* chemical  
15 measurements agree well (differences < 11%) with results from a multiple scattering actinic flux  
16 model. The linearity of the correlation between these two computations of J<sub>NO<sub>2</sub></sub> over the SZA  
17 range 80 to 93° demonstrates the model scattering calculation is accurate for twilight conditions  
18 (Gao *et al.*, 2001a).

19 Loss of ozone by NO<sub>x</sub> chemistry in the summer polar regions may become more important  
20 in the future due to rising levels of NO<sub>2</sub> (Liley *et al.*, 2000; McLinden *et al.*, 2001). Nitrous  
21 oxide (N<sub>2</sub>O), the source gas for NO<sub>x</sub> and NO<sub>y</sub>, is rising at about 3% per decade (*e.g.*, McLinden  
22 *et al.*, 2001). Interestingly, concentrations of NO<sub>2</sub> at Southern Hemisphere mid-latitudes have  
23 been observed to be increasing at a faster rate of 5% per decade (Liley *et al.*, 2000). This  
24 increase has been interpreted as being due to rising N<sub>2</sub>O as well as declining levels of O<sub>3</sub>, which  
25 alters the NO/NO<sub>2</sub> partitioning and the diurnal variation of NO<sub>x</sub> (McLinden *et al.*, 2001).

## 26 **2.4.2 SUMMERTIME HO<sub>x</sub> CHEMISTRY**

27  
28 Measurements of OH and hydroperoxyl radical (HO<sub>2</sub>) in the high latitude stratosphere  
29 during spring provide an important test of our understanding of twilight sources of HO<sub>x</sub> because

1 abundances of these species are nearly in photochemical steady state under the slowly varying  
2 SZA conditions up to  $93^\circ$ . Observed abundances of OH and HO<sub>2</sub> in the lower stratosphere  
3 significantly exceeded those from standard model calculations for SZA >  $85^\circ$  (Wennberg *et al.*,  
4 1999); agreement is much better at lower zenith angles. The high zenith angle discrepancy is  
5 larger than can be explained by any reasonable adjustments to the rate of bromine nitrate  
6 (BrNO<sub>3</sub>) hydrolysis and /or assumptions regarding Br<sub>y</sub> (Salawitch *et al.*, 2002b). The data  
7 suggest the presence of a photolytic source of HO<sub>x</sub> that operates more efficiently than known  
8 HO<sub>x</sub> sources during twilight (Wennberg *et al.*, 1999). Including a photolytic pathway for  
9 photolysis of HNO<sub>4</sub> via excitation of purely vibration modes longward of 760 nm (the near IR)  
10 based on recent laboratory measurements (Roehl *et al.*, 2002), a process first suggested by  
11 Donaldson *et al.* (1997), leads to significant improvements in measured and modeled HO<sub>x</sub> near  
12 twilight due to the rapid photolysis of HNO<sub>4</sub> (Salawitch *et al.*, 2002b). This process also reduces  
13 the efficiency of the OH+HNO<sub>4</sub> sink of HO<sub>x</sub>, altering the coupling between NO<sub>x</sub> and HO<sub>x</sub> in  
14 stratospheric and upper tropospheric models (Salawitch *et al.*, 2002b). The global implications  
15 of this process have yet to be evaluated.

16 Balloon-borne observations of OH, HO<sub>2</sub>, H<sub>2</sub>O, and O<sub>3</sub> obtained over Fairbanks, Alaska  
17 suggest important gaps in our understanding of several HO<sub>x</sub> reactions (Jucks *et al.*, 1998).  
18 Discrepancies between measured and modeled abundances of OH and HO<sub>2</sub> are reduced with a  
19 ~25% downward adjustment of the ratio of the rate constants for atomic oxygen (O) + HO<sub>2</sub> and  
20 O + OH and either a 25% reduction to the rate constant for OH + HO<sub>2</sub> (the primary HO<sub>x</sub> sink) or  
21 a 25% increase in the HO<sub>x</sub> production rate (Jucks *et al.*, 1998). These modifications are within  
22 the uncertainties of the laboratory measurements and are consistent with the results of HO<sub>x</sub>  
23 model/measurement studies discussed in the previous assessment. The new insight provided by  
24 the simultaneous observations of OH and HO<sub>2</sub> is that the required modifications to the rate  
25 constants appear not to appreciably affect odd oxygen production rates in the upper stratosphere  
26 (Jucks *et al.*, 1998).

### 27 2.4.3 SUMMERTIME Cl<sub>y</sub> CHEMISTRY

28  
29 The first *in situ* observations of ClNO<sub>3</sub> were obtained in the high-latitude stratosphere  
30 during the summer of 1997 (Stimpfle *et al.*, 1999). These observations are in good agreement

1 with values of  $\text{ClNO}_3$  determined using a photochemical steady state relation constrained by  
2 simultaneous observations of  $[\text{ClO}]$  and  $[\text{NO}_2]$  (ratio of measured to modeled  $\text{ClNO}_3$  is  
3  $1.15 \pm 0.36$ ). These results, together with a study that used balloon-borne remote measurements  
4 (Sen *et al.*, 1999), confirm the photochemical mechanism by which abundances of  $\text{NO}_x$  regulate  
5 the abundance of  $\text{ClO}$  in regions of the stratosphere that are  $\text{NO}_x$ -limited (*i.e.*, mixing ratio of  
6  $\text{NO}_x >$  mixing ratio of  $\text{ClO}_x$ ).

7 Simultaneous observations of  $\text{ClNO}_3$  and  $\text{HCl}$  from a balloon (Sen *et al.*, 1999) and the  
8 ER-2 aircraft (Voss *et al.*, 2001) test our understanding of the kinetic processes that regulate the  
9 partitioning within the inorganic chlorine ( $\text{Cl}_y$ ) family. Model calculations using JPL 00-3  
10 recommendations agree extremely well with the balloon-borne remote observations of both  
11  $\text{ClNO}_3$  and  $\text{HCl}$  (Figure 2.4-2), whereas the aircraft *in situ* measurements of the ratio  
12  $[\text{ClNO}_3]/[\text{HCl}]$  are ~55 to 60% lower than values based on a steady-state calculation (Voss *et al.*,  
13 2001). This discrepancy has not been resolved and is the subject of ongoing investigations.

14 Simultaneous observations of the major inorganic and organic chlorine species in the  
15 summer polar stratosphere provide a test of the chlorine budget. The observed increase in the  
16 inorganic chlorine content (*e.g.*,  $\text{HCl} + \text{ClNO}_3 + \text{HOCl} + \text{ClO}$ ) of stratospheric air with decreasing  
17  $\text{N}_2\text{O}$  from both the ER-2 and MkIV agrees well (differences less than ~10%) with estimates of  
18 inorganic chlorine based on the observed disappearance of organic source molecules (Sen *et al.*,  
19 1999; Bonne *et al.*, 2000) (Figure 2.4-2). However, the ER-2 based estimate of inorganic  
20 chlorine is ~15% less than the MkIV estimate for mixing ratios of  $\text{N}_2\text{O}$  below about 175 ppbv.  
21 This offset is probably due to differences in the measurements of  $\text{ClNO}_3$  noted in the previous  
22 paragraph. These results extend the conclusions of the previous assessment regarding the good  
23 quantitative link between abundances of inorganic chlorine species and their halogen sources to a  
24 new region of the atmosphere (*i.e.*, polar summer) and to a new class of observations (*i.e.*, *in*  
25 *situ*). These findings are particularly relevant for the discussion of the chlorine budget for the  
26 winter polar stratosphere (Section 2.2.1.3).

27

### 3 QUANTIFICATION OF POLAR OZONE LOSS: OBSERVATIONS AND MODELS

Quantification of the degree of chemical ozone loss in the polar stratosphere is hampered by the pronounced dynamically induced variability of the ozone layer in these regions in winter/spring. Precise quantification of the chemically induced contribution to observed changes in the ozone abundance are particularly difficult in the Arctic stratosphere, where the degree of ozone loss is smaller and the dynamic activity is more pronounced than in the Antarctic. Over the last decade a number of approaches have been developed to overcome these difficulties. Major challenges of recent years have been to (a) assess how reliable the results of these approaches are and hence how precise current estimates of the degree of Arctic ozone losses are, and (b) determine whether the degrees of ozone losses calculated by up to date chemical models agree with the observational results within the combined uncertainties of the models and the observations. The latter question is crucial to assess our current ability to make projections of future polar ozone losses in a potentially colder stratosphere.

Severe Arctic ozone loss has been reported for some recent cold Arctic winters. No significant loss was found during warmer winters. Overwhelming evidence exists that large Arctic ozone losses were the result of increased levels of radical halogen species that resulted from heterogeneous chemical processing on the surface of Polar Stratospheric Clouds (WMO 1998, c.f. also Section 2). About 80 % of the stratospheric chlorine and bromine loading are of anthropogenic origin. Since the relevant ozone destruction cycles are linear to quadratic in the concentration of active chlorine, by far the largest fraction of the ozone losses discussed in this section is anthropogenic. However, no quantitative study exists to precisely quantify the small degree of ozone loss that would be expected in a cold Arctic winter for natural levels of halogens in the stratosphere.

#### 3.1 Approaches to Quantify Chemically Induced Ozone Loss in the Arctic

Two principal techniques are currently used to quantify chemically induced ozone losses in the Arctic:

1. Studies that take into account the effect of transport explicitly by using transport calculations based on meteorological analyses, or



1           2. Studies that allow for transport effects implicitly by using the relation between ozone  
2           and a long lived chemical tracer.

3           In the following the approaches that have been used in a consistent way for several winters  
4           are briefly assessed.

### 5   **3.1.1    APPROACHES THAT USE EXPLICIT TRANSPORT CALCULATIONS**

#### 6    7   ***Bulk Advection [3.1.1.1]***

8             
9           In this section approaches are assessed that use explicit transport calculations to advect  
10          bulk quantities like vortex averages or gridded ozone fields and compare these with later  
11          measurements of ozone, a concept first published by Manney *et al.* (1994).

12          The ‘vortex average’ technique involves analysis of the temporal evolution of the mean  
13          profile of ozone within the polar vortex on surfaces of potential temperature. Ozone  
14          measurements by ozone sondes (*e.g.*, Knudsen *et al.*, 1998; Rex *et al.*, 1998; Lucic *et al.*, 1999)  
15          or a remote sensing instrument, *e.g.*, the POAM II satellite instrument (Bevilacqua *et al.*, 1997)  
16          have been analyzed with this approach. The boundary of the polar vortex is usually defined by  
17          isolines of potential vorticity. Potential temperature and potential vorticity are conserved  
18          quantities in the polar stratosphere over time scales of a couple of weeks, so this coordinate  
19          system largely eliminates variability due to rapid and reversible dynamics. The slow irreversible  
20          descent of air across surfaces of potential temperature is usually accounted for by a diabatic  
21          correction calculated from descent rates using a radiative transfer model that is based on  
22          temperatures from a meteorological assimilation system. In the absence of mixing across the  
23          vortex edge, changes in ozone can be attributed to chemical loss. The largest uncertainties  
24          connected with this approach are (a) possible mixing across the vortex edge, that may impact the  
25          average ozone abundance inside the polar vortex, (b) any bias in sampling of the vortex that  
26          changes with time may lead to changes in the derived vortex average, since ozone is not uniform  
27          within the vortex, and (c) uncertainties in the calculated diabatic corrections. Knudsen *et al.*  
28          (1998) used an approach based on domain filling trajectory calculations to estimate the effect of  
29          mixing across the vortex edge for the Arctic winter 1996/1997. For this winter at the altitude of  
30          the maximum loss they found an insignificant impact of mixing on the ozone loss derived from  
31          the vortex average technique.

1 In the 'transport model' approach a 3-D Chemical Transport Model (3-D-CTM) is  
2 initialized with ozone observations during the early winter period. The model advects ozone  
3 passively, *i.e.*, without chemical conversion, throughout the winter, using analyzed winds and,  
4 depending on the vertical transport scheme in the model, also temperatures. Ozone  
5 measurements throughout the winter are compared with the passively advected ozone. Evolving  
6 deficits between observed ozone and the model passive ozone indicate chemical loss. This  
7 approach has been used with the REPROBUS model using data from the POAM satellite instru-  
8 ments and from the ground based network of Système d'Analyse par Observation Zénithale  
9 (SAOZ) instruments (*e.g.*, Lefèvre *et al.* 1998; Goutail *et al.* 1999; Deniel *et al.* 2000). Hansen  
10 *et al.* (1997); Guirlet *et al.* (2000); and Sinnhuber *et al.* (2000) have used this approach with the  
11 SLIMCAT model, using ozone lidar data, SAOZ data and ozone sonde data respectively. This  
12 approach relies on the assumption that the model transport scheme realistically represents the  
13 transport of air over a time period of several months. But when the derived ozone loss is  
14 averaged over the polar vortex as is the case in many studies, the approach only depends on a  
15 correct representation of average transport properties like *e.g.*, vortex averaged vertical  
16 subsidence and average rates of exchange of air across the vortex edge. Possible systematic  
17 errors in these average properties are the largest source of uncertainty in the transport model  
18 approach. Another source of concern is the initialization of the model ozone with data from a  
19 different type of instrument (usually measurements of the HALOE or MLS satellite instruments)  
20 than is used for the ozone observations later on. Systematic discrepancies between the different  
21 instruments make altitude dependent correction factors necessary, that are often in the order of  
22 5% which is a substantial fraction of the ozone changes observed over the course of warmer  
23 Arctic winters. The method is sensitive to the vertical variation of the correction, because early  
24 winter measurements from one instrument at higher altitude are compared with late winter  
25 measurements from another instrument at lower altitude.

26 Manney *et al.* (*e.g.*, 1995a, b, 1996a, b, 1997) used a similar approach based on 'trajectory  
27 ensemble' calculations to analyze ozone data of the Microwave Limb Sounder (MLS) on the  
28 UARS satellite. Trajectory calculations are started at all points on the gridded MLS data and are  
29 run forward in time for a few weeks. Succeeding MLS measurements are interpolated to the  
30 locations of the trajectories. Differences in ozone are attributed to chemistry. The results are  
31 stated as vortex averaged ozone loss or are analyzed versus equivalent latitude, PV, etc. During

1 one north looking yaw cycle continuous time-series of ozone loss can be derived, accumulated  
2 losses are stated for the south looking yaw cycles, when measurements in the Arctic are not  
3 available. [Schoeberl \*et al.\*, \(2002\)](#) used trajectory ensemble calculations to advect early winter  
4 ozone observations throughout the winter and comparing it to succeeding ozone observations.  
5 Again the advected and the observed ozone fields are averaged over the polar vortex before they  
6 are compared, thus reducing the sensitivity of the approach to transport features of individual air  
7 masses. The trajectory ensemble approach uses 3-D trajectory calculations that are several  
8 months long for the advection. By using trajectories instead of a grid point advection scheme,  
9 any potential bias due to numerical diffusion of the advection scheme is eliminated. The largest  
10 uncertainty of the trajectory ensemble method comes from possible systematic biases in the long  
11 term trajectory calculations, *e.g.*, due to possible uncertainties in the vertical transport, that is  
12 based on calculated diabatic descent rates.

13  
14 ***Lagrangian Ozone Measurements (Match) [3.1.1.2]***  
15

16 'Match' is a Lagrangian technique to determine the rate of chemical ozone loss. In active  
17 Match campaigns ozonesonde launches from a large network of about 35 ground stations are  
18 coordinated in real time to probe individual air masses twice over an interval of a few days (so  
19 called 'match events,' *e.g.*, von der Gathen *et al.*, 1995; Rex *et al.*, 1997, 1998, 1999b, [2002a](#)).  
20 The coordination is based on calculations of air parcel trajectories that allow for diabatic descent.  
21 Several hundreds to more than a thousand ozonesondes are launched in a Match campaign,  
22 typically producing several match events per sonde, each at a different altitude and with different  
23 soundings as respective first measurement of the air mass. The coordination results in hundreds  
24 to thousands match events per winter. Chemical ozone loss rates are derived from a statistical  
25 analysis of subsets of match events from a certain time period (typically 14 days long) and  
26 altitude region (typically 20 K broad) by calculating linear regressions of the difference in ozone  
27 between both measurements and the sunlit time that the air mass encountered. The overall ozone  
28 loss during the winter is calculated by accumulating the measured loss rates. A similar approach  
29 has been used by Sasano *et al.* (2000) and [Terao \*et al.\* \(2002\)](#) to analyze the ozone measurements  
30 from the ILAS satellite instrument.

31 The largest uncertainties in this method are possible systematic errors in the trajectory  
32 calculations including the calculated diabatic subsidence rates. Individual Match events depend

1 on a correct representation of the motion of individual air masses by the trajectories. Therefore  
2 the length of the trajectory calculations used in Match is limited to 10 days and the majority of  
3 the Match events relies on ~5-7 days trajectories. But ozone loss rates are calculated in a  
4 statistical process from subsets of several tens of Match events, so that the derived average ozone  
5 loss rates are only sensitive to systematic trajectory errors, *e.g.*, possible systematic biases in the  
6 calculated diabatic descent rates. A statistical analysis of the data shows that observed ozone  
7 losses occur exclusively during sunlit periods along the trajectories. This suggests that any  
8 systematic biases in the trajectory calculations, if present, are so small that they do not  
9 significantly affect the derived ozone loss rates (*e.g.*, Rex *et al.*, 1998, 1999b, 2002b).

### 10 **3.1.2 APPROACHES THAT USE THE RELATION OF OZONE TO AN INERT TRACER**

11  
12 In mid-winter ozone abundances inside the polar vortex show a relatively compact relation  
13 to abundances of many long-lived tracer species such as N<sub>2</sub>O or CH<sub>4</sub>. In the absence of mixing  
14 any reduction of ozone versus an inert tracer indicates chemical loss of ozone. This approach  
15 has first been used by Proffitt *et al.* (1990). More recently early winter and late winter  
16 measurements of ozone, N<sub>2</sub>O, CH<sub>4</sub> and HF by the HALOE satellite instrument have been used to  
17 identify chemical loss of ozone during various winters (*e.g.*, Müller *et al.* 1996, 1997). The  
18 evolution of the ozone versus N<sub>2</sub>O relation through the winter 1999/2000 was studied using data  
19 from in-situ instruments on board of two balloon borne platforms and the high altitude aircraft  
20 ER-2 (Salawitch *et al.*, 2002a; Richard *et al.*, 2001).

21 Two fundamental issues have been brought up regarding the validity of the tracer relation  
22 approach. First, the existence of a compact universal relation between ozone and inert tracers  
23 has been questioned, and second the impact of mixing on results from ozone versus tracer  
24 relation studies has been discussed. Here we assess the current status of the discussion on these  
25 two points.

26 During polar summer the chemical lifetime of ozone in the middle and upper stratosphere  
27 is comparable or shorter than transport timescales, so the ozone-tracer relationship in the Arctic  
28 stratosphere in fall is not expected to be compact and universal (Plumb and Ko, 1992). But in  
29 fall the lifetime of ozone in the middle and lower stratosphere gets sufficiently long and it can be  
30 expected that mixing within the early polar vortex leads to compacting of the ozone-tracer  
31 relations inside the vortex. These slowly evolving more compact relations inside the vortex are

1 quite different from the extra vortex relations, with less ozone at a given tracer level than outside.  
2 The degree of compactness and the definition of this inner vortex 'early winter relation' is  
3 critical for the validity of the tracer relation approach. Richard *et al.* (2001) and Salawitch *et al.*  
4 (2002a) used initial O<sub>3</sub> versus N<sub>2</sub>O reference relations measured well inside the polar vortex in  
5 mid-winter (December/early January). They showed that these relations were sufficiently  
6 compact and representative of initial conditions inside the polar vortex, an essential condition for  
7 the validity of the approach. But observations of the O<sub>3</sub> versus CH<sub>4</sub> relation measured well  
8 inside the Arctic vortex in mid-winter for 1999/2000 were significantly lower (differences of O<sub>3</sub>  
9 of ~1.5 parts per million by volume (ppmv) for values of CH<sub>4</sub>≈0.5 ppmv) than the suite of initial  
10 HALOE based reference relations (Müller *et al.*, 1999 and references therein) measured in the  
11 vortex edge region in October for earlier Arctic winters (Salawitch *et al.*, 2002a). The validity of  
12 these early winter HALOE reference relations is currently the subject of numerous on-going  
13 investigations. Generally results from the tracer relation approach are more reliable when the  
14 initial reference relation is measured late (*i.e.*, December / early January) and deep inside the  
15 vortex.

16 The second issue brought up regarding the validity of tracer relation studies is related to  
17 mixing. These considerations apply also for studies that assess the degree of denitrification  
18 based on changes in the otherwise very compact relation between NO<sub>y</sub> and N<sub>2</sub>O. If the relation  
19 between two tracers is curved, as is the case for both these relations, the results of the tracer  
20 relation approach can be compromised by mixing between air masses that are widely separated  
21 in tracer space (*e.g.*, Waugh *et al.* 1997, Michelsen *et al.*, 1998; Rex *et al.*, 1999a; Plumb *et al.*,  
22 2000; Ray *et al.*, 2002). Isentropic mixing across the edge of the polar vortex or mixing of air  
23 masses inside the vortex that underwent different descent during the winter are examples for  
24 such long range mixing in tracer space. Furthermore the ozone / tracer relations inside the vortex  
25 are different from the relation outside of the polar vortex. After substantial ozone loss these  
26 differences can be very pronounced (several ppmv). Hence, any mixing across the vortex edge  
27 directly impacts the ozone / tracer relation inside of the vortex and could represent a potential  
28 source of uncertainty for the tracer relation approach.

29 One can attempt to distinguish mixing and chemical ozone loss (or denitrification) by using  
30 simultaneous measurements of two long-lived tracers (*e.g.*, CH<sub>4</sub> and N<sub>2</sub>O) to estimate the impact  
31 of mixing (Rex *et al.*, 1999a). However, this method is dependent on the assumption that there

1 had been a single mixing event after the bulk of the descent and is not applicable if there is  
2 intermittent mixing at descent (Plumb *et al.* 2000). A more general approach is the use of a  
3 linear combination of several long-lived tracers to form an artificial tracer that has a compact and  
4 linear relationship with O<sub>3</sub> (or NO<sub>y</sub>) (Esler and Waugh 2002). Due to its linearity this artificial  
5 relation is unaffected by mixing within the vortex, so deviations from this relationship can be  
6 more directly attributed to chemical ozone loss (denitrification). But mixing across the edge of  
7 the vortex edge is still a source of uncertainty, because the outside vortex relations are often  
8 different from the inside relations (for ozone versus N<sub>2</sub>O this is always the case, for NO<sub>y</sub> versus  
9 N<sub>2</sub>O this is the case after denitrification inside of the vortex). These attempts to correct for the  
10 impact of mixing in tracer relation studies were mainly focused on studies that used the relation  
11 of NO<sub>y</sub> versus N<sub>2</sub>O to assess denitrification.

12 [Salawitch \*et al.\* \(2002a\)](#) noted that considerations that are valid for the NO<sub>y</sub> versus N<sub>2</sub>O  
13 relation (*e.g.*, the relation  $\chi_2$  versus  $\chi_1$  in Plumb *et al.* (2000) resembles NO<sub>y</sub> versus N<sub>2</sub>O) should  
14 not be applied to the interpretation of the ozone versus N<sub>2</sub>O relation in the vortex, because ozone  
15 mixing ratios, unlike NO<sub>y</sub>, do not approach zero at the top of the vortex due to the influence of  
16 photochemistry at 40 km. Hence the curvature of the ozone versus N<sub>2</sub>O relation for low N<sub>2</sub>O  
17 (*i.e.*, N<sub>2</sub>O between 10 and 40 ppbv) is much less pronounced than that of NO<sub>y</sub> versus N<sub>2</sub>O and  
18 mixing can not lead to the observed changes in the ozone tracer relations that have been observed  
19 *e.g.*, by HALOE. More quantitatively simultaneous measurement of multiple long-lived tracers  
20 have been used to argue that the impact of mixing on estimates of chemical ozone loss by the  
21 tracer relation approach for the Arctic winter of 1999/2000 was negligible. Based on the  
22 temporal evolution of CO<sub>2</sub>, CFC-11, N<sub>2</sub>O, and O<sub>3</sub> within the vortex Richard *et al.* (2001) and  
23 [Salawitch \*et al.\* \(2002a\)](#) demonstrated that the vast majority of the observed changes in the  
24 O<sub>3</sub>/N<sub>2</sub>O relations were due to chemistry and could not have been caused by dynamics. The  
25 isolation of the Arctic vortex for this winter was also noted by a multivariate analysis of the time  
26 evolution of nearly a dozen tracers with varying lifetimes (Ray *et al.*, 2002). [Rex \*et al.\* \(2002a\)](#)  
27 showed that during January to March 2002 any mixing across the vortex edge would have led to  
28 an underestimation of the ozone loss by tracer relation studies, so that the results of tracer  
29 relation studies that rely on initial relations from early January can be regarded as conservative  
30 estimates of the loss. These results from the Arctic winter of 1999/2000 support the validity of

1 the tracer relation approach, provided the reference relation is defined in mid-winter, but it is  
2 currently not clear whether these results can be applied to other, more dynamically active winters  
3 (e.g., [Salawitch et al. 2002a](#)).

## 4 **3.2 Arctic Ozone Loss during the Last Decade**

5  
6 Since WMO (1998) a number of approaches to quantify the degree of chemical ozone loss  
7 in the Arctic have been used in a consistent way for several winters during the 1990s. Due to  
8 these long-term efforts the extent and the variability of Arctic ozone losses is now well  
9 characterized for the last ten years. Several techniques have revealed a large interannual  
10 variability of chemical ozone losses in the Arctic.

### 11 **3.2.1 OZONE LOSS RATES NEAR THE MAXIMUM OF THE OZONE CONCENTRATION**

12  
13 The Match approach was used consistently over the last decade to study the evolution of  
14 chemical ozone loss at about 475 K potential temperature (~19 km altitude). At polar latitudes  
15 this level is close to the maximum concentration of ozone in the ozone layer. Figure 3-1 shows  
16 the measured ozone loss rates for the winters 1991/1992 to 2000/2001 (compilation of Match  
17 results based on [Rex et al., 1997, 1998, 1999b, 2002a](#); [Schulz et al., 2000, 2001](#)). Little or no  
18 significant ozone loss was observed in 1997/1998 and 1998/1999. The accumulated ozone loss  
19 during the winter was particularly large in 1995/1996 and 1999/2000, when relatively large loss  
20 rates have been sustained for extended periods of time. The chemical ozone loss rate in the  
21 Arctic stratosphere is clearly controlled by temperature. Blue shaded areas in Figure 3-1 indicate  
22 the geographical areas ( $A_{PSC}$ ) where temperatures have been below  $T_{PSC}$  (the NAT equilibrium  
23 temperature based on 5 ppmv water vapor and an average  $HNO_3$  profile based on measurements;  
24  $T_{PSC}$  is a convenient threshold that roughly indicates the onset of rapid heterogeneous chemistry  
25 in the stratosphere, independent of the actual composition of the PSCs). All periods of rapid  
26 chemical ozone loss in Figure 3-1 are associated with preceding large values of  $A_{PSC}$ . No  
27 significant chemical loss of ozone has been observed in warm winters, when  $T_{PSC}$  was not or  
28 only barely reached.

1 **3.2.2 VERTICAL PROFILES OF OZONE LOSS**

2  
3 The determination of vertical profiles of ozone loss requires ozone losses quantifications in  
4 a broad altitude range. Ozone loss observations are typically most reliable at levels around 475  
5 K. Below 400 K or above 550 K the uncertainty of observational studies is typically  
6 significantly larger. The problems at lower levels are (a) a strong vertical gradient in the average  
7 ozone mixing ratio profile largely amplifies the uncertainty introduced by diabatic descent, and  
8 (b) larger small scale dynamical activity (the presence of higher wave numbers) makes explicit  
9 transport calculations less reliable and leads to larger degrees of mixing, which is problematic for  
10 all approaches. Above 550 K average poleward motion and influx into the polar vortex,  
11 followed by mixing, is the main problem. The strong diabatic descent at higher altitudes causes  
12 additional uncertainty only in winters when the vertical gradient in the average ozone mixing  
13 ratio profile is significant at these levels, which is not always the case (*e.g.*, compare 1998/1999  
14 with 1997/1998 in Figure 3-2).

15 Figure 3-2 shows ozone losses derived from the vortex average approach in the vertical  
16 region between  $\Theta=360$  and 570 K (update from [Rex \*et al.\* \(2002a\)](#) for various winters). Results  
17 at the lowest and highest levels shown are less reliable. It is based on several hundred  
18 ozonesonde measurements per winter inside the vortex from a network of about 35 sounding  
19 stations. The vortex-averaged ozone profiles have been plotted against the ‘spring-equivalent  
20 potential temperature,’  $e\Theta$ , which is the potential temperature that a given air mass reached at the  
21 end of March due to diabatic subsidence. By using  $e\Theta$ , which is a conserved quantity, diabatic  
22 effects are accounted for. In the absence of mixing across the vortex edge, any change in the  
23 vortex-averaged ozone versus  $e\Theta$  profile indicates chemical loss of ozone. In Figure 3-2 the  
24 large interannual variability of the ozone loss stands out. During winter 1998/1999 no  
25 significant loss of ozone was found at any part of the profile. In contrast, the loss of ozone in  
26 1999/2000 exceeded 70% in a ~1 km thick region centered around 460 K. This local loss is  
27 slightly more than in any previous Arctic winter, with 64% local loss in winter 1995/1996 as the  
28 previous record. However, in 1995/1996 ozone loss occurred over a broader vertical region  
29 (*e.g.*, ozone loss of more than 1 ppmv occurred between ~390-530K in 1995/1996, compared to  
30 ~420-510 K in 1999/2000), so that the vertically integrated losses in both years are comparable.



5/7/02

1        The average value of APSC ( $\bar{A}_{PSC}$ ), averaged from mid-December to end of March  
2 between 400 and 550 K potential temperature is given in Figure 3-2. Figure 3-3 shows the  
3 relation between  $\bar{A}_{PSC}$  and the average accumulated ozone loss between 400 and 550 K  $e\Theta$ . A  
4 surprisingly close quantitative relation between both quantities suggests that the chemical loss of  
5 ozone in the Arctic stratosphere in a given winter correlates strongly with the parameter  $\bar{A}_{PSC}$ .  
6 The compactness of the relation shown in Figure 3-3 is currently not fully understood. To  
7 reproduce this empirical relation is a major challenge for global chemistry transport models. The  
8 ability of models to reproduce the slope of the relation shown in Figure 3-3 is crucial, when  
9 models are to be used to predict the impact of climate changes on future ozone losses.

### 10 **3.2.3 EFFECT OF OZONE LOSS ON THE TOTAL OZONE COLUMN**

11  
12        Estimating the total column loss of ozone also requires a good quantification of ozone  
13 losses in a broad vertical region. The region above 550 K is of less concern for ozone column  
14 loss estimates because it contributes little to the total column amount of ozone, due to the small  
15 ozone concentrations at these altitudes. But uncertainties in the ozone loss estimates at altitudes  
16 below 400 K make ozone column loss estimates generally less reliable than estimates of local  
17 ozone losses near 19-20 km. The ozone column loss has been estimated for all winters since  
18 1993/1994 with the transport model approach. Figure 3-4 shows the difference between ozone  
19 columns as measured by the SAOZ UV-visible network in the Arctic (Ny Ålesund, Thule,  
20 Scoresbysund, Sodankylä, Salekhard, Zhigansk, and Harestua) and the column of passive ozone  
21 in REPROBUS (again, initialized with POAM measurements in early winter) above these  
22 stations. In many winters, large deficits of observed ozone compared with passively advected  
23 ozone have been observed. These deficits are attributed to chemical loss of ozone. Associated  
24 with persistently low temperatures in the winters of 1994/1995, 1995/1996, 1996/1997, and  
25 1999/2000 large chemically induced ozone reductions of 22-31% have been observed inside the  
26 vortex. The ozone loss during the warmer winter 1998/1999 has been smaller and is hardly  
27 significant. In the relatively warm winter 1997/1998 ozone column losses derived from the  
28 transport model approach were still significant (20%). In this winter temperatures dropped  
29 below the PSC threshold only in very limited geographical regions inside the vortex and only  
30 during short periods (see Figure 3-1). From the vortex average approach (Figure 3-2) some  
31 limited ozone loss in 1997/1998 is also visible, but only below 450 K. During that year March

1 results at 475 K indicate no significant loss, but results for 450 K and below are not available  
2 from Match of that year.

### 3 **3.2.4 CHEMICAL OZONE LOSS IN THE ARCTIC WINTER 1999/2000**

4  
5 The winter of 1999-2000 had the largest potential for PSC formation for at least the last 20  
6 years. Due to the extensive SOLVE-THESEO 2000 campaign during the winter 1999/2000 all  
7 basic approaches outlined in Section 3.1 were used to study the ozone loss throughout the winter,  
8 resulting in a better characterization of the ozone losses in 1999/2000 than in any previous winter  
9 and providing a unique opportunity to compare results from the different techniques.

10 All approaches identified extensive chemical loss of ozone. Figure 3-5(a) shows the  
11 evolution of the vortex averaged ozone loss in a vertical section as determined with the Match  
12 approach. Ozone loss started at altitudes above 500 K in mid January. The largest loss rates of  
13  $61 \pm 4$  ppbv per day (vortex average) were observed at 450 K in early March. [Rex \*et al.\* \(2002a\)](#)  
14 showed that the vertical structure and the time evolution of the observed ozone loss agrees well  
15 with the vertical structure and the time evolution of observations of high levels of active  
16 chlorine. During the winter 1999/2000 only approaches that are based on ozonesonde  
17 measurements, like Match and the vortex average approach, were able to capture the full extent  
18 of the ozone loss, *i.e.*, cover the full altitude range of the loss and the time period from early  
19 January to late March in vertical resolution. Comparisons of the results with other approaches  
20 are possible for a slightly shorter period and focus on the region close to 450 K. Here the results  
21 of all approaches agree very well (see Section 3.3).

22 Figure 3-6 shows the impact of the cumulative ozone loss through the winter on the vortex  
23 averaged vertical ozone profile at the end of March. In a layer of air around 18 km altitude the  
24 degree of chemical ozone destruction reached 70%.

25 Table 3.1 gives an overview over various estimates for the deficit in the total column  
26 amount of ozone due to chemical loss of ozone. The numbers given are the difference between  
27 the actually observed column amount of ozone and the column amount of ozone that would have  
28 been present at a given day in the absence of chemical ozone loss, dynamics being equal. For  
29 comparable time periods the agreement between results from all approaches is within the error  
30 bars. The results from the SAOZ/transport model study are generally somewhat higher than the  
31 other approaches and have larger uncertainties. The results of the other approaches agree to

1 better than 20%. Figure 3.5c shows the evolution of the total column loss through January to  
2 March, as determined by Match. By the end of March the chemically induced ozone deficit  
3 amounted to 90 to 100 DU. This is roughly the amount of total ozone that has been supplied to  
4 the polar vortex by dynamic effects during the same time, so that the total ozone column  
5 remained relatively constant during January to March (Rex *et al.*, 2002a), which is in contrast to  
6 the natural, climatological increase of the Arctic ozone column during this season.

7 **Table 3-1.** Comparisons of chemical loss of column ozone, column [O<sub>3</sub>\*-O<sub>3</sub>] (see Rex *et al.*,  
8 2002a), inside the Arctic vortex for the winter of 1999/2000 as of the indicated date. N/A  
9 indicates that data for that date is not available.

10  
11

<b>Data Source:</b>	OMS Balloon	POAM III Satellite	SAOZ Network	Ozonesondes
<b>Method:</b>	Tracer-Tracer (O <sub>3</sub> vs. N <sub>2</sub> O)	Vortex Averaged Descent	Transport model	Match
<b>Reference:</b>	Salawitch <i>et al.</i> (2002a)	Hoppel <i>et al.</i> (2002)	Goutail <i>et al.</i> (2002)	Rex <i>et al.</i> (2002a)
<b>5 March 2000</b>	61 ± 14 DU	51 ± 11 DU	85 ± 24 DU	53 ± 11 DU
<b>15 March 2000</b>	N/A	67 ± 11 DU	98 ± 25 DU	71 ± 12 DU
<b>28 March 2000</b>	N/A	N/A	101 ± 30 DU	88 ± 13 DU

12

### 13 3.3 Consistency between the Different Observational Techniques

14

15 Comparisons of the different approaches used to infer Arctic ozone loss are often hampered  
16 by the fact that the altitude range, horizontal extent (vortex definition) and time periods used in  
17 the various published works are different. These differences are partly unavoidable due to the  
18 constraints of the data sets used. But often the data sets can be reanalyzed for certain time  
19 periods and regions where they overlap, so that the results can be directly compared.

20

21 For the winter 1999/2000 basically all approaches can be used to calculate the amount of  
ozone loss that occurred inside the polar vortex between 20 January and 12 March in the layer of

1 air that subsided from about 475 to 450 K during this time. This subsiding layer of air is  
2 indicated in Figure 3-5(a) by the solid black lines. Figure 3-7 summarizes the accumulated  
3 ozone losses as determined for this layer of air with the various techniques. The average of the  
4 various estimates is 1.65 ppmv of ozone loss for this specific time period and vertical region.  
5 The results from all techniques are within +/-20% of this value, all but two are within +/-10% of  
6 the average.

7 The winter 1999/2000 was characterized by relatively weak dynamic activity and perhaps  
8 less than average exchange of air across the vortex edge (see Section 2.1). It is reasonable to  
9 assume that for the winter 1999/2000 the agreement between different techniques to estimate the  
10 degree of chemical ozone loss from ozone observations may be better than for dynamically more  
11 active winters. However, to investigate this [Harris \*et al.\* \(2002\)](#) reanalyzed data from past  
12 winters during the 90s, using different techniques and data sets, focusing on time periods where  
13 the data sets overlap. Based on results from many winters they found an agreement of generally  
14 better than 20% between techniques that use explicit transport calculations. Results from tracer  
15 relation studies showed slightly larger discrepancies compared with these results, when the initial  
16 tracer relation was measured early in fall. This agreement is 25% or better, when the initial  
17 tracer relation is measured in mid-winter, *e.g.*, in December.

18 Based on these studies, the results from current estimates of the degree of chemically  
19 induced Arctic ozone losses appear to have an accuracy of about 20%.

### 20 **3.4 The Effect of Denitrification on Ozone Loss in the Arctic**

21  
22 The effect of denitrification on ozone loss has been quantified (to some extent) in both  
23 hemispheres. In the Antarctic (complete) denitrification is shown to cause a 10% increase in the  
24 column ozone loss ([Brasseur \*et al.\*, 1997](#); [Portmann \*et al.\*, 1996](#)).

25 Evidence for a much more significant impact of denitrification (see Section 2.3) on Arctic  
26 ozone losses in recent cold winters has increased. Observational results indicate that the degree  
27 of ozone loss in the Arctic was significantly amplified by denitrification during the winters of  
28 1994/1995, 1995/1996 and 1999/2000. Using model studies [Rex \*et al.\* \(1997\)](#) concluded that in  
29 winter 1995/1996 observed ongoing chemical ozone loss in certain air masses more than one  
30 month after the last exposure to PSCs can only be explained by approximately 80%  
31 denitrification in about half of the air masses inside the polar vortex. In this winter the heavily

1 denitrified layer of air was limited to a very narrow vertical region of less than 1 km thickness at  
2 about 20 km altitude.

3 Waibel *et al.* (1999) presented measurements of denitrification in the Arctic winter  
4 1994/1995, based on the  $\text{NO}_y$  versus  $\text{N}_2\text{O}$  relation, and used a chemical model to conclude that  
5 in the denitrified air masses the degree of ozone loss was enhanced by at least 30% compared to  
6 what would have occurred without denitrification. They show, that the model results can come  
7 close to the observed ozone loss only when the observed denitrification is taken into account.

8 Gao *et al.* (2001b) present measurements of varying degrees of denitrification (also based  
9 on the  $\text{NO}_y$  versus  $\text{N}_2\text{O}$  relation) in different areas of the polar vortex, as characterized by fixed  
10 ranges of  $\text{N}_2\text{O}$  and potential temperature. Succeeding observations of the rate of ozone loss  
11 based on analyzing sets of photochemically intercomparable air masses indicate largest loss rates  
12 at the  $\text{N}_2\text{O}$  levels that were most severely denitrified (about 30% larger losses than in less  
13 denitrified air). Gao *et al.* (2001b) show that these differences in the ozone loss rate can not be  
14 explained by differences in solar exposure or initial chlorine activation and hence are most likely  
15 a result of the denitrification.

16 These observational studies have shown that denitrification in cold Arctic winters can  
17 cause up to 30% increase in ozone loss at a given altitude, a result that is confirmed by model  
18 studies (Chipperfield and Pyle, 1998; Tabazadeh *et al.*, 2000; Drdla and Schoeberl, 2002). The  
19 more pronounced effect of denitrification on ozone loss in the Arctic, compared to the Antarctic  
20 is the result of higher temperatures in the Arctic. In the Antarctic reactivation of chlorine out of  
21 the reforming  $\text{ClNO}_3$  reservoir via reactions on cold liquid aerosol particles (*e.g.*,  $\text{ClNO}_3 + \text{H}_2\text{O}$ )  
22 can sustain a high level of active chlorine in spring (Portmann *et al.*, 1996) This is much less  
23 effective in the Arctic, since the heterogeneous reaction of  $\text{ClNO}_3 + \text{H}_2\text{O}$  is much slower at the  
24 higher temperatures typical for the Arctic spring and hence the lifetime of active chlorine is  
25 strongly dependent on the rate of formation of  $\text{ClNO}_3$  and hence the abundance of  $\text{HNO}_3$ . The  
26 overall effect of denitrification on Arctic column ozone loss depends on the vertical range of  
27 severe denitrification. Currently, the effect of denitrification on Arctic ozone is limited to the  
28 altitude range of ~18 to 21 km, where most parcels are shown to be severely denitrified in cold  
29 winters (Hintsa *et al.*, 1998; Kondo *et al.*, 2000; Fahey *et al.*, 2001). Microphysical sensitivity  
30 studies have shown that a cooling of the lower stratosphere could significantly extend the vertical  
31 range of severe denitrification in the Arctic (Waibel *et al.*, 1999; Tabazadeh *et al.*, 2001).

1 It is important to note that current denitrification schemes that are used *e.g.*, in 3-D-CTMs  
2 have severe difficulties to correctly represent the degree of denitrification in cold Arctic winters  
3 (*e.g.*, Davies *et al.*, 2002, see also Section 2.2). In the light of the recent results that extensive  
4 denitrification (up to 80%) occurred in cold Arctic winters and that it had significant impact on  
5 the degree of ozone loss in these years, the correct representation of denitrification remains one  
6 of the major challenges for 3-D-CTMs, when they are used to study the variability of chemical  
7 ozone loss in the Arctic (*e.g.*, Chipperfield and Jones, 1999) or to predict future ozone losses in a  
8 potentially changing climate.

9 Dehydration, unlike denitrification, can moderate ozone loss for two reasons (Portmann *et*  
10 *al.*, 1996, Chipperfield and Pyle, 1998). First, in a drier atmosphere it is harder for PSCs to  
11 form. Second, heterogeneous reaction rates that lead to active chlorine production drop  
12 exponentially with decrease in relative humidity. Sensitivity studies show that dehydration (to  
13 the level of ice saturation) in the Antarctic can decrease column ozone loss by about 20%  
14 (Portmann *et al.*, 1996; Brasseur *et al.*, 1997). No large-scale model calculations have yet been  
15 performed to evaluate the role that dehydration may play in Arctic ozone loss and recovery in the  
16 future. However, it is unlikely that climate change in the near future could cause extensive  
17 dehydration in the Arctic region. Some air mass trajectory statistical analyses indicate that even  
18 a substantial cooling of lower stratospheric temperatures (by 3 to 4 K) is still insufficient to  
19 trigger the occurrence of severe dehydration in the Arctic vortex (Tabazadeh *et al.*, 2000).

### 20 **3.5 Model Studies of Arctic Ozone Loss**

21  
22 Model investigation of polar ozone loss was the subject of intense research in recent years.  
23 Most studies concentrated on the Arctic region due to the high interannual variability of the  
24 Arctic ozone loss in relation with the year-to-year meteorological conditions. 3-D CTMs, which  
25 proved to be particularly well fitted to the non zonal character of the Arctic polar vortex, have  
26 been used to estimate the overall degree of polar ozone loss for several winters. For more  
27 specific studies or highly constrained comparisons between models and ozone loss observations  
28 photochemical box models were used.

### 1 3.5.1 CHEMICAL TRANSPORT MODELS

2  
3 Studies using the transport model approach to estimate ozone loss from ozone  
4 measurements typically include a comparison with the ozone loss calculated by the chemistry  
5 module of the model. Chemical ozone loss inferred from the POAM II and III measurements  
6 was compared with that obtained from the REPROBUS model (Deniel *et al.*, 1998; 2000). In the  
7 same way, total ozone measurements by the SAOZ network were compared with REPROBUS  
8 and SLIMCAT simulations for various Arctic winters from 1993/1994 (Figure 3.4; Goutail *et al.*,  
9 1999; 2002). The agreement between the observed ozone loss and the model result varies from  
10 winter to winter. Overall a couple of points can be seen in Figure 3.4. (a) The overall interannual  
11 variability of the Arctic ozone loss is reasonably well represented by the models. A large  
12 fraction (between about 60 and 100%) of the overall Arctic ozone loss is reproduced by the  
13 models. (b) In winters when substantial ozone loss was observed during January (1994/1995,  
14 1995/1996, and 1999/2000), the models fall short of reproducing this January loss. Typically, by  
15 the end of January, only about 50% of the observed loss is accounted for by the models. The  
16 loss in January is part of the reason, why the overall loss at the end of the winter is sometimes  
17 underestimated (*e.g.*, 1994/1995). In other winters the January loss contributes only a minor  
18 fraction to the overall loss (*e.g.*, 1999/2000) or the model overestimates the loss rate later during  
19 the winter so that the overall loss at the end of the winter is better reproduced than the time  
20 evolution of the loss (*e.g.*, 1995/1996). Also, in 1995/1996 the simulated vertical distribution of  
21 the ozone loss at the end of March differs from that estimated from POAM II measurements with  
22 the model resulting in larger losses at lower altitudes and smaller losses at higher altitudes  
23 compared to the observations (Deniel *et al.*, 2000). It appears that a good agreement between  
24 observations and modeled total ozone loss at the end of the winter alone may be fortuitous and  
25 does not necessarily prove that the ozone loss mechanisms in the model are well-reproduced.

26 Extensive modeling studies were performed as part of SOLVE/THESEO 2000 in order to  
27 estimate the ozone loss in the winter 1999/2000. Sinnhuber *et al.* (2000) compared the chemical  
28 ozone loss estimated with SLIMCAT with that derived from the model ozone passive tracer and  
29 ozonesondes observations at Ny Ålesund (Figure 3-8). They found good agreement between the  
30 modeled ozone and observations, both indicating more than 2.5 ppmv ozone destruction by late  
31 March, corresponding to 70% ozone loss at the 450 K isentropic level, the largest ozone loss ever

1 produced by SLIMCAT. The reason for the large loss of ozone in the model was extensive  
2 formation of large denitrifying ice particles by the model's microphysical scheme. But the large  
3 scale formation of ice clouds in the model was merely the result of a cold bias in the UKMO  
4 temperature fields used in SLIMCAT and is not consistent with observations during  
5 SOLVE/THESEO 2000. Coincidentally the extensive denitrification produced by the erroneous  
6 representation of ice clouds in the model is in agreement with observations of denitrification.  
7 The mechanism how the observed denitrification occurred in the atmosphere is still under  
8 investigation (see Section 2.2.3) and is not included in the model used by Sinnhuber *et al.*  
9 (2000). Using a correct temperature field SLIMCAT would have significantly underestimated the  
10 ozone loss during winter 1999/2000, as in many earlier cold Arctic winters (*e.g.*, Hansen *et al.*,  
11 1997).

12 The KASIMA (Karlsruhe Simulation model of the Middle Atmosphere) CTM driven by  
13 ECMWF analyses was compared with ozone measurements by a FTIR spectrometer and a  
14 millimeter wave radiometer in Kiruna for the winter 1999/2000. The modeled total ozone loss  
15 underestimates the observations by 30% and 20% respectively (Kopp *et al.*, 2002).

16 The Langley Research Center (LaRC) Lagrangian chemical transport model (LCTM) was  
17 used in conjunction with HALOE and POAM III satellite observations to simulate the large-scale  
18 photochemical evolution of the Arctic vortex in 1999/2000 from vortex ensemble of air mass  
19 trajectories using UKMO analyses (Pierce *et al.*, 2001). The model shows significant  
20 denitrification within the vortex in late December and early January. A significant  
21 overprediction of the level of chlorine activation is found in early March but the predicted peak  
22 ozone loss rate is in good agreement with that inferred from the Match campaign during the same  
23 period. Conversely it can be concluded that for a realistic level of active chlorine the model  
24 would have significantly underestimated the observed ozone loss rate during this period.

25 Grooss *et al.*, (2002) report simulations with the Chemical Lagrangian Model of the  
26 Stratosphere (CLaMS). This model simulates the dynamics and chemistry of multiple air parcels  
27 along their trajectories which are determined from ECMWF winds. The model includes mixing  
28 between neighboring air parcels. In this model study, the degree of denitrification was described  
29 from observations by using observed relations between  $\text{NO}_y$  and  $\text{N}_2\text{O}$  and the temperature  
30 history based on ER-2 measurements. The simulation was initialized on 10 February, and the



1 ozone loss during the mid-February to mid-March period (up to 60% at 425-450 K) agrees  
2 roughly with estimates from observations.

3 The various 3-D model studies focusing on the winter 1999/2000 reveal a consistent  
4 picture. The ozone loss after mid-February is well reproduced if the degree of denitrification in  
5 the model is correct, be it by coincidence like in Sinnhuber *et al.* (2000) or because it was  
6 specified from observations like in Grooss *et al.* (2002). Currently 3-D CTMs are not able to  
7 reliably reproduce the degree of denitrification within the model. This deficit limits the current  
8 ability to reliably reproduce the degree of ozone loss in cold Arctic winters.

### 9 **3.5.2 SPECIFIC MODEL STUDIES**

10  
11 Several modeling studies using box models were conducted to compare specific ozone loss  
12 observations with model results and test our understanding of the chemical processes involved in  
13 the loss. These calculations are performed specifically for the air masses in which the ozone  
14 losses have been observed. Hence the temperature and solar zenith angle history in these studies  
15 are much more constrained than in comparisons of vortex averaged ozone losses. Becker *et al.*  
16 (1998; 2000) performed box model simulations along each trajectories of the Match data set for  
17 1991/1992 and 1994/1995. They concluded that the model underestimated the ozone losses  
18 observed by Match in late January 1992 and 1995 by up to a factor of two above 475 K. During  
19 the other months the observed losses were also underestimated by the model but within the large  
20 uncertainties of the model mainly linked to the extent of denitrification.

21 Match ozone loss rates were also compared to SLIMCAT simulations for the winters  
22 1994/1995 and 1995/1996 (Kilbane-Dawe *et al.*, 2001). The study suggests that Match may  
23 have overestimated the ozone loss rates above 525 K in January 1995 due to deficiencies in the  
24 ECMWF wind fields close to the top level of the ECMWF assimilation model (the top level was  
25 shifted to higher levels since then). In January 1995 at levels below 525 K and in January  
26 1995/1996 SLIMCAT generally underestimated Match ozone loss rates by about 30 to 50%. It  
27 was found that the SLIMCAT photochemistry was the least able to reproduce observed ozone  
28 losses when low temperatures coincide with high solar zenith angles.

29 Woyke *et al.* (1999) used the tracer relation approach to quantify ozone loss in air masses  
30 that have been probed by a balloon payload providing observations of ClO, BrO, O<sub>3</sub>, and long-  
31 lived tracers, on 3 February 1995. They used box model runs constrained by ClO and BrO

1 concentrations observed by the balloon, to calculate the ozone loss throughout January along the  
2 back trajectories of the air masses. Using this highly constrained approach they could explain  
3 only half of the observed ozone loss.

4 These results confirm that ozone losses observed during cold Arctic Januarys are currently  
5 not understood.

### 6 **3.6 Quantifying Antarctic Ozone Loss**

7  
8 As emphasized in Section 1, the Antarctic ozone depletion is monitored by ground-based  
9 and satellite measurements since the mid-eighties. However, relatively few studies have recently  
10 concentrated on a detailed quantification of Antarctic ozone loss rates with state-of-the-art  
11 approaches to separate chemical loss from dynamical impacts. Hence our quantitative knowledge  
12 of Antarctic ozone loss rates is not as good as in the Arctic. The quantification of the  
13 accumulated overall ozone loss in the Antarctic is not challenging since by the end of the winter  
14 ozone is basically completely lost in a broad vertical region.

15 Hofmann *et al.*, 1997 quantified Antarctic ozone loss from the analysis of ten years of  
16 ozonesonde measurements at the south pole and made recommendations for the detection of the  
17 recovery of the Antarctic ozone. Indicators for recovery include an end to springtime ozone  
18 depletion at 22-24 km and a 12-20 km ozone column value of more than 70 DU on 15  
19 September. Bevilacqua *et al.* (1997) used POAM II ozone observations above Antarctica to  
20 derive vortex average ozone loss rates in August and September from 1994 to 1996 in the 450-  
21 800 K potential temperature range. Over the three years significant loss of ozone is found over  
22 the whole period, except in 1994, when ozone loss was not observed in August, due to the  
23 sampling of the POAM instrument. The largest loss rates are found in September 1996 where  
24 they reach 0.1 ppmv/d below 500 K. From the analysis of the temporal evolution of total ozone  
25 at the Faraday station together with model calculations, Roscoe *et al.* (1997) showed that the  
26 ozone chemical depletion starts in June at the sunlit vortex edge, and Waters *et al.* (1999) show  
27 that enhanced abundances of ClO are observed on the sunlit edge of the Antarctic vortex by late  
28 May or early June. Ozone loss rates were evaluated above the Antarctic station of Dumont  
29 d'Urville (66.4°S, 140°E) from ozonesonde and lidar measurements on an interannual basis  
30 (Godin *et al.*, 2001). Interpretation of the data required careful analysis of PV-equivalent  
31 latitude to determine whether each observation was inside, in the edge or outside the vortex at

1 different isentropic levels. Measurements inside the vortex showed complete ozone destruction  
2 from 400 to 500 K with ozone loss rates reaching 0.06 ppmv/d in the late August-September  
3 period.

### 4 **3.7 Model Studies of Antarctic Ozone Loss**

5  
6 The few recent model studies of the Antarctic ozone loss generally point to an agreement  
7 between models and observations. The SLIMCAT model was used to study the austral  
8 stratosphere in winter and spring 1996 together with ozonesonde measurements from various  
9 Antarctic stations (Lee *et al.*, 2000). The model shows very good agreement with measured  
10 ozone values and both the model and observations show that chemical ozone depletion follows  
11 the edge of polar night with little mixing poleward until the terminator reaches 80°S. In a follow  
12 up study, Lee *et al.*, (2001) analyze the isentropic transport processes within the Antarctic polar  
13 vortex. Their calculations indicate two distinct regions within the vortex: a strongly mixed  
14 vortex core and a broad ring of weakly mixed air that remains isolated from the core between  
15 late winter and mid-spring and where the ozone loss is not complete. This result has an  
16 implication for the recovery of Antarctic ozone since a cooling of the stratosphere could enhance  
17 the ozone loss in the edge region and delay the ozone recovery. In another study of Antarctic  
18 ozone loss, Wu and Dessler, (2001) test the current understanding of polar ozone chemistry with  
19 version 4 MLS measurements of O<sub>3</sub> and ClO. By comparing the observed ozone loss estimated  
20 from the MLS ozone evolution at 465 K with a modeled ozone loss inferred from the  
21 simultaneous ClO measurements and a fixed BrO mixing ratio, they find a good agreement  
22 between both methods. However, MLS version 5 data, that has a better vertical definition of the  
23 ClO profile, resulted in a significantly reduction of the ClO concentrations at 465K compared to  
24 version 4 data that has been used in Wu and Dessler (2001). This reduction would lead to a  
25 reduction in the modeled ozone loss rate in Wu and Dessler (2001). A slight change in the ozone  
26 profile in MLS version 5 data compared to version 4 data would also reduce the ozone loss rate  
27 deduced from observations. A quantitative study would be required to assess how the  
28 conclusions of Wu and Dessler (2001) would change if MLS version 5 data had been used.

1 **3.8 Conclusion**

2  
3 Arctic chemical ozone losses during the last decade have been determined by a variety of  
4 approaches and ozone loss rates are now better quantified in the Arctic than in the Antarctic.  
5 The uncertainty of state-of-the-art approaches to quantify Arctic ozone losses from ozone  
6 observations is below 20% for local losses between 400 and 550 K potential temperature and  
7 perhaps somewhat larger for total column loss estimates. Large interannual variability of the  
8 Arctic ozone loss, ranging from 0-70% loss at about 20 km for individual winters during the past  
9 decade, is driven by the variable extent of temperatures low enough for PSC formation in a given  
10 winter. Global chemical transport models reproduce a large fraction (60-100%, depending on  
11 the winter) of the observed ozone loss in the Arctic and its variability. The largest uncertainties  
12 are due to the current unrealistic representation of denitrification processes in 3-d CTMs and  
13 unexplained ozone losses during cold Arctic Januarys. These uncertainties currently prevent  
14 reliable predictions of future Arctic ozone losses in a potentially changing climate.

15 **4 CAUSES OF POLAR STRATOSPHERIC TEMPERATURE TRENDS**

16 **4.1 Introduction**

17  
18 In WMO 1999, it was recognized that the future development of the ozone layer does not  
19 depend just on changes in stratospheric halogen loading but also, very importantly, on a number  
20 of other factors connecting chemistry and climate. While the observations of temperatures are  
21 discussed in Section 1.2.2, the causes of trends in polar stratospheric temperatures are discussed  
22 here: the role of changes in well-mixed greenhouse gases (WMGHGs), in ozone, water vapor  
23 and aerosol particles are reviewed. Solar effects are also noted. The onset of cold temperatures  
24 during the polar winter/ spring, its duration, interannual variations and the statistical significance  
25 of trends over the past two decades are issues that impact upon our knowledge of the chemistry-  
26 climate interactions and the detection and attribution of climate change in the polar stratosphere  
27 due to ozone and other greenhouse gases.

28 Observations, from radiosondes and satellites have shown a general cooling of the polar  
29 lower-stratosphere over the last few decades (WMO, 1999; Ramaswamy *et al.*, 2001). For a  
30 number of reasons detection and attribution of temperature change in the lower-stratosphere may

1 be easier than at the surface (IPCC, 1996). Firstly, the observed temperature change in the  
2 stratosphere is large and the response time of the stratosphere is shorter, compared to the surface.  
3 There are relatively good satellite observations of both temperature and the important  
4 atmospheric constituents over the last few decades, corresponding to the timing of polar ozone  
5 depletion. There are also potentially fewer relatively uncertain mechanisms involved in  
6 stratospheric temperature change; many of the large and uncertain surface radiative forcings,  
7 such as the anthropogenic sulfate aerosol forcing, are expected to have a minimal effect on  
8 stratospheric temperatures. Further, the magnitude of the response in the stratosphere to a given  
9 mechanism has been shown to be reasonably well approximated by purely radiative processes,  
10 and therefore may be better quantifiable than the surface temperature response (Ramaswamy *et*  
11 *al.*, 2001). However, the WMO (1999) ozone assessment acknowledged that the large variability  
12 of temperatures, particularly in the Arctic winter and spring, and a possible stratosphere-wide  
13 trend in stratospheric water vapor complicate the attribution issue. It is now recognized that  
14 ozone and WMGHG changes can not be considered in isolation and there is an increasing  
15 acknowledgement that it is important to attempt to quantify the feedbacks between temperature  
16 change, chemistry and stratospheric dynamics, to better understand the stratospheric temperature  
17 response.

18 Since the last assessment there has been improved quantification of atmospheric  
19 constituent changes and development of more sophisticated stratospheric models, especially  
20 coupled chemistry general circulation models. These have provided important insights into our  
21 understanding of polar temperature changes in the lower-stratosphere.

22 This section uses the updated temperature lower-stratospheric high latitude temperature  
23 trends (discussed in Section 1.2.2) and discusses the recent modeling efforts that have attempted  
24 to understand them. It concentrates on the analysis and understanding of past decadal-timescale  
25 trends in the polar lower- stratosphere; the upper stratospheric response is often more  
26 independent of latitude and is discussed in the global ozone chapter (Chapter 4). Possible future  
27 temperature-change scenarios are discussed more fully in the next section (Section 5).

## 1 **4.2 Modeling Techniques**

2  
3 Several different types of model have been adopted for the study of stratospheric  
4 temperature change. Two types of commonly used models are briefly assessed here. Table 4.1  
5 presents recent model results.

### 6 **4.2.1 FIXED DYNAMICAL HEATING (FDH) MODELS**

7  
8 Fixed Dynamical Heating (FDH) models and Seasonally Evolving Fixed Dynamical  
9 Heating models (SEFDH) (WMO, 1999; IPCC, 2001) employ a method of calculating  
10 temperature changes using only a radiative transfer model. They have been shown to agree well  
11 with calculations using GCMs (Rosier and Shine, 2000; Ramaswamy *et al.*, 2001) and, compared  
12 to these, they are generally faster and allow the use of more sophisticated radiative transfer  
13 schemes. In contrast to the FDH technique, SEFDH techniques include a calculation for the time  
14 evolution of temperature and have been shown to improve the temperature response in the high  
15 latitude polar stratosphere, compared to GCM integrations (Forster *et al.*, 1997; Rosier and  
16 Shine, 2000). This was a region where the equilibrium temperature response calculated with  
17 FDH models overestimated the cooling resulting from short-term polar ozone depletion. Both  
18 FDH and SEFDH techniques are unable to model the response of atmospheric dynamics.

### 19 **4.2.2 GENERAL CIRCULATION MODELS (GCMs)**

20  
21 An assessment of the performance of current middle atmosphere GCMs is currently being  
22 performed by the 'GCM-Reality Intercomparison Project for SPARC' (GRIPS) (Pawson *et al.*,  
23 2000). Preliminary analysis of their results suggest that all models have a cold-bias, at most  
24 levels in the troposphere and stratosphere, which may be indicative of errors in the radiative  
25 transfer, or input data (Pawson *et al.*, 2000). This is particularly pronounced at the poles (see  
26 Section 5.1.1); one of the largest uncertainties remains the parameterization of small-scale  
27 gravity waves (see Section 2.1.2 and Section 5.1.1). The upper boundary and vertical resolution  
28 may also be important for an accurate simulation (see Section 5.1.3). Due to large inter-annual  
29 variability particularly in the Arctic temperatures (see Section 5.1.4 and Section 2.1.2), either  
30 many transient integrations (indicated by the suffix 'T' in the model column of Table 4.1) or  
31 many years of equilibrium experiments need to be performed for statistically significant trend

1 calculations. It must be noted, however, that the real atmosphere has evolved through only one  
2 specific realization and that the global observational record only spans ~20 years. Experiments  
3 have been performed with both prescribed changes in atmospheric constituents (referred to as  
4 GCM in the model column of Table 4.1) and coupled chemistry GCMs (discussed in more detail  
5 in Section 5 and referred to as GCM-CHEM in Table 4.1). Whilst coupled chemistry GCMs  
6 allow interaction between radiation, chemistry and dynamics (one coupled model does not  
7 include stratospheric water vapor feedback), they have two main drawbacks when attempting to  
8 attribute stratospheric temperature change to a particular cause. Firstly their complexity makes  
9 them computationally expensive; it is therefore difficult to run them for long enough to produce  
10 statistically significant trends. Secondly, their simulation of the ozone change is imperfect; this  
11 is to be contrasted with GCMs that employ the ozone trends inferred from observations to deter-  
12 mine the temperature response.

### 13 **4.3 Causes of Stratospheric Temperature Trends**

14  
15 This sub-section assesses the role of different mechanisms on polar lower-stratospheric  
16 temperature trends. A variety of recent model results are compared to the satellite-derived  
17 temperature trends (discussed in Section 1.2.2). Table 4-1 and Figure 4-1 summarize the  
18 findings for the lower stratospheric temperature response at 70°N and 70°S to: a) stratospheric  
19 ozone changes, b) Well mixed greenhouse gas (WMGHG) changes, c) combined changes in  
20 WMGHGs and stratospheric ozone changes, and d) stratospheric water vapor changes. Annual  
21 and Seasonal temperature trends are shown at pressures of 50 hPa and 100 hPa. There are  
22 several factors that affect the interpretation of the comparisons of the observations and model  
23 simulations presented in this section.

- 24 (a) The satellite measurements comprise radiances from a range of altitudes. This  
25 introduces some uncertainty when model results at 50 and 100 hPa are compared with  
26 the satellite observations.
- 27 (b) This section examines a single latitude belt in the polar regions where there is a large  
28 dynamical variability.
- 29 (c) The polar trends, especially for the winter/spring season, are influenced by the end-  
30 year considered for the analysis.

1 **4.3.1 OZONE**

2  
3 The stratospheric cooling over Antarctica has previously been shown to be very well  
4 correlated with ozone losses (WMO, 1999; Randel and Wu, 1999a). Shine (1986) was the first  
5 to show that such a stratospheric cooling could be due to the direct radiative response of the  
6 ozone loss. GCM and radiative model studies since then have largely confirmed this early work  
7 (Mahlman *et al.*, 1994; Ramaswamy *et al.*, 1996; WMO, 1999). In the Northern Hemisphere  
8 studies have also found a correlation between springtime Arctic temperatures and ozone (WMO,  
9 1999; Randel and Wu, 1999a). However, the correlations are not as strong and the cooling  
10 observed during the Arctic winter is not expected from a simple radiative response to the ozone  
11 loss (Randel and Wu, 1999a). In addition, reductions of planetary wave driving reduce the  
12 strength of the residual circulation, leading to a cooling trend. This also weakens the transport of  
13 ozone rich air to the polar lower stratosphere, and could give larger heterogeneous loss rates.  
14 Hence, a correlation of temperature and ozone does not necessarily imply a causal linkage of  
15 ozone loss with temperature.

16 Since the last assessment several studies have employed the monthly averaged vertical  
17 trend data, based on ozone observations over the 1979-1997 period (SPARC, 1998), with most  
18 studies employing the combined trend dataset of Randel and Wu (1999b). The results of these  
19 prescribed ozone change studies are shown in the 'STRAT OZONE' section of Table 4.1. The  
20 calculations presented in the table had the benefit of more detailed ozone-trend vertical  
21 resolution compared to previous work. The ozone dataset employs stratospheric-only trends  
22 derived from the Syowa (69°S) and Resolute (75°N) ozonesondes as representative of the polar  
23 regions. The Rosier and Shine (2000) results shown in the table are slightly updated versions of  
24 the GCM runs described in their paper.

25 Figure 4.2 shows an illustration of the annual cycle of model-derived 100 hPa trends from  
26 the Berlin model and compares them to trends derived from reanalysis data. It is noted that  
27 trends from re-analyses data (Figure 4.2 panel c) must be interpreted with caution (WMO, 1999,  
28 Chapter 5). The Antarctic and Arctic response are discussed separately below.

29  
30 ***Antarctic [4.3.1.1]***

31  
32 All studies report an ozone-induced cooling at 70°S for most seasons, with the largest  
33 cooling in all models occurring in SON and DJF. [Langematz \*et al.\* \(2002\)](#) and [Ramaswamy and](#)



1 [Schwarzkopf \(2002\)](#) find that the largest cooling at 100 hPa occurs in DJF not SON (see Section  
2 4.4). There is a dynamically induced heating in the middle atmosphere, which adds to the  
3 radiative heating owing to more upwelling longwave initiated by the depletion of ozone in the  
4 lower stratosphere. This effect is simulated by several models (Kiehl *et al.*, 1988; Mahlman *et*  
5 *al.*, 1994; Ramaswamy *et al.*, 1996; Rosier and Shine, 2000), and is consistent with observations  
6 (Ramaswamy *et al.*, 2001), but is not statistically significant, in either models or observations.

7 Compared to the observed trends the [Langematz \*et al.\* \(2002\)](#) response underestimates the  
8 SON cooling at 50 hPa but gives a better fit with the MSU-4 observations which are  
9 representative of 100 hPa. The other models tend to overestimate the observed spring and  
10 summer cooling at 100 hPa, particularly during DJF (see Section 4.4). Caution needs to be  
11 applied to this satellite-model comparison as there are uncertainties with regards to the  
12 representation of the altitude profile of ozone loss in the models over the winter/spring period,  
13 and with regards to the interpretation of seasonal trends at 50 and 100 hPa from satellite data.

14 Two versions of the same model (Rosier and Shine, 2000 (updated); and Smith, 2001)  
15 produce significantly different trends in SON (Table 4.1). Both models are versions of the  
16 Reading Intermediate GCM performing 20- year equilibrium experiments. Differences between  
17 the simulations are also found in the Arctic (see below), which may imply a difference between  
18 the way the ozone trends are implemented and/or differences in the variability of the model.

19  
20 ***Arctic [4.3.1.2]***

21  
22 All four models in Table 4-1 find an annually averaged cooling in the Arctic. Three of the  
23 four models find the largest cooling in MAM – which agrees qualitatively well with the satellite  
24 data. However, this modeled cooling is only about half the size of the cooling trend in the  
25 satellite data. Smith (2001), in contrast, finds a maximum cooling in DJF and smaller cooling in  
26 MAM, although differences again may be due to the large variability in the Arctic winter and are  
27 of limited significance. When comparing trends Graf *et al.*, (1998); Waugh *et al.* (1999);  
28 [Langematz \*et al.\* \(2002\)](#) and [Ramaswamy and Schwarzkopf \(2002\)](#) make the important point that  
29 the large natural variability in the Arctic may mean that the modeled and observed trends are not  
30 easily compared.

1 **4.3.2 WELL-MIXED GREENHOUSE GASES (WMGHG)**

2  
3 In general, considering their radiative effects only, WMGHG increases are expected to  
4 have a much smaller effect on lower stratospheric temperatures than they do on temperatures  
5 above 30 hPa (Forster and Shine, 1997; WMO, 1999; Chapter 4; Ramaswamy and Schwarzkopf,  
6 2002). This is borne out by the results presented in Table 4.1. The Langematz *et al.* (2002)  
7 trend was derived for CO<sub>2</sub> changes only and has been estimated by taking the difference between  
8 the results of their STRAT-OZONE and WMGHG experiment and those of their OZONE  
9 experiment. The same method has been adopted in connection with the Ramaswamy-  
10 Schwarzkopf results. This is in contrast to the updated Rosier and Shine study where WMGHG  
11 effects were studied directly. Few of the modeling studies show significant temperature trends.  
12 Some models are seen to cool their annual-mean lower stratospheres in response to WMGHG  
13 increases. The magnitude of cooling (~0.3 K/decade) agrees with earlier FDH calculations (*e.g.*,  
14 Ramaswamy *et al.*, 2001). For further discussion on the role of WMGHGs in annual-mean  
15 trends see Chapter 4.

16 **4.3.3 COMBINED CHANGES IN WMGHGS AND STRATOSPHERIC OZONE**

17  
18 Since WMO (1999) several experiments with coupled chemistry-climate models have been  
19 performed for different time periods to simulate the combined effect of changes in ozone and  
20 WMGHGs. These experiments are discussed in more detail in Section 5. Here we only examine  
21 how the coupled chemistry modeling studies influence the attribution of high latitude  
22 temperature trends. Results from five of coupled chemistry experiments are presented in Table  
23 4.1 Temperature trends are also shown for 2 different prescribed WMGHG and ozone  
24 experiments and the updated Rosier and Shine (2000) result, where individual ozone and  
25 WMGHG trends have been added.

26  
27 ***Antarctic [4.3.3.1]***

28  
29 The agreement between the different models in Table 4.1 is encouraging considering: a) the  
30 range of different models employed; b) the differences between the responses, for models  
31 employing the same ozone trend dataset (Section 4.4.1.1); and c) the large uncertainty in trends  
32 derived from transient integrations. As the overall effect of WMGHG changes on lower

1 stratospheric temperatures is minimal (annual-mean results in Section 4.4.2), there is little  
2 difference with respect to the annual-mean temperature trends from the stratospheric ozone  
3 experiments. Therefore, for all seasons the observed cooling can be explained by either  
4 combined WMOGHG and stratospheric ozone changes or stratospheric ozone changes alone (see  
5 Figure 4.1). Most of the coupled chemistry models and [Ramaswamy and Schwarzkopf \(2002\)](#)  
6 tend to overestimate the observed 100 hPa cooling in SON, although most results are still within  
7 the observational uncertainty range. In contrast, at 50 hPa, these models are closer to  
8 observations while some of the other models underestimate the cooling. The differences seen  
9 amongst the models at 50 and 100 hPa suggest the height profile of the applied ozone loss as a  
10 possible cause of the dipole-like behavior in the biases. Schnadt *et al.* (2002) and the study of  
11 Austin (2002) find an SON cooling whose position is too high compared to observations. These  
12 discrepancies were found to be consistent with model ozone-biases (Austin, 2002). Most models  
13 simulate the annual-mean change at 50 hPa well while all overestimate the 100 hPa trend.

14 Generally, the Antarctic springtime cooling is captured by the models but further  
15 improvements are needed to simulate the magnitude of the cooling and its vertical extent.

#### 16 17 *Arctic [4.3.3.2]*

18  
19 As for Antarctica the models are generally consistent with the observed trends, and inter-  
20 model differences are generally smaller than the  $2\sigma$  uncertainty in the observations (Figure 4.1).  
21 At 50 hPa all models underestimate the MAM cooling. At 100 hPa all models (bar one)  
22 underestimate this cooling, which could indicate: 1) an underestimate of the ozone-related  
23 cooling; 2) a contribution of a missing effect, such as increases in stratospheric water vapor; 3)  
24 an underestimate of the role of natural variability. Some models yield a warming in DJF which  
25 is in contrast to the observations. In the annual-mean, only one of the models (a coupled model)  
26 is close to the observations, the rest underestimate the observed cooling.

#### 27 **4.3.4 STRATOSPHERIC WATER VAPOR**

28  
29 Since the last assessment a major development has been the burgeoning interest in the role  
30 of stratospheric water vapor. Increases in stratospheric water vapor have now been measured by  
31 satellite and ground based observing systems which are roughly twice the expected increase from

1 methane oxidation (see Chapter 4, Rosenlof *et al.*, 2001, SPARC, 2000). Several recent papers  
2 have examined the consequences of this increase for stratospheric temperatures.

3 The study of Forster and Shine (1999) used an over-simplified representation of the water  
4 vapor change, both in the perturbation and background stratospheric water values (Forster and  
5 Shine, 2002) and, perhaps, its radiative transfer scheme (Oinas *et al.*, 2001). In general,  
6 inadequacies of broadband radiative transfer codes are readily accounted for (see Forster *et al.*,  
7 2001; Forster and Shine, 2002). Since this study, Smith (2001) (see also, Smith *et al.*, 2001),  
8 used trends derived from HALOE data over the 1992-1999 period to better represent the water  
9 vapor change. Likewise, Forster and Shine (2002) used an improved representation of the  
10 background water vapor a simulated +1 ppmv water vapor increase, derived from SPARC (2000)  
11 data. Shindell (2001) also modeled the effect on increases in stratospheric water vapor, from  
12 methane oxidation, using a coupled chemistry GCM. Although large uncertainties in the water  
13 vapor trend remain, these studies indicate a possible cooling of up to 0.5 K/decade in both hemi-  
14 spheres, comparable to that due to ozone. Given the present level of uncertainty in the  
15 observational trend analysis and notwithstanding the contribution of WMGHGs and stratospheric  
16 ozone to the cooling, one cannot rule out a significant effect due to stratospheric water vapor.  
17 There is an indication that a water vapor contribution is required for a quantitative accounting of  
18 the observed polar cooling (also see the discussion in Chapter 4).

#### 19 4.3.5 SOLAR CHANGES

20  
21 Following on from work discussed in the reviews of WMO (1999) and Ramaswamy *et al.*  
22 (2001), Van Loon and Labitzke (2000) correlate the solar cycle with stratospheric temperatures  
23 and find that the ‘response’ of the Arctic stratosphere depends on the phase of the QBO. During  
24 solar maximum easterly phases of the QBO coincide with a cooler Arctic stratosphere, whereas  
25 westerly phases of the QBO give a warmer stratosphere. A model simulation (Cubasch and  
26 Voss, 2000) is unable to simulate this response, although their model did not include a  
27 modulation of ozone with ultraviolet radiation. Inclusion of this feedback affects the Arctic  
28 temperature response (Haigh, 1999; Larkin *et al.*, 2000). Both these modeling studies found a  
29 warmer wintertime Arctic stratosphere during solar maximum. Recent studies with coupled  
30 chemistry models (Williams *et al.*, 2001; Labitzke *et al.*, 2002) find increased sensitivity of  
31 lower stratospheric ozone to the solar cycle, compared to earlier modeling experiments, giving

1 greater consistency with observations (see also EUR, 2001). Generally the latest modeling stud-  
2 ies indicate a possible influence of the solar cycle on high latitude temperatures. However, any  
3 effect is still too uncertain to quantify and remains somewhat speculative.

#### 4 **4.3.6 VOLCANOES**

5  
6 In the last 20 years the two large volcanic eruptions of Mt. Pinatubo and El Chichón  
7 created significant amounts of aerosol in the low-latitude stratosphere. Whilst several  
8 simulations show a low-latitude stratospheric warming the response at high latitudes is less  
9 certain (WMO, 1999). Ramachandran *et al.* (2000) simulated the Mt Pinatubo eruption in a  
10 GCM and found that the dynamical response to the aerosol forcing led to an annually averaged  
11 cooling at high latitudes up to 2 K for the two years following the eruption. Ramaswamy *et al.*  
12 (2002b) find that the high-latitude simulations of Pinatubo aerosol effects are affected  
13 substantially by the initial conditions in the model ensemble integrations. Timmreck *et al.*,  
14 (1999) also found that volcanic aerosol caused a stronger Arctic vortex. While both model and  
15 observations in the Pinatubo case indicate that polar effects were not statistically significant, the  
16 suggestion remains that volcanic eruptions may have contributed to the observed high latitude  
17 stratospheric cooling. Following a volcanic eruption, enhanced ozone loss is expected from  
18 heterogeneous chemical reactions on the volcanic aerosol (see WMO, 1999). This ozone loss  
19 would cool the stratosphere. Pawson *et al.* (1999) postulate a stepwise decrease in stratospheric  
20 temperatures following volcanic eruptions that may be connected with changes in heterogeneous  
21 ozone chemistry (Solomon *et al.*, 1998).

#### 22 **4.4 Timing of the Springtime Cooling Trend**

23  
24 Observational evidence shows that the maximum springtime stratospheric cooling trend  
25 occurs at roughly the same time as a maximum ozone loss (March in the NH and October-  
26 November in the SH (*e.g.*, Randel and Wu, 1999a, see Figure 4.2, panel c). However, most  
27 modeling studies of ozone loss and simple radiative arguments would suggest that the maximum  
28 cooling lags the ozone loss in the lower stratosphere by a month or more (*see* Figure 4.2, panels  
29 a) and b), and also: Forster *et al.*, 1997; Ramaswamy *et al.*, 2001; Langematz, 2000; Rosier and  
30 Shine, 2000; Graf *et al.*, 1998, Langematz *et al.*, 2002). For example, in Antarctica a number of  
31 the models show approximately similar cooling trends in SON and DJF for their stratospheric

1 ozone experiments (Table 4.1). This is especially true of the 100 hPa where radiative relaxation  
2 times are longer. The NCEP reanalyses also hints at this feature (Figure 4.2, panel c). This  
3 feature is not observed in the satellite record. Graf *et al.*, 1998 investigated whether WMGHG  
4 increases could compensate for this lag and found it could not, at least in their model.  
5 [Ramaswamy and Schwarzkopf \(2002\)](#) find that the effects due to ozone and WMGHG over the  
6 1980-2000 period in the northern polar region are swamped by the dynamical variability seen in  
7 both model and observations. The finding is probably true of the other models (see Table 4.1  
8 and especially Figure 4.2). Graf *et al.*, 1998 further suggested that the discrepancy could be due  
9 to an incorrect modeling of the dynamical response and concluded that until reasons for this are  
10 adequately resolved it represents a problem in the attribution, of particularly the Arctic cooling,  
11 to an anthropogenic cause.

#### 12 **4.5 Summary and Conclusions**

13  
14 Generally, modeling studies now demonstrate that the springtime cooling in the Arctic  
15 lower stratosphere over the 1980-2000 period is, in part, due to stratospheric ozone depletion, but  
16 the degree of attribution is hindered by the large dynamical variability in this region. In  
17 Antarctica, modeling studies re-affirm that ozone loss is the major cause of the springtime  
18 cooling. They also indicate that WMGHG and stratospheric water vapor increases are likely  
19 contributors to the annually-averaged cooling.

20 For combined changes in stratospheric ozone and WMGHGs there is generally a  
21 reasonable agreement between the various modeling studies; inter-model differences are  
22 generally smaller than the uncertainty in observations. However, this good agreement is  
23 probably somewhat fortuitous, as the models which used *the same* prescribed ozone change still  
24 differed in the sign of their temperature response, especially in the Arctic. Furthermore, some of  
25 the ozone-change modeling studies were equilibrium experiments and as such were less prone to  
26 differences caused by the high variability of the Arctic vortex.

27 In summary the cooling of the springtime high latitude stratosphere is likely influenced to a  
28 substantial extent by various mechanisms (WMGHG increases, ozone loss, stratospheric water  
29 vapor increases, volcanic eruptions and natural variability). Attribution of polar temperatures is  
30 hampered by the large variability in the polar vortices (see Figure 1.2.1). This variability not  
31 only increases the uncertainty of observational trend analyses it also means that either many

5/7/02

1 years of equilibrium studies or many ensemble integrations are needed for reliable statistics.  
2 Further, it implies that model studies performed under equilibrium conditions may be inadequate  
3 for examination of polar trends, especially in the Arctic, over a time-period of two decades. At  
4 present 20 years of an equilibrium GCM run are barely sufficient to resolve temperature changes  
5 in the Arctic winter. This would imply that 20+ member ensembles would also be needed for  
6 transient integrations. Comparison between observations and models, or between different  
7 models, is also complicated by uncertainty in the vertical profile of ozone loss, which leads to  
8 uncertainty in the temperature response. In models which simulate the chemistry this uncertainty  
9 could be larger than in those models which prescribe the ozone loss from observations. These  
10 coupled-chemistry models are discussed next.

11

5/7/02

Study	Model	Period	Notes	50 hPa (K/decade)									
				70N					70 S				
				DJF	MAM	JJA	SON	Annual	DJF	MAM	JJA	SON	Annual
				<i>Satellite observations</i>									
SSU		1979-1998		-0.93	-2.99	-0.49	-0.27	-1.17	-0.74	-1.01	-0.66	-2.90	-1.33
Berlin sondes		1979-2000						<b>-0.61</b>					
UKRAOB sondes		1979-2000						<b>-0.90</b>					
Russia sondes		1979-2000						<b>-0.70</b>					
CPC analysis		1979-2000						<b>-0.52</b>					<b>-0.64</b>
				<i>STRAT OZONE</i>									
Schwarzkopf & Ramaswamy, 2002	GCM	1979-1997		-0.34	-0.80	-0.42	0.23	<b>-0.33</b>	-1.61	-0.41	-0.13	-2.42	<b>-1.08</b>
Rosier and Shine, 2000(updated)	GCM	1979-1997		-0.17	-1.02	-0.30	-0.30	<b>-0.45</b>	-1.04	-0.27	0.41	-1.99	<b>-0.72</b>
Langematz, 2000	GCM	1979-1996		-0.64	-0.96	-0.26	-0.25	<b>-0.53</b>	-0.36	-0.13	0.00	-0.04	<b>-0.11</b>
Smith, 2001	GCM	1979-1997		-1.58	-0.25	-0.71	-0.76	<b>-0.83</b>	-1.75	-0.47	-0.91	-3.66	<b>-1.70</b>
				<i>WMGHG</i>									
Schwarzkopf & Ramaswamy, 2002	GCM	1979-1997		1.12	-0.19	-0.25	-0.33	<b>0.10</b>	0.03	-0.24	0.10	2.16	<b>-0.13</b>
Rosier and Shine, 2000(updated)	GCM	1979-1997		-0.11	0.09	0.07	-0.07	<b>0.00</b>	-0.23	-0.32	-0.80	0.51	<b>-0.21</b>
Langematz et al., 2002	GCM	1979-1996	co2, diff.	-0.31	0.20	-0.06	-0.32	<b>-0.12</b>	0.19	-0.04	-0.14	-0.12	<b>-0.05</b>
Butchart et al, 2001	GCM-T	1991-2001	2 run avg.	2.02	-0.74	-0.02	-0.01	<b>0.28</b>	0.29	-1.35	-1.99	-1.06	<b>-1.04</b>
Shindell, 2001	GCM-T	1980-2000		-1.90	-1.20	-0.50	-0.60	<b>-0.90</b>	-0.80	-0.70	-0.60	-0.80	<b>-0.70</b>
				<i>STRAT OZONE + WMGHG</i>									
Schwarzkopf & Ramaswamy, 2002	GCM	1979-1997		0.78	-0.99	-0.67	-0.10	<b>-0.23</b>	-1.58	-0.65	-0.03	-0.26	<b>-1.21</b>
Rosier and Shine, 2000(updated)	GCM	1979-1997	summed	-0.28	-0.94	-0.22	-0.37	<b>-0.46</b>	-1.27	-0.58	-0.39	-1.48	<b>-0.92</b>
Langematz et al, 2002	GCM	1979-1996	co2 only	-0.95	-0.76	-0.32	-0.57	<b>-0.65</b>	-0.17	-0.17	-0.14	-0.16	<b>-0.16</b>
Austin, 2002	GCM-CHEM-T	1979-1999	wat-feed	1.06	-0.75	-0.31	-0.34	<b>0.09</b>	-0.56	-0.15	-0.02	-2.85	<b>-0.89</b>
Shindell, 2001	GCM-CHEM-T	1980-2000		-1.60	-1.80	-0.50	-0.40	<b>-1.00</b>	-0.50	-0.70	-0.40	-2.80	<b>-0.70</b>
Shindell, 2001	GCM-CHEM-T	1980-2000	wat-feed	-1.70	-1.90	-0.60	-0.70	<b>-1.20</b>	-1.00	-1.00	-0.80	-2.80	<b>-1.40</b>
Schnadt et al., 2002	GCM-CHEM	1980-1990	wat-feed	-0.20	-0.72	-0.37	-0.43	<b>-0.37</b>	-1.23	0.44	-0.26	-4.02	<b>-1.31</b>
				<i>STRAT WATER VAPOUR</i>									
Forster and Shine, 2002	FDH	1980-2000	+1 ppmv	-0.58	-0.47	-0.44	-0.56	<b>-0.51</b>	-0.49	-0.60	-0.70	-0.65	<b>-0.61</b>
Shindell, 2001	GCM-CHEM-T	1980-2000		-0.20	-0.50	-0.20	-0.10	<b>-0.30</b>	-0.10	-0.20	-0.20	-0.40	<b>-0.30</b>
Smith, 2001	GCM	1992-1999	HALOE	0.03	0.28	-0.01	-0.21	<b>0.02</b>	-0.09	-0.20	-1.00	-1.12	<b>-0.60</b>
Smith, 2001	2Dmodel	1992-1999	HALOE	0.11	0.10	0.11	0.08	<b>0.10</b>	-0.33	-0.31	-0.25	-0.23	<b>-0.28</b>
				<i>100 hPa (K/decade)</i>									
Study	Model	Period	Notes	100 hPa (K/decade)									
				70N					70 S				
				DJF	MAM	JJA	SON	Annual	DJF	MAM	JJA	SON	Annual

**Table 4.1:** Observed and modeled 70°N and 70°S seasonal lower stratospheric temperature trends over the last two decades. Trends are shown in units of K/decade for altitudes at 50 hPa and 100 hPa, for: December, January and February (DJF), March, April, and May (MAM); June,



1 July and August (JJA); September, October, and November (SON), and the annual-averaged  
2 trend. Dark (light) shading represents significant trends at the 2s (1s) level. Observations are  
3 described in Section 1.2.2 and models in Section 4.2

## 4 **5 CHEMISTRY-CLIMATE MODELING OF THE POLAR STRATOSPHERE**

### 6 **5.1 Introduction**

7  
8 Despite considerable research, the extent to which stratospheric change can influence  
9 climate is only beginning to be understood. Before the discovery of the Antarctic ozone hole  
10 (Farman *et al.*, 1985) it was thought that increases in WMGHGs would cool the stratosphere and  
11 increase ozone (*e.g.*, Groves and Tuck, 1980). However, it is now recognized that an increase in  
12 WMGHGs may increase PSCs and decrease ozone. Possibly one of the most extreme examples  
13 of chemistry-climate coupling is the effect of increasing WMGHGs on Arctic ozone. Using a  
14 mechanistic model with reasonably comprehensive chemistry Austin *et al.* (1992) showed that a  
15 doubling of CO<sub>2</sub> concentrations, expected towards the end of the 21st century, could lead to  
16 severe Arctic ozone loss if large halogen abundances persisted until that time. On the other  
17 hand, the calculations of Pitari *et al.* (1992) showed only a slight reduction in Arctic ozone due  
18 to a CO<sub>2</sub> doubling, while again keeping chlorine amounts fixed.

19 Since the early 1990s, the amendments to the Montreal protocol have resulted in a  
20 considerable constraint on the evolution of halogen amounts and more recent calculations have  
21 been able to take this into consideration. For example, in a coupled chemistry-climate  
22 simulation, Shindell *et al.* (1998a) specified currently projected concentrations of halogens and  
23 WMGHGs and calculated increased ozone depletion over the next decade or so, with severe  
24 ozone loss in the Arctic in years with lower than normal temperatures. Many of the conclusions  
25 of the last report (WMO, 1999, Chapter 12), were based on the Shindell *et al.* (1998a) study.  
26 Since then a number of coupled chemistry-climate models have been developed and run. One of  
27 the main reasons for using coupled models to investigate future ozone changes is that the  
28 changes in temperatures and transport occur in a way that is consistent with the underlying  
29 physics. For example reductions in ozone can cool the stratosphere via radiative processes and  
30 this results in further changes in ozone and transport. Simulations with, for example, a CTM  
31 require the specification of temperature and winds from another source such as a different model.

1 This would necessarily introduce some differences between the model results, which may be  
2 significant, particularly if severe ozone loss is predicted.

3 Traditionally, climate models have been run with fixed WMGHGs for both present and  
4 doubled CO<sub>2</sub> with the investigation of the subsequent ‘equilibrium climate.’ Several coupled  
5 chemistry-climate runs have followed this route with multi-year ‘timeslice’ simulations  
6 applicable to greenhouse gases (GHG) concentrations for specific years (*e.g.*, Rozanov *et al.*,  
7 2001; Schnadt *et al.*, 2002; Pitari *et al.* 2002b; Steil *et al.*, 2001). Other climate simulations have  
8 involved transient changes in the WMGHGs, and several coupled chemistry-climate simulations  
9 have followed this pattern (*e.g.*, Shindell *et al.*, 1998a; Austin 2002; Nagashima *et al.*, 2002).  
10 The advantage of transient experiments is that the detailed evolution of ozone can be determined  
11 in the same way that it is likely to occur (in principle) in the atmosphere, albeit with some  
12 statistical error. Comparisons with observations are direct since both atmosphere and model  
13 cover the period when WMGHGs and halogens are changing. Timeslice simulations need  
14 sufficient duration (at least 10 and preferably 20 years) to allow the interannual variability to be  
15 determined but in principle, 20 years evaluations of the same conditions may have less  
16 variability than the atmosphere in which halogens may be changing rapidly. Timeslice runs also  
17 have the advantage that several realizations of the same year are available, from which future  
18 predictions can be assessed. However, in practice this may be of less value than examining the  
19 behavior of different models, since a given model will tend to have systematic errors.

20 In this section, results are brought together only from 3-D models, as 2-D models are much  
21 less able to capture the dynamical processes of the polar regions. Also, because 2-D models do  
22 not treat the planetary wave dynamics in a fully realistic manner they are less able to capture the  
23 processes which give rise to trends in transport and temperature which are essential to the future  
24 predictions of ozone recovery. 2-D models are therefore better suited to process studies  
25 investigating the impacts of chemical changes, as indicated in Chapter 4. For the GCMs used in  
26 this section, both transient simulations and timeslice simulations are used, with results from both  
27 sets of simulations collected together specifically for this report, with the purpose of illustrating  
28 how the polar stratosphere might evolve during the next 50 years. A more complete model  
29 intercomparison is included in Austin *et al.* (2002).

30

1 **Table 1.** Models used in the comparisons. The resolution is given in degrees latitude x  
2 degrees longitude (grid point models) and T32 etc. are the resolutions in spectral models  
3 corresponding to triangular truncation of the wave space with 32 wave numbers. IS92a, refers  
4 to scenario IS92a of IPCC (1992) and WMO refers to the halogen scenario indicate in WMO  
5 (1999), Chapter 12.

Model	Horizontal Resolution	# Levels/ Upper Boundary	GHG/ Halogen Scenarios	Reference
UMETRAC	2.5x3.75	64/0.01 hPa	IS92a/WMO	Austin (2002) (Rayleigh Friction version)
CMAM	T32	65/0.0006 hPa	Observations	deGrandpre <i>et al.</i> (2000)
MAECHAM / CHEM	T30	39/0.01 hPa	IS92a/WMO	<a href="#">Steil <i>et al.</i> (2001)</a> <a href="#">Manzini <i>et al.</i> (2002)</a>
ECHAM4.L39 (DLR)/ CHEM	T30	39/10 hPa	IS92a/WMO	Schnadt <i>et al.</i> (2002)
UIUC	4x5	25/1 hPa	Observations	Rozanov <i>et al.</i> (2001)
CCSR/NIES	T21	30/0.06 hPa	IS92a/WMO	Takigawa <i>et al.</i> (1999), <a href="#">Nagashima <i>et al.</i> (2002)</a>
GISS	8x10	23/0.002 hPa	IS92a/WMO	Shindell <i>et al.</i> (1998b)
ULAQ	10x20	18/1 hPa	IS92a/WMO	<a href="#">Pitari <i>et al.</i> (2002a)</a>

7  
8  
9 The models used in the comparisons are indicated in Table 1, in order of decreasing  
10 horizontal resolution. ULAQ is the only model with a substantial aerosol package and has  
11 reasonably detailed chemistry, albeit diurnally averaged. This model has been run in timeslice  
12 mode. Of the other models run in this mode, the Canadian Middle Atmosphere Model (CMAM)  
13 and the Middle Atmosphere European Centre Hamburg model (ECHAM) with chemistry  
14 (MAECHAM/CHEM) have reasonably detailed chemistry and a high upper boundary (0.01 hPa  
15 and above), while the University of Illinois at Urbana-Champaign (UIUC) model and the  
16 ECHAM model with chemistry run at DLR (ECHAM4.L39(DLR)/CHEM) have a much lower  
17 upper boundary (1 hPa and below). The Unified Model with Eulerian Transport and Chemistry

1 (UMETRAC), CCSR/NIES, and GISS have been run in transient mode and the first two models  
2 have reasonably detailed chemistry while the GISS model has parameterized chemistry.

## 3 **5.2 The Uncertainties in Chemistry-Climate Models**

### 4 **5.2.1 TEMPERATURE BIASES**

5  
6 As noted in Section 4.3.2, many climate models without chemistry but with a fully resolved  
7 stratosphere have a cold bias of the order of 5-10 K over Antarctica in the lower stratosphere.  
8 This suggests that their residual circulations are too weak (Pawson *et al.*, 2000), *i.e.*, there is too  
9 little downwelling in high latitudes and too little upwelling in low latitudes. This cold  
10 temperature bias would significantly impact model heterogeneous chemistry, and enhance ozone  
11 destruction. The ‘cold pole problem’ extends to higher stratospheric levels causing a polar night  
12 jet that is too strong and too vertically oriented, whereas the observed polar night jet slopes with  
13 height towards the equator in the upper stratosphere. The weaker jet and vertical slope allows  
14 waves to propagate into higher latitudes and maintain higher polar temperatures. A potentially  
15 important component of climate change is whether these waves will be stronger in the future,  
16 since this will likely affect the evolution of ozone: see Section 5.2.4. A practical solution to  
17 those models with a cold bias is to increase the temperatures in the heterogeneous chemistry  
18 routines (*e.g.*, Austin *et al.*, 2000) by a fixed amount (*e.g.*, 5K). The strong polar night jet is also  
19 associated with a polar vortex that breaks down later in the spring, particularly in the Southern  
20 Hemisphere. In a chemistry-climate model this can lead to ozone depletion that continues for  
21 longer than observed.

22 Gravity waves generated by processes other than orography (*e.g.*, clouds) are thought to  
23 play an important role in the momentum balance of the stratosphere. Nonorographic gravity-  
24 wave drag (gwd) schemes have now been developed for climate models (*e.g.*, Medvedev and  
25 Klaassen, 1995; Hines, 1997; Warner and McIntyre, 1999) and their use has resulted in a  
26 significant reduction in the cold pole problem relative to simulations that rely on Rayleigh  
27 friction to decelerate the polar night jet (*e.g.*, Manzini and McFarlane, 1998). Two of these  
28 schemes have also been shown to produce a QBO when run in a climate model (Scaife *et al.*,  
29 2000a). The latest versions of several coupled chemistry-climate models now employ such  
30 schemes: CMAM uses the Medvedev-Klaassen scheme (Medvedev *et al.* 1998) or the Hines  
31 scheme (McLandress, 1998); UMETRAC uses the Warner and McIntyre scheme; and

1 MAECHAM/CHEM uses the Hines scheme (Steil *et al.*, 2001). The GISS GCM has used a non-  
2 orographic gravity wave drag scheme for many years (Rind *et al.*, 1988a, b), which is able to  
3 reproduce high latitude temperatures reasonably well (Shindell *et al.*, 1998b) but does not  
4 simulate a QBO in the tropics.

5 Figure 5.1 shows model temperature biases as a function of height for 80°N and 80°S,  
6 which are representative of the polar regions, for the winter and spring seasons. To determine  
7 the biases, a 10-year temperature climatology determined from UKMO data assimilation fields  
8 (Swinbank and O'Neill, 1994) was subtracted from the mean model temperature profiles  
9 applicable to the 1990s. The UKMO temperatures are considered to be about 2K too high at low  
10 temperatures (*e.g.*, Pullen and Jones, 1997; Manney *et al.*, 2002; Pommereau *et al.*, 2002;  
11 Knudsen *et al.*, 2002) but this is somewhat smaller than typical model biases. The upper  
12 stratospheric cold pole problem is particularly noticeable in the south in the UMETRAC (with  
13 Rayleigh friction), CCSR/NIES (which also uses Rayleigh friction) and MAECHAM/CHEM  
14 results. In the results of the UIUC and ULAQ models a warm bias is present. For the ULAQ  
15 model this is likely to be due to the inclusion of vertical diffusion (in addition to Rayleigh  
16 friction). As seen in the UMETRAC results, the winter and spring polar temperature bias can be  
17 dramatically reduced by the use of non-orographic gwd. Both UMETRAC and CMAM have  
18 very similar biases, within a few K of each other in the seasons investigated. The  
19 MAECHAM/CHEM model, which uses the Hines non-orographic gwd scheme, is only a slight  
20 improvement on the Rayleigh friction results of UMETRAC and CCSR/NIES.  
21 ECHAM4.L39(DLR)/CHEM is very similar to the MAECHAM/CHEM model, and gives similar  
22 results below 30 hPa, but does not have a non-orographic gwd scheme. At 80°N temperature  
23 biases are somewhat smaller than at 80°S and are sometimes positive. The northern lower  
24 stratospheric temperature biases would generally lead to insufficient heterogeneous ozone  
25 depletion in early winter but excessive ozone depletion in the more important spring period. In  
26 the Southern Hemisphere, spring cold biases could lead to more extensive PSCs than observed  
27 and delayed recovery in Antarctic ozone.

28 Some indication of the source of the model temperature biases in the lower stratosphere is  
29 given by Figure 5.2, which shows the heat flux [ $v'T$ ] at 100 hPa averaged over the domain 40-  
30 80°N for January and February plotted against temperature averaged over the domain 60-90°N at  
31 50 hPa for February and March. As argued by Newman *et al.* (2001), the heat flux at 100 hPa is

1 indicative of the wave forcing from the troposphere and this is highly correlated with lower  
2 stratospheric temperature slightly later in the year. Newman *et al.* (2001) chose a 1-15 March  
3 temperature average, but here we choose a longer period for the temperature average to smooth  
4 model and atmospheric transients. The model results (Figures 5.2 and 5.3) are in general  
5 agreement with observations and in Table 2 results of the linear regression between the two  
6 variables are shown (see table caption for explanation of the terms  $T_0$  and  $\beta$ ). The results  
7 indicate that horizontal resolution may have affected the model results: in general the model  
8 regression lines were less steep (smaller  $\beta$  in Table 2) as the model resolution decreased,  
9 particularly in the Northern Hemisphere. This could be because low-resolution models capture  
10 the low-amplitude wave, small heat flux case, but have difficulty capturing the large heat flux  
11 case with its significant potential enstrophy cascade to larger wavenumbers. The performance of  
12 the models might also depend on the dissipation that the models have at short spatial scales,  
13 although this is more difficult to compare. The values of  $\beta$  are generally much smaller in the  
14 Southern Hemisphere, except for the CCSR/NIES and CMAM models. The implication of these  
15 results therefore is that models need higher resolution and non-orographic gwd schemes to  
16 improve the relationship between heat flux and temperature in order to reduce their polar  
17 temperature biases.

## 18 **5.2.2 THE SIMULATION OF POLAR STRATOSPHERIC CLOUDS**

19  
20 PSCs have a significant impact on stratospheric ozone depletion in polar regions and recent  
21 developments in their understanding are discussed in detail in Carslaw *et al.* (2001) and Section  
22 2.3. Coupled chemistry-climate models have a variety of PSC schemes with and without  
23 sedimentation, but such models have in some cases large climatological temperature biases in the  
24 polar regions, as indicated in Section 5.2.1. If the models are to be effective, the temperature  
25 field must give realistic distributions near the PSC temperature thresholds.

26 The areal coverage of PSCs provides a model comparison diagnostic. We use the  
27 temperature at 50 hPa as an indicator of likely PSC amounts, and ignore the effect of  $\text{HNO}_3$  and  
28 sulfate concentrations on the determination of PSC surface areas (following Pawson and  
29 Naujokat, 1997; and Pawson *et al.*, 1999). Figure 5.4 shows for the models and observations the  
30 time integral throughout the winter of the PSC area at 50 hPa.  $A_\tau$  is here measured in terms of  
31 the fraction of the hemisphere covered in % times their duration in days. For the ice amount,  $A_\tau$

1 varies dramatically in the Arctic, between zero (ULAQ and CMAM models, not shown) and  
 2 70% of the hemisphere times days. The models have large interannual variability. Arctic NAT  
 3 also covers a large range, both for different models and in the interannual variability for each  
 4 simulation. In accordance with their temperature biases, several models have larger areas of  
 5 NAT than are typically derived from observations. The ULAQ PSCs are in good agreement with  
 6 observations, despite a slight positive temperature bias, while UMETRAC and CMAM have  
 7 lower PSCs than are derived from observations. In the Antarctic each model has much lower  
 8 fractional interannual variation, but again the results for separate models cover an exceedingly  
 9 large range for the ice amount. Clearly, the differences between different models will have a  
 10 profound impact on the amount of chemical ozone depletion calculated and will be discussed  
 11 further in Section 5.3.

12  
13

14 **Table 2.** Statistical analysis of the linear regression between the area averaged temperature  
 15 (K) at 50 hPa poleward of 60°N for Feb and March, and the heat flux (Km/s) at 100 hPa  
 16 between 40 and 80°N for Jan. and Feb (Northern Hemisphere). The Southern Hemisphere  
 17 results are for the months Aug. and Sept. and July and Aug. respectively. R is the correlation  
 18 coefficient between the variables,  $T_0$  is the intercept of the line at zero heat flux, and  $\beta$  is the  
 19 gradient of the line.

20

Model/Observations	Northern Hemisphere			Southern Hemisphere		
	R	$T_0$	$\beta$	R	$T_0$	$\beta$
NCEP (Observations)	<b>0.77</b>	<b>195.1</b>	<b>1.49</b>	<b>0.78</b>	<b>189.4</b>	<b>0.89</b>
UMETRAC Non-orographic gwd	0.74	196.9	1.21	0.66	188.5	0.98
Rayleigh Friction	0.67	196.2	1.21	0.51	187.7	0.67
CMAM 2000	0.54	204.6	0.76	0.48	191.2	0.86
MAECHAM/CHEM 1990	0.79	196.3	1.10	0.70	190.0	0.50
ECHAM4.L39(DLR) CHEM	0.62	198.3	0.93	0.86	186.3	0.56
CCSR/NIES	0.74	199.4	0.80	0.74	186.6	1.17
ULAQ	0.58	203.0	0.48	----	----	----

21

### 1 5.2.3 THE POSITION OF THE UPPER BOUNDARY OF THE GCM

2  
3 There is strong evidence from a number of modeling studies (Garcia and Boville, 1994;  
4 Shepherd *et al.*, 1996; Lawrence, 1997; Austin *et al.*, 1997; Rind *et al.*, 1998; Beagley *et al.*,  
5 2000) that the position of the model upper boundary can play a significant role in influencing  
6 transport and stratospheric dynamics due to the ‘downward control principle’ (Haynes *et al.*,  
7 1991). The sensitivity of the dynamical fields to the position of the upper boundary may be  
8 larger when using non-orographic gwd schemes than when Rayleigh friction is used, although if  
9 all the non-orographic gwd that is produced above the model boundary is placed instead in the  
10 top model layer, assuming that the upward propagating waves are not simply absorbed in the top  
11 layer, this sensitivity reduces (Lawrence, 1997). Model simulations with an upper boundary as  
12 low as 10 hPa have been completed (*e.g.*, Schnadt *et al.*, 2002; Hein *et al.*, 2001; Dameris *et al.*,  
13 1998). Schnadt *et al.* (2002) show the meridional circulation of the DLR model and this gives  
14 the expected upward motion from the summer hemisphere and downward motion over the winter  
15 hemisphere, although modeled meridional circulations are known to extend into the mesosphere  
16 (*e.g.*, Butchart and Austin, 1998). Schnadt *et al.* (2002) argue is that it is less important to have a  
17 high upper boundary, but more important to have high resolution in the vicinity of the  
18 tropopause. At present the evidence appears ambiguous: for example in the total ozone  
19 presented by Hein *et al.* (2001), insufficient ozone is transported to the North Pole, but there is  
20 excessive subtropical ozone transport. This could be related to the cold pole problem, rather than  
21 the position of the upper boundary. While the transport effect on ozone is direct, other  
22 considerations are the transport of long-lived tracers such as NO<sub>y</sub> and water vapor that have a  
23 photochemical impact on ozone. Consequently, it is generally recognized that the upper  
24 boundary should be placed at least as high as 1 hPa (*e.g.*, Rozanov *et al.*, 2001; Pitari *et al.*,  
25 2002b) with many models now placing their boundary at about 0.01 hPa (*e.g.*, Shindell *et al.*,  
26 1998b; Austin *et al.*, 2001; Steil *et al.*, 2001; Nagashima *et al.*, 2002). In comparison, CMAM  
27 (de Grandpre *et al.*, 2000) has an upper boundary somewhat higher (c. 0.0006 hPa) to allow a  
28 more complete representation of gwd to reduce the cold-pole problem (Section 5.1.1) and to  
29 simulate upper atmosphere phenomena.



1 **5.2.4 PREDICTIONS OF PLANETARY WAVES**

2  
3 In some GCMs, there is a significant trend in planetary wave propagation with time. In the  
4 GISS GCM, planetary waves are refracted equatorward as greenhouse gases increase (Shindell *et*  
5 *al.*, 2001) while in the ULAQ model a marked reduction in the propagation of planetary waves 1  
6 and 2 to high northern latitudes is found in the doubled CO<sub>2</sub> climate simulated by Pitari *et al.*  
7 (2002b). In the GISS model the impact of changed planetary wave drag is largest during winter  
8 when the enhanced polar night jet strengthens the polar vortex over the Arctic (Shindell *et al.*,  
9 1998a; Rind *et al.*, 1998). Planetary wave refraction is governed by wind shear, among other  
10 factors, so that enhanced wave refraction occurs as the waves coming up from the surface  
11 approach the area of increased wind. They are refracted by the increased vertical shear below  
12 the altitude of the maximum wind increase. Equatorward refraction of planetary waves at the  
13 lower edge of the wind anomaly leads to wave divergence and hence an acceleration of the zonal  
14 wind in that region. Over time, the wind anomaly itself propagates downward within through the  
15 stratosphere (*e.g.*, Baldwin and Dunkerton, 2001), and subsequently, from the tropopause to the  
16 surface in the GISS model.

17 The direct radiative cooling by greenhouse gases at high latitudes in the lower stratosphere  
18 causes an increase in the strength of the polar vortex. Planetary wave changes may be a  
19 feedback that strengthens this effect. One proposed planetary wave feedback mechanism  
20 (Shindell, 2001) works as follows: tropical and subtropical sea surface temperatures increase,  
21 leading to a warmer tropical and subtropical upper troposphere via moist convective processes.  
22 This results in an increased latitudinal temperature gradient at around 100-200 hPa leading to  
23 enhanced lower stratospheric westerly winds, which refract upward propagating tropospheric  
24 planetary waves equatorward. This results in a strengthened polar vortex.

25 However, climate experiments containing different physics with higher spatial resolution  
26 models (*e.g.*, Schnadt *et al.*, 2002) do not show a future trend towards reduced high latitude wave  
27 propagation. Without chemical feedback, the Unified Model (UM) predicts a future increase in  
28 overall generation of planetary waves, which leads to a greater wave flux to the Arctic  
29 stratosphere, and is even able to overcome the radiatively induced increase in the westerly zonal  
30 wind so that the overall trend is to more easterly flow. This also occurs in the Deutschen  
31 Zentrum für Luft- und Raumfahrt (DLR) model with chemical feedback (Schnadt *et al.*, 2002)

1 whereas in the UM with chemical feedback (UMETRAC) the trend in the heat flux during the  
2 period 1975-2020 is downwards but is not statistically significant. The Center for Climate  
3 System Research/National Institute for Environmental Studies (CCSR/NIES) model, of lower  
4 resolution than UMETRAC, has systematically lower heat fluxes but does show a downward  
5 trend during the period 1986-2050 which is marginally statistically significant. In general, the  
6 strengthening of the polar vortex appears to be critically dependent upon the relative importance  
7 of changes in wave generation versus wave propagation. These changes are likely to be highly  
8 model and resolution dependent, resulting from the particular wave forcing and drag schemes  
9 employed in each climate model. To some degree this sensitivity of the changes in planetary  
10 waves to the model simulation reflects similar uncertainties in the atmosphere: for example in the  
11 observations of the last five northern winters, four have been warm with a weaker polar vortex  
12 (see Section 1.2.2). As a result the strengthening of the vortex over the last twenty years noted  
13 by some authors (Tanaka *et al.*, 1996; Zurek *et al.*, 1996; Waugh *et al.*, 1999; Hood *et al.*, 1999).  
14 will have been modified by recent measurements.

#### 15 **5.2.5 UNCERTAINTIES IN THE RATE OF WATER VAPOR INCREASE**

16 Observations of atmospheric water vapor concentrations have revealed significant  
17 increases over the period 1964-2000 (Oltmans and Hofmann, 1995; Oltmans *et al.*, 2000). These  
18 observations and their possible implications and causes are discussed in Sections 2.2, 3, 4 and  
19 Chapter 4. In general, the increases are uncertain in magnitude and their causes have not been  
20 established.  
21

22 Increased water vapor directly affects ozone chemistry, and also alters local temperatures  
23 by radiative cooling, slowing down the reaction rates of ozone depletion chemistry, which  
24 indirectly leads to more ozone. The effects on homogeneous chemistry have been studied by  
25 Evans *et al.* (1998); Dvortsov and Solomon (2001); and Shindell (2001). The models all show  
26 that increases in water vapor reduce ozone in the upper and lower stratosphere, and increase  
27 ozone in the middle stratosphere. The model results differ most in the lower stratosphere where  
28 the largest impact on total ozone column occurs. In the model of Evans *et al.* (1998), lower  
29 stratospheric ozone is reduced only in the tropics when water vapor increases, while in the other  
30 models, ozone reductions extend to mid-latitudes or to the poles. Thus, the models of Dvortsov  
31 and Solomon (2001) and Shindell (2001) show a slower ozone recovery by about 10-20 years,

1 and a 1-2% reduction during the next 50 years due to water vapor increase, assuming that the  
2 water vapor increase continues at the current rate. The Evans *et al.* (1998) model disagrees with  
3 these results, presumably due to differences in the model's temperature response to increasing  
4 water, which seems to dominate over its chemical impacts.

5 Water vapor increases also affect heterogeneous chemistry, enhancing the formation of  
6 PSCs. Kirk-Davidoff *et al.* (1999) calculated a significant enhancement to Arctic ozone loss in a  
7 more humid atmosphere. Much of this effect was based on a very large estimate of 6 to 9 K per  
8 ppmv radiative cooling induced by increased water vapor. This value has been superseded by  
9 newer results showing that this value is almost certainly much smaller, about 1.5 to 2.5 K  
10 cooling per ppmv of water (Section 4.3.3). This would in turn imply a reduced role for water  
11 vapor in enhancing PSC formation. Tabazadeh *et al.* (2000) showed that the enhancement of  
12 PSC formation due to the addition of 1 ppmv of water vapor is approximately the same as the  
13 PSC enhancement due to cooling of about 1 K. This suggests that the radiative impact of water  
14 vapor is larger than its effects on chemistry or microphysics but that all these processes should be  
15 considered in numerical models. Given the potential for denitrification in the Arctic, and the  
16 large ozone losses that could result from a slight cooling there (Tabazadeh *et al.*, 2000), it is  
17 important both to understand trends in stratospheric water vapor, and to resolve model  
18 differences in the radiative impact of those trends.

19 Model simulations of past water vapor trends do not agree well with observations. In  
20 UMETRAC (Austin, 2002), water vapor increases by only about 1% per decade in the  
21 stratosphere, despite the inclusion of a methane oxidation scheme. In UMETRAC the tropical  
22 tropopause temperature decreases slightly, counteracting the methane impact. In  
23 ECHAM4.L39(DLR)/CHEM (Schnadt *et al.*, 2002), water vapor increases in the lower  
24 stratosphere are significantly larger (about 3% per decade) but are still about a factor of 2-3  
25 lower than observed. Similar results are also obtained in the GISS model. In general the  
26 modeled water vapor trend tends to be driven by methane oxidation and trends in tropopause  
27 temperature, suggesting the need to investigate the microphysics of dehydration and how this is  
28 represented in models. See EUR (2001), Section 4.3.3.

1 **5.3 Model Assessments**

2  
3 In the Arctic the processes leading to stratospheric ozone depletion may undergo too much  
4 natural variability to provide a definite answer of how ozone will actually evolve. Each model  
5 may be considered as supplying a single simulation (or range of simulations in the case of the  
6 timeslice experiments) of a larger ensemble. While the mean of the ensemble can be readily  
7 computed, the atmosphere may in practice evolve in a manner anywhere within, or even outside,  
8 the envelope of the model simulations. In the Antarctic, the dominant processes are less  
9 dependent on interannual variability and hence the ozone evolution is in principle more  
10 predictable.

11 One of the emphases here has been on spring ozone recovery. In view of the range of  
12 results obtained, it is important to define this term carefully and it is here used in two senses: (i)  
13 the start of ozone recovery, defined as the date of the minimum spring column ozone as a  
14 function of year in the decadal averaged results, (ii) full ozone recovery defined as the date of  
15 the return of the decadal averaged spring column ozone to the value obtained in 1980.

16 **5.3.1 THE 1960 - 2000 TIME FRAME: OZONE DEPLETION**

17  
18 As is well established from observations (Section 1), polar ozone has been decreasing over  
19 the last few decades. Figure 5.5 (top panel) shows the minimum daily ozone throughout the  
20 range 60-90N for the range of models of Table 1 together with TOMS data. Each model has a  
21 large interannual variability, similar to that of the observations, and hence detecting a signal is  
22 difficult. The continuous lines indicate the 10-year running means of the individual datasets for  
23 the transient model runs, which help to identify the timing of the minima. All the models  
24 indicate a slight high bias relative to observations. In the Arctic, the trends in the minimum are  
25 consistent with the observations for most of the models, although only the observed trend is  
26 statistically significant. See Table 3.

27 In the Antarctic (Figure 5.5, lower panel), the model runs all agree reasonably well with  
28 observations for the past and show the steady development of the ozone hole during the period.  
29 The calculated trends depend on the period chosen but even when this is taken into account both  
30 GISS and CMAM under predict the trend over the period 1980 – 2000. While the interannual  
31 variability in most of the models is similar to that observed, both CMAM and UMETRAC have a

1 large interannual variability. In the case of UMETRAC, this may to some extent be a product of  
2 the non-orographic gwd scheme. In CMAM the ozone minima are slightly high for the current  
3 atmosphere, but too low for 1980, giving a much-reduced trend.

4  
5  
6 **Table 3.** Past trends (1979-2000) in minimum ozone (DU/decade) with 2 sigma error bars for  
7 participating models and TOMS. The results for the CCSR/NIES model covers the period 1986-  
8 2000, the ECHAM.L39(DLR)/CHEM results cover the period 1960 to 1990 (Arctic) and 1980 to  
9 1990 (Antarctic). The MAECHAM/CHEM results cover the period 1960-2000 (Arctic) and 1960-  
10 1990 (Antarctic).

Model/Observations	Northern Hemisphere trend	Southern Hemisphere trend
TOMS	-21 +/- 16	-59 +/- 12
UMETRAC	-6 +/- 22	-80 +/- 31
CMAM	-8 +/- 17	-14 +/- 17
MAECHAM/CHEM	-14 +/- 17	-46 +/- 5
ECHAM.L39(DLR)/CHEM	-16 +/- 14	-64 +/- 7
CCSR/NIES	-33 +/- 38	-41 +/- 21
GISS	-21 +/- 34	-34 +/- 12

12  
13  
14 The maximum size of the Antarctic ozone hole during each spring, as given by the area  
15 within the 220-DU, total-ozone contour, is shown in Figure 5.6. The results for GISS,  
16 ECHAM.L39(DLR)/CHEM and CCSR/NIES are in good agreement with observations, but may  
17 indicate a slight under prediction. A much smaller ozone hole is simulated by UMETRAC, but  
18 recent model runs, with an NO<sub>y</sub> distribution consistent with observations show an ozone hole  
19 about 50% larger for 1995, which is in close agreement with observations. The small ozone hole  
20 area for CMAM reflects the bias and large interannual variability noted in Figure 5.5. Errors in  
21 the modeling of the size of the ozone hole can have important implications. Firstly, comparisons  
22 between models and observations for ozone amounts near 60°S will give poor agreement if the  
23 ozone hole area is too small, even though the underlying physics of the model may be correct.  
24 Secondly, a model with a smaller ozone hole may evolve differently from that of the atmosphere  
25 due to transport and chemistry effects relating to radiative effects.

1 **5.3.2 THE 2000 - 2020 TIME FRAME: START OF OZONE RECOVERY**

2  
3 The first signs of ozone recovery are expected within the next two decades (Shindell *et al.*,  
4 1998a; Austin *et al.*, 2000; Schnadt *et al.* 2002; Rosenfield *et al.*, 2002; Nagashima *et al.*, 2002).  
5 Two-dimensional (2-D) model simulations (*e.g.*, Rosenfield *et al.*, 2002) indicate a slight delay  
6 in Arctic and Antarctic spring ozone recovery following the maximum values in halogen loading.  
7 The GISS model has a larger response than the other models with the simulation indicating a  
8 minimum in the smoothed results of about 175 DU compared with almost 100 DU higher in the  
9 other transient runs. The date of minimum Arctic ozone, again as indicated by the minimum of  
10 the smoothed curves, varies from 2004 for the CCSR/NIES model to 2019 for the GISS model.  
11 UMETRAC indicates a minimum at about the year 2015, but the simulation ends shortly  
12 afterwards and the smoothed curve is virtually flat in the final decade. All three transient runs  
13 indicate some delay in the onset of ozone recovery, due to increases in GHGs, although such a  
14 result is subject to considerable uncertainty because of the large interannual variability.  
15 Although the timeslice experiments do not have the temporal resolution to give a precise  
16 indication of the timing of future ozone recovery, the ECHAM4.L39(DLR)/CHEM model results  
17 (Schnadt *et al.*, 2002) may go against the transient model results by suggesting that increases in  
18 planetary waves occur in the Arctic speeding up ozone recovery. This may be considered the  
19 ‘dynamical effect on chemistry’: Increases in planetary waves transport more ozone as well as  
20 raise temperatures and decrease heterogeneous chemistry. Therefore, the net effect on ozone is  
21 that of the two potentially competing processes of dynamics and radiation. If planetary waves  
22 increase, the ‘dynamical’ effect increases ozone and the ‘radiative’ effect decreases ozone, giving  
23 a relatively small response. If planetary waves decrease, both the ‘dynamical’ and ‘radiative’  
24 effects are negative, leading to enhanced ozone depletion. To resolve whether increases in  
25 GHGs are delaying the onset of ozone recovery, from the timeslice simulations would require  
26 more results for the period 1990 to 2015.

27 In the Antarctic, the runs are all in fairly good agreement. Of the transient runs, as in the  
28 Arctic, the CCSR/NIES model indicates the earliest start of ozone recovery (2001) followed by  
29 UMETRAC (2005) and GISS (2008). The minima in the smoothed curves are all comparable  
30 (109, 86, and 98 DU respectively). On the basis of the decadal averaged model results this  
31 would appear to indicate that ozone recovery would begin earlier in the Antarctic than in the

1 Arctic. Such an earlier start to recovery would also be detectable earlier in observations in  
2 Antarctica, because of the smaller interannual variability.

3 Observations of the size of the ozone hole (Figure 5.6, see also Section 1.2.1) do not  
4 indicate any clear recovery by October 2001, with interannual variability now dominating over  
5 the current trends. Indeed, the smoothed curve for the GISS results has its maximum size in  
6 2011. For UMETRAC the maximum ozone hole area is in 2019, although the curve is virtually  
7 flat from 1995 onwards. In contrast the decadal smoothed results for the CCSR/NIES model  
8 indicate a clear peak as early as the year 2002.

### 9 **5.3.3 THE 2020 - 2060 TIME FRAME: COMPLETE OZONE RECOVERY**

10  
11 Those models that have run beyond the year 2020 indicate some recovery in ozone. Of  
12 particular importance is the return to '1980-like conditions,' when the effects of anthropogenic  
13 halogen concentrations were negligible. As noted in WMO (1999), Chapter 12, this recovery  
14 would be to a different vertical distribution of ozone, with higher middle and upper stratospheric  
15 ozone due to the change in vertical temperature profile (see Chapter 4). Using a 2-D model,  
16 [Rosenfield \*et al.\* \(2002\)](#), determined the date for the recovery of total ozone to 1980 levels as a  
17 function of day of year and latitude. In the Arctic, this recovery was latest at the end of spring  
18 (after 2050) and earliest in autumn (before 2035). Further, the impact of CO<sub>2</sub> increases was  
19 shown to accelerate the recovery from that due to chemical changes alone by increasing the  
20 downwelling. In contrast, if methane amounts do not increase at the current rate, ozone recovery  
21 could be slowed down in the future by the increased importance of NO<sub>x</sub> chemistry ([Randeniya \*et al.\*, 2002](#)).  
22 Over Antarctica, downwelling is less important in speeding up the ozone recovery.

23 The results of Figure 5.5 show similar results for the spring for 3-D models. However, in  
24 the Arctic, most models do not show substantial Arctic ozone change throughout the period 2020  
25 to 2050, while the low values of the GISS model for the decade 2010 to 2020, are no longer  
26 present after 2030. In the Antarctic, the recovery of spring ozone, already underway by 2020,  
27 continues in the simulations completed (Figure 5-6). Recovery to 1980-like conditions occurs in  
28 the CCSR/NIES and GISS models by about 2045, and perhaps a decade later in the UMETRAC  
29 snapshot and CMAM results. The CCSR/NIES and GISS transient model results suggest a near  
30 monotonic recovery of ozone, but the UMETRAC snapshot results suggest that ozone could  
31 undergo further loss over the period 2025 to 2045. This was identified as due to increases in ice

1 PSCs as the lower stratospheric climate cools (Austin *et al.*, 2001), but would need to be  
2 confirmed by model simulations with more detailed PSC schemes. Of the timeslice experiments,  
3 the MAECHAM/CHEM results indicate a significant (but not 'full') recovery in the Antarctic by  
4 2030, consistent with the transient experiments. The MAECHAM/CHEM model also simulates  
5 full or near full recovery in the Arctic by 2030.

#### 6 **5.3.4 ATTRIBUTION OF MODEL OZONE CHANGES**

7  
8 In a coupled chemistry-climate model the attribution of ozone changes to dynamical and  
9 chemical processes may be ambiguous since the dynamical changes themselves may have been  
10 caused by chemical changes to the ozone amounts. This is discussed further in Chapter 4.  
11 Figure 5.4, illustrating the approximate amounts of PSCs in the model simulations, should in  
12 principle reflect the amount of chemical ozone depletion (cf. Figure 3.4). This would suggest,  
13 for example that UMETRAC has slightly less Arctic ozone depletion relative to observations and  
14 this is reflected in the Arctic ozone trend (Figure 5.5, Table 3) that is smaller than observed,  
15 although the difference is not statistically significant. Also, both MAECHAM/CHEM and  
16 ECHAM4.L39(DLR)/CHEM results for PSCs in Figure 5.4 suggest that their chemical ozone  
17 depletion is larger than observed in the Arctic although the net ozone trend is similar to  
18 observations. The implication is that transport into the polar regions is enhanced to compensate.  
19 However, this does not appear to be consistent with earlier results, *e.g.*, Hein *et al.* (2001) which  
20 if anything indicates reduced transport into the polar regions.

21 Similar results apply in the Antarctic. Here many of the models have similar ozone  
22 depletion rates (Figure 5.5, Table 3), similar amounts of PSCs and similar ozone trends, when  
23 allowance is made for the different periods under consideration. The main exceptions are the  
24 GISS model for which PSC diagnostics are not available, and CMAM, which has larger ozone  
25 depletion than observed in 1980. These inconsistencies in both hemispheres suggest the need for  
26 further investigation of the sizes of the transport versus chemical depletion terms in all the  
27 models included herein.

#### 28 **5.4 Summary**

29  
30 The main uncertainties of 3-D coupled chemistry-climate models stem from the  
31 performance of the underlying dynamical models. Temperature biases lead to errors in the



1 spatial extent of PSCs and the degree of chemical ozone depletion. The model results also  
2 suggest significant differences in the transport of ozone to high latitudes, although this is in need  
3 of further clarification. At the current stage of model performance, uncertainties in the details of  
4 PSC formation and sedimentation are probably less important in simulating ozone amounts than  
5 the model temperature biases. Nonetheless, the accurate representation of PSC processes will  
6 prove to be increasingly important as temperature biases become smaller, by for example, the  
7 inclusion of non-orographic gravity wave parameterizations. Another uncertainty is the amount  
8 of aerosol present due to future unpredictable volcanic eruptions. For a large eruption such as  
9 that of Mt. Pinatubo, sufficient aerosol would be present to provide additional sites for  
10 heterogeneous chemistry and possible severe ozone loss for a period of a few years, although this  
11 perturbation would not affect the long-term ozone trend. The impact of volcanic eruptions on  
12 coupled chemistry-climate model results has not been discussed in this Section, but further  
13 details may be found in Chapter 4.

14 For the transient model simulations the start of ozone recovery, as defined in Section 5.3,  
15 occurs in the Antarctic in the range 2001 to 2008, depending on the model and in the Arctic  
16 occurs in the range 2004 to 2019. In the Antarctic, however, model results suggest that the  
17 vertical and horizontal extent of the ozone hole may increase slightly further over the next few  
18 years. Thus, the results here suggest that the start of ozone recovery will occur slightly later in  
19 the Arctic than in the Antarctic. Further, since the halogen amounts are thought to have  
20 maximized in 2002 (see Chapter 1), the start of ozone recovery in the Arctic in the models is  
21 delayed by 3-18 years by greenhouse gas increases. Most of the models come to similar  
22 conclusions on this issue, but one of the coupled chemistry-climate model experiments (Schnadt  
23 *et al.*, 2002) suggests that greenhouse gas increases would tend to speed up rather than slow  
24 down ozone recovery in the Arctic. It should also be recognized that interannual variability on  
25 the sub-decadal timescale may still lead to ozone extremes. In the worst-case scenario, therefore,  
26 it may take until at least the end of the 2020s before we can be certain that ozone recovery has  
27 started in the Arctic. To put this into perspective, most models predict relatively modest changes  
28 in future spring Arctic column ozone (under 10%). The one model that does predict a major  
29 Arctic ozone change in the near future (described in Shindell *et al.*, 1998), has lower spatial  
30 resolution, simplified ozone transport, and parameterized ozone chemistry. In comparison, the  
31 other models have more accurate treatments of these processes.

5/7/02

1           On the longer timescale, to the middle of the 21st century, model predictions appear to be  
2 more uncertain. Hence, although recovery of Antarctic ozone to 1980-like conditions ('full  
3 ozone recovery') is to be expected by about 2050, models will need to have a better  
4 representation of the water vapor increase than has hitherto been possible, as well as an accurate  
5 specification of methane changes, for full confidence in their predictions. Although the results  
6 for the Arctic are less certain, since most models indicate relatively modest change in ozone, it is  
7 possible that 'full recovery' may occur somewhat earlier there.

1 **REFERENCES**

- 2
- 3 Abrams, M. C., G. L. Manney, M. R. Gunson, M. M. Abbas, A. Y. Chang, A. Goldman, F. W. Irion, H.  
4 A. Michelsen, M. J. Newchurch, C. P. Rinsland, R. J. Salawitch, G. P. Stiller, and R. Zander,  
5 ATMOS/ATLAS-3 observations of long-lived tracers and descent in the Antarctic vortex in  
6 November 1994, *Geophys. Res. Lett.*, 23, 2341-2344, 1996.
- 7 Allen, D. R., J. L. Stanford, N. Nakamura, M. A. Lopez-Valverde, M. Lopez-Puertas, F. W. Taylor, and J.  
8 J. Remedios, Antarctic polar descent and planetary wave activity observed in ISAMS CO from  
9 April to July 1992, *Geophys. Res. Lett.*, 27, 665-668, 2000.
- 10 Allen, D. R., and N. Nakamura, A seasonal climatology of effective diffusivity in the stratosphere, *J.*  
11 *Geophys. Res.*, 106, 7917-7935, 2001.
- 12 Ambaum, M. H. P., B. J. Hoskins, and D. B. Stephenson, Arctic Oscillation or North Atlantic  
13 Oscillation?, *J. Climate*, 14, 3495-3507, 2001.
- 14 Andersen, S. B., and B. M. Knudsen, The influence of polar vortex ozone depletion on Arctic ozone  
15 trends, *Geophys. Res. Lett.*, in press, 2002.
- 16 Appenzeller, C., and J. R. Holton, Tracer lamination in the stratosphere: A global climatology *J.*  
17 *Geophys. Res.*, 102, 13555-13569, 1997.
- 18 Atkinson, R. J., and R. A. Plumb, Three-dimensional ozone transport during the ozone-hole breakup in  
19 December 1987, *J. Geophys. Res.*, 102, 1451-1466, 1997.
- 20 Austin, J., A three-dimensional coupled chemistry-climate model simulation of past stratospheric trends,  
21 *J. Atmos. Sci.*, 59, 218-232, 2002.
- 22 Austin, J., N. Butchart, and K. P. Shine, Possibility of an Arctic ozone hole in a doubled-CO<sub>2</sub> climate,  
23 *Nature*, 360, 221-225, 1992.
- 24 Austin, J., N. Butchart, and R. S. Swinbank, Sensitivity of ozone and temperature to vertical resolution in  
25 a GCM with coupled stratospheric chemistry, *Q. J. R. Meteorol. Soc.*, 123, 1405-1431, 1997.
- 26 Austin, J., J. Knight, and N. Butchart, Three-dimensional chemical model simulations of the ozone layer:  
27 1979-2015, *Q. J. R. Meteorol. Soc.*, 126, 1533-1556, 2000.
- 28 Austin, J., N. Butchart, and J. Knight, Three-dimensional chemical model simulations of the ozone layer:  
29 2015-2055, *Q. J. R. Meteorol. Soc.*, 127, 959-974, 2001.
- 30 Austin, J., D. Shindell, S. Beagley, C. Brühl, M. Damerid, E. Manzini, T. Nagashima, P. Newman, S.  
31 Pawson, G. Pitari, E. Rozanov, C. Schnadt, and T. G. Shepherd, Uncertainties and assessments of  
32 chemistry-climate models of the stratosphere, *Surveys in Geophysics*, to be submitted in April 2002.
- 33 Avallone, L. M., D. W. Toohey, S. M. Schauffler, W. H. Pollock, L. E. Heidt, E. L. Atlas, and K. R.  
34 Chan, *In situ* measurements of BrO during AASE-II, *Geophys. Res. Lett.*, 22, 831-834, 1995.
- 35 Avallone, L. M., and D. W. Toohey, Tests of halogen photochemistry using *in situ* measurements of ClO  
36 and BrO in the lower polar stratosphere, *J. Geophys. Res.*, 106, 10411-10421, 2001.
- 37 Bacmeister, J. T., S. D. Eckermann, A. Tsias, K. S. Carslaw, and T. Peter, Mesoscale temperature  
38 fluctuations induced by a spectrum of gravity waves: A comparison of parameterizations and their  
39 impact on stratospheric microphysics, *J. Atmos. Sci.*, 56, 1913-1924, 1999.
- 40 Baldwin, M. P., and T. J. Dunkerton, Propagation of the Arctic Oscillation from the stratosphere to the

5/7/02

- 1 troposphere, *J. Geophys. Res.*, *104*, 30937-30946, 1999.
- 2 Baldwin, M. P., and T. J. Dunkerton, Stratospheric harbingers of anomalous weather regimes, *Science*,  
3 *294*, 581-584, 2001.
- 4 Beagley, S. R., C. McLandress, V. I. Fomichev, and W. E. Ward, The extended Canadian middle  
5 atmosphere model, *Geophys. Res. Lett.*, *27*, 2529-2532, 2000.
- 6 Becker, G., R. Müller, D. S. McKenna, M. Rex, and K. S. Carslaw, Ozone loss rates in the Arctic  
7 stratosphere in the winter 1991/92: Model calculations compared with Match results, *Geophys. Res.*  
8 *Lett.*, *25*, 4325-4328, 1998.
- 9 Becker, G., R. Müller, D. S. McKenna, M. Rex, K. S. Carslaw, and H. Oelhaf, Ozone loss rates in the  
10 Arctic stratosphere in the winter 1994/1995: Model simulations underestimate results of the Match  
11 analysis, *J. Geophys. Res.*, *105*, 15175-15184, 2000.
- 12 Bertram, A. K., and J. J. Sloan, Temperature-dependent nucleation rate constants and freezing behavior of  
13 submicron nitric acid dihydrate aerosol particles under stratospheric conditions, *J. Geophys. Res.*,  
14 *103*, 3553, 1998a.
- 15 Bertram, A. K., and J. J. Sloan, The nucleation rate constants and freezing mechanism of nitric acid  
16 trihydrate aerosol under stratospheric conditions, *J. Geophys. Res.*, *103*, 13261-13265, 1998b.
- 17 Bevilacqua, R. M., C. P. Aellig, D. J. Debrestian, M. D. Fromm, K. Hoppel, J. D. Lumpe, E. P. Shettle, J.  
18 S. Hornstein, C. E. Randall, D. W. Rusch, and J. E. Rosenfield, POAM II ozone observation in the  
19 Antarctic ozone hole in 1994, 1995, and 1996, *J. Geophys. Res.*, *102*, 23643-23657, 1997.
- 20 Bevilacqua, R. M., M. D. Fromm, J. M. Alfred, J. S. Hornstein, G. E. Nedoluha, K. W. Hoppel, J. D.  
21 Lumpe, C. E. Randall, E. P. Shettle, E. V. Browell, C. Butler, A. Dörnbrack, and A. W. Strawa,  
22 Observations and analysis of PSCs detected by POAM III during the 1999/2000 Northern  
23 Hemisphere winter, *J. Geophys. Res.*, in press, 2002.
- 24 Biele, J., A. Tsias, B. P. Luo, K. S. Carslaw, R. Neuber, G. Beyerle, and T. Peter, Nonequilibrium  
25 coexistence of solid and liquid particles in Arctic stratospheric clouds, *J. Geophys. Res.*, *106*,  
26 22991-23007, 2001.
- 27 Biermann, U. M., T. Presper, T. Koop, J. Mossinger, P. J., Crutzen, and T. Peter, The unsuitability of  
28 meteoritic and other nuclei for polar stratospheric cloud freezing, *Geophys. Res. Lett.*, *23*, 1693-  
29 1696, 1996.
- 30 Bird, J. C., S. R. Pal, A. I. Carswell, D. P. Donovan, G. L. Manney, J. M. Harris, and O. Uchino,  
31 Observations of ozone structures in the Arctic polar vortex, *J. Geophys. Res.*, *102*, 10785-10800,  
32 1997.
- 33 Bloss, W. J., S. L. Nikolaisen, R. J. Salawitch, R. R. Friedl, and S. P. Sander, Kinetics of the ClO self-  
34 reaction and 210 nm absorption cross section of the ClO dimer, *J. Phys. Chem.*, *105*, 11226-11239,  
35 2001.
- 36 Bodeker, G. E., J. C. Scott, K. Kreher, and R. L. McKenzie, Global ozone trends in potential vorticity  
37 coordinates using TOMS and GOME intercompared against the Dobson network: 1978-1998, *J.*  
38 *Geophys. Res.*, *106*, 23029-23042, 2001.
- 39 Bodeker, G. E., H. Struthers, and B. J. Connor, Dynamical containment of Antarctic ozone depletion,  
40 *Geophys. Res. Lett.*, *29*, 10.1029/2001GL014206, 2002.
- 41 Bonne, G. P., R. M. Stimpfle, R. C. Cohen, P. B. Voss, K. K. Perkins, J. G. Anderson, R. J. Salawitch, J.  
42 W. Elkins, G. S. Dutton, K. W. Jucks, and G. C. Toon, An examination of the inorganic chlorine

- 1 budget in the lower stratosphere, *J. Geophys. Res.*, *105*, 1957-1971, 2000.
- 2 Bowman, K. P., Rossby wave phase speeds and mixing barriers in the stratosphere: 1. Observations, *J.*  
3 *Atmos. Sci.*, *53*, 905-916, 1996.
- 4 Bowman, K. P., and A. J. Krueger, A global climatology of total ozone from the Nimbus-7 Total Ozone  
5 Mapping Spectrometer, *J. Geophys. Res.*, *90*, 7967-7976, 1985.
- 6 Brasseur, G. P., The response of the middle atmosphere to long-term and short-term solar variability: A  
7 two-dimensional model, *J. Geophys. Res.*, *98*, 23079-23090, 1993.
- 8 Brasseur, G. P., X. Tie, P. J. Rasch, and F. Lefèvre, A three-dimensional simulation of the Antarctic  
9 ozone hole: Impact of anthropogenic chlorine on the lower stratosphere and upper troposphere, *J.*  
10 *Geophys. Res.*, *102*, 8909-8930, 1997.
- 11 Bridgeman, A. J., and J. Rothery, Bonding in mixed halogen and hydrogen peroxides, *J. Chem. Soc.*  
12 *Dalton*, *22*, 4077-4082, 1999.
- 13 Brown, S. S., R. K. Talukdar, and A. R. Ravishankara, Rate constants for the reaction  $\text{OH} + \text{NO}_2 + \text{M} \rightarrow$   
14  $\text{HNO}_3 + \text{M}$  under atmospheric conditions, *Chem. Phys. Lett.* *299*, 277-284, 1999a.
- 15 Brown, S. S., R. K. Talukdar, and A. R. Ravishankara, Reconsideration of the rate constant for the  
16 reaction of hydroxyl radicals with nitric acid, *J. Phys. Chem.*, *103*, 3031-3037, 1999b.
- 17 Brühl, C., P. J. Crutzen, and J.-U. Grooss, High-latitude, summertime  $\text{NO}_x$  activation and seasonal ozone  
18 decline in the lower stratosphere: Model calculations based on observations by HALOE on UARS,  
19 *J. Geophys. Res.*, *103*, 3587-3597, 1998.
- 20 Burrows, J. P., M. Weber, M. Buchwitz, V. V. Rozanov, A. Ladstadter-Weissenmayer, A. Richter, R. de  
21 Beek, R. Hoogen, K. Bramstedt, K.-U. Eichmann, M. Eisigner, and D. Perner, The Global Ozone  
22 Monitoring Experiment (GOME): Mission concept and first scientific results, *J. Atmos. Sci.*, *56*,  
23 151-175, 1999.
- 24 Butchart, N., and J. Austin, Middle atmosphere climatologies from the troposphere-stratosphere  
25 configuration of the UKMO's Unified Model, *J. Atmos. Sci.*, *55*, 2782-2809, 1998.
- 26 Carslaw, K. S., T. Peter, and S. L. Clegg, Modeling the composition of liquid stratospheric aerosols, *Rev.*  
27 *Geophys.*, *35*, 125-154, 1997a.
- 28 Carslaw, K. S., T. Peter, and R. Müller, Uncertainties in reactive uptake coefficients for solid  
29 stratospheric particles: 2. Effect on ozone depletion, *Geophys. Res. Lett.*, *24*, 1747-1750, 1997b.
- 30 Carslaw, K. S., M. Wirth, A. Tsias, B. P. Luo, A. Dörnbrack, M. Leutbecher, H. Volkert, W. Renger, J. T.  
31 Bacmeister, and T. Peter, Particle microphysics and chemistry in remotely observed mountain polar  
32 stratospheric clouds, *J. Geophys. Res.*, *103*, 5785-5796, 1998a.
- 33 Carslaw, K. S., M. Wirth, A. Tsias, B. P. Luo, A. Dörnbrack, M. Leutbecher, H. Volkert, W. Renger, J. T.  
34 Bacmeister, E. Reimer, and T. Peter, Increased stratospheric ozone depletion due to mountain-  
35 induced atmospheric waves, *Nature*, *391*, 675-678, 1998b.
- 36 Carslaw, K. S., T. Peter, J. T. Bacmeister, and S. D. Eckermann, Widespread solid particle formation by  
37 mountain waves in the Arctic stratosphere, *J. Geophys. Res.*, *104*, 1827-1836, 1999.
- 38 Carslaw, K., H. Oelhaf, J. Crowley, F. Goutail, B. Knudsen, N. Larsen, G. Redaelli, M. Rex, H. Roscoe,  
39 R. Ruhnke, and M. Volk, Polar Ozone, European Research in the Stratosphere 1996-2000,  
40 Advances in our understanding of the ozone layer during THESEO, Directorate-General for  
41 Research, Environment and Sustainable Development Programme, Office for Official Publications

- 1 of the European Communities EUR 19867, Chapter 3, 69-132, 2001.
- 2 Carslaw, K. S., J. Kettleborough, M. J. Northway, S. Davies, R. S. Gao, D. W. Fahey, D. G.  
3 Baumgardner, M. P. Chipperfield, and A. Kleinböhl, A vortex-scale simulation of the growth and  
4 sedimentation of large nitric acid particles observed during SOLVE/THESEO-2000, *J. Geophys.*  
5 *Res.*, in press, 2002.
- 6 Chen, P., The permeability of the Antarctic vortex edge, *J. Geophys. Res.*, 99, 20563-20571, 1994.
- 7 Chipperfield, M. P., Multiannual simulations with a three-dimensional chemical transport model, *J.*  
8 *Geophys. Res.*, 104, 1781-1805, 1999.
- 9 Chipperfield, M. P., and R. L. Jones, Relative influences of atmospheric chemistry and transport on Arctic  
10 ozone trends, *Nature*, 400, 551-554, 1999.
- 11 Chipperfield, M. P., and J. A. Pyle, Model sensitivity studies of Arctic ozone depletion, *J. Geophys. Res.*,  
12 103, 28389-28403, 1998.
- 13 Chipperfield, M. P., D. Cariolle, P. Simon, R. Ramaroson, and D. J. Lary, A 3-dimensional modeling  
14 study of trace species in the arctic lower stratosphere during winter 1989-1990, *J. Geophys. Res.*,  
15 98, 7199-7218, 1993.
- 16 Chipperfield, M. P., T. Glassup, I. Pundt, and O. V. Rattigan, Model calculations of stratospheric OBrO  
17 indicating very small abundances, *Geophys. Res. Lett.*, 25, 3575-3578, 1998.
- 18 Christiansen, B., Downward propagation of zonal mean zonal wind anomalies from the stratosphere to the  
19 troposphere: Model and reanalysis, *J. Geophys. Res.*, 106, 27307-27322, 2001.
- 20 Cohen, R. C., K. K. Perkins, L. C. Koch, R. M. Stimpfle, P. O. Wennberg, T. F. Hanisco, E. J.  
21 Lanzendorf, G. P. Bonne, P. B. Voss, R. J. Salawitch, L. A. Del Negro, J. C. Wilson, C. T.  
22 McElroy, and T. P. Bui, Quantitative constraints on the atmospheric chemistry of nitrogen oxides:  
23 An analysis along chemical coordinates, *J. Geophys. Res.*, 105, 24283-24304, 2000.
- 24 Considine, D. B., A. R. Douglass, P. S. Connell, D. E. Kinnison, and D. A. Rotman, A polar stratospheric  
25 cloud parameterization for the global modeling initiative three-dimensional model and its response  
26 to stratospheric aircraft, *J. Geophys. Res.*, 105, 3955-3973, 2000.
- 27 Corlett, G. K., and P. S. Monks, A comparison of total column ozone values derived from the Global  
28 Ozone Monitoring Experiment (GOME), the TIROS Operational Vertical Sounder (TOVS), and the  
29 Total Ozone Mapping Spectrometer (TOMS), *J. Atmos. Sci.*, 58, 1103-1116, 2001.
- 30 Cubasch, U., and R. Voss, The influence of total solar irradiance on climate, *Space Sci. Rev.*, 94, 185-198,  
31 2000.
- 32 Dameris, M., V. Grewe, R. Hein, and C. Schnadt, Assessment of future development of the ozone layer,  
33 *Geophys. Res. Lett.*, 25, 3579-3582, 1998.
- 34 Danilin, M. Y., M. L. Santee, J. M. Rodriguez, M. K. W. Ko, J. M. Mergenthaler, J. B. Kumer, A.  
35 Tabazadeh, and N. J. Livesey, Trajectory hunting: A case study of rapid chlorine activation in  
36 December 1992 as seen by UARS, *J. Geophys. Res.*, 105, 4003-4018, 2000.
- 37 Davies, S. M. P. Chipperfield, K. S. Carslaw, B.-M. Sinnhuber, J. G. Anderson, R. M. Stimpfle, D. M.  
38 Wilmouth, D. W. Fahey, P. J. Popp, E. C. Richard, P. von der Gathen, H. Jost, and C. R. Webster,  
39 Modeling the effect of denitrification on Arctic ozone depletion during winter 1999/2000, *J.*  
40 *Geophys. Res.*, in press, 2002.
- 41 de Grandpre, J., S. R. Beagley, V. I. Fomichev, E. Griffioen, J. C. McConnell, and A. S. Medvedev,  
42 Ozone climatology using interactive chemistry, results from the Canadian Middle Atmosphere

5/7/02

- 1 Model, *J. Geophys. Res.*, *105*, 26475-26491, 2000.
- 2 Del Negro, L. A., D. W. Fahey, R. S. Gao, S. G. Donnelly, E. R. Keim, J. A. Neuman, R. C. Cohen, K. K.  
3 Perkins, L. C. Koch, R. J. Salawitch, S. A. Lloyd, M. H. Proffitt, J. J. Margitan, R. M. Stimpfle, G.  
4 P. Bonne, P. B. Voss, P. O. Wennberg, C. T. McElroy, W. H. Swartz, T. L. Kusterer, D. E.  
5 Anderson, L. R. Lait, and T. P. Bui, Comparison of modeled and observed values of NO<sub>2</sub> and JNO<sub>2</sub>  
6 during the POLARIS mission, *J. Geophys. Res.*, *104*, 26687-26703, 1999.
- 7 DeMore, W. B. S. P. Sander, D. M. Golden, R. F. Hampson, M. J. Kurylo, C. J. Howard, A. R.  
8 Ravishankara, C. E. Kolb, and M. J. Molina, *Chemical Kinetics and Photochemical Data for Use in*  
9 *Stratospheric Modeling, Evaluation No. 12*, JPL Publ. 97-4, Jet Propulsion Laboratory, Pasadena,  
10 CA, USA, 1997.
- 11 Deniel, C., J. P. Pommereau, R. M. Bevilacqua, and F. Lefèvre, Arctic chemical ozone depletion during  
12 the 1994/95 winter deduced from POAM II satellite observations and the REPROBUS 3-D model,  
13 *J. Geophys. Res.*, *103*, 19231-19244, 1998.
- 14 Deniel, C., *et al.*, Arctic ozone loss deduced by POAM, *Proc. 5th European Symp. on Polar Ozone, Air*  
15 *Pollution Research Report 73*, Harris, Guirlet, and Amanatidis, (ed.), European Commission, 421-  
16 424, 2000. [Need complete author list.]
- 17 Deshler, T., and S. J. Oltmans, Vertical profiles of volcanic aerosol and polar stratospheric clouds above  
18 Kiruna, Sweden: Winters 1993 and 1995, *J. Atmos. Chem.*, *30*, 11-23, 1998.
- 19 Deshler, T., A. Adriani, D. J. Hofmann, and G. P. Gobbi, Evidence for denitrification in the 1990  
20 Antarctic spring stratosphere: II, lidar and aerosol measurements, *Geophys. Res. Lett.*, *18*, 1999-  
21 2002, 1991.
- 22 Deshler, T., T. Peter, R. Muller, and P. Crutzen, The lifetime of leewave-induced ice particles in the  
23 Arctic stratosphere: 1. Balloonborne observations, *Geophys. Res. Lett.*, *21*, 1327-1330, 1994.
- 24 Dessler, A. E., J. Wu, M. L. Santee, and M. R. Schoeberl, Satellite observations of temporary and  
25 irreversible denitrification, *J. Geophys. Res.*, *104*, 13993-14002, 1999.
- 26 Dhaniyala, S., K. A. McKinney, and P. O. Wennberg, Lee-wave clouds and denitrification in the polar  
27 stratosphere, submitted to *Geophys. Res. Lett.*, 2001.
- 28 Disselkamp, R. S., S. E. Anthony, A. J. Prenni, T. B. Onasch, and M. A. Tolbert, Crystallization kinetics  
29 of nitric acid dihydrate aerosols, *J. Phys. Chem.*, *100*, 9127-9137, 1996.
- 30 Dobson, G. M. B., Annual variation of ozone in Antarctica, *Quart. J. Roy. Met. Soc.*, *92*, 549-552, 1966.
- 31 Donaldson, D. J., G. J. Frost, K. H. Rosenlof, A. F. Tuck, and V. Vaida, Atmospheric radical production  
32 by excitation of vibrational overtones via absorption of visible light, *Geophys. Res. Lett.*, *24*, 2651-  
33 2654, 1997.
- 34 Dörnbrack, A., M. Leutbecher, J. Reichardt, A. Behrendt, K.-P. Müller, and G. Baumgarten, Relevance of  
35 mountain wave cooling for the formation of polar stratospheric clouds over Scandinavia: mesoscale  
36 dynamics and observations for January, 1997, *J. Geophys. Res.*, *106*, 1569-1581, 2001.
- 37 Dörnbrack, A., T. Birner, A. Fix, H. Flentje, A. Meister, H. Schmid, E. V. Browell, and M. J. Mahoney,  
38 Evidence for inertia-gravity waves forming polar stratospheric clouds over Scandinavia, *J.*  
39 *Geophys. Res.*, in press, 2002.
- 40 Douglass, A. R., M. R. Schoeberl, R. S. Stolarski, J. W. Waters, J. M. Russell III, A. E. Roche, and S. T.  
41 Massie, Interhemispheric differences in springtime production of HCl and ClONO<sub>2</sub> in the polar  
42 vortices, *J. Geophys. Res.*, *100*, 13967-13978, 1995.

5/7/02

- 1 Douglass, A. R., M. R. Schoeberl, S. R. Kawa, and E. V. Browell, A composite view of ozone evolution  
2 in the 1995-1996 northern winter polar vortex developed from airborne lidar and satellite  
3 observations, *J. Geophys. Res.*, *106*, 9879-9895, 2001.
- 4 Dransfield, T. J., K. K. Perkins, N. M. Donahue, J. G. Anderson, M. M. Sprengnether, and K. L.  
5 Demerjian, Temperature and pressure dependent kinetics of the gas-phase reaction of the hydroxyl  
6 radical with nitrogen dioxide, *Geophys. Res. Lett.*, *26*, 687-690, 1999.
- 7 Drdla, K., and M. R. Schoeberl, Microphysical modeling of the 1999-2000 winter: 2. Chlorine activation  
8 and ozone depletion, *J. Geophys. Res.*, in press, 2002.
- 9 Drdla, K., M. R. Schoeberl, and E. Browell, Microphysical modeling of the 1999-2000 winter: 1.  
10 Chlorine activation and ozone depletion, *J. Geophys. Res.*, in press, 2002.
- 11 Dütsch, H. U., Ozone distribution in atmosphere, *Canadian J. Chem.* *52*, 1491-1504, 1974.
- 12 Dvortsov, V. L., and S. Solomon, Response of the stratospheric temperatures and ozone to past and future  
13 increases in stratospheric humidity, *J. Geophys. Res.*, *106*, 7505-7514, 2001.
- 14 Dye, J. E., D. Baumgardner, B. W. Gandrud, S. R. Kawa, K. K. Kelly, M. Loewenstein, G. V. Ferry, K.  
15 R. Chan, and B. L. Gary, Particle size distribution in Arctic polar stratospheric clouds, growth and  
16 freezing of sulfuric acid droplets, and implications for cloud formation, *J. Geophys. Res.*, *30*, 8015-  
17 8034, 1992.
- 18 Engel, A., U. Schmidt, and R. A. Stachnik, Partitioning between chlorine reservoir species deduced from  
19 observations in the Arctic winter stratosphere, *J. Atmos. Chem.*, *27*, 107-126, 1997.
- 20 Erle, F., U. Platt, and K. Pfeilsticker, Measurement of OBrO upper limits in the nighttime stratosphere,  
21 *Geophys. Res. Lett.*, *27*, 2217-2220, 2000.
- 22 Esler, J. G., and D. W. Waugh, A method for estimating the extent of denitrification of Arctic polar  
23 vortex air from tracer-tracer scatter plots, submitted to *J. Geophys. Res.*, 2002.
- 24 EUR, European Research in the Stratosphere 1996-2000, European Union Report 19867, 2001.
- 25 Evans, S. J., R. Toumi, J. E. Harries, M. P. Chipperfield, and J. M. Russell, Trends in stratospheric  
26 humidity and the sensitivity of ozone to these trends, *J. Geophys. Res.*, *103*, 8715-8725, 1998.
- 27 Fahey, D. W., and A. R. Ravishankara, Summer in the stratosphere, *Nature*, *285*, 208-210, 1999.
- 28 Fahey, D. W., R. S. Gao, L. A. Del Negro, E. R. Keim, S. R. Kawa, R. J. Salawitch, P. O. Wennberg, T.  
29 F. Hanisco, E. J. Lanzendorf, K. K. Perkins, S. A. Lloyd, W. H. Swartz, M. H. Proffitt, J. J.  
30 Margitan, J. C. Wilson, R. M. Stimpfle, R. C. Cohen, C. T. McElroy, C. R. Webster, M.  
31 Loewenstein, J. W. Elkins, and T. P. Bui, Ozone destruction and production rates between spring  
32 and autumn in the Arctic stratosphere, *Geophys. Res. Lett.*, *27*, 2605-2608, 2000.
- 33 Fahey, D. W., R. S. Gao, K. S. Carslaw, J. Kettleborough, P. J. Popp, M. J. Northway, J. C. Holecek, S.  
34 C. Ciciora, R. J. McLaughlin, T. L. Thompson, R. H. Winkler, D. G. Baumgardner, B. Gandrud, P.  
35 O. Wennberg, S. Dhaniyala, K. McKinney, T. Peter, R. J. Salawitch, T. P. Bui, J. W. Elkins, C. R.  
36 Webster, E. L. Atlas, H. Jost, J. C. Wilson, R. L. Herman, A. Kleinböhl, and M. von König, The  
37 detection of large HNO<sub>3</sub>-containing particles in the winter Arctic stratosphere, *Science*, *291*, 1026-  
38 1031, 2001.
- 39 Farman, J. C., B. G. Gardiner, and J. D. Shanklin, Large losses of total ozone in Antarctica reveal  
40 seasonal ClO<sub>x</sub>/NO<sub>x</sub> interaction, *Nature*, *315*, 207, 1985.
- 41 Fels, S. B., Radiative dynamical interactions in the middle atmosphere, *Adv. Geophys.*, *28*, 277-300,



- 1 1985.
- 2 Fitzenberger, R., H. Bösch, C. Camy-Peyret, M. P. Chipperfield, H. Harder, U. Platt, B.-M. Sinnhuber, T.  
3 Wagner, and K. Pfeilsticker, First profile measurements of tropospheric BrO, *Geophys. Res. Lett.*,  
4 27, 2921-2924, 2000.
- 5 Flentje, H., W. Renger, and M. Wirth, Validation of Contour Advection simulations with airborne lidar  
6 measurements of filaments during the Second European Stratospheric Arctic and Midlatitude  
7 Experiment (SESAME), *J. Geophys. Res.*, 105, 15417-15437, 2000. [Need to verify reference.]
- 8 Forster, P. M. de F., and K. P. Shine, Radiative forcing and temperature trends from stratospheric ozone  
9 changes, *J. Geophys. Res.*, 102, 10841-10855, 1997.
- 10 Forster, P. M. de F., and K. P. Shine, Stratospheric water vapor changes as a possible contributor to  
11 observed stratospheric cooling, *Geophys. Res. Lett.*, 26, 3309-3312, 1999.
- 12 Forster, P. M. de F., and K. P. Shine, [Assessing the climate impact and its uncertainty for trends in](#)  
13 [stratospheric water vapor, submitted to \*Geophys. Res. Lett.\*, 2002.](#)
- 14 Forster, P. M. de F., R. S. Freckleton, and K. P. Shine, On the aspects of the concept of radiative forcing,  
15 *Clim. Dyn.*, 13, 547-560, 1997.
- 16 Forster, P. M. de F., M. Ponater, and W. Y. Zhong, Testing broadband radiation schemes for their ability  
17 to calculate the radiative forcing and temperature response to stratospheric water vapour and ozone  
18 changes, *Meteorol. Z.*, 10, 387-393, 2001.
- 19 Friess, U., M. P. Chipperfield, H. Harder, C. Otten, U. Platt, J. Pyle, T. Wagner, and K. Pfeilsticker,  
20 Intercomparison of measured and modeled BrO slant column amounts for the Arctic winter and  
21 spring 1994/95, *Geophys. Res. Lett.*, 26, 1861-1864, 1999.
- 22 Fromm, M. D., J. D. Lumpe, R. M. Bevilacqua, E. P. Shettle, J. Hornstein, S. T. Massie, and K. H. Fricke,  
23 Observations of Antarctic polar stratospheric clouds by POAM II: 1994-1996, *J. Geophys. Res.*,  
24 102, 23659-23672, 1997.
- 25 Fromm, M. D., R. M. Bevilacqua, J. Hornstein, E. Shettle, K. Hoppel, and J. D. Lumpe, An analysis of  
26 Polar Ozone and Aerosol Measurement (POAM) II Arctic polar stratospheric cloud observations,  
27 1993-1996, *J. Geophys. Res.*, 104, 24341-24358, 1999.
- 28 Füglistaler, S., B. P. Luo, T. Peter, and K. S. Carslaw, [Arctic stratospheric denitrification: Model study of](#)  
29 [NAT-rock formation by mother clouds, submitted to \*J. Geophys. Res.\*, 2001.](#)
- 30 Gao, R. S., D. W. Fahey, L. A. Del Negro, S. G. Donnelly, E. R. Keim, J. A. Neuman, E. Teverovskaia,  
31 P. O. Wennberg, T. F. Hanisco, E. J. Lanzendorf, M. H. Proffitt, J. J. Margitan, J. C. Wilson, J. W.  
32 Elkins, R. M. Stimpfle, R. C. Cohen, C. T. McElroy, T. P. Bui, R. J. Salawitch, S. S. Brown, A. R.  
33 Ravishankara, R. W. Portmann, M. K. W. Ko, D. K. Weisenstein, and P. A. Newman, A  
34 comparison of observations and model simulations of NO<sub>x</sub>/NO<sub>y</sub> in the lower stratosphere, *Geophys.*  
35 *Res. Lett.*, 26, 1153-1156, 1999.
- 36 Gao, R. S., L. A. Del Negro, W. H. Swartz, R. J. Salawitch, S. A. Lloyd, M. H. Proffitt, D. W. Fahey, S.  
37 G. Donnelly, J. A. Neuman, R. M. Stimpfle, and T. P. Bui, J<sub>NO<sub>2</sub></sub> at high solar zenith angles in the  
38 lower stratosphere, *Geophys. Res. Lett.*, 28, 2405-2408, 2001a
- 39 Gao, R. S., E. C. Richard, P. J. Popp, G. C. Toon, D. F. Hurst, P. A. Newman, J. C. Holecek, M. J.  
40 Northway, D. W. Fahey, M. Y. Danilin, B. Sen, K. Aikin, P. A. Romashkin, J. W. Elkins, C. R.  
41 Webster, S. M. Schauffler, J. B. Greenblatt, C. T. McElroy, L. R. Lait, T. P. Bui, and D.  
42 Baumgardner, Observational evidence for the role of denitrification in Arctic stratospheric ozone  
43 loss, *Geophys. Res. Lett.*, 28, 2879-2882, 2001b.

- 1 Garcia, R. R., and Boville, B. A., 'Downward control' of the mean meridional circulation and temperature  
2 distribution of the polar winter stratosphere, *J. Atmos. Sci.*, 51, 2238-2245, 1994.
- 3 Gleghorn, J. T., A G1 study of the isomers of ClOOBr and related systems, *Chem. Phys. Lett.*, 271, 296-  
4 301, 1997.
- 5 Gobbi, P. G., G. D. Donfrancesco, and A. Adriani, Physical properties of stratospheric clouds during the  
6 Antarctic winter of 1995, *J. Geophys. Res.*, 103, 10859, 1998.
- 7 Godin, S., V. Bergeret, S. Bekki, C. David, and G. Mégie, Study of the interannual ozone loss and the  
8 permeability of the Antarctic Polar Vortex from long-term aerosol and ozone lidar measurements in  
9 Dumont d'Urville (66.4S°, 140°E), *J. Geophys. Res.*, 106, 1311-1330, 2001.
- 10 Gomez, P. C., and L. F. Pacios, Bromine and mixed bromine chlorine oxides: Wave function (CCSD(T)  
11 and MP2) versus density functional theory (B3LYP) calculations, *J. Phys. Chem.*, 103, 739-743,  
12 1999.
- 13 Goutail, F., J.-P. Pommereau, C. Phillips, C. Deniel, A. Sarkissian, F. Lefèvre, E. Kyrö, M.  
14 Rummukainen, P. Ericksen, S. B. Andersen, B. A. Kåstad-Høiskar, G. O. Braathen, V. Dorokhov,  
15 V. U. Khattatov, Depletion of column ozone in the Arctic during the winters of 1993-94 and 1994-  
16 95, *J. Atmos. Chem.*, 32, 1-34, 1999.
- 17 Goutail, F., *et al.*, Total ozone loss in the Arctic winter vortex of 2000 and comparison to previous years,  
18 submitted to *J. Geophys. Res.*, 2002. [Need complete author list.]
- 19 Graf, H. F., I. Kirchner, and J. Perlwitz, Changing lower stratospheric circulation: The role of ozone and  
20 greenhouse gases, *J. Geophys. Res.*, 103, 11251-11261, 1998.
- 21 Gray, L. J., S. J. Phipps, T. J. Dunkerton, M. P. Baldwin, E. F. Drysdale, and M. R. Allen, A data study of  
22 the influence of the equatorial upper stratosphere on northern-hemisphere stratospheric sudden  
23 warmings, *Q. J. R. Meteorol. Soc.*, 127, 1985-2003, 2001.
- 24 Grewe, V., and M. Dameris, Heterogeneous PSC ozone loss during an ozone mini-hole, *Geophys. Res.*  
25 *Lett.*, 24, 2503-2506, 1997.
- 26 Grooss, J.-U., G. Günther, P. Konopka, R. Müller, D. S. McKenna, F. Stroh, B. Vogel, A. Engel, M.  
27 Müller, K. Hoppel, R. Bevilacqua, E. Richard, C. R. Webster, J. W. Elkins, D. F. Hurst, P.A.  
28 Romashkin, and D. G. Baumgardner, Simulation of ozone depletion in spring 2000 with the  
29 Chemical Lagrangian Model of the Stratosphere (CLaMS), *J. Geophys. Res.*, in press, 2002.
- 30 Groves, K. S., and A. F. Tuck, Stratospheric O<sub>3</sub> – CO<sub>2</sub> coupling in a photochemical model, I: Without  
31 chlorine chemistry, II: With chlorine chemistry, *Q. J. R. Meteorol. Soc.*, 106, 125-157, 1980.
- 32 Guirlet, M., M. P. Chipperfield, J. A. Pyle, F. Goutail, J. P. Pommereau, and E. Kyrö, Modeled Arctic  
33 ozone depletion in winter 1997/1998 and comparison with previous winters, *J. Geophys. Res.*, 105,  
34 22185-22200, 2000.
- 35 Hadjinicolau, P., A. Jrrar, J. A. Pyle, and L. Bishop, The dynamically-driven long-term trend in  
36 stratospheric ozone over high latitudes, *Q. J. R. Meteorol. Soc.*, in press, 2002.
- 37 Haigh, J. D., The role of stratospheric ozone in modulating the solar radiative forcing of climate. *Nature*,  
38 370, 544-546, 1994.
- 39 Haigh, J. D., A GCM study of climate change in response to the 11-year solar cycle, *Quart. J. Roy.*  
40 *Meteorol. Soc.*, 125, 871-892, 1999.
- 41 Hamilton, K., Effects of an imposed quasi-biennial oscillation in a comprehensive troposphere-  
42 stratosphere-mesosphere general circulation model, *J. Atmos. Sci.*, 55, 2393-2418, 1998.

5/7/02

- 1 Hamilton, K., R. J. Wilson, and R. S. Hemler, Middle atmosphere simulated with high vertical and  
2 horizontal resolution versions of a GCM: Improvements in the cold pole bias and generation of a  
3 QBO-like oscillation in the tropics, *J. Atmos. Sci.*, *56*, 3829-3846, 1999.
- 4 Hanisco, T. F., J. B. Smith, R. M. Stimpfle, D. M. Wilmouth, K. K. Perkins, J. R. Spackman, J. G.  
5 Anderson, D. Baumgardner, B. Gandrud, C. R. Webster, S. Dhaniyala, K. A. McKinney, and T. P.  
6 Bui, Quantifying the rate of heterogeneous processing in the Arctic polar vortex with in situ  
7 observations of OH, *J. Geophys. Res.*, in press, 2002.
- 8 Hansen, G., T. Svenøe, M. P. Chipperfield, A. Dahlback, and U.-P. Hoppe, Evidence of substantial ozone  
9 depletion in winter 1995/96 over northern Norway, *Geophys. Res. Lett.*, *24*, 799-802, 1997.
- 10 Hansen, G., A. Dahlback, F. Tonnessen, and T. Svenøe, Validation of GOME total ozone by means of the  
11 Norwegian ozone monitoring network, *Annales Geophysicae*, *17*, 430-436, 1999.
- 12 Hanson, D., and K. Mauersberger, Vapor pressures of HNO<sub>3</sub>/H<sub>2</sub>O solutions at low temperatures, *J. Phys.*  
13 *Chem.*, *92*, 6167-6170, 1988.
- 14 Harder, H., C. Camy-Peyret, F. Ferlemann, R. Fitzenberger, T. Hawat, H. Osterkamp, M. Schneider, D.  
15 Perner, U. Platt, P. Vradelis, and K. Pfeilsticker, Stratospheric BrO profiles measured at different  
16 latitudes and seasons: Atmospheric observations, *Geophys. Res. Lett.*, *25*, 3843-3846, 1998.
- 17 Harris, N. R. P., M. Rex, F. Goutail, B. M. Knudsen, G. L. Manney, R. Müller, and P. von der Gathen,  
18 Comparison of Empirically Derived Ozone Losses in the Arctic Vortex, *J. Geophys. Res.*, in press,  
19 2002.
- 20 Hartmann, D. L., J. M. Wallace, V. Limpasuvan, D. W. J. Thompson, and J. R. Holton, Can ozone  
21 depletion and global warming interact to produce rapid climate change, *Proc. Natl. Acad. Sci.*, *97*,  
22 1412-1417, 2000.
- 23 Haynes, P. H., C. J. Marks, M. E. McIntyre, T. G. Shepherd, and K. P. Shine, on the 'Downward Control'  
24 of extratropical diabatic circulations by eddy-induced mean zonal forces, *J. Atmos. Sci.*, *48*, 651-  
25 678, 1991.
- 26 Hein, R., M. Dameris, C. Schnadt, C. Land, V. Grewe, I. Kohler, M. Ponater, R. Sausen, B. Steil, J.  
27 Landgraf, and C. Brühl, Results of an interactively coupled atmospheric chemistry - general  
28 circulation model: comparison with observations, *Annales Geophysicae*, *19*, 435-457, 2001.
- 29 Hendricks, J., F. Baier, G. Gunther, B. C. Kruger, and A. Ebel, Stratospheric ozone depletion during the  
30 1995-1996 Arctic winter: 3-D simulations on the potential role of different PSC types, *Annales*  
31 *Geophysicae*, 1163-1181, 2001.
- 32 Herman, R. L., K. Drdla, J. R. Spackman, D. F. Hurst, P. J. Popp, C. R. Webster, J. W. Elkins, E. M.  
33 Weinstock, B. W. Gandrud, G. C. Toon, M. R. Schoeberl, H. Jost, E. L. Atlas, and T. P. Bui,  
34 Hydration, dehydration, and the total hydrogen budget of the 1999-2000 winter Arctic stratosphere,  
35 *J. Geophys. Res.*, in press, 2002.
- 36 Hines, C. O., Doppler spread parameterization of gravity wave momentum deposition in the middle  
37 atmosphere, Part 1: Basic formulation, Part 2: Broad and quasi-monochromatic spectra and  
38 implementation, *J. Atmos. Solar Terr. Phys.*, *59*, 371-400, 1997.
- 39 Hints, H. J., P. A. Newman, H. H. Jonsson, C. R. Webster, R. D. May, R. L. Herman, L. R. Lait, M. R.  
40 Schoeberl, J. W. Elkins, P. R. Wamsley, G. S. Dutton, T. P. Bui, D. W. Kohn, and J. G. Anderson,  
41 Dehydration and denitrification in the Arctic polar vortex during the 1995-1996 winter, *Geophys.*  
42 *Res. Lett.*, *25*, 501-504, 1998.
- 43 Hofmann, D. J., and T. Deshler, Stratospheric cloud observations during formation of the Antarctic ozone

- 1 hole in 1989, *J. Geophys. Res.*, 96, 2897-2912, 1991.
- 2 Hofmann, D. J., S. J. Oltmans, J. M. Harris, B. J. Johnson, and J. A. Lathrop, Ten years of ozonesonde  
3 measurements at the south pole: Implication for recovery of springtime Antarctic ozone, *J.*  
4 *Geophys. Res.*, 102, 8931-8943, 1997.
- 5 Holton, J. R., Meridional distribution of stratospheric trace constituents. *J. Atmos. Sci.*, 43, 1238-1242,  
6 1986.
- 7 Hood, L. L., and S. Zhou, Stratospheric effects of 27-day solar ultraviolet variations: The column ozone  
8 response and comparisons of solar cycles 21 and 22, , *J. Geophys. Res.*, 104, 26473-26479, 1999.
- 9 Hood, L., S. Rossi, and M. Beulen, Trends in lower stratospheric zonal winds, Rossby wave breaking  
10 behavior, and column ozone at northern midlatitudes, *J. Geophys. Res.*, 104, 24,321-24,339, 1999.
- 11 Hood, L. L., B. E. Soukharev, M. Fromm, and J. P. McCormack, Origin of extreme ozone minima at  
12 middle to high northern latitudes, *J. Geophys. Res.*, 106, 20925-20940, 2001.
- 13 Hoogen, R., V.V. Rozanov, and J.P. Burrows, Ozone profiles from GOME satellite data: Algorithm  
14 description and first validation, *J. Geophys. Res.*, 104, 8263-8280, 1999.
- 15 Hopfner, M., C. E. Blom, H. Fischer, N. Glatthor, T. Gulde, C. Piesch, W. Renger, and M. Wirth, HNO<sub>3</sub>  
16 and PSC measurements from the TRANSALL: Sequestering of HNO<sub>3</sub> in the winter of 1994/95, *J.*  
17 *Atmos. Chem.*, 30, 61-79, 1998.
- 18 Hoppel, K. W., R. M. Bevilacqua, G. Nedoluha, C. Deniel, F. Lefèvre, J. D. Lumpe, M. D. Fromm, C. E.  
19 Randall, J. Rosenfield, and M. Rex, POAM III observations of Arctic ozone loss for the 1999/2000  
20 winter, *J. Geophys. Res.*, in press, 2002.
- 21 Hu, R., K. S. Carslaw, C. Hostetler, L. R. Poole, B. P. Luo, T. Peter, S. Füglistaler, T. J. McGee, and J. F.  
22 Burris, The microphysical properties of wave PSCs retrieved from lidar measurements during  
23 SOLVE, *J. Geophys. Res.*, in press, 2002.
- 24 Huder, K. J., and W. B. DeMore, Absorption cross sections of the ClO dimer, *J. Phys. Chem.*, 99, 3905-  
25 3908, 1995.
- 26 Ionov, D. V., Y. M. Timofeev, V. V. Ionov, A. M. Shalamyanskii, O. M. Johannessen, and J. P. Burrows,  
27 Comparison of measurements of total ozone by the GOME (ERS-2) spectrometer with data from  
28 the Russian ozonometric network, *Earth Obs. Rem. Sens.*, 16, 527-539, 2001.
- 29 IPCC, *Climate Change 1992: The Intergovernmental Panel on Climate Change Scientific Assessment,*  
30 *Supplementary Report*, J. T. Houghton, B. A. Callander, and S. K. Varney, (eds.), Cambridge  
31 University Press, Cambridge, U.K., 1992.
- 32 IPCC, *Climate Change 1995: The Science of Climate Change*, The Intergovernmental Panel on Climate  
33 Change, Cambridge University Press, Cambridge, U.K., 1996.
- 34 IPCC, *Climate Change 2001: The Scientific Basis*, The Intergovernmental Panel on Climate Change,  
35 Cambridge University Press, Cambridge, U.K., 2001.
- 36 Iraci, L. T., A. M. Middlebrook, M. A. Wilson, and M. A. Tolbert., Growth of nitric-acid hydrates on thin  
37 sulfuric-acid films, *Geophys. Res. Lett.*, 21, 867-870 , 1994.
- 38 Iraci, L. T., A. M. Middlebrook, and M. A. Tolbert, Laboratory studies of the formation of polar  
39 stratospheric clouds - nitric-acid condensation on thin sulfuric-acid films, *J. Geophys. Res.*, 100,  
40 20969-20977, 1995.
- 41 Iraci, L. T., T. J. Fortin, and M. A. Tolbert, Dissolution of sulfuric acid tetrahydrate at low temperatures

- 1 and subsequent growth of nitric acid trihydrate, *J. Geophys. Res.*, *103*, 8491-8498, 1998.
- 2 Irie, H., M. Koike, Y. Kondo, G. E. Bodeker, M. Y. Danilin, and Y. Sasano, Redistribution of nitric acid  
3 in the Arctic lower stratosphere during the winter of 1996-1997, *J. Geophys. Res.*, *106*, 23139,  
4 2001.
- 5 Irie, H., Y. Kondo, M. Koike, M. Y. Danilin, C. Camy-Peyret, S. Payan, J. P. Pommereau, F. Goutail, H.  
6 Oelhaf, G. Wetzel, G. C. Toon, B. Sen, R. M. Bevilacqua, J. M. Russell III, J. B. Renard, H.  
7 Kanzawa, H. Nakajima, T. Yokota, T. Sugita and Y. Sasano, Validation of NO<sub>2</sub> and HNO<sub>3</sub>  
8 measurements from the Improved Limb Atmospheric Spectrometer (ILAS) with the version 5.20  
9 retrieval algorithm, *J. Geophys. Res.*, in press, 2002.
- 10 Jensen, E., O. B. Toon, K. Drdla, and A. Tabazadeh, Impact of polar stratospheric cloud particle  
11 composition, number density, and lifetime on denitrification, *J. Geophys. Res.*, in press, 2002.
- 12 Johnsson, K., A. Engdahl, J. Kolm, J. Nieminen, and B. Nelander, The ClOClO, BrOClO, and IOClO  
13 molecules and their photoisomerization – A matrix isolation study, *J. Chem. Phys.*, *99*, 3902-3904,  
14 1995.
- 15 Jones, R. L., and A. R. MacKenzie, Observational studies of the role of the polar regions in mid-latitude  
16 ozone loss, *Geophys. Res. Lett.*, *22*, 3485-3488, 1995.
- 17 Juckes, M. N., and M. E. McIntyre, A high-resolution, one-layer model of breaking planetary waves in  
18 the stratosphere, *Nature*, *328*, 590-596, 1987.
- 19 Jucks, K. W., D. G. Johnson, K. V. Chance, W. A. Traub, and R. J. Salawitch, Nitric acid in the middle  
20 stratosphere as a function of altitude and aerosol loading, *J. Geophys. Res.*, *104*, 26715-26723,  
21 1999.
- 22 Jucks, K. W., D. G. Johnson, K. V. Chance, W. A. Traub, J. J. Margitan, G. B. Osterman, R. J. Salawitch,  
23 and Y. Sasano, Observations of OH, HO<sub>2</sub>, H<sub>2</sub>O, and O<sub>3</sub> in the upper stratosphere: implications for  
24 HO<sub>x</sub> photochemistry, *Geophys. Res. Lett.*, *25*, 3935-3938, 1998.
- 25 Kaledin, A., and K. Morokuma, An *ab initio* direct study of the photodissociation of ClOOCl, *J. Chem.*  
26 *Phys.*, *113*, 5750-5762, 2000.
- 27 Kanzawa, H., C. Schiller, J. Ovarlez, C. Camy-Peyret, S. Payan, P. Jeseck, H. Oelhaf, M. Stowasser, W.  
28 A. Traub, K. Jucks, D. G. Johnson, G. C. Toon, J. H. Park, G. Bodeker, L. Pan, T. Sugita, H.  
29 Nakajima, T. Yokota, M. Suzuki, M. Shiotani, and Y. Sasano, Validation and data characteristics of  
30 water vapor profiles observed by the Improved Limb Atmospheric Spectrometer (ILAS) and  
31 processed with Version 5.20 algorithm, *J. Geophys. Res.*, in press, 2002.
- 32 Kawamoto, N., and M. Shiotani, Interannual variability of the vertical descent rate in the Antarctic polar  
33 vortex, *J. Geophys. Res.*, *105*, 11935-11946, 2000.
- 34 Kettleborough, J. A., and J. R. Holton, Limitations of a diagnostic of stratospheric tracer lamination. *J.*  
35 *Geophys. Res.*, *104*, 21621-21628, 1999.
- 36 Kilbane-Dawe, I., N. R. P. Harris, J. A. Pyle, M. Rex, A. M. Lee, and M. P. Chipperfield, A comparison  
37 of Match ozonesonde-derived and 3-D model ozone loss rates in the Arctic polar vortex during the  
38 winters of 1994/95 and 1995/96, *J. Atmos. Chem.*, *39*, 123-138, 2001.
- 39 Kiehl, J. T., B. A. Boville, and B. P. Briegleb, Response of a general-circulation model to a prescribed  
40 Antarctic ozone hole, *Nature*, *332*, 501-504, 1988.
- 41 Kirchner, I., G. L. Stenchikov, H.-F. Graf, A. Robock, and J. C. Antuna, Climate model simulation of  
42 winter warming and summer cooling following the 1991 Mt. Pinatubo eruption, *J. Geophys. Res.*,

- 1 104, 19039-19055, 1999.
- 2 Kirk-Davidoff, D. B., E. J. Hints, J. G. Anderson, and D. W. Keith, The effect of climate change on  
3 ozone depletion through changes in stratospheric water vapour, *Nature*, 402, 399-401, 1999.
- 4 Klein, U., K. Linder, I. Wohltmann, and K. F. Künzi, Winter and spring observations of stratospheric  
5 chlorine monoxide from Ny-Ålesund, Spitsbergen in 1997/98 and 1998/99, *Geophys. Res. Lett.*, 27,  
6 4093-4096, 2000.
- 7 Knudsen, B. M., N. Larsen, I. S. Mikkelsen, J.-J. Morcrette, G. O. Braathen, E. Kyrö, H. Fast, H.  
8 Gernandt, H. Kanzawa, H. Nakane, V. Dorokhov, V. Yushkov, G. Hansen, M. Gil, and R. J.  
9 Shearman, Ozone depletion in and below the Arctic vortex for 1997, *Geophys. Res. Lett.*, 25, 627-  
10 630, 1998.
- 11 Knudsen, B. M., J.-P. Pommereau, A. Garnier, M. Nunes-Pinharanda, L. Denis, P. A. Newman, G.  
12 Letrenne, and M. Durand, Accuracy of analyzed stratospheric temperature in the winter Arctic  
13 vortex from infra-red Montgolfier long duration balloon flights, Part II: Results, *J. Geophys. Res.*,  
14 in press, 2002.
- 15 Kodera, K., Influence of volcanic eruptions on the troposphere through stratospheric dynamical processes  
16 in the Northern Hemisphere winter. *J. Geophys. Res.*, 99, 1273-1282, 1994.
- 17 Kodera, K., and Y. Kuroda, Tropospheric and stratospheric aspects of the Arctic Oscillation, *Geophys.*  
18 *Res. Lett.*, 27, 3349-3352, 2000.
- 19 Kodera, K., M. Chiba, H. Koide, A. Kitoh, and Y. Nikaidou, Interannual variability of the winter  
20 stratosphere and troposphere in the Northern Hemisphere, *J. Meteorol. Soc. Japan*, 74, 365-382,  
21 1996.
- 22 Kodera, K., Y. Kuroda, and S. Pawson, Stratospheric sudden warmings and slowly propagating zonal-  
23 mean wind anomalies, *J. Geophys. Res.*, 105, 12351-12359, 2000.
- 24 Koike, M., Y. Kondo, H. Irie, F. J. Murcray, J. Williams, P. Fogal, R. Blatherwick, C. Camy-Peyret, S.  
25 Payan, H. Oelhaf, G. Wetzel, W. Traub, D. Johnson, K. Jucks, G. C. Toon, B. Sen, J.-F. Blavier, H.  
26 Schlager, H. Ziereis, N. Toriyama, M. Y. Danilin, J. M. Rodriguez, H. Kanzawa, and Y. Sasano, A  
27 comparison of Arctic HNO<sub>3</sub> profiles measured by ILAS and balloon-borne sensors, *J. Geophys.*  
28 *Res.*, 105, 6761-6771, 2000.
- 29 Kondo, Y., H. Irie, M. Koike, and G. E. Bodeker, Denitrification and nitrification in the Arctic  
30 stratospheric during the winter of 1996-1997, *Geophys. Res. Lett.*, 27, 337, 2000.
- 31 Koop, T., B. Luo, U. M. Biermann, P. J. Crutzen, and Th. Peter, Freezing of HNO<sub>3</sub>/H<sub>2</sub>SO<sub>4</sub>/H<sub>2</sub>O solutions  
32 at stratospheric temperatures: Nucleation statistics and experiments, *J. Phys. Chem.*, 101, 1117-  
33 1133, 1997.
- 34 Koop, T., U. M. Biermann, W. Raber, B. P. Luo, P. J. Crutzen, and Th. Peter, Do stratospheric aerosol  
35 droplets freeze above the ice frost point?, *Geophys. Res. Lett.*, 22, 917-920, 1995.
- 36 Kopp, G., H. Berg, T. Blumenstock, H. Fischer, F. Hase, G. Hochschild, M. Hoepfner, W. Kouker, I.  
37 Langbein, T. Reddmann, R. Ruhnke, U. Raffalski, and Y. Kondo, Evolution of ozone and ozone  
38 related species over Kiruna during the THESEO 2000-SOLVE campaign retrieved from ground-  
39 based millimeter wave and infrared observations, *J. Geophys. Res.*, in press, 2002.
- 40 Kuroda, Y., and K. Kodera, Interannual variability in the troposphere and stratosphere of the Southern  
41 Hemisphere winter, *J. Geophys. Res.*, 103, 13787-13799, 1998.
- 42 Kuroda, Y., and K. Kodera, Role of planetary waves in the stratosphere-troposphere coupled variability in

- 1 the Northern Hemisphere winter, *Geophys. Res. Lett.*, 26, 2375-2378, 1999.
- 2 Labitzke, K., On the interannual variability of the middle stratosphere during the northern winters, *J. Met.*  
3 *Soc. Japan*, 60, 124-139, 1982.
- 4 Labitzke, K., and H. van Loon, The southern oscillation, Part IX: The influence of volcanic-eruptions on  
5 the southern oscillation in the stratosphere, *J. Climate*, 2, 1223-1226, 1989.
- 6 Labitzke, K., and H. van Loon, A note on the distribution of trends below 10 hPa: The extratropical  
7 Northern Hemisphere, *J. Met. Soc. Japan*, 73, 8883-8889, 1995.
- 8 Labitzke, K., and H. van Loon, The signal of the 11-year solar cycle in the upper troposphere-lower  
9 stratosphere, *Space Sci. Rev.*, 80, 393-410, 1997.
- 10 Labitzke, K., J. Austin, N. Butchart, J. Knight, J. Haigh, and V. Williams, The global signal of the 11-  
11 year solar cycle in the stratosphere, *J. Atmos. Sol.-Terr. Phys.*, in press, 2002.
- 12 Langematz, U., An estimate of the impact of observed ozone losses on stratospheric temperature.  
13 *Geophys. Res. Lett.*, 27, 2077-2080, 2000.
- 14 Langematz, U., K. Kirstin, M. Kunze, M. Labitzke, G. L. Roff, Thermal and dynamical changes of the  
15 stratosphere since 1979 and their link to ozone and CO<sub>2</sub> changes, submitted to *J. Geophys. Res.*,  
16 2002.
- 17 Larkin, A., J. D. Haigh, and S. Djavidnia, The effect of solar UV irradiance variations on the Earth's  
18 atmosphere, *Space Sci. Rev.*, 94, 199-214, 2000.
- 19 Larsen, N., I. S. Mikkelsen, B. M. Knudsen, J. Schreiner, C. Voigt, K. Mauersberger, J. M. Rosen, and N.  
20 T. Kjome, Comparison of chemical and optical in-situ measurements of polar stratospheric clouds,  
21 *J. Geophys. Res.*, 105, 1491-1502, 2000.
- 22 Larsen, N., S. Høyer Svendsen, B. M. Knudsen, C. Voigt, A. Kohlmann, J. Schreiner, K. Mauersberger, T.  
23 Deshler, C. Kröger, J. M. Rosen, N. T. Kjome, A. Adriani, F. Cairo, G. Di Donfrancesco, J.  
24 Ovarlez, H. Ovarlez, A. Dörnbrack and T. Birner, Microphysical mesoscale simulations of polar  
25 stratospheric cloud formation constrained by in-situ measurements of chemical and optical cloud  
26 properties, accepted, *J. Geophys. Res.*, 2002.
- 27 Lawrence, B. N., Some aspects of the sensitivity of stratospheric climate simulation to model lid height,  
28 *J. Geophys. Res.*, 102, 23805-23811, 1997.
- 29 Lee, A. M., H. K. Roscoe, and S. Oltmans, Model and measurements show Antarctic ozone loss follows  
30 edge of polar night, *Geophys. Res. Lett.*, 27, 3845-3848, 2000.
- 31 Lee, A. M., H. K. Roscoe, A. E. Jones, P. H. Haynes, E. F. Shuckburgh, M. W. Morrey, and H. C.  
32 Pumphrey, The impact of the mixing properties within the Antarctic stratospheric vortex on ozone  
33 loss in spring, *J. Geophys. Res.*, 106, 3203-3211, 2001.
- 34 Lefèvre, F., F. Figarol, K. S. Carslaw, and T. Peter, The 1997 Arctic ozone depletion quantified from  
35 three-dimensional model simulations, *Geophys. Res. Lett.*, 25, 2425-2428, 1998.
- 36 Li, S., E. C. Cordero, and D. J. Karoly, Transport out of the Antarctic polar vortex from a three-  
37 dimensional transport model, *J. Geophys. Res.*, in press, 2002.
- 38 Liley, J. B., P. V. Johnston, R. L. McKenzie, A. J. Thomas, and I. S. Boyd, Stratospheric NO<sub>2</sub> variations  
39 from a long time series at Lauder, New Zealand, *J. Geophys. Res.*, 105, 11633-11640, 2000.
- 40 Lloyd, S., W. H. Swartz, T. Kusterer, D. Anderson, C. T. McElroy, C. Midwinter, R. Hall, K. Nassim, D.  
41 Jaffe, W. Simpson, J. Kelley, D. Nicks, D. Griffin, B. Johnson, R. Evans, D. Quincey, S. Oltmans, P.

5/7/02

- 1 Newman, R. McPeters, G. Labow, L. Moy, C. Seftor, G. Toon, B. Sen, and J.-F. Blavier,  
2 Intercomparison of total ozone observations at Fairbanks, Alaska during POLARIS, *J. Geophys.*  
3 *Res.*, *104*, 26767-26778, 1999.
- 4 Lucic, D., N. R. P. Harris, J. A. Pyle, and R. L. Jones, A technique for estimating polar ozone loss:  
5 Results from the northern 1991/92 winter using EASOE data, *J. Atmos. Chem.*, *34*, 365-383, 1999.
- 6 Lucke, R. L., D. R. Korwan, R. M. Bevilacqua, J. S. Hornstein, E. P. Shettle, D. T. Chen, M. Dähler, J. D.  
7 Lumpe, M. D. Fromm, D. Debrestian, B. Neff, M. Squire, G. König-Langlo, and J. Davies, The  
8 Polar Ozone and Aerosol Measurement (POAM) III instrument and early validation results, *J.*  
9 *Geophys. Res.*, *104*, 18785-18799, 1999.
- 10 Lumpe, J. D., M. Fromm, K. Hoppel, R. M. Bevilacqua, C. E. Randall, E. V. Browell, W. B. Grant, T.  
11 McGee, J. Burris, L. Twigg, E. Richard, G. C. Toon, J. J. Margitan, B. Sen, K. Pfeilsticker, H.  
12 Boesch, R. Fitzenberger, F. Goutail, and J.-P. Pommereau, Comparison of POAM III ozone  
13 measurements with correlative aircraft and balloon data during SOLVE, *J. Geophys. Res.*, in press,  
14 2002.
- 15 Mahlman, J. D., J. P. Pinto, and L. J. Umscheid, Transport radiative and dynamical effects of the  
16 Antarctic ozone hole - A GFDL SKYHI Model experiment, *J. Atmos. Sci.*, *51*, 489-508, 1994.
- 17 Mann, G. W., S. Davies, K. S. Carslaw, M. P. Chipperfield, and J. Kettleborough, Influence of vortex  
18 baroclinicity on Arctic denitrification, *J. Geophys. Res.*, in press, 2002.
- 19 Manney, G. L., L. Froidevaux, J. W. Waters, R. W. Zurek, W. G. Read, L. S. Elson, J. B. Kumer, J. L.  
20 Mergenthaler, A. E. Roche, A. O'Neill, R. S. Harwood, I. MacKenzie, and R. Swinbank, Chemical  
21 depletion of ozone in the Arctic lower stratosphere during winter 1992-93, *Nature*, *370*, 429, 1994.
- 22 Manney, G. L., R. W. Zurek, L. Froidevaux, J. W. Waters, A. O'Neill, and R. Swinbank, Lagrangian  
23 transport calculations using UARS data. Part II: Ozone, *J. Atmos. Sci.*, *52*, 3069-3081, 1995a.
- 24 Manney, G. L., R. W. Zurek, L. Froidevaux, and J. W. Waters, Evidence for Arctic ozone depletion in  
25 late February and early March 1994, *Geophys. Res. Lett.*, *22*, 2941-2944, 1995b.
- 26 Manney, G. L., M. L. Santee, L. Froidevaux, J. W. Waters, and R. W. Zurek, Polar vortex conditions  
27 during the 1995-96 Arctic winter: Meteorology and MLS ozone, *Geophys. Res. Lett.*, *23*, 3203-  
28 3206, 1996a.
- 29 Manney, G. L., L. Froidevaux, J. W. Waters, M. L. Santee, W. G. Read, D. A. Flower, R. F. Garnet, and  
30 R. W. Zurek, Arctic ozone depletion observed by UARS MLS during the 1994-95 winter, *Geophys.*  
31 *Res. Lett.*, *23*, 85-88, 1996b.
- 32 Manney, G. L., L. Froidevaux, M. L. Santee, R. W. Zurek, and J. W. Waters, MLS observations of Arctic  
33 ozone loss in 1996-1997, *Geophys. Res. Lett.*, *24*, 2697-2700, 1997.
- 34 Manney, G. L., J. C. Bird, D. P. Donovan, T. J. Duck, J. A. Whiteway, S. R. Pal, and A. I. Carswell,  
35 Modeling ozone laminae in ground-based Arctic wintertime observations using trajectory  
36 calculations and satellite data, *J. Geophys. Res.*, *103*, 5797-5814, 1998.
- 37 Manney, G. L., W. A. Lahoz, R. Swinbank, A. O'Neill, P. M. Connaw, and R. W. Zurek, Simulation of  
38 the December 1998 stratospheric major warming, *Geophys. Res. Lett.*, *26*, 2733-2736, 1999.
- 39 Manney, G. L., H. A. Michelsen, F. W. Irion, G. C. Toon, M. R. Gunson, and A. E. Roche, Lamination  
40 and polar vortex development in fall from ATMOS long-lived trace gases observed during  
41 November 1994, *J. Geophys. Res.*, *105*, 29023-29038, 2000.
- 42 Manney, G. L., J. L. Sabutis, and R. Swinbank, A unique stratospheric warming event in December 2000,



- 1        *Geophys. Res. Lett.*, 28, 2629-2632, 2001.
- 2        Manney, G. L., J. L. Sabutis, S. Pawson, M. L. Santee, B. Naujokat, R. Swinbank, M. E. Gelman, and W.  
3        Ebisuzaki, Lower stratospheric temperature differences between meteorological analyses in two  
4        cold Arctic winters and their impact on polar processing studies, *J. Geophys. Res.*, in press, 2002.
- 5        Manzini, E., and N. A. McFarlane, The effect of varying the source spectrum of a gravity wave  
6        parameterization in a middle atmosphere general circulation model, *J. Geophys. Res.*, 103, 31523-  
7        31539, 1998.
- 8        Manzini, E., B. Steil, C. Brühl, M. Giorgetta, and K. Krüger, Interactive chemistry-climate modeling of  
9        the middle atmosphere, Part 2: Sensitivity to changes from near past to present conditions and  
10       comparison with observed trends, manuscript in preparation, 2002.
- 11       Massie, S. T., X. Tie, G. P. Brasseur, R. M. Bevilacqua, M. D. Fromm, and M. L. Santee, Chlorine  
12       activation during the early 1995-1996 Arctic winter, *J. Geophys. Res.*, 105, 7111-7132, 2000.
- 13       McCormick, M. P., W. P. Chu, G. W. Grams, P. Hamill, B. M. Herman, L. R. McMaster, T. J. Pepin, P.  
14       B. Russell, H. M. Steele, and T. J. Swissler, High-latitude stratospheric aerosols measured by the  
15       SAM II satellite system in 1978 and 1979, *Science*, 214, 328-331, 1981.
- 16       McKenna, D., R. L. Jones, J. Austin, E. V. Browell, M. P. McCormick, A. J. Krueger, and A. F. Tuck,  
17       Diagnostic studies of the Antarctic Vortex during the 1987 Airborne Antarctic Ozone Experiment:  
18       Ozone mini-holes, *J. Geophys. Res.*, 94, 11641-11668, 1989.
- 19       McLandress, C., On the importance of gravity waves in the middle atmosphere and their parameterization  
20       in general circulation models, *J. Atmos. Sol.-Terr. Phys.*, 60, 1357-1383, 1998.
- 21       McLinden, C. A., S. C. Olsen, M. J. Prather, and J. B. Liley, Understanding trends in stratospheric NO<sub>y</sub>  
22       and NO<sub>2</sub>, *J. Geophys. Res.*, 106, 27787- 27793, 2001.
- 23       Medvedev, A. S., and G. P. Klaassen, Vertical evolution of gravity wave spectra and the parameterization  
24       of associated wave drag, *J. Geophys. Res.*, 100, 25841-25853, 1995.
- 25       Medvedev, A. S., G. P. Klaassen, and S. R. Beagley, In the role of anisotropic gravity wave spectrum in  
26       maintaining the circulation of the middle atmosphere, *Geophys. Res. Lett.*, 25, 509-512, 1998.
- 27       Meilinger, S. K., T. Koop, B. P. Luo, T. Huthwelker, K. S. Carslaw, U. Kreiger, P. J. Crutzen, and T.  
28       Peter, Size-dependent stratospheric droplet composition in lee wave temperature-fluctuations and  
29       their potential role in PSC freezing, *Geophys. Res. Lett.*, 22, 3031-3034, 1995.
- 30       Mergenthaler, J. L., J. B. Kumer, A. E. Roche, and S. T. Massie, Distribution of Antarctic polar  
31       stratospheric clouds as seen by the CLAES experiment, *J. Geophys. Res.*, 102, 19161-19170, 1997.
- 32       Michelsen, H. A., G. L. Manney, M. R. Gunson, and R. Zander, Correlations of stratospheric abundances  
33       of NO<sub>y</sub>, O<sub>3</sub>, N<sub>2</sub>O, and CH<sub>4</sub> derived from ATMOS measurements, *J. Geophys. Res.*, 103, 28347-  
34       28359, 1998.
- 35       Michelsen, H. A., C. R. Webster, G. L. Manney, D. C. Scott, J. J. Margitan, R. D. May, F. W. Irion, M. R.  
36       Gunson, J. M. Russell III, and C. M. Spivakovsky, Maintenance of high HCl/Cl<sub>y</sub> and NO<sub>x</sub>/NO<sub>y</sub> in  
37       the Antarctic vortex: A chemical signature of confinement during spring, *J. Geophys. Res.*, 104,  
38       26419-26436, 1999.
- 39       Mickley, L. J., J. P. D. Abbatt, J. E. Frederick, and J. M. Russell III, Evolution of chlorine and nitrogen  
40       species in the lower stratosphere during Antarctic spring: Use of tracers to determine chemical  
41       change, *J. Geophys. Res.*, 102, 21479-21491, 1997.

5/7/02

- 1 Millard, G. A., A. M. Lee, and J. A. Pyle, A model study of the connection between polar and mid-  
2 latitude ozone loss in the Northern Hemisphere lower stratosphere, *J. Geophys. Res.*, in press, 2002.
- 3 Miller, H. L., R. W. Sanders, and S. Solomon, Observations and interpretation of column OClO seasonal  
4 cycles at polar sites, *J. Geophys. Res.*, *104*, 18769-18783, 1999.
- 5 Mo, R. P., O. Buhler, and M. E. McIntyre, Permeability of the vortex edge: on the mean mass flux due to  
6 thermally dissipating, steady, non-breaking Rossby waves, *Quart. J. Roy. Meteorol. Soc.*, *124*,  
7 2129-2148, 1998.
- 8 Moore, T. A., M. Okumura, J. W. Seale, and T. K. Minton, UV Photolysis of ClOOCl, *J. Phys. Chem.*,  
9 *103*, 1691-1695, 1999.
- 10 Müller, R., P. J. Crutzen, J.-E. Grooss, C. Brühl, J. M. Russell III, and A. F. Tuck, Chlorine activation and  
11 ozone depletion in the Arctic vortex: Observations by the Halogen Occultation Experiment on the  
12 Upper Atmosphere Research Satellite, *J. Geophys. Res.*, *101*, 12531-12554, 1996.
- 13 Müller, R., P. J. Crutzen, J.-U. Grooss, C. Brühl, J. M. Russell, H. Gernandt, D. S. McKenna, and A. F.  
14 Tuck, Severe chemical ozone loss in the Arctic during the winter 1995-96, *Nature*, *389*, 709-712,  
15 1997.
- 16 Müller, R., J.-U. Grooss, D. S. McKenna, P. J. Crutzen, C. Brühl, J. M. Russell, L. L. Gordley, J. P.  
17 Burrows, and A. F. Tuck, Chemical ozone loss in the Arctic vortex in the winter 1995-96: HALOE  
18 measurements in conjunction with other observations, *Annales Geophysicae*, *17*, 101-114, 1999.
- 19 Nagashima, T., M. Takahashi, M. Takigawa, and H. Akiyoshi, Future development of the ozone layer  
20 calculated by a general circulation model with fully interactive chemistry, *Geophys. Res. Lett.*, in  
21 press, 2002.
- 22 Nakajima, H., M. Suzuki, A. Matsuzaki, T. Ishigaki, K. Waragai, Y. Mogi, N. Kimura, N. Araki, T.  
23 Yokota, H. Kanzawa, T. Sugita, Y. Sasano, Characteristics and performance of the Improved Limb  
24 Atmospheric Spectrometer (ILAS) in orbit, *J. Geophys. Res.*, in press, 2002.
- 25 Nash, E. R., P. A. Newman, J. E. Rosenfield, and M. R. Schoeberl, An objective determination of the  
26 polar vortex using Ertel's potential vorticity, *J. Geophys. Res.*, *101*, 9471-9478, 1996.
- 27 Nedoluha, G. E., R. M. Bevilacqua, K. W. Hoppel, M. Dähler, E. P. Shettle, J. H. Hornstein, M. D.  
28 Fromm, J. D. Lumpe, and J. E. Rosenfield, POAM III measurements of dehydration in the  
29 Antarctic lower stratosphere, *Geophys. Res. Lett.*, *27*, 1683-1686, 2000.
- 30 Newman, P. A., and M. R. Schoeberl, A reinterpretation of the data from the NASA Stratosphere-  
31 Troposphere Exchange Project, *Geophys. Res. Lett.*, *22*, 2501-2504, 1995.
- 32 Newman, P. A., L. R. Lait, and M. R. Schoeberl, The morphology and meteorology of Southern-  
33 Hemisphere spring total ozone mini-holes, *Geophys. Res. Lett.*, *15*, 923-926, 1988.
- 34 Newman, P. A., L. R. Lait, M. Seablom, L. Coy, R. Rood, R. Swinbank, M. Proffitt, M. Loewenstein, J.  
35 R. Podolske, J. W. Elkins, C. R. Webster, R. D. May, D. W. Fahey, G. S. Dutton, and K. R. Chan,  
36 Measurements of polar vortex air in the midlatitudes, *J. Geophys. Res.*, *101*, 12879-12891, 1996.
- 37 Newman, P. A., J. F. Gleason, R. D. McPeters, and R. S. Stolarski, Anomalously low ozone over the  
38 Arctic, *Geophys. Res. Lett.*, *24*, 2689-2692, 1997.
- 39 Newman, P. A., D. Fahey, W. Brune, M. Kurylo, and S. R. Kawa, Preface: Photochemistry of Ozone  
40 Loss in the Arctic Region in Summer (POLARIS), *J. Geophys. Res.*, *104*, 26481-26496, 1999.
- 41 Newman, P. A., E. R. Nash, and J. E. Rosenfield, What controls temperature of the Arctic stratosphere  
42 during spring?, *J. Geophys. Res.*, *106*, 19999-20010, 2001.

5/7/02

- 1 Niwano, M., and M. Takahashi, The influence of the equatorial QBO on the Northern Hemisphere winter  
2 circulation of a GCM, *J. Met. Soc. Japan.*, 76, 453-461, 1998.
- 3 Northway, M. J., R.-S. Gao, P. J. Popp, J. C. Holecek, D. W. Fahey, K. S. Carslaw, M. A. Tolbert, L. R.  
4 Lait, S. Dhaniyala, R. C. Flagan, P. O. Wennberg, M. J. Mahoney, R. L. Herman, G. C. Toon, and  
5 T. P. Bui., An analysis of large HNO<sub>3</sub>-containing particles sampled in the Arctic stratosphere  
6 during the winter of 1999-2000, *J. Geophys. Res.*, in press, 2002a.
- 7 Northway, M. J., P. J. Popp, R. S. Gao, D. W. Fahey, G. C. Toon, and T. P. Bui, Relating inferred HNO<sub>3</sub>  
8 flux values to the denitrification of the 1999-2000 Arctic vortex, submitted to *Geophys. Res. Lett.*,  
9 2002b.
- 10 Norton, W. A., and M. P. Chipperfield, Quantification of the transport of chemically processed air from  
11 the Northern Hemisphere polar vortex, *J. Geophys. Res.*, 100, 25817-25840, 1995.
- 12 Oinas, V., A. A. Lacis, D. Rind, D. T. Shindell, and J. E. Hansen, Radiative cooling by stratospheric  
13 water vapor: Big differences in GCM results, *Geophys. Res. Lett.*, 28, 2791-2794, 2001.
- 14 Oltmans, S. J., and D. J. Hofmann, Increase in lower-stratospheric water vapour at a mid-latitude  
15 Northern Hemisphere site from 1981 to 1994, *Nature*, 374, 146-149, 1995.
- 16 Oltmans, S. J., H. Vömel, D. J. Hofmann, K. H. Rosenlof, and D. Kley, The increase in stratospheric  
17 water vapor from balloonborne, frostpoint hygrometer measurements at Washington, DC, and  
18 Boulder, Colorado, *Geophys. Res. Lett.*, 27, 3453-3456, 2000.
- 19 Orsolini, Y. J., Long-lived tracer patterns in the summer polar stratosphere, *Geophys. Res. Lett.*, 28, 3855-  
20 3858, 2001.
- 21 Orsolini, Y. J., and V. Limpasuvan, The North Atlantic Oscillation and the occurrences of ozone  
22 miniholes, *Geophys. Res. Lett.*, 28, 4099-4102, 2001.
- 23 Orsolini, Y. J., G. Hansen, U. P. Hoppe, G. L. Manney, and K. H. Fricke, Dynamical modeling of  
24 wintertime lidar observations in the Arctic: Ozone laminae and ozone depletion, *Quart. J. Roy Met.  
25 Soc.*, 123, 785-800, 1997.
- 26 Osterman, G. B., B. Sen, G. C. Toon, R. J. Salawitch, J. J. Margitan, J.-F. Blavier, D. W. Fahey, and R. S.  
27 Gao, The partitioning of reactive nitrogen species in the summer Arctic stratosphere, *Geophys. Res.  
28 Lett.*, 26, 1157-1160, 1999.
- 29 Pan, L. L., *et al.*, Satellite observations of dehydration in the Arctic polar vortex, *Geophys. Res. Lett.*, in  
30 press, 2002. [Need complete author list.]
- 31 Papayannis, D. K., A. M. Kosmas, and V. S. R. Melissas, Quantum mechanical studies on the BrO plus  
32 ClO reaction, *J. Phys. Chem.*, 105, 2209-2215, 2001.
- 33 Pawson, S., and B. Naujokat, Trends in daily wintertime temperatures in the northern stratosphere,  
34 *Geophys. Res. Lett.*, 24, 575-578, 1997.
- 35 Pawson, S., and B. Naujokat, The cold winters of the middle 1990s in the northern lower stratosphere. *J.  
36 Geophys. Res.*, 104, 14209-14222, 1999.
- 37 Pawson, S., B. Naujokat, and K. Labitzke, On the polar stratospheric cloud formation potential of the  
38 northern stratosphere. *J. Geophys. Res.*, 100, 23215-23225, 1995.
- 39 Pawson, S., K. Kruger, R. Swinbank, M. Bailey, and A. O'Neill, Intercomparison of two stratospheric  
40 analyses: Temperatures relevant to polar stratospheric cloud formation, *J. Geophys. Res.*, 104,  
41 2041-2050, 1999.

5/7/02

- 1 Pawson, S., K. Kodera, K. Hamilton, T. H. Shepherd, S. R. Beagley, B. A. Boville, J. D. Farrara, T. D. A.  
2 Fairlie, A. Kitoh, W. A. Lahoz, U. Langematz, E. Manzini, D. H. Rind, A. A. Scaife, K. Shibata, P.  
3 Simon, R. Swinbank, L. Takacs, R. J. Wilson, J. A. Al-Saadi, M. Amodei, M. Chiba, L. Coy, J. de  
4 Grandpre, R. S. Eckman, M. Fiorino, W. L. Grose, H. Koide, J. N. Koshyk, D. Li, J. Lerner, J. D.  
5 Mahlman, N. A. McFarlane, C. R. Mechoso, A. Molod, A. O'Neill, R. B. Pierce, W. J. Randel, R.  
6 B. Rood, F. Wu, The GCM-reality intercomparison project for SPARC (GRIPS): Scientific issues  
7 and initial results, *Bull. Amer. Met. Soc.*, 81, 781-796, 2000.
- 8 Perez, A., E. de Crino, I. A. de Carcer, and F. Jaque, Low ozone events and three-dimensional transport at  
9 midlatitudes of South America during springs of 1996 and 1997. *J. Geophys. Res.*, 105, 4553-4561,  
10 2000.
- 11 Perkins, K. K., T. F. Hanisco, R. C. Cohen, L. C. Koch, R. M. Stimpfle, P. B. Voss, G. P. Bonne, E. J.  
12 Lanzendorf, J. G. Anderson, P. O. Wennberg, R. S. Gao, L. A. Del Negro, R. J. Salawitch, C. T.  
13 McElroy, E. J. Hintsa, M. Loewenstein, and T. P. Bui, The NO<sub>x</sub>-HNO<sub>3</sub> system in the lower  
14 stratosphere: Insights from *in situ* measurements and implications of the J<sub>HNO<sub>3</sub></sub>-[OH] relationship,  
15 *J. Phys. Chem. A.*, 105, 1521-1534, 2001.
- 16 Perlwitz, J., and H.-F. Graf, The variability of the horizontal circulation in the troposphere and  
17 stratosphere - A comparison, *Accepted Theoretical and Applied Climatology*, 2001.
- 18 Pfeilsticker, K., W. T. Sturges, H. Bösch, C. Camy-Peyret, M. P. Chipperfield, A. Engel, R. Fitzenberger,  
19 M. Müller, S. Payan, and B.-M. Sinnhuber, Lower stratospheric organic and inorganic bromine  
20 budget for the Arctic winter 1998/99, *Geophys. Res. Lett.*, 27, 3305-3308, 2000.
- 21 Pfenniger, M., A. Z. Liu, G. C. Papen, and C. S. Gardner, Gravity wave characteristics in the lower  
22 atmosphere at South Pole, *J. Geophys. Res.*, 104, 5963-5984, 1999.
- 23 Pierce, R. B., J. A. Al-Saadi, T. D. Fairlie, J. R. Olson, R. S. Eckman, W. L. Grose, G. S. Lingenfelter, J.-  
24 U. Grooss, and J. M. Russell III, Large-scale stratospheric ozone photochemistry and transport  
25 during the POLARIS campaign, *J. Geophys. Res.*, 104, 26525-26545, 1999.
- 26 Pierce, B., J. Al-Saadi, T. D. Fairlie, M. Natarajan, V. L. Harvey, W. L. Grose, J. M. Russell, R. M.  
27 Bevilacqua, S. Eckermann, D. W. Fahey, R.-S. Gao, G. C. Toon, E. Richard, R. Stimpfle, C. R.  
28 Webster, and J. W. Elkins, Large-scale chemical evolution of the arctic vortex during the 1999-  
29 2000 winter: HALOE/POAM3 Lagrangian photochemical modeling for the SAGE III ozone loss  
30 and validation experiment (SOLVE) campaign, submitted to *J. Geophys. Res.*, 2001.
- 31 Pierson, J. M., K. A. McKinney, D. W. Toohey, J. J. Margitan, U. Schmidt, A. Engel, and P. A. Newman,  
32 An investigation of ClO photochemistry in the chemically perturbed Arctic vortex, *J. Atmos.*  
33 *Chem.*, 32, 61-81, 1999.
- 34 Pitari, G., S. Palermi, G. Visconti, and R. G. Prinn, Ozone response to a CO<sub>2</sub> doubling: Results from a  
35 stratospheric circulation model with heterogeneous chemistry, *J. Geophys. Res.*, 97, 5953-5962,  
36 1992.
- 37 Pitari, G., E. Mancini, and D. Shindell, Feedback of future climate and sulfur emission changes an  
38 stratospheric aerosols and ozone, *J. Atmos. Sci.*, in press, 2002a.
- 39 Pitari, G., E. Mancini, V. Rizi, and D. Shindell, Impact of future climate and emission changes on  
40 stratospheric aerosols and ozone, *J. Atmos. Sci.*, in press, 2002b.
- 41 Piters, A. J. M., P. F. Levelt, M. A. F. Allaart, and H. M. Kelder, Validation of GOME total ozone  
42 column with the Assimilation Model KNMI, *Remote Sensing: Earth, Ocean and Atmosphere*  
43 *Advances in Space Research*, 22, 1501-1504, 1999.

5/7/02

- 1 Plumb, R. A., and M. K. W. Ko, Interrelationships between mixing ratios of long-lived stratospheric  
2 constituents, *J. Geophys. Res.*, *97*, 10145-10156, 1992.
- 3 Plumb, R. A., D. W. Waugh, and M. P. Chipperfield, The effects of mixing on tracer-tracer relationships  
4 in the polar vortices, *J. Geophys. Res.*, *105*, 10047-10062, 2000.
- 5 Pommereau, J. P., A. Garnier, B. M. Knudsen, G. Letrenne, M. Durand, M. Nunes-Pinharanda, L. Denis,  
6 F. Vial, A. Hertzog, and F. Cairo, Accuracy of analyzed stratospheric temperature in the winter  
7 Arctic vortex from infra-red Montgolfier long duration balloon flights, Part I: Measurements, *J.*  
8 *Geophys. Res.*, in press, 2002.
- 9 Popp, P. J., M. J. Northway, J. C. Holecek, R. S. Gao, D. W. Fahey, J. W. Elkins, D. F. Hurst, P. A.  
10 Romashkin, G. C. Toon, B. Sen, S. M. Schauffler, R. J. Salawitch, C. R. Webster, R. L. Herman, H.  
11 Jost, T. P. Bui, P. A. Newman, and L. R. Lait, Severe and extensive denitrification in the 1999-  
12 2000 Arctic winter stratosphere, *Geophys. Res. Lett.*, *28*, 2875-2878, 2001.
- 13 Portmann, R. W., S. Solomon, R. R. Garcia, L. W. Thomason, L. R. Poole, and M. P. McCormick, Role  
14 of aerosol variations in anthropogenic ozone depletion in the polar regions, *J. Geophys. Res.*, *101*,  
15 22991-23006, 1996.
- 16 Prenni, A. J., T. B. Onasch, R. T. Tisdale, R. L. Siefert, and M. A. Tolbert, Composition-dependent  
17 freezing nucleation rates for HNO<sub>3</sub>-H<sub>2</sub>O aerosols resembling gravity-wave-perturbed stratospheric  
18 particles, *J. Geophys. Res.*, *103*, 28439-28450, 1998.
- 19 Proffitt, M. H., J. J. Margitan, K. K. Kelly, M. Loewenstein, J. R. Podolske, and K. R. Chan, Ozone loss  
20 in the Arctic polar vortex inferred from high altitude aircraft measurements, *Nature*, *347*, 31-36,  
21 1990.
- 22 Pullen, S., and R. L. Jones, Accuracy of temperatures from UKMO analyses of 1994/95 in the Arctic  
23 winter stratosphere, *Geophys. Res. Lett.*, *24*, 845-848, 1997.
- 24 Raffalski, U., U. Klein, B. Franke, J. Langer, B. M. Sinnhuber, J. Trentmann, K. F. Künzi, and O.  
25 Schrems, Ground based millimeter-wave observations of Arctic chlorine activation during winter  
26 and spring 1996/97, *Geophys. Res. Lett.*, *25*, 3331-3334, 1998.
- 27 Ramachandran, S., V. Ramaswamy, G. L. Stenchikov, and A. Robock, Radiative impact of the Mount  
28 Pinatubo Volcanic eruption: Lower stratospheric response, *J. Geophys. Res.*, *105*, 24409-24429,  
29 2000.
- 30 Ramaswamy, V., and M. D. Schwarzkopf, Effects of ozone and well-mixed gases on annual-mean  
31 stratospheric temperature trends, submitted to *Geophys. Res. Lett.*, 2002.
- 32 Ramaswamy, V., M. D. Schwarzkopf, and W. J. Randel, Fingerprint of ozone depletion in the spatial and  
33 temporal pattern of recent lower-stratospheric cooling, *Nature*, *382*, 616-618, 1996.
- 34 Ramaswamy, V., M.-L. Chanin, J. Angell, J. Barnett, D. Gaffen, M. Gelman, P. Keckhut, Y. Koshelkov,  
35 K. Labitzke, J. J. R. Lin, A. O'Neill, J. Nash, W. Randel, R. Rood, K. Shine, M. Shiotani, and R.  
36 Swinbank, Stratospheric temperature trends: observations and model simulations, *Rev. Geophysics*,  
37 *39*, 71-122, 2001.
- 38 Ramaswamy, V., M. Gelman, M. D. Schwarzkopf, and R. Lin, An update of stratospheric temperature  
39 trends, *SPARC newsletter*, *18*, January 2002a.
- 40 Ramaswamy, V., S. Ramachandran, G. Stenchikov, and A. Robock, A model study of the effect of  
41 Pinatubo volcanic aerosols on stratospheric temperatures, Proceedings of Symposium in honor of  
42 Robert Cess (held in San Diego, USA, October, 1999), Oxford University Press, in press, 2002b.

5/7/02

- 1 Randall, C. E., J. D. Lumpe, R. M. Bevilacqua, K. W. Hoppel, M. D. Fromm, R. J. Salawitch, W. H.  
2 Swartz, S. A. Lloyd, E. Kyrö, P. von der Gathen, H. Claude, J. Davies, H. De Backer, H. Dier, M. J.  
3 Molyneux, and J. Sancho, Reconstruction of 3-D ozone fields using POAM III during SOLVE, *J.*  
4 *Geophys. Res.*, in press, 2002.
- 5 Randel, W. J., and P. A. Newman, The stratosphere in the Southern Hemisphere. The Meteorology of the  
6 Southern Hemisphere, Chapter 6, 1998.
- 7 Randel, W. J., and F. Wu, Cooling of the Arctic and Antarctic polar stratospheres due to ozone depletion,  
8 *J. Clim.*, 12, 1467-1479, 1999a.
- 9 Randel, W. J., and F. Wu, A stratospheric ozone trends data set for global modeling studies. *Geophys.*  
10 *Res. Lett.*, 26, 3089-3092, 1999b.
- 11 Randeniya, L. K., P. F. Vohralik, and I. C. Plumb, Stratospheric ozone depletion at northern mid-latitudes  
12 in the 21<sup>st</sup> century: The importance of future concentrations of greenhouse gases nitrous oxide and  
13 methane, *Geophys. Res. Lett.*, 2002.
- 14 Rathman, W., P. S. Monks, D. Llewellyn Jones, and J. P. Burrows, A preliminary comparison between  
15 TOVS and GOME level 2 ozone data, *Geophys. Res. Lett.*, 24, 2191-2194, 1997.
- 16 Ray, E., F. L. Moore, J. W. Elkins, D. F. Hurst, P. A. Romashkin, G. S. Dutton, and D. W. Fahey,  
17 Descent and mixing in the northern polar vortex from *in situ* tracer measurements, submitted to *J.*  
18 *Geophys. Res.*, 2002.
- 19 Renard, J.-B., M. Pirre, C. Robert, and D. Huguenin, Is OBrO present in the stratosphere?, *C. R. Acad.*  
20 *Sci. Paris, Sciences de la Terre et des Planetes*, 325, 921-924, 1997.
- 21 Renard, J.-B., M. Pirre, C. Robert, and D. Huguenin, The possible detection of OBrO in the stratosphere,  
22 *J. Geophys. Res.*, 103, 25383-25395, 1998.
- 23 Rex, M., N. R. P. Harris, P. von der Gathen, R. Lehmann, G. O. Braathen, E. Reimer, A. Beck, M. P.  
24 Chipperfield, R. Alfier, M. Allaart, F. O'Connor, H. Dier, V. Dorokhov, H. Fast, M. Gil, E. Kyrö,  
25 Z. Litynska, I. S. Mikkelsen, M. G. Molyneux, H. Nakane, J. Notholt, M. Rummukainen, P. Viatte,  
26 and J. Wenger, Prolonged stratospheric ozone loss in the 1995-96 Arctic winter, *Nature*, 389, 835-  
27 838, 1997.
- 28 Rex, M., P. von der Gathen, N. R. P. Harris, D. Lucic, B. M. Knudsen, G. O. Braathen, S. J. Reid, H. De  
29 Backer, H. Claude, R. Fabian, H. Fast, M. Gil, E. Kyrö, I. S. Mikkelsen, M. Rummukainen, H. G.  
30 Smit, J. Stähelin, C. Varotsos, and I. Zaitcev, *In situ* measurements of stratospheric ozone depletion  
31 rates in the Arctic winter 1991/1992: A Lagrangian approach, *J. Geophys. Res.*, 103, 5843-5853,  
32 1998.
- 33 Rex, M., R. J. Salawitch, G. C. Toon, B. Sen, J. J. Margitan, G. B. Osterman, J. F. Blavier, R.-S. Gao, S.  
34 Donnelly, E. Keim, J. Neuman, D. W. Fahey, C. R. Webster, D. C. Scott, R. L. Herman, R. D. May,  
35 E. J. Moyer, M. R. Gunson, F. W. Irion, A. Y. Chang, C. P. Rinsland, and T. P. Bui, Subsidence,  
36 mixing, and denitrification of Arctic polar vortex air measured during POLARIS, *J. Geophys. Res.*,  
37 104, 26611-26623, 1999a.
- 38 Rex, M., P. von der Gathen, G. O. Braathen, N. R. P. Harris, E. Reimer, A. Beck, R. Alfier, R. Krüger-  
39 Carstensen, M. Chipperfield, H. De Backer, D. Balis, F. O'Connor, H. Dier, V. Dorokhov, H. Fast,  
40 A. Gamma, M. Gil, E. Kyrö, Z. Litynska, I. S. Mikkelsen, M. Molyneux, G. Murphy, S. J. Reid, M.  
41 Rummukainen, and C. Zerefos, Chemical ozone loss in the Arctic winter 1994/95 as determined by  
42 the Match technique, *J. Atmos. Chem.*, 32, 35-39, 1999b.
- 43 Rex, M. R., J. Salawitch, N. R. P. Harris, P. von der Gathen, G. O. Braathen, A. Schulz, H. Deckelman,

5/7/02

- 1 M. Chipperfield, B. M. Sinnhuber, E. Reimer, R. Alfier, R. Bevilacqua, K. Hoppel, M. Fromm, J.  
2 Lumpe, H. Küllmann, A. Kleinböhl, H. Bremer, M. von König, K. Künzi, D. Toohey, H. Vömel, E.  
3 Richard, K. Aikin, H. Jost, J. B. Greenblatt, M. Loewenstein, J. R. Podolske, C. R. Webster, G. J.  
4 Flesch, D. C. Scott, R. L. Herman, J. W. Elkins, E. A. Ray, F. L. Moore, D. F. Hurst, P.  
5 Romashkin, G. C. Toon, B. Sen, J. J. Margitan, P. Wennberg, R. Neuber, M. Allaart, R. B. Bojkov,  
6 H. Claude, J. Davies, W. Davies, H. De Backer, H. Dier, V. Dorokhov, H. Fast, Y. Kondo, E. Kyrö,  
7 Z. Litynska, I. S. Mikkelsen, M. J. Molyneux, E. Moran, T. Nagai, H. Nakane, C. Parrondo, F.  
8 Ravegnani, P. Skrivankova, P. Viatte, and V. Yushkov, Chemical depletion of Arctic ozone in  
9 winter 1999/2000, *J. Geophys. Res.*, in press, 2002a.
- 10 Rex, M., *et al.*, Theory and observation of Arctic ozone loss rates, manuscript in preparation, 2002b.
- 11 Ricaud, P., E. Monnier, F. Goutail, J. P. Pommereau, C. David, S. Godin, L. Froidevaux, J. W. Waters, J.  
12 Mergenthaler, A. E. Roche, H. Pumphrey, and M. P. Chipperfield, Stratosphere over Dumont  
13 d'Urville, Antarctica, in winter 1992, *J. Geophys. Res.*, 103, 13267-13284, 1998.
- 14 Richard, E. C., K. C. Aikin, A. E. Andrews, B. C. Daube, C. Gerbig, S. C. Wofsy, P. A. Romashkin, D. F.  
15 Hurst, E. A. Ray, F. L. Moore, J. W. Elkins, T. Deshler, and G. C. Toon, Severe chemical ozone  
16 loss inside the Arctic Polar Vortex during winter 1999-2000 inferred from *in situ* airborne  
17 measurements, *Geophys. Res. Lett.*, 28, 2197-2200, 2001.
- 18 Rind, D., R. Suozzo, N. K. Balachandran, A. Lacis, and G. Russell, The GISS global climate/middle  
19 atmosphere model, I, Model structure and climatology, *J. Atmos. Sci.*, 45, 329-370, 1988a.
- 20 Rind, D., R. Suozzo, and N. K. Balachandran, The GISS global climate/middle atmosphere model, II,  
21 Model variability due to interactions between planetary waves, the mean circulation, and gravity  
22 wave drag, *J. Atmos. Sci.*, 45, 371-386, 1988b.
- 23 Rind, D., D. Shindell, P. Lonergan, and N. K. Balachandran, Climate change and the middle atmosphere:  
24 Part III: The doubled CO<sub>2</sub> climate revisited, *J. Climate*, 11, 876-894, 1998.
- 25 Robock, A., Volcanic eruptions and climate, *Rev. Geophys.*, 38, 191-219, 2000.
- 26 Roehl, C. M., T. L. Mazely, R. R. Friedl, Y. M. Li, J. S. Francisco, and S. P. Sander, NO<sub>2</sub> quantum yield  
27 from the 248-nm photodissociation of peroxyoxynitric acid (HO<sub>2</sub>NO<sub>2</sub>), *J. Phys. Chem.*, 105, 1592-  
28 1598, 2001.
- 29 Rood R.B., A.R. Douglass, M.C. Cerniglia, and W.G. Read, Synoptic-scale mass exchange from the  
30 troposphere to the stratosphere, *J. Geophys. Res.*, 102 23467-23485, 1997.
- 31 Roscoe, H. K., A. E. Jones, and A. M. Lee, Midwinter start to Antarctic ozone depletion: Evidence from  
32 observations and models, *Science*, 278, 93-96, 1997.
- 33 Rosier, S. M., and K. P. Shine, The effect of two decades of ozone change on stratospheric temperatures  
34 as indicated by a general circulation model, *Geophys. Res. Lett.*, 27, 2617-2620, 2000.
- 35 Rosenfield, J. E., and M. R. Schoeberl, On the origin of polar vortex air, *J. Geophys. Res.*, 106, 33485-  
36 33497, 2001.
- 37 Rosenfield, J. E., A. R. Douglass, and D. B. Considine, The impact of increasing carbon dioxide on ozone  
38 recovery, *J. Geophys. Res.*, in press, 2002.
- 39 Rosenlof, K. H., Estimates of the seasonal cycle of mass and ozone transport at high northern latitudes, *J.*  
40 *Geophys. Res.*, 104, 26511-26523, 1999.
- 41 Rosenlof, K. H., S. J. Oltmans, D. Kley, J. M. Russell III, E.-W. Chiou, W. P. Chu, D. G. Johnson, K. K.  
42 Kelly, H. A. Michelsen, G. E. Nedoluha, E. E. Remsberg, G. C. Toon, and M. P. McCormick,

5/7/02

- 1 Stratospheric water vapor increases over the past half-century, *Geophys. Res. Lett.*, 28, 1195-1198,  
2 2001.
- 3 Rozanov, E. V., M. E. Schlesinger, and V. A. Zubov, The University of Illinois at Urbana-Champaign  
4 three-dimensional stratosphere-troposphere general circulation model with interactive ozone  
5 photochemistry: Fifteen-year control run climatology, *J. Geophys. Res.*, 106, 27233-27254, 2001.
- 6 Saitoh, N. S., S. Hayashida, Y. Sasano, and L. L. Pan, Characteristics of Arctic polar stratospheric clouds  
7 in winter of 1996/1997 inferred from ILAS measurements, *J. Geophys. Res.*, in press, 2002.
- 8 Salawitch, R. J., J. J. Margitan, B. Sen, G. C. Toon, G. B. Osterman, M. Rex, J. W. Elkins, E. A. Ray, F.  
9 L. Moore, D. F. Hurst, P. A. Romashkin, R. M. Bevilacqua, K. W. Hoppel, E. C. Richard, and T. P.  
10 Bui, Chemical loss of ozone during the Arctic winter of 1999-2000: An analysis based on balloon-  
11 borne observations, in press, *J. Geophys. Res.*, 2002a.
- 12 Salawitch, R. J., P. O. Wennberg, G. C. Toon, B. Sen, and J-F Blavier, Near IR photolysis of HO<sub>2</sub>NO<sub>2</sub>:  
13 Implications for HO<sub>x</sub>, *Geophys. Res. Lett.*, submitted, 2002b.
- 14 Salawitch, R. J. *et al.*, The budget and partitioning of chlorine in the Arctic winter stratosphere, *Geophys.*  
15 *Res. Lett.*, manuscript in preparation, 2002c.
- 16 Salcedo, D., L. T. Molina, and M. J. Molina, Homogeneous freezing of concentrated aqueous nitric acid  
17 solutions at polar stratospheric temperatures, *J. Phys. Chem.*, 105, 1433, 2001.
- 18 Sander, S. P., A. R. Ravishankara, R. R. Friedl, W. B. DeMore, D. M. Golden, C. E. Kolb, M. J. Kurylo,  
19 M. J. Molina, R. F. Hampson, R. E. Huie, and G. K. Moortgat, *Chemical kinetics and*  
20 *photochemical data for use in stratospheric modeling, Evaluation number 12: Update of key*  
21 *reactions*, JPL Publication 00-3, Pasadena, CA, 2000.
- 22 Santee, M. L., G. L. Manney, L. Froidevaux, W. G. Read, and J. W. Waters, Six years of UARS  
23 microwave limb sounder HNO<sub>3</sub> observations: Seasonal, interhemispheric, and interannual  
24 variations in the lower stratosphere, *J. Geophys. Res.*, 104, 8225, 1999.
- 25 Santee, M. L., G. L. Manney, N. J. Livesey, and J. W. Waters, UARS Microwave Limb Sounder  
26 observations of denitrification and ozone loss in the 2000 Arctic late winter, *Geophys. Res. Lett.*,  
27 27, 3213-3216, 2000.
- 28 Santee, M. L., A. Tabazadeh, G. L. Manney, M. D. Fromm, R. M. Bevilacqua, N. J. Livesey, E. J. Jensen,  
29 A Lagrangian approach to studying Arctic polar stratospheric clouds using UARS MLS HNO<sub>3</sub> and  
30 POAM II aerosol extinction measurements, *J. Geophys. Res.*, in press, 2002.
- 31 Sasano, Y., M. Suzuki, T. Yokota, and H. Kanzawa, Improved Limb Atmospheric Spectrometer (ILAS)  
32 for stratospheric ozone layer measurements by solar occultation technique, *Geophys. Res. Lett.*, 26,  
33 197-200, 1999.
- 34 Sasano, Y., Y. Terao, H. L. Tanaka, T. Yasunari, H. Kanzawa, H. Nakajima, T. Yokota, H. Nakane, S.  
35 Hayashida, and N. Saitoh, ILAS observations of chemical ozone loss in the Arctic vortex during  
36 early spring 1997, *Geophys. Res. Lett.*, 27, 213-216, 2000.
- 37 Sato, K., K. Yamada, and I. Hirota, Global characteristics of medium-scale tropopausal waves observed  
38 in ECMWF operational data, *Mon. Wea. Rev.*, 128, 3808-3823, 2000.
- 39 Scaife, A. A., N. Butchart, C. D. Warner, D. Stainforth, W. Norton, and J. Austin, Realistic quasi-biennial  
40 oscillations in a simulation of the global climate, *Geophys. Res. Lett.*, 27, 3481-3484, 2000a.
- 41 Scaife, A. A., J. Austin, N. Butchart, S. Pawson, M. Keil, J. Nash, and I. N. James, Seasonal and  
42 interannual variability of the stratosphere diagnosed from UKMO TOVS analyses, *Q. J. R.*



- 1 *Meteorol. Soc.*, 126, 2585-2604, 2000b.
- 2 Schnadt, C., M. Dameris, M. Ponater, R. Hein, V. Grewe, and B. Steil, Interaction of atmospheric  
3 chemistry and climate and its impact on stratospheric ozone, *Clim. Dyn.*, 18, 501-517, 2002.
- 4 Schoeberl, M. R., and P. A. Newman, A multi-level trajectory analysis of vortex filaments *J. Geophys.*  
5 *Res.*, 100, 25801-25815, 1995.
- 6 Schoeberl, M. R., M. H. Proffitt, K. K. Kelly, L. R. Lait, P. A. Newman, J. E. Rosenfield, M.  
7 Loewenstein, J. R. Podolske, S. E. Strahan, and K. R. Chan, Stratospheric constituent trends from  
8 ER-2 profile data, *Geophys. Res. Lett.*, 17, 469-472, 1990.
- 9 Schoeberl, M. R., M. Z. Lu, and J. E. Rosenfield, An analysis of the Antarctic Halogen Occultation  
10 Experiment Trace Gas Observations, *J. Geophys. Res.*, 100, 5159-5172, 1995.
- 11 Schoeberl, M. R., P. A. Newman, L. R. Lait, T. J. McGee, J. F. Burris, E. V. Browell, W. B. Grant E. C.  
12 Richard, P. von der Gathen, R. Bevilacqua, I. S. Mikkelsen, and M. J. Molyneux, A multi-  
13 instrument assessment of the ozone loss during the 1999-2000 SOLVE campaign, *J. Geophys. Res.*,  
14 in press, 2002.
- 15 Schreiner, J., C. Voigt, A. Kohlmann, F. Arnold, K. Mauersberger, and N. Larsen, Chemical analysis of  
16 polar stratospheric cloud particles, *Science*, 283, 968-970, 1999.
- 17 Schreiner, J., C. Voigt, C. Weisser, A. Kohlmann, K. Mauersberger, T. Deshler, C. Kröger, J. Rosen, N.  
18 Kjome, N. Larsen, A. Adriani, F. Cairo, G. Di Donfrancesco, J. Ovarlez, H. Ovarlez, and A.  
19 Dörnbrack, Chemical, microphysical and optical properties of polar stratospheric clouds, *J.*  
20 *Geophys. Res.*, in press, 2002.
- 21 Schulz, A., M. Rex, J. Steger, N. R. P. Harris, G. O. Braathen, E. Reimer, R. Alfier, A. Beck, M. Alpers,  
22 J. Cisneros, H. Claude, H. De Backer, H. Dier, V. Dorokhov, H. Fast, S. Godin, G. Hansen, H.  
23 Kanzawa, B. Kois, Y. Kondo, E. Kosmidis, E. Kyrö, Z. Litynska, M. J. Molyneux, G. Murphy, H.  
24 Nakane, C. Parrondo, F. Ravegnani, C. Varotsos, C. Vialle, P. Viatte, V. Yushkov, C. Zerefos, and  
25 P. von der Gathen, Match observations in the Arctic winter 1996/97: High stratospheric ozone loss  
26 rates correlate with low temperatures deep inside the polar vortex, *Geophys. Res. Lett.*, 27, 205-208,  
27 2000.
- 28 Schulz, A., M. Rex, N. R. P. Harris, G. O. Braathen, E. Reimer, R. Alfier, I. Kilbane-Dawe, S.  
29 Eckermann, M. Allaart, M. Alpers, B. Bojkov, J. Cisneros, H. Claude, E. Cuevas, J. Davies, H. De  
30 Backer, H. Dier, V. Dorokhov, H. Fast, S. Godin, B. Johnson, B. Kois, Y. Kondo, E. Kosmidis, E.  
31 Kyrö, Z. Litynska, I. S. Mikkelsen, M. J. Molyneux, G. Murphy, T. Nagai, H. Nakane, F.  
32 O'Connor, C. Parrondo, F. J. Schmidlin, P. Skrivankova, C. Varotsos, C. Vialle, P. Viatte, V.  
33 Yushkov, C. Zerefos, and P. von der Gathen, Arctic ozone loss in threshold conditions: Match  
34 observations in 1997/1998 and 1998/1999, *J. Geophys. Res.*, 106, 7495-7503, 2001.
- 35 Sen, B., G. B. Osterman, R. J. Salawitch, G. C. Toon, J. J. Margitan, J.-F. Blavier, A. Y. Chang, R. D.  
36 May, C. R. Webster, R. M. Stimpfle, G. P. Bonne, P. B. Voss, K. K. Perkins, J. G. Anderson, R. C.  
37 Cohen, J. W. Elkins, G. S. Dutton, D. F. Hurst, P. A. Romashkin, E. L. Atlas, S. M. Schauffler, and  
38 M. Loewenstein, The budget and partitioning of stratospheric chlorine during the 1997 Arctic  
39 summer, *J. Geophys. Res.*, 104, 26653-26665, 1999.
- 40 Shepherd, T., K. Semeniuk, and J. Koshyk, Sponge-layer feedbacks in middle atmosphere models, *J.*  
41 *Geophys. Res.*, 101, 23447-23464, 1996.
- 42 Shindell, D. T., Climate and ozone response to increased stratospheric water vapor, *Geophys. Res. Lett.*,  
43 28, 1551-1554, 2001.

5/7/02

- 1 Shindell, D. T., and R. L. de Zafra, The chlorine budget of the lower polar stratosphere - upper limits on  
2 ClO and implications of new Cl<sub>2</sub>O<sub>2</sub> photolysis cross-sections, *Geophys. Res. Lett.*, 22, 3215-3218,  
3 1995.
- 4 Shindell, D. T., D. Rind, and P. Lonergan, Increased polar stratospheric ozone losses and delayed  
5 eventual recovery owing to increasing greenhouse-gas concentrations, *Nature*, 392, 589-592,  
6 1998a.
- 7 Shindell, D. T., D. Rind, and P. Lonergan, Climate change and the middle atmosphere. Part IV: Ozone  
8 response to doubled CO<sub>2</sub>, *J. Clim.*, 11, 895-918, 1998b.
- 9 Shindell, D., D. H. Rind, N. Balachandran, J. Lean, and P. Lonergan, Solar cycle variability, ozone, and  
10 climate, *Science*, 284, 305-308, 1999a.
- 11 Shindell, D. T., D. Rind, and N. Balachandran, Interannual variability of the Antarctic ozone hole in a  
12 GCM, Part II: A comparison of unforced and QBO-induced variability, *J. Atmos. Sci.*, 56, 1873-  
13 1884, 1999b.
- 14 Shindell, D. T., G. A. Schmidt, R. L. Miller, and D. Rind, Northern Hemisphere winter climate response  
15 to greenhouse gas, volcanic, ozone and solar forcing, *J. Geophys. Res.*, 106, 7193-7210, 2001.
- 16 Shine, K. P., On the modeled thermal response of the Antarctic stratosphere to a depletion of ozone,  
17 *Geophys. Res. Lett.*, 13, 1331-1334, 1986.
- 18 Sinnhuber, B.-M., M. P. Chipperfield, S. Davies, J. P. Burrows, K.-U., Eichmann, M. Weber, P. Von der  
19 Gathen, M. Guirlet, G. A. Cahill, A. M. Lee, and J. A. Pyle, Large loss of total ozone during the  
20 Arctic winter of 1999/2000, *Geophys. Res. Lett.*, 27, 3473-3476, 2000.
- 21 Sinnhuber, B.-M., D. W. Arlander, H. Bovensmann, J. P. Burrows, M. P. Chipperfield, C.-F. Enell, U.  
22 Friess, F. Hendrick, P. V. Johnston, R. L. Jones, K. Kreher, N. Mohamed-Tahrin, R. Mueller, K.  
23 Pfeilsticker, U. Platt, J.-P. Pommereau, I. Pundt, A. Richter, A. South, K. K. Tørnkvist, M. Van  
24 Roozendaal, T. Wagner, and F. Wittrock, The global distribution of stratospheric bromine oxide:  
25 Intercomparison of measured and modelled slant column densities, *J. Geophys. Res.*, in press, 2002.
- 26 Smith, C. A., The radiative effects of observed trends in stratospheric water vapour, Ph.D. thesis, Imperial  
27 College, London, 2001.
- 28 Smith, C. A., J. D. Haigh, and R. Toumi, Radiative forcing due to trends in stratospheric water vapour,  
29 *Geophys. Res. Lett.*, 28, 179-182, 2001.
- 30 Sobel, A., and R. A. Plumb, Quantitative diagnostics of mixing in a shallow water model of the  
31 stratosphere, *J. Atmos. Sci.*, 56, 2811-2829, 1999.
- 32 Solomon, P., J. Barrett, B. Connor, S. Zoonematkermani, A. Parrish, A. Lee, J. Pyle, and M. Chipperfield,  
33 Seasonal observations of chlorine monoxide in the stratosphere over Antarctica during the 1996-  
34 1998 ozone holes and comparison with the SLIMCAT three-dimensional model, *J. Geophys. Res.*,  
35 105, 28979-29001, 2000.
- 36 Solomon, P. *et al.*, Stratospheric ClO over Antarctica, comparison of measurements with the SLIMCAT  
37 3-D model, manuscript in preparation, 2002.
- 38 Solomon, S., Stratospheric ozone depletion: A review of concepts and history, *Rev. Geophys.*, 37, 275-  
39 316, 1999.
- 40 Solomon, S., R. W. Portmann, R. R. Garcia, W. J. Randel, F. Wu, R. Nagatani, J. Gleason, L. Thomason,  
41 L. R. Poole, and M. P. McCormick, Ozone depletion at mid-latitudes: Coupling of volcanic  
42 aerosols and temperature variability to anthropogenic chlorine, *Geophys. Res. Lett.*, 25, 1871-2874,

- 1 1998.
- 2 Spang, R., M. Riese, and D. Offermann, CRISTA-2 observations of the south polar vortex in winter 1997:  
3 A new dataset for polar process studies, *Geophys. Res. Lett.*, 28, 3159-3162, 2001.
- 4 SPARC, *SPARC-IOC-GAW Assessment of Trends in the Vertical Distribution of Ozone*, SPARC Report  
5 No. 1, WMO Global Ozone Research and Monitoring Project Report No. 43, 1998.
- 6 SPARC, SPARC Assessment of Upper Tropospheric and Stratospheric Water Vapour, in *Stratospheric*  
7 *Processes and their Role in Climate*, WCRP-113, WMO-TD No 1043, SPARC Report 2, Verrières  
8 le Buisson Cedex, 2000.
- 9 Stachnik, R. A., R. J. Salawitch, A. Engel, and U. Schmidt, Measurements of chlorine partitioning in the  
10 winter Arctic stratosphere, *Geophys. Res. Lett.*, 26, 3093-3096, 1999.
- 11 Steele, H. M., K. Drdla, R. P. Turco, J. D. Lumpe, R. M. Bevilacqua, Tracking polar stratospheric cloud  
12 development with POAM II and a microphysical model, *Geophys. Res. Lett.*, 26, 287-290, 1999.
- 13 [Steil, B., C. Brühl, E. Manzini, P. J. Crutzen, J. Lelieveld, P. J. Rasch, and E. Roeckner, Interactive  
14 chemistry-climate modeling of the middle atmosphere, Part 1: Present conditions, validation with 9  
15 years of HALOE/UARS satellite data, submitted to \*J. Geophys. Res.\*, 2001.](#)
- 16 Steinbrecht, W., H. Claude, U. Kohler, and K. P. Hoinka, Correlations between tropopause height and  
17 total ozone: Implications for long-term changes, *J. Geophys. Res.*, 103, 19183-19192, 1998.
- 18 Stimpfle, R. M., R. C. Cohen, G. P. Bonne, P. B. Voss, K. K. Perkins, L. C. Koch, J. G. Anderson, R. J.  
19 Salawitch, S. A. Lloyd, R. S. Gao, L. A. Del Negro, E. R. Keim, and T. P. Bui, The coupling of  
20 ClONO<sub>2</sub>, ClO, and NO<sub>2</sub> in the lower stratosphere from *in situ* observations using the NASA ER-2  
21 aircraft, *J. Geophys. Res.*, 104, 26705-26714, 1999.
- 22 [Stimpfle, R. M., D. M. Wilmouth, R. J. Salawitch, J. G. Anderson, and T. P. Bui, First measurements of  
23 ClOOCl in the stratosphere: The coupling of ClOOCl and ClO in the Arctic polar vortex,  
24 submitted to \*J. Geophys. Res.\*, 2002.](#)
- 25 Stone, E. M., A. Tabazadeh, E. J. Jensen, H. C. Pumphrey, K. L. Santee, and J. L. Mergenthaler, Onset,  
26 extent, and duration of dehydration in the Southern Hemisphere polar vortex, *J. Geophys. Res.*, 106,  
27 22979-22990, 2001.
- 28 [Strawa, A. W., K. Drdla, M. Fromm, R. F. Pueschel, K. W. Hoppel, E. V. Browell, P. Hamill, and D. P.  
29 Dempsey, Discriminating type Ia and Ib polar stratospheric clouds in POAM satellite data, \*J.  
30 Geophys. Res.\*, in press, 2002.](#)
- 31 Sugita, T., Y. Kondo, H. Nakajima, U. Schmidt, A. Engel, H. Oelhaf, G. Wetzal, M. Koike, and P. A.  
32 Newman, Denitrification observed inside the Arctic vortex in February 1995, *J. Geophys. Res.*, 103,  
33 16221-16233, 1998.
- 34 [Sugita, T., T. Yokota, H. Nakajima, H. Kanzawa, H. Nakane, H. Germandt, V. Yushkov, K. Shibasaki, T.  
35 Deshler, Y. Kondo, S. Godin, F. Goutail, J.-P. Pommereau, C. Camy-Peyret, S. Payan, P. Jeseck, J.  
36 B. Renard, H. Bosch, R. Fitzenberger, K. Pfeilsticker, M. Von König, H. Bremer, H. Küllmann, H.  
37 Schlager, J. J. Margitan, R. Stachnik, G. Toon, K. Jucks, W. Traub, D. G. Johnson, I. Murata, H.  
38 Fukunishi, and Y. Sasano, Validation of ozone measurements from the Improved Limb  
39 Atmospheric Spectrometer \(ILAS\), \*J. Geophys. Res.\*, in press, 2002.](#)
- 40 Swinbank, R., and A. O'Neill, A stratosphere-troposphere data assimilation system, *Mon. Weather Rev.*,  
41 122, 686-702, 1994.
- 42 Tabazadeh, A., M. L. Santee, M. Y. Danilin, H. C. Pumphrey, P. A. Newman, P. J. Hamill, and J. L.

5/7/02

- 1 Mergenthaler, Quantifying denitrification and its effect on ozone recovery, *Science*, 288, 1407-  
2 1411, 2000.
- 3 Tabazadeh, A., E. J. Jensen, O. B. Toon, K. Drdla, and M. R. Schoeberl, Role of the stratospheric polar  
4 freezing belt in denitrification, *Science*, 291, 2591, 2001.
- 5 Takigawa, M., M. Takahashi, and H. Akiyoshi, Simulation of ozone and other chemical species using a  
6 Center for Climate Systems Research/National Institute for Environmental Studies atmospheric  
7 GCM with coupled stratospheric chemistry, *J. Geophys. Res.*, 104, 14003-14018, 1999.
- 8 Tanaka, H. L., R. Kanohgi, and T. Yasunari, Recent abrupt intensification of the northern polar vortex  
9 since 1988, *J. Meteorol. Soc. Japan.*, 74, 947-954, 1996.
- 10 Teitelbaum, H., M. Moustououi, P. F. J. van Velthoven, and H. Kelder, Decrease of total ozone at low  
11 latitudes in the Southern Hemisphere by a combination of linear and non-linear processes, *Quart. J.*  
12 *Roy. Met. Soc.*, 124, 2625-2644, 1999.
- 13 Teitelbaum, H., C. Basdevant, and M. Moustououi, Explanations of simultaneous laminae in water vapor  
14 and aerosols profiles found during the SESAME experiment, *Tellus*, 52A, 442-455, 2000.
- 15 Teitelbaum, H., M. Moustououi, M. Fromm, Exploring polar stratospheric cloud and ozone minihole  
16 formation: The primary importance of synoptic-scale flow perturbations, *J. Geophys. Res.*, 106,  
17 28173- 28188, 2001.
- 18 [Terao et al., J. Geophys. Res., in press, 2002. \[Need complete reference info.\]](#)
- 19 Thompson, D. W. J., and J. M. Wallace, The Arctic Oscillation signature in the wintertime geopotential  
20 height and temperature fields, *Geophys. Res. Lett.*, 25, 1297-1300, 1998.
- 21 Thompson, D. W. J., and J. M. Wallace, Annular modes in the extratropical circulation, Part I: Month-to-  
22 month variability, *J. Clim.*, 13, 1000-1016, 2000.
- 23 Thompson, D. W. J., J. M. Wallace, and G. C. Hegerl, Annular modes in the extratropical circulation, Part  
24 II: Trends, *J. Clim.*, 13, 1018-1036, 2000.
- 25 Thuburn, J., and V. Lagneau, Eulerian mean, contour integral, and finite-amplitude wave activity  
26 diagnostics applied to a single-layer model of the winter stratosphere, *J. Atmos. Sci.*, 56, 689-710,  
27 1999.
- 28 Timmreck, C., H.-F. Graf, and I. Kirchner, A one-and-half-year interactive MA/ECHAM4 simulation of  
29 Mount Pinatubo aerosol, *J. Geophys. Res.*, 104, 9337-9359, 1999.
- 30 Tolbert, M. A., and O. B. Toon, Solving the PSC mystery, *Science*, 292, 61, 2001.
- 31 Toniolo, A., M. Persico, and D. Pitea, Theoretical photoabsorption spectra of ClOOCl and Cl<sub>2</sub>O, *J. Phys.*  
32 *Chem.*, 104, 7278-7283, 2000.
- 33 [Toohey, D. W. et al., BrO trends in the Arctic stratosphere, manuscript in preparation, 2002.](#)
- 34 Toon, G. C., J.-F. Blavier, B. Sen, R. J. Salawitch, G. B. Osterman, J. Notholt, M. Rex, C. T. McElroy,  
35 and J. M. Russell III, Ground-based observations of Arctic O<sub>3</sub> loss during spring and summer 1997,  
36 *J. Geophys. Res.*, 104, 26497-26510, 1999.
- 37 Toon, O. B., A. Tabazadeh, E. V. Browell, and J. Jordan, Analysis of lidar observations of Arctic polar  
38 stratospheric clouds during January 1989, *J. Geophys. Res.*, 105, 20589-20615, 2000.
- 39 Tsias, A., M. Wirth, K. S. Carslaw, J. Biele, H. Mehrtens, J. Reichardt, C. Wedekind, V. Weiss, W.  
40 Renger, R. Neuber, U. von Zahn, B. Stein, V. Santacesaria, L. Stefanutti, F. Fierli, J. Bacmeister,

5/7/02

- 1 and T. Peter, Aircraft lidar observations of an enhanced type Ia polar stratospheric clouds during  
2 APE-POLECAT, *J. Geophys. Res.*, *104*, 23961-23969, 1999.
- 3 Tuck, A. F., K. K. Kelly, C. R. Webster, M. Loewenstein, R. M. Stimpfle, M. H. Proffitt, and R. K. Chan,  
4 Airborne chemistry and dynamics at the edge of the 1994 Antarctic vortex, *J. Chem. Soc. - Faraday*  
5 *Trans.*, *91*, 3063-3071, 1995.
- 6 Uchino, O., R. D. Bojkov, D. S. Balis, K. Akagi, M. Hayashi, and R. Kajiwara, Essential characteristics  
7 of the Antarctic ozone decline: Update to 1998, *Geophys. Res. Lett.*, *26*, 1377-1380, 1999.
- 8 van den Broek, M. M. P., A. Bregman, and J. Lelieveld, Model study of stratospheric chlorine activation  
9 and ozone loss during the 1996-1997 winter, *J. Geophys. Res.*, *105*, 28961- 28977, 2000.
- 10 van Loon, H., and K. Labitzke, The Southern Oscillation, Part V: The anomalies in the lower  
11 stratosphere of the Northern Hemisphere in winter and comparison with the quasi-biennial  
12 oscillation, *Mon. Wea. Rev.*, *115*, 357-369, 1987.
- 13 van Loon, H., and K. Labitzke, The influence of the 11-year solar cycle on the stratosphere below 30 km:  
14 A review, *Space Sci. Rev.*, *94*, 259-278, 2000.
- 15 Vincent, A. P., and B. J. S. Tranchant, Anisotropic diffusion for ozone transport at 520 K, *J. Geophys.*  
16 *Res.*, *104*, 27209-27215, 1999.
- 17 Voigt, C., J. Schreiner, A. Kohlmann, P. Zink, K. Mauersberger, N. Larsen, T. Deshler, C. Kroger, J.  
18 Rosen, A. Adriani, F. Cairo, G. Di Donfrancesco, M. Viterbini, J. Ovarlez, H. Ovarlez, C. David,  
19 and A. Dörnbrack, Nitric acid trihydrate (NAT) in polar stratospheric clouds, *Science*, *290*, 1756-  
20 1758, 2000a.
- 21 Voigt, C., A. Tsias, A. Dörnbrack, S. Meilinger, B. Luo, J. Schreiner, N. Larsen, K. Mauersberger, and T.  
22 Peter, Non-equilibrium compositions of liquid polar stratospheric clouds in gravity waves,  
23 *Geophys. Res. Lett.*, *27*, 3873-3876, 2000b.
- 24 Volkert, H., and D. Intes, Orographically forced stratospheric waves over northern Scandinavia, *Geophys.*  
25 *Res. Lett.*, *19*, 1205-1208, 1992.
- 26 Vömel, H. M. Rummukainen, R. Kivi, J. Karhu, T. Turunen, E. Kyrö, J. Rosen, N. Kjome, and S.  
27 Oltmans, Dehydration and sedimentation of ice particles in the Arctic stratospheric vortex,  
28 *Geophys. Res. Lett.*, *24*, 795-798, 1997.
- 29 Vömel, H., D. W. Toohey, T. Deshler, and C. Kröger, Sunset observations of ClO in the Arctic polar  
30 vortex and implications for ozone loss, *Geophys. Res. Lett.*, *28*, 4183-4186, 2001.
- 31 von Clarmann, T., A. Linden, H. Oelhaf, H. Fischer, F. Friedl-Vallon, C. Piesch, M. Seefeldner, W.  
32 Völker, R. Bauer, A. Engel, and U. Schmidt, Determination of the stratospheric organic chlorine  
33 budget in the spring Arctic vortex from MIPAS B limb emission spectra and air sampling  
34 experiments, *J. Geophys. Res.*, *100*, 13979-13997, 1995.
- 35 von der Gathen, P., M. Rex, N. R. P. Harris, D. Lucic, B. M. Knudsen, G. O. Braathen, H. De Backer, R.  
36 Fabian, H. Fast, M. Gil, E. Kyrö, I. S. Mikkelsen, M. Rummukainen, J. Stähelin, and C. Varotsos,  
37 Observational evidence for chemical ozone depletion over the Arctic winter 1991-92, *Nature*, *375*,  
38 131-134, 1995.
- 39 Voss, P. B., R. M. Stimpfle, R. C. Cohen, T. F. Hanisco, G. P. Bonne, K. K. Perkins, E. J. Lanzendorf, J.  
40 G. Anderson, R. J. Salawitch, C. R. Webster, D. C. Scott, R. D. May, P. O. Wennberg, P. A.  
41 Newman, L. R. Lait, J. W. Elkins, and T. P. Bui, Inorganic chlorine partitioning in the summer  
42 lower stratosphere: Modeled and measured [ClONO<sub>2</sub>]/[HCl] during POLARIS, *J. Geophys. Res.*,  
43 *106*, 1713-1732, 2001.

5/7/02

- 1 Wagner, R. E., and K. P. Bowman, Wavebreaking and mixing in the Northern Hemisphere summer  
2 stratosphere, *J. Geophys. Res.*, *105*, 24799-24807, 2000.
- 3 Wagner, T., C. Leue, K. Pfeilsticker, and U. Platt, Monitoring of the stratospheric chlorine activation by  
4 Global Ozone Monitoring Experiment (GOME) OCIO measurements in the austral and boreal  
5 winters 1995 through 1999, *J. Geophys. Res.*, *106*, 4971, 2001.
- 6 Wagner, T., F. Wittrock, A. Richter, M. Wenig, J.P. Burrows, and U. Platt, Continuous monitoring of the  
7 high and persistent chlorine activation during the Arctic winter 1999/2000 by the GOME  
8 instrument on ERS-2, *J. Geophys. Res.*, in press, 2002.
- 9 Wahner, A., and C. Schiller, Twilight variation of vertical column abundances of OCIO and BrO in the  
10 North Polar region, *J. Geophys. Res.*, *97*, 8047-8055, 1992.
- 11 Waibel, A. E., T. Peter, K. S. Carslaw, H. Oelhaf, G. Wetzell, P. J. Crutzen, U. Poschl, A. Tsias, E.  
12 Reimer, and H. Fisher, Arctic ozone loss due to denitrification, *Science*, *283*, 2064-2069, 1999.
- 13 Wamsley, P. R., J. W. Elkins, D. W. Fahey, G. S. Dutton, C. M. Volk, R. C. Meyers, S. A. Montzka, J. H.  
14 Butler, A. D. Clarke, P. J. Fraser, L. P. Steele, M. P. Lucarelli, E. L. Atlas, S. M. Schauffler, D. R.  
15 Blake, F. S. Rowland, W. T. Sturges, J. M. Lee, S. A. Penkett, A. Engel, R. M. Stimpfle, K. R.  
16 Chan, D. K. Weisenstein, M. K. W. Ko, and R. J. Salawitch, Distribution of halon-1211 in the  
17 upper troposphere and lower stratosphere and the 1994 total bromine budget, *J. Geophys. Res.*, *103*,  
18 1513-1526, 1998.
- 19 Warner, C. D., and M. E. McIntyre, Toward an ultra-simple spectral gravity wave parameterization for  
20 general circulation models, *Earth Planets Space*, *51*, 475-484, 1999.
- 21 Waters, J. W., W. G. Read, L. Froidevaux, R. F. Jarnot, R. E. Cofield, D. A. Flower, G. K. Lau, H. M.  
22 Pickett, M. L. Santee, D. L. Wu, M. A. Boyles, J. R. Burke, R. R. Lay, M. S. Loo, N. J. Livesey, T.  
23 A. Lungu, G. L. Manney, L. L. Nakamura, V. S. Perun, B. P. Ridenoure, Z. Shippony, P. H. Siegel,  
24 R. P. Thurstans, R. S. Harwood, H. C. Pumphrey, and M. J. Filipiak, The UARS and EOS  
25 Microwave Limb Sounder experiments, *J. Atmos. Sci.*, *56*, 194-218, 1999.
- 26 Waugh, D. W., and D. G. Dritschel, The dependence of Rossby wave breaking on the vertical structure of  
27 the polar vortex, *J. Atmos. Sci.*, *56*, 2359-2375, 1999.
- 28 Waugh, D. W., R. A. Plumb, J. W. Elkins, D. W. Fahey, K. A. Boering, G. S. Dutton, C. M. Volk, E.  
29 Keim, R.-S. Gao, B. C. Daube, S. C. Wofsy, M. Loewenstein, J. R. Podolske, K. R. Chan, M. H.  
30 Proffitt, K. K. Kelly, P. A. Newman, and L. R. Lait, Mixing of polar vortex air into middle latitudes  
31 as revealed by tracer-tracer scatterplots, *J. Geophys. Res.*, *102*, 13119-13134, 1997.
- 32 Waugh, D. W., W. J. Randel, S. Pawson, P. A. Newman, and E. R. Nash, Persistence of the lower  
33 stratospheric polar vortices, *J. Geophys. Res.*, *104*, 27191-27201, 1999.
- 34 Weber, M, K.-U. Eichmann, F. Wittrock, K. Bramstedt, L. Hild, A. Richter, J. P. Burrows, and R. Müller,  
35 The cold Arctic winter 1995/96 as observed by the Global Ozone Monitoring Experiment GOME  
36 and HALOE: Tropospheric wave activity and chemical ozone loss, *Q. J. R. Meteorol. Soc.*, in press,  
37 2002.
- 38 Webster, C. R., R. D. May, D. W. Toohey, L. M. Avallone, J. G. Anderson, P. Newman, L. R. Lait, M. R.  
39 Schoeberl, J. W. Elkins, and K. R. Chan, Hydrochloric acid loss and chlorine chemistry on polar  
40 stratospheric clouds in the Arctic winter, *Science*, *261*, 1130-1134, 1993.
- 41 Webster, C. R., H. A. Michelsen, M. R. Gunson, J. J. Margitan, J. M. Russell III, G. C. Toon, and W. A.  
42 Traub, Response of lower stratospheric HCl/Cl<sub>y</sub> to volcanic aerosol: Observations from aircraft,  
43 balloon, space shuttle, and satellite instruments, *J. Geophys. Res.*, *105*, 11711-11719, 2000.

5/7/02

- 1 Wennberg, P. O., R. J. Salawitch, D. J. Donaldson, T. F. Hanisco, E. J. Lanzendorf, K. K. Perkins, S. A.  
2 Lloyd, V. Vaida, R. S. Gao, E. J. Hints, R. C. Cohen, W. H. Swartz, T. L. Kusterer, and D. E.  
3 Anderson, Twilight observations suggest unknown sources of HO<sub>x</sub>, *Geophys. Res. Lett.*, 26, 1373-  
4 1376, 1999.
- 5 Whiteway, J. A., and T. J. Duck, Enhanced stratospheric gravity wave activity above a tropospheric jet,  
6 *Geophys. Res. Lett.*, 26, 2453-2456, 1999.
- 7 Williams, V. J. Austin, and J. D. Haigh, Model simulations of the impact of the 27-day solar rotation  
8 period on stratospheric ozone and temperatures: Ozone variations of the solar origin, *Advances in*  
9 *Space Research*, 1933-1942, 2001.
- 10 Wirth, M., A. Tsias, A. Dörnbrack, V. Weiss, K. S. Carslaw, M. Leutbecher, W. Renger, H. Volkert, and  
11 T. Peter, Model-guided Lagrangian observation and simulation of mountain polar stratospheric  
12 clouds, *J. Geophys. Res.*, 104, 23971-23981, 1999.
- 13 WMO, *Scientific Assessment of Ozone Depletion: 1994*, World Meteorological Organization Global  
14 Ozone Research and Monitoring Project Report No. 37, 1995.
- 15 WMO, *Scientific Assessment of Ozone Depletion: 1998*, World Meteorological Organization Global  
16 Ozone Research and Monitoring Project Report No. 44, 1999.
- 17 Woyke, T., R. Müller, F. Stroh, D. S. McKenna, A. Engel, J. J. Margitan, M. Rex, and K. S. Carslaw, A  
18 test of our understanding of the ozone chemistry in the Arctic polar vortex based on *in situ*  
19 measurements of ClO, BrO, and O<sub>3</sub> in the 1994/1995 winter, *J. Geophys. Res.*, 104, 18755-18768,  
20 1999.
- 21 Wu, J., and A. E. Dessler, Comparison between measurements and models of Antarctic ozone loss, *J.*  
22 *Geophys. Res.*, 106, 3195-3201, 2001.
- 23 Yoden, S., T. Yamaga, S. Pawson S, and U. Langematz, A composite analysis of the stratospheric sudden  
24 warmings simulated in a perpetual January integration of the Berlin TSM GCM, *J. Meteorol. Soc.*  
25 *Japan.*, 77, 431-445, 1999.
- 26 Yoshiki, M., and K. Sato, A statistical study of gravity waves in the polar regions based on operational  
27 radiosonde data, *J. Geophys. Res.*, 105, 17995-18011, 2000.
- 28 Zink, F., and R. A. Vincent, Wavelet analysis of stratospheric gravity wave packets over Macquarie  
29 Island, 2, Intermittency and mean-flow accelerations, *J. Geophys. Res.*, 106, 10289-10297, 2001.
- 30 Zurek, R. W., G. L. Manney, A. J. Miller, M. E. Gelman, and R. M. Nagatani, Interannual variability of  
31 the north polar vortex in the lower stratosphere during the UARS mission, *Geophys. Res. Lett.*, 23,  
32 289-292, 1996.

1 **CHAPTER 3 ACRONYMS AND ABBREVIATIONS**

2		
3	2-D	two-dimensional
4	3-D	three-dimensional
5		
6	AASE	Airborne Arctic Stratospheric Expedition
7	ADEOS	ADvanced Earth Observing Satellite
8	AES	Atmospheric Environment Service (Canada)
9	AM	annular mode
10	AO	Arctic Oscillation
11	ATMOS	Atmospheric Trace Molecule Spectroscopy
12	AWI	Alfred Wegener Institute (Germany)
13		
14	BAS	British Antarctic Survey (United Kingdom)
15	BISA	Belgian Institute for Space Aeronomy (Belgisch Instituut voor Ruimte-Aëronomie, Institut d'Aéronomie Spatiale de Belgique)
17	CCSR	Center for Climate System Research (University of Tokyo) ( <a href="#">verify</a> )
18	CFC	chlorofluorocarbon
19	ClAMS	Chemical Lagrangian Model of the Stratosphere
20	CMAM	Canadian Middle Atmosphere Model
21	CNES	Centre National d'Études Spatiales (France)
22	CNRS	Centre National de la Recherche Scientifique (France)
23	CPC	
24	CRISTA	Cryogenic Infrared Spectrometers and Telescopes for the Atmosphere
25		
26	CTM	Chemical Transport Model
27		
28	DAO	Data Assimilation Office (NASA Goddard, USA)
29	DJF	December, January, and February
30	DLR	Deutschen Zentrum für Luft- und Raumfahrt (German Aerospace Research Establishment)?
31		
32	DMI	Danish Meteorological Institute
33	DOAS	Differential Optical Absorption Spectroscopy
34	DU	Dobson unit
35		
36	ECHAM4.L39(DLR)/CHEM	European Centre Hamburg Model with Chemistry (Germany)
37	ECMWF	European Centre for Medium-Range Weather Forecasts (Reading, United Kingdom)
38		
39	ENEA	Ente Nazionale Energie Alternative (Italy)
40	ENSO	El Niño-Southern Oscillation
41	EP	Earth Probe
42	ERS-2	second European Remote Sensing satellite
43	ESA	European Space Agency
44	EU	European Union
45		



5/7/02

1	FDH	Fixed Dynamical Heating
2	FSSP	forward scattering spectrometer probe
3	FTIR	Fourier transform infrared
4		
5	GCM	General circulation model
6	GHG	greenhouse gases
7	GISS	Goddard Institute for Space Studies (NASA, United States)
8	GOME	Global Ozone Monitoring Experiment
9	GRIPS	GCM-Reality Intercomparison Project for SPARC
10	gwd	gravity wave drag
11		
12	HALOE	Halogen Occultation Experiment
13		
14	IFOV	instantaneous field of view
15	IGY	International Geophysical Year
16	ILAS	Improved Limb Atmospheric Spectrometer
17	IMK	Institut für Meteorologie und Klimaforschung (Institute of Meteorology and Climate Research, Karlsruhe, Germany)
18		
19	IRF	Institut für Rumdfysik (Institute of Space Physics, Sweden)
20	IROE	Instituto di Ricerca Sulle Onde Elettromagnetiche (Italy)
21	ISAMS	Improved Stratospheric and Mesospheric Sounder
22	ISTS	Institute for Space and Terrestrial Science (Canadian Space Agency, Canada)
23		
24	IVL	Institutet för Vatten- och Luftvårdsforskning) (Swedish Environmental Research Institute, Sweden)
25		
26	JJA	June, July, and August
27	JPL	Jet Propulsion Laboratory (California Institute of Technology, United States)
28		
29	KASIMA	Karlsruhe SIMulation model of the Middle atmosphere
30		
31	LaRC	Langley Research Center (NASA, United States)
32	LCTM	Lagrangian chemical transport model
33		
34	MAECHAM/CHEM	Middle Atmosphere ECHAM with chemistry
35	MAM	March, April, and May
36	MASP	Multiangle Aerosol Spectrometer Probe
37	MIPAS	Michelson Interferometric Passive Atmosphere Sounder
38	MLM	Modified Lagrangian Mean
39	MLS	Microwave Limb Sounder
40	MOS	metal oxide semiconductor
41	MRI	Meteorological Research Institute (Japan)
42	MSU	Microwave Sounding Unit
43		
44	NAD	nitric acid dihydrate
45	NAO	North Atlantic oscillation
46	NASA	National Aeronautics and Space Administration

5/7/02

1	NAT	nitric acid trihydrate
2	NCAR	National Center for Atmospheric Research (United States)
3	NCEP	National Center for Environmental Protection
4	NDSC	Network for the Detection of Stratospheric Change
5	NH	Northern Hemisphere
6	NIES	National Institute for Environmental Studies (Japan)
7	NILU	Norwegian Institute for Air Research (Norway)
8	NMC	National Meteorological Center
9	NIWA	National Institute of Water and Atmosphere (New Zealand)
10	NOAA	National Oceanic and Atmospheric Administration
11		
12	OPC	Optical Particle Counter (OPC)
13		
14	PMD	polarization monitoring devices
15	PNJ	polar night jet
16	POAM	Polar Ozone and Aerosol Measurement
17	POLARIS	Photochemistry of Ozone Loss in the Arctic Region in Summer
18	ppbv	parts per billion by volume
19	ppmv	parts per million by volume
20	ppt	parts per trillion
21	PSC	Polar Stratospheric Cloud
22	PV	potential vorticity
23		
24	QBO	quasi-biennial oscillation
25		
26	SAGE	Stratospheric Aerosol and Gas Experiment
27	SAOD	stratospheric aerosol optical depth
28	SAOZ	Système d'Analyse par Observation Zénithale
29	SBUV	Solar Backscatter Ultraviolet spectrometer
30	SCD	slant column density
31	SEFDH	Seasonally Evolving Fixed Dynamical Heating models
32	SH	Southern Hemisphere
33	SOLVE	SAGE III Ozone Loss and Validation Experiment
34	SON	September, October, and November
35	SPADE	Stratospheric Photochemistry, Aerosols, and Dynamics Expedition
36	SPARC	Stratospheric Processes and their Role in Climate (WCRP)
37	SPOT	Satellite Pour l'Observation de la Terre
38	SSU	Stratospheric Sounding Unit
39	STEL	Solar Terrestrial Environment Laboratory (Japan)
40	STS	supercooled ternary solutions
41	STTA	Stratospheric Temperature Trend Analysis
42	SUNY	State University of New York (United States)
43	SZA	solar zenith angle
44		
45	TEM	transformed Eulerian mean
46	TOMS	Total Ozone Mapping Spectrometer

5/7/02

1	TOVS	Television and InfraRed Observational Satellite (TIROS)
2		Operational Vertical Sounder
3		
4	UARS	Upper Atmosphere Research Satellite
5	UIUC	University of Illinois at Urbana-Champaign (United States)
6	UKMO	United Kingdom Meteorological Office
7	ULAQ	Università degli Studi dell'Aquila (Italy)
8	UM	Unified Model
9	UMETRAC	Unified Model with Eulerian Transport and Chemistry
10	UV	ultraviolet
11	UV-C	UV-radiation (approximately 200-280 nm)
12		
13	WMGHG	well-mixed greenhouse gas
14	WMO	World Meteorological Organization
15		

1 **CHAPTER 3 CHEMICAL FORMULAE AND NOMENCLATURE**

2		
3	Br	atomic bromine
4	Br <sub>y</sub> <sup>org</sup>	organic bromine profile
5	Br <sub>y</sub> <sup>inorg</sup>	inorganic bromine profile
6	BrCl	bromide chloride
7	BrO	bromine monoxide
8	BrONO <sub>2</sub>	bromine nitrate
9	BrOOCl	bromo chloro peroxide (verify)
10		
11	CH <sub>4</sub>	methane
12	Cl	atomic chlorine
13	ClO	chlorine monoxide
14	ClOO	chloro peroxy radical (verify)
15	ClO <sub>x</sub>	chlorine radicals
16	ClONO <sub>2</sub> ,	chlorine nitrate
17	ClOOCl	chlorine monoxide dimer
18	Cl <sub>y</sub> <sup>inorg</sup>	inorganic chlorine species
19	Cl <sub>y</sub> <sup>org</sup>	organic source compounds
20	Cl <sub>y</sub>	total inorganic chlorine
21	CO	carbon monoxide
22	CO <sub>2</sub>	carbon dioxide
23		
24	H <sub>2</sub> O	water
25	HBr	hydrogen bromide
26	HCl	hydrogen chloride (hydrochloric acid)
27	HF	hydrogen fluoride (hydrofluoric acid)
28	HNO <sub>3</sub>	nitric acid
29	HNO <sub>4</sub>	peroxynitric acid
30	HO <sub>2</sub>	hydroperoxyl radical
31	HOBr	hypobromous acid
32	HO <sub>x</sub>	odd hydrogen (H, OH, HO <sub>2</sub> , H <sub>2</sub> O <sub>2</sub> )
33		
34	IO	iodine monoxide
35		
36	J <sub>1b</sub>	photolysis rate
37		
38	k <sub>1a</sub>	first-order reaction-rate constant
39		
40	NO	nitric oxide
41	NO <sub>2</sub>	nitrogen dioxide
42	NO <sub>x</sub>	nitrogen oxides (NO + NO <sub>2</sub> )

5/7/02

1	$\text{NO}_y$	odd nitrogen (usually includes NO, NO <sub>2</sub> , NO <sub>3</sub> , N <sub>2</sub> O <sub>5</sub> , ClONO <sub>2</sub> ,
2		HNO <sub>4</sub> , HNO <sub>3</sub> )
3	$\text{N}_2\text{O}$	nitrous oxide
4	$\text{N}_2\text{O}_5$	dinitrogen pentoxide
5		
6	O	atomic oxygen
7	OBrO	bromine dioxide
8	OCIO	chlorine dioxide
9	O <sub>2</sub>	molecular oxygen
10	O <sub>3</sub>	ozone
11	O <sub>3</sub> MD	ozone mass deficiency
12		
13	SF <sub>6</sub>	sulfur hexafluoride
14	SO <sub>2</sub>	sulfur dioxide
15		